Obesity, 11β-hydroxysteroid dehydrogenase and metabolic changes in the pathogenesis of Idiopathic Intracranial Hypertension

by

Alexandra Sinclair

A thesis submitted to the University of Birmingham for the degree of Doctor of Philosophy

Academic Unit of Ophthalmology, School of Immunity and Infection, and
Centre for Diabetes, Endocrinology and Metabolism,
School of Clinical and Experimental Medicine,
College of Medical and Dental Sciences,
University of Birmingham,
United Kingdom.
March 2010

Abstract

Idiopathic intracranial hypertension (IIH) is a blinding condition amongst the young obese female population characterised by elevated intracranial pressure (ICP). The aetiology of IIH is not known and, as highlighted in the 2005 Cochrane review, an evidence base for treatment has not been established, although weight loss is frequently advocated.

Obesity is associated with dysregulation of cortisol metabolism by 11β-hydroxysteroid dehydrogenase type 1 (11β-HSD1). Additionally, 11β-HSD1 has a role in the regulation of intraocular pressure. This thesis hypothesised that 11β-HSD1 is involved in the aetiology of IIH and examined the roles of obesity, 11β-HSD1 and metabolic changes in the pathogenesis and treatment of IIH.

We demonstrated that ICP regulating structures (choroid plexus and arachnoid granulation tissue), are potential glucocorticoid target tissues expressing 11β-HSD1. Metabolomic analysis identified a unique biofluid metabolite biomarker profile, with potential implications for IIH pathogenesis. We established the therapeutic efficacy of weight loss in IIH (improving headaches, papilloedema and ICP) and provided evidence that the beneficial effects may relate to alterations in the glucocorticoid profile driving 11β-HSD1 and potentially, 5α reductase. These studies have started to address the important issues of causation and treatment in IIH and provide avenues for future research into this complex condition.

Dedications

For Andy

Acknowledgments

Table of Contents

List of Figures

List of Tables

Abbreviations

%B	percentage beta cell function
%S	percentage insulin sensitivity
11β-HSD	11beta-hydroxysteroid dehydrogenase
11β-HSD1	11beta-hydroxysteroid dehydrogenase type 1
11β-HSD2	11beta-hydroxysteroid dehydrogenase type 2
1D	one dimension
2D	two dimensions
^{3}H-E	tritiated cortisone
^{3}H-F	tritiated cortisol
ACRD	apparent cortisone reductase deficiency
ACTH	adrenocorticotropic hormone
AG	arachnoid granulation
AGEpi	arachnoid granulation epithelial cell line
AGT	arachnoid granulation tissue
AH	aqueous humour
An	androsterone
ANOVA	analysis-of-variance
AQP	aquaporin
au	arbitrary units
BBB	blood brain barrier
BMI	body mass index
BSA	bovine serum albumin
B-scan	brightness scan
CA	carbonic anhydrase
CB	ciliary body
CBG	corticosteroid binding globulin
CD	collecting ducts
cDNA	complementary deoxyribonucleic acid
CP	choroid plexus
CPE	choroid plexus epithelial cells
CPP	cerebral perfusion pressure
CSF	cerebrospinal fluid
Ct	cycle threshold
CT	computerised tomography
CV	central vein
CVD	cerebrovascular disease
DAB	3,3'-diaminobenzidine tetrahydochloride
DEXA	dual energy x-ray absorptiometry
DHAS	dehydroepiandrosterone sulphate
DHEA	dehydroepiandrosterone
DHT	dihydrotestosterone
DMEM	Dulbecco's Modified Eagle's medium
DNase I	deoxyribonuclease I
DNAse	deoxyribonuclease
DPX	dibutyl-polystyrene-xylene
E	cortisone
EDTA	ethylenediaminetetraacetic acid

ELISA	enzyme linked immunosorbant assay
EMA	epithelial membrane antigen
ENaC	epithelial sodium channel
EPiCM	epithelial cell media
Et	etiocholanolone
F	cortisol
FAM	6-carboxyfluorescein
FBS	foetal bovine serum
FCS	foetal calf serum
FV111	factor V111 related antigen
GAG	glycosaminoglycans
GC	glucocorticoids
GC/MS	gas chromatography / mass spectrometry
GE	glycyrrhetinic acid
glog	generalised log
GR	glucocorticoid receptor
GRE	glucocorticoid response element
GRα	glucocorticoid receptor alpha
GRβ	glucocorticoid receptor beta
H&E	haematoxylin and eosin
H6PD	hexose- 6-phosphate dehydrogenase
HCPEpi	human choroid plexus epithelial cell line
HIT-6	headache impact test-6
HOMA	Homeostasis Model Assessment
HPA	hypothalamic pituitary adrenal
HPLC	high performance liquid chromatography
HRP	horseradish peroxidase
HRT	Heidelberg Retina Tomography
HSP	heat shock protein
HVF	Humphrey visual field
ICP	intracranial pressure
Ig	immunoglobulin
IHS	International Headache Society
IIH	idiopathic intracranial hypertension
IOP	intraocular pressure
IR	insulin resistance
JRES	J-resolved spectroscopy
LC/MS	liquid chromatography / mass spectrometry
LogMAR	logarithm of the minimum angle of resolution
LP	lumbar puncture
LPS	lumboperitoneal shunting
LV	latent variable
MD	mineralocorticoid receptor
MRI	magnetic resonance imaging
mRNA	messenger RNA
MRV	magnetic resonance venography
MS	multiple sclerosis
MYOC	myocilin
NAD$^+$	nicotinamide adenine dinucleotide
NADH	reduced nicotinamide adenine dinucleotide

NADP$^+$	nicotinamide adenine dinucleotide phosphate
NADPH	reduced nicotinamide adenine dinucleotide phosphate
NDS	normal donkey serum
NMR	nuclear magnetic resonance
NPE	non-pigmented epithelium
NSD	nerve sheath diameter
NTP	nucleotide triphosphates
NZWAR	New Zealand White Albino rabbit
OCT	optical coherence tomography
ONSF	optic nerve sheath fenestration
P/S	penicillin and streptomycin
PBS	phosphate buffered saline
PC	principal components
PCOS	polycystic ovarian syndrome
PCR	polymerase chain reaction
PE	pigmented epithelium
p-JRES	1D projections of 2D JRES spectra
PLSDA	partial least squares discriminant analysis
POAG	primary open angle glaucoma
ppm	parts per million
PSD	pattern standard deviation
QC	quality control
RIA	radioimmunoassay
RNA	ribonucleic acid
RNFL	retinal nerve fibre layer
SEM	standard error of the mean
sgk 1	serum and glucocorticoid regulated kinase
SHBG	sex hormone binding globulin
SUMO -1	small ubiquitin related modifier-1
T_2	transverse
TG	triglycerides
THE	tetrahydrocortisone
THF	tetrahydrocortisol
TIGR	trabecular meshwork inducible glucocorticoid response
TLC	thin layer chromatography
TM	trabecular meshwork
TMSP	trimethylsilyl-2,2,3,3-tetradeuteropropionic acid
TOVS	total obscuration of major vessel segments
USG	ultrasonography
VAS	visual analogue pain scale
VLCD	very low calorie total meal replacement liquid diet
VPS	ventriculoperitoneal shunt

Chapter 1. General Introduction

Chapter 1

1.1. Introduction to Idiopathic Intracranial Hypertension

Idiopathic intracranial hypertension (IIH), formerly referred to as serous meningitis, pseudotumour cerebri or benign intracranial hypertension, is a condition of unknown aetiology characterised by elevated intracranial pressure (ICP) and papilloedema in the absence of intra-cerebral space occupation or venous sinus thrombosis (Friedman and Jacobson 2002). The previous nomenclature of "benign" intracranial hypertensions was felt inappropriate in a condition where affected individuals suffer with significant morbidity from chronic headaches, together with progressive visual loss, which is severe and permanent in up to 25% of case (Corbett *et al.* 1982). Of particular interest is that IIH is almost exclusively diagnosed, greater than 93% of cases, amongst young obese female subjects (Giuseffi *et al.* 1991). The reasons for this association are unclear and will be discussed in more detail in section 1.5.

The reported incidence of IIH is 0.9 to 2.2 per 100,000 in the general population (Durcan *et al.* 1988; Radhakrishnan *et al.* 1993), rising to above 19 per 100,000 in studies confined to young, overweight women. This background incidence is likely to increase further in developed countries with the epidemic of obesity.

Despite the disability associated with IIH, the pathogenesis remains unidentified and an evidence base for treatment has not been established. This thesis, will explore the putative role of obesity, metabolic changes and glucocorticoid regulation, via 11β-hydroxysteroid dehydrogenase (11β-HSD), in ICP regulation and IIH. The therapeutic role of weight loss in IIH will also be assessed and metabolic implications characterised.

1.2. Intracranial pressure homeostasis

ICP homeostasis is dependent on cerebrospinal fluid (CSF) dynamics and cerebral blood circulating pressure. ICP in turn influences the cerebral perfusion pressure (CPP) which controls cerebral blood flow (Miller *et al.* 1972), a vital determinant of viable brain tissue.

CPP = mean arterial blood pressure – ICP

As the fragile tissue of the brain is enclosed in a rigid cranium, relatively small changes in either CSF pressure or cerebral blood volume can significantly alter the ICP. In turn, fluctuations in ICP can have dramatic effects on cerebral blood volume through compression of the venous sinuses with consequential reduction in venous blood flow. Significantly impaired venous blood flow may contribute to venous infarction with resultant loss of brain function. Numerous pathological and physiological processes (space occupying lesion, obstructed CSF flow, jugular vein compression) can impair ICP homeostasis and result in either locally or globally impaired cerebral blood flow with potential implications for brain function.

1.3. Cerebrospinal fluid dynamics

CSF dynamics are dependent on the balance between CSF production and drainage. The brain is surrounded by approximately 150 ml of CSF (Praetorius 2007), this has two predominant functions. Firstly, to protect the brain from external mechanical trauma, and secondly, to provide a medium for the transfer of nutrients and waste products to and from the brain tissue. 80 % of the CSF is produced in the lateral, third and fourth ventricles by the choroid plexus (CP) (Welch 1963) with a smaller volume being produced by the ventricular ependyma, arachnoidal membrane and brain tissue itself (McComb 1983;

Adams and Graham 1988). CSF circulation is shown in Figure 1-1. CSF drains

predominantly via the arachnoid granulation tissue (AGT) into the venous circulation.
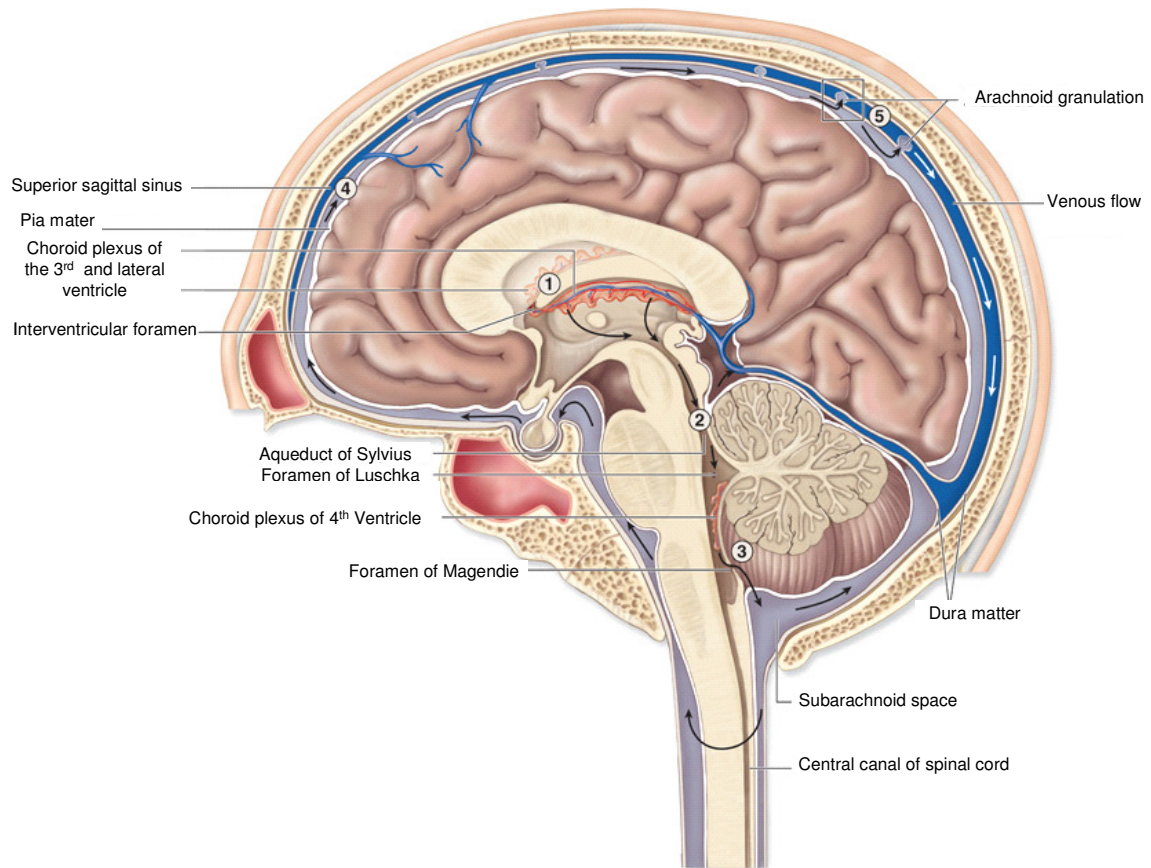
Figure 1-1   *Sagittal section through the brain illustrating the circulation of cerebrospinal fluid.*

CSF is secreted by the choroid plexus (1), CSF then flows from the lateral and third ventricle through the aqueduct of Sylvius into the forth ventricle (2),CSF then passes into the cisterna magna via the bilateral foramen of Luschka and the midline foramen of Magendie (3). CSF in the cisterna magna is in continuity with the subarachnoid space and flows upwards over the cranium towards the arachnoid granulations (4), finally, CSF drains via the arachnoid granulations into the venous blood (5). The arrows indicate the direction of CSF flow. Reproduced and adapted with permission from McGraw-Hill Companies Inc, USA.

There is evidence that CSF drainage can occur via sites other than the AGT. As long ago

as 1869, it was suggested that CSF could drain via lymphatic channels (Schwalbe 1869)

and this has been demonstrated in a number of animal studies (McComb 1983). More recently, post-mortem subarachnoid injection of microfil has demonstrated the drainage of CSF via nasal lymphatics in large mammals, and also in one human (Johnston *et al.* 2004). The precise pathway by which CSF enters the nasal lymphatics is unclear. In addition, the extent to which extra-arachnoid CSF drainage takes place needs to be established.

1.3.1. Arachnoid granulation tissue

AGT is continuous with the arachnoid membrane and projects into venous sinuses, predominantly at the superior sagittal sinus but also into veins associated with spinal nerve roots (Weller 1974) (Figure 1-2).
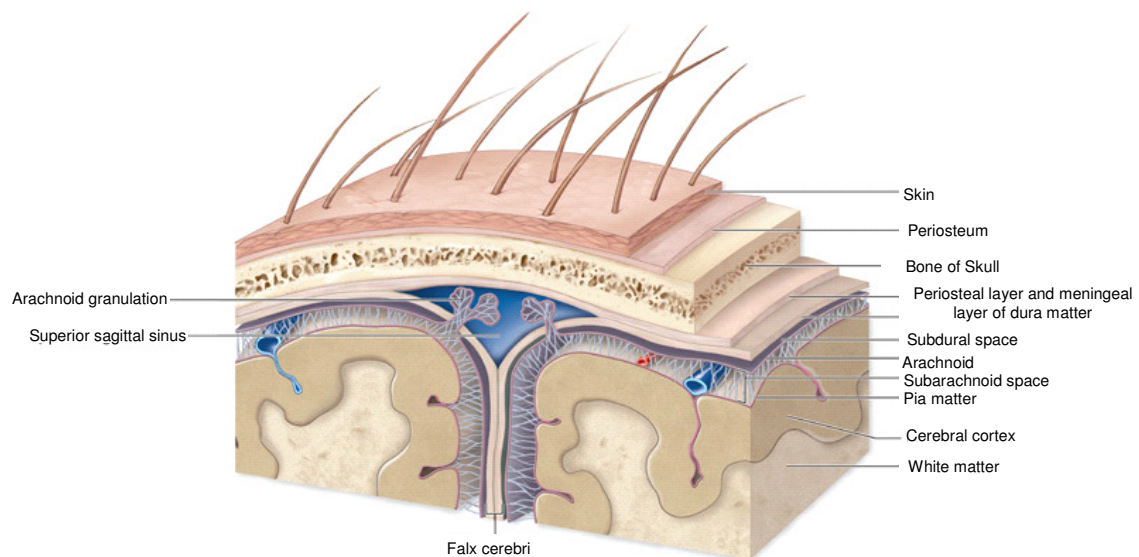
Figure 1-2   ***Coronal section through the brain illustrating the location of arachnoid granulation tissue.***

Reproduced and adapted from McGraw-Hill Companies Inc, USA (with permission).

The number of arachnoid granulations (AG) varies with gender and ethnicity, being higher in men and in African Americans (Grzybowski *et al.* 2006a). By convention AGT

visible to the naked eye are known as AG's (around 4 mm in diameter); arachnoid villi are smaller (Upton and Weller 1985). AGT increases in size with increasing age (Turner 1961) and becomes more lobulated. Each AG is composed of four zones: an arachnoid cell layer, a cap cell cluster, a fibrous capsule and a central core (Kida *et al.* 1988) (Figure 1-3). Arachnoid cells are mesothelial cells with both epithelial and fibroblastic characteristics. Epithelial cells cover the AG and form a thickened layer at the apex of the granulation, the cap cell cluster. The cap cell cluster projects into the lumen of the venous sinus and is not covered by a fibrous, endothelial capsule (Kida et al. 1988).

The central core of the AG is made up of arachnoid cells and connective tissue formed into multiple channels of variable diameter. The core contains no blood vessels or nervous tissue.

It is thought that CSF travels through the honeycomb of channels to the venous sinus (Figure 1-4). In support of this, the channels have been shown to contain red blood cells after subarachnoid haemorrhage (Upton and Weller 1985). Mechanisms which control CSF movement across the AG are not known. Vacuoles have been noted in the AG core from the basal to the apical region and it has been suggested that they may transfer fluid and proteins into the venous sinus (Tripathi and Tripathi 1974).

Histological identification of AGT is facilitated by vimentin which stains both the cap cell cluster and the central core, while factor eight related-antigen (FVIII) localises exclusively to the AG endothelium, and epithelial membrane antigen to the cap cell cluster epithelium (Kida et al. 1988).
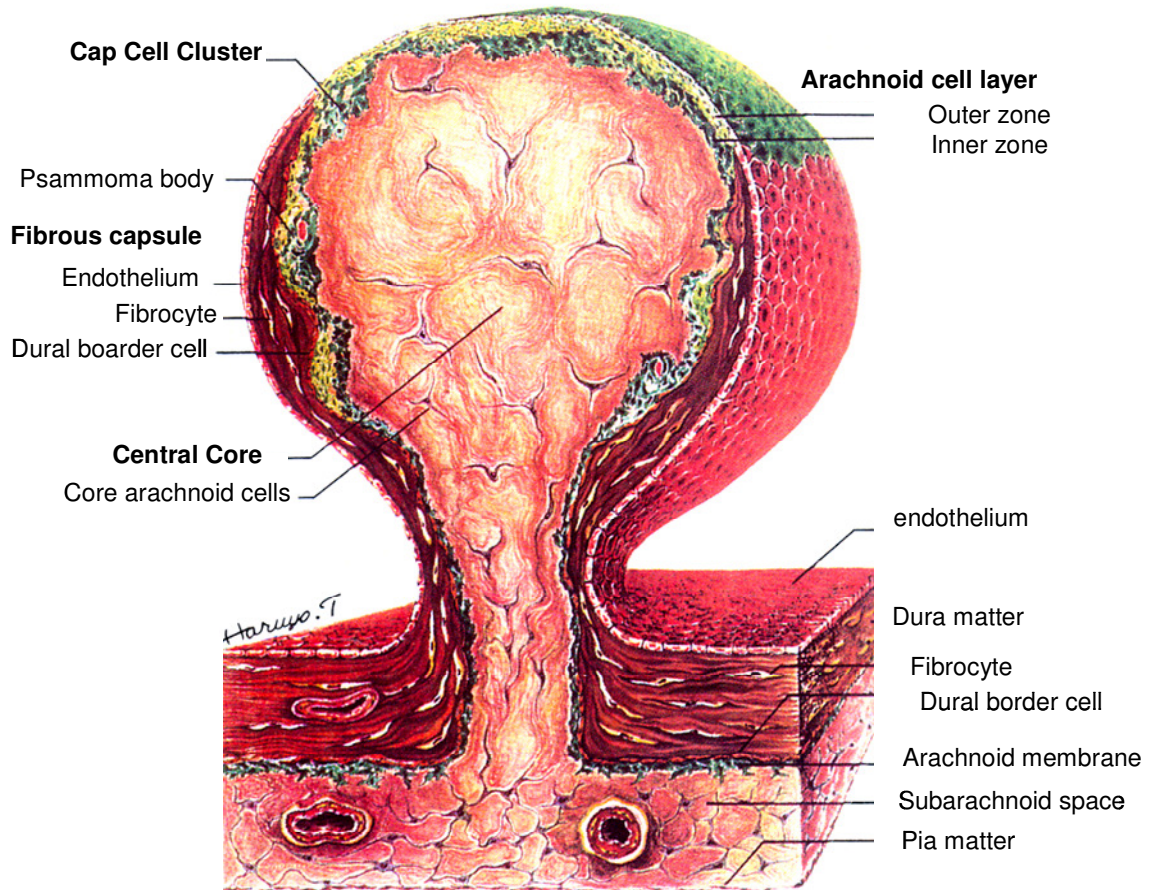
Figure 1-3 *Schematic drawing of a human arachnoid granulation*

CSF travels through the channels of the central core towards the apex of the arachnoid granulation and then into the venous sinus. The apex is composed of the cap cell cluster covered by a layer of epithelium, the arachnoid cell layer, which projects into the lumen of the venous sinus. A fibrous capsule encloses the granulation, except at the apex. Adapted and modified from Kida et al. J Neurosurgery 1988; 69:429-435.
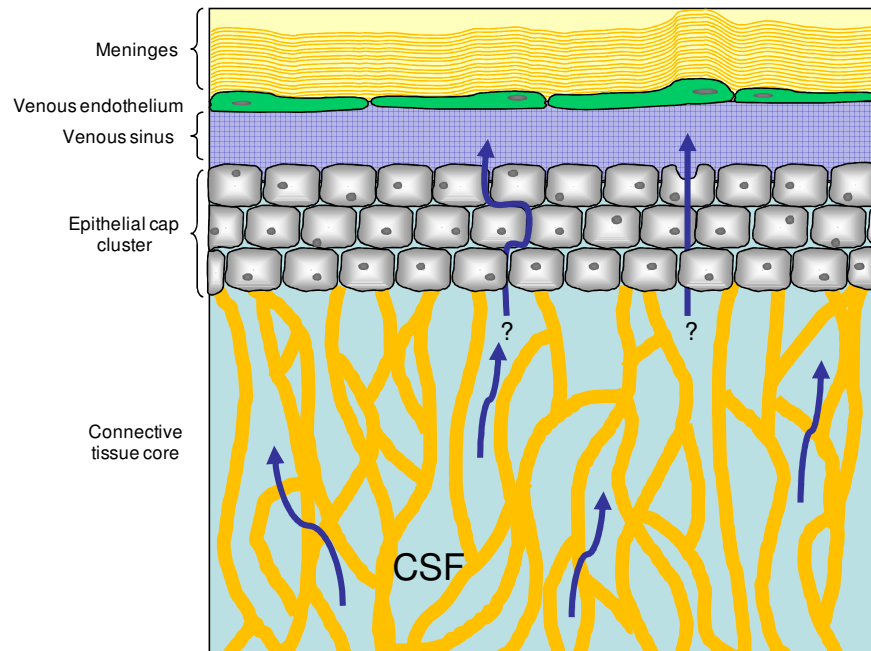
Figure 1-4   Schematic diagram of a sagittal section through an arachnoid granulation

CSF flows through the connective tissue core to the epithelial cap cell cluster and then into the venous sinus. The mechanisms that control CSF flow across the connective tissue core and epithelial cap cell cluster are not known.

1.3.2. Choroid plexus and cerebrospinal fluid secretion

The dynamic circulation of CSF is driven by the secretion of CSF from the CP at the rate of 25 ml/h (Wright 1978). The CP is one of the most efficient secretory tissues in the body (Speake *et al.* 2001). Macroscopically the CP is a branched structure of microvilli. Each villus is composed of a core of connective tissue and fenestrated capillaries surrounded by an epithelial monolayer (Figure 1-5). The epithelial cells are joined by tight junctions at their apical surface; this arrangement forms the blood-CSF barrier. The epithelial cells of the CP are highly specialised in their orientation and structure. The apical surface is composed of a brush border facing into the ventricle, while the folded, basal surface, is orientated towards the capillary endothelium (Speake et al. 2001).
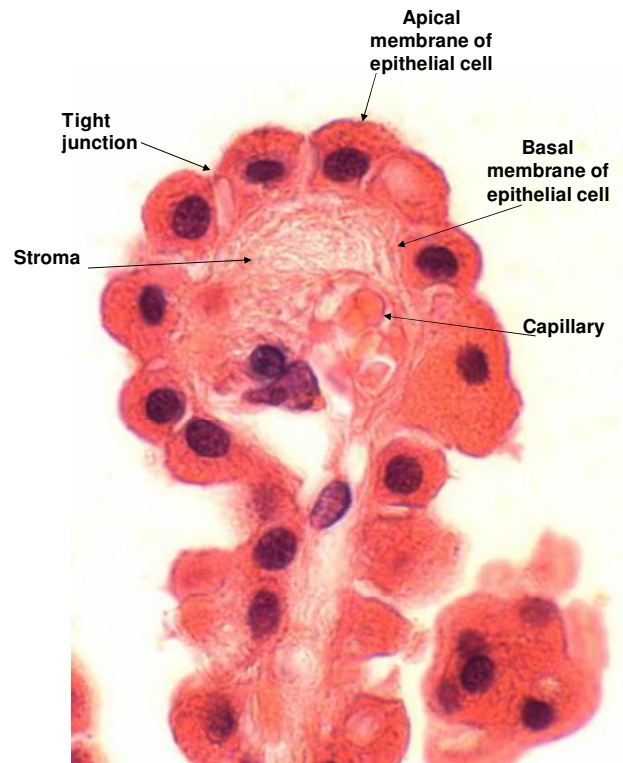
Figure 1-5   ***Haematoxylin and eosin stain of a choroid plexus villus***

> *The villus is composed of single layer of epithelial cells surrounding an abundant capillary net work and stromal cells. The villus projects into the cerebrospinal fluid filled ventricle.*

The initial step in CSF secretion is likely to be passive due to ultrafiltration of plasma from the leaky, fenestrated capillary network into the connective tissue stroma of the CP. Thereafter, CSF secretion is thought to be predominantly an active process. This is supported by the findings that 1) CSF is hypertonic compared to plasma (Table 1-1), 2) ion concentrations in the CSF remain stable despite wide fluctuations in plasma ion concentrations, 3) capillary pressure is insufficient to drive ultrafiltration and 4) there is an electrical potential difference of 5mV across the CP epithelium (Speake et al. 2001; Praetorius 2007).

	Plasma	CSF
Na^+ (mM)	155	151
K^+ (mM)	4.6	3.0
HCO_3^- (mM)	26.2	25.8
Glucose	6.3	4.2
Amino acids (mM)	2.3	0.8
pH	7.4	7.4
Osmolality (mosmol/Kg H_2O)	300	305
Protein (mg/100g)	6500	25

Table 1-1   Comparison of CSF and plasma constituents in the dog.
Adapted from Davson et al. 1987.

The process of CSF secretion from the CP epithelial cells is not fully characterised but is known to involve multiple ion channels on both the basal and apical surfaces of the CP epithelium. Sodium ions are transported from the CP connective tissue across the CP epithelial cell and into the ventricular space containing CSF. This creates an osmotic gradient which pulls water into the ventricles. This process is analogous to fluid secretion in other epithelia e.g. saliva and sweat secretion (Speake et al. 2001), and was originally described in the shark rectal gland (Silva *et al.* 1977). Central to this process is the Na^+K^+ ATPase which is located exclusively on the apical surface of the CP epithelial cell (Ernst *et al.* 1986). This localisation is unusual, as in most other secretory epithelia, the Na^+K^+ ATPase is on the basal surface (Speake et al. 2001). The Na^+K^+ ATPase consists of 3 subunits, which vary between tissues but in the CP consist of the $\alpha 1$, $\beta 1$ and $\beta 2$ subunits, in conjunction with a membrane spanning protein, phospholemman (Feschenko *et al.* 2003). The importance of the Na^+K^+ ATPase is highlighted by the finding that ventricular application of ouabain, a Na^+K^+ ATPase inhibitor, completely abolishes Na^+ influx and CSF secretion (Welch 1963; Davson and Segal 1970; Zeuthen and Wright 1978).

Chapter 1

There is considerable interplay between numerous other ion transporters in the CP epithelial cells (Figure 1-6). The effects of these other ion transporters, on CSF secretion are illustrated by the ability of inhibitors to reduce CSF secretion. CSF secretion is impaired by bumetanide, via its actions on the Na^+ K^+ $2Cl^-$ co transporter (Wu *et al.* 1998), frusemide, due to inhibition of the K^+ Cl^- co transporter (Zeuthen and Wright 1981) and amiloride, due to inhibition of the basal Na^+/H^+ exchanger (Murphy and Johanson 1989), which is thought to control Na^+ entry into the epithelial cell. In addition Cl^- secretion is blocked by 4,4'-diisothiocyanatostilbene-2,2'-disulphonic acid at the Cl-/HCO3- transporter in the CP (Deng and Johanson 1989)

Carbonic anhydrase, an enzyme which catalyses the reversible hydration of carbon dioxide (CO_2 + H_2O «to» H_2CO_3 «to» H^+ + HCO_3^-) also has a role in CSF secretion. Twelve isoforms of carbonic anhydrase have been identified, which vary between tissues and species (Halmi *et al.* 2006). Carbonic anhydrase II has been localised to the cytoplasm of rat CP epithelial cells (Masuzawa and Sato 1983; Masuzawa *et al.* 1984) while carbonic anhydrase III has been identified in the lateral ventricle of rat CP as well as in human CP epithelial cells (Nogradi *et al.* 1993). Acetazolamide, a carbonic anhydrase inhibitor, reduces CSF secretion in rats by 50% (Vogh *et al.* 1987), supporting the importance of this enzyme in CSF secretion. Acetazolamide does not inhibit carbonic anhydrase III, potentially explaining why it is only partially effective in inhibiting CSF secretion. The effects of acetazolamide on reducing CSF secretion and thus potentially ICP have lead to its widespread use in the treatment of patients with IIH. The use of acetazolamide in IIH has, however, been questioned, following the results of a randomised controlled study which failed to demonstrate clinical efficacy (Ball *et al.* 2009a).

Aquaporins, small hydrophobic integral membrane proteins with the primary function of facilitating water transport, are also thought to have a role in CSF secretion (Speake et al. 2001). 13 mammalian aquaporin channels have been identified and are expressed in both epithelium and endothelium involved in fluid transport, as well as in brain glia and adipocytes (Verkman 2009). There has been considerable recent interest in anti aquaporin 4 antibodies due to their discovery in association with Devic's disease, a multiple sclerosis (MS) variant (Lennon *et al.* 2004; Lennon *et al.* 2005). Within the CP, aquaporin 1 and 4 have been identified in rat models (Nielsen *et al.* 1993; Venero *et al.* 1999) although the contribution of aquaporin channels to CSF production has not been studied.
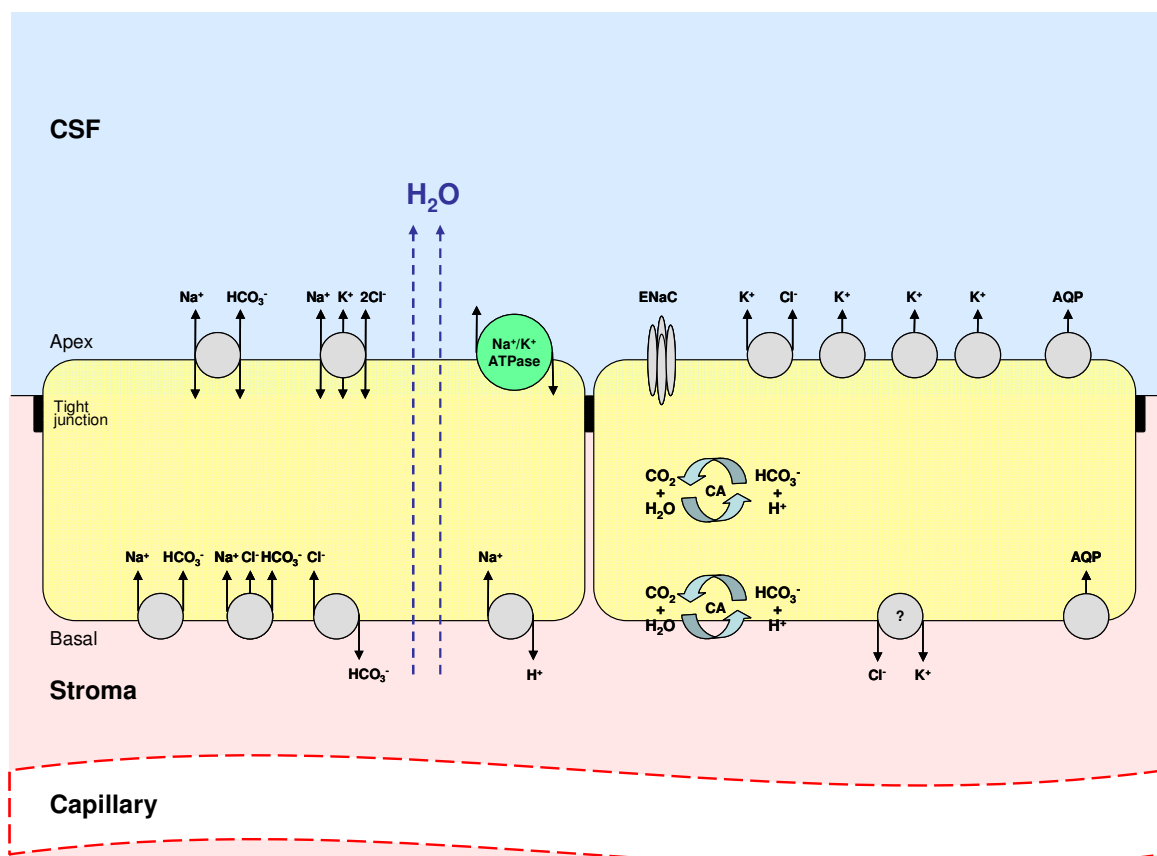
Figure 1-6   Schematic representation of CSF secretion in the CP by ion transporters

ENaC indicates epithelial sodium channel, CA, carbonic anhydrase, AQP, aquaporin channel.

1.4. Pathogenesis of IIH

1.4.1. What is known about the pathogenesis of IIH?

Although the hallmark of IIH is raised ICP, the underlying aetiology of IIH is not known. Elevated ICP is likely to relate to abnormalities in the balance between production, by the CP, and drainage, primarily at the AGT, of CSF. Several possible mechanisms for the raised ICP have been postulated: increased CSF secretion, increased cerebral volume, increased CSF outflow resistance and increased cerebral venous pressure.

1.4.2. CSF hypersecretion

The first suggestion that CSF hypersecretion resulted in IIH was made over a century ago (Quincke *et al.* 1897) when alcohol, stress or changes in the weather were thought to lead to CSF hypersecretion and subsequent raised ICP. In 1979, ventricular infusion studies (which monitor CSF dilution and calculate the rate of CSF production), demonstrated elevated CSF secretion in five patients with IIH (Donaldson 1979). These findings were supported by velocity sensitive magnetic resonance imaging (MRI), a calculation of CSF flow, which also showed hypersecretion in IIH (Gideon *et al.* 1994). These studies, however, were confounded by small numbers and assumptions made in the mathematical modelling. Nevertheless the observation that CSF protein levels are reduced in IIH supports the theory of CSF hypersecretion (Chandra *et al.* 1986), although low protein in IIH is not a universal finding (Johnston *et al.* 1991). In other conditions in which there is CSF hypersecretion, such as choroid plexus papilloma, hydrocephalus is a feature. The absence of hydrocephalus in IIH suggests that increased CSF secretion may not be a feature. Increased brain water content has been postulated as the cause of IIH but evidence, based on histology of brain biopsies and diffusion weighted MRI scanning, is

sparse (Gideon *et al.* 1995; Wall *et al.* 1995). In summary, the limited studies investigating CSF hypersecretion in IIH have been inconclusive but continues to be debated in the literature (Ball and Clarke 2006).

1.4.3. Increased CSF outflow resistance

Impaired CSF drainage is increasingly recognised as a probable cause of IIH. The majority of evidence to support this has come from CSF infusion studies which demonstrated reduced CSF drainage in IIH (Malm *et al.* 1992). Studies scrutinising the transit time of a radio-labelled tracer injected into the CSF (cisternography) have demonstrated delayed uptake into the circulation in patients with IIH, implicating compromised CSF drainage (Orefice *et al.* 1992). These findings have not been universally replicated (Janny *et al.* 1981).

The importance of CSF drainage in CSF dynamics is highlighted by observations of secondary intracranial hypertension in conditions such as Guillain Barré syndrome (Ropper and Marmarou 1984), spinal cord tumour (Feldmann *et al.* 1986), malignant / infective meningitis (Cremer *et al.* 1997) and subarachnoid haemorrhage (Kida et al., 1988). These conditions are characterised by CSF hypercellularity or hyperproteinaemia which is believed to block the AGT, thereby restricting drainage and elevating CSF pressure. This has been shown histologically in cases of subarachnoid haemorrhage which demonstrate red blood cells obstructing the AGT core (Kida et al. 1988). Elevated ICP is also noted in patients with AGT agenesis (Gilles and Davidson 1971; Gutierrez *et al.* 1975). These observations emphasise the importance of AGT in CSF drainage and ICP homeostasis

1.4.4. Increased cerebral venous pressure

There is considerable evidence from venography and manometry studies that venous sinus pressure is raised in IIH, particularly in the transverse and superior sagittal sinus (Karahalios et al., 1996) (King *et al.* 1995). In addition, focal cerebral venous stenoses have been reported in IIH patients (Higgins *et al.* 2004), and stenting the stenosed veins has been shown to improve symptoms in a few cases of IIH (Higgins *et al.* 2003; Rajpal *et al.* 2005). The underlying cause for the stenoses remains controversial and may represent either small venous sinus thromboses, congenital variations (Johnston *et al.* 2002), intra-luminal septa (Subramaniam *et al.* 2004) or indentations from giant arachnoid granulations swollen by raised ICP (Kollar *et al.* 2001). It is most likely, however, that the stenoses are a consequence of raised pressure, originating from brain parenchyma or the CSF compartment, on the venous system (Farb *et al.* 2003). This is substantiated in an elegant study by King et al in 2002 in which patients with IIH underwent cerebral venous manometry before and after a lumbar puncture (LP) (King *et al.* 2002). The pressure in the superior sagittal and transverse sinus, which was initially elevated, significantly reduced following LP, with subsequent reduction of CSF pressure and disappearance of the apparent venous stenoses. This study, and others, conclude that the cerebral venous stenoses and elevated venous pressure in IIH result from collapse of the venous sinus walls due to raised intracranial pressure, that is the stenoses occur as a secondary phenomenon and are not the primary cause of IIH (Goodwin 2003; McGonigal *et al.* 2004). It is also possible that the cerebral venous stenoses play an important role in aggravating IIH by further decreasing CSF drainage across the AGT and thus further increasing the CSF pressure (Pickard *et al.* 2008).

1.4.5. Other

A number of other studies have highlighted possible aetiological factors in IIH. Elevated retinol has been identified in the CSF of patients with IIH (Warner *et al.* 2007). In addition, elevated ICP has been noted in individuals taking vitamin A containing drugs and following ingestion of vitamin A rich foods, such as polar bear liver (Rodahl and Moore 1943). Vitamin A has, therefore, been implicated in the pathogenesis of IIH, although the mechanism remains unclear. Elevated plasma and CSF leptin levels have also been documented in patients with IIH (Lampl *et al.* 2002; Ball *et al.* 2009b). Leptin, an adipokine (cytokine predominantly secreted by adipose tissue), has a key role in appetite regulation (Klok *et al.* 2007) but its role in ICP regulation has not been studied. Microthrombi obstructing the AGT have been postulated as a cause of IIH with thrombophilic defects being reported in between 14 and 68% of patients with IIH (Sussman *et al.* 1997; Glueck *et al.* 2005), although a number of patients in these studies had underlying venous sinus thrombosis.

In summary although raised ICP in IIH suggests disordered CSF dynamics, there is no consensus regarding the mechanism. This thesis will, therefore, focus on the control of CSF dynamics via CSF secretion at the CP and drainage at the AGT.

1.5. Obesity and IIH

IIH is strikingly associated with obesity, 87.8 – 94% of patients with IIH being obese (Giuseffi et al. 1991; Wall and George 1991; Galvin and Van Stavern 2004). The incidence of IIH increases to between 19.3 and 21 per 100,000 in the obese population compared with 0.9 to 2.2 per 100,000 in the general population (Durcan *et al.* 1988; Ireland *et al.* 1990; Radhakrishnan *et al.* 1993).

Chapter 1

The mechanism by which obesity causes IIH is debated. Obstructive sleep apnoea, a condition associated with obesity, leads to nocturnal hypercapnia, right heart failure and surges in intra-thoracic pressure which can elevate ICP particularly in the morning compared to the evening (Jennum and Borgesen 1989). It has also been suggested that pressure effects of centrally distributed adiposity elevate intra-abdominal pressure which subsequently elevates intra-thoracic pressure and cerebral venous pressure and finally ICP (Sugerman *et al.* 1995). This theory does not explain why despite ubiquitous elevation of intra-abdominal pressure in obese patients (Sugerman *et al.* 1997; Whiteley *et al.* 2006), only a small proportion of patients develop IIH. Furthermore, there is only a weak, non significant relationship between BMI and LP opening pressure (Whiteley et al. 2006). The current literature does not establish whether obesity in IIH represents cause or effect. In addition, these mechanisms do not explain the sexual dimorphism seen in IIH. We therefore suggest that the relationship of IIH to obese patients strongly suggests that neuroendocrine dysfunction plays an important aetiological role in these patients.

1.5.1. Obesity, glucocorticoids and 11β-HSD1

The effects of glucocorticoids on body mass index (BMI) have long been recognised and are illustrated in Cushing's syndrome; a condition characterised by central obesity and elevated plasma cortisol levels. Although patients with obesity are not characterised by elevated plasma cortisol (Fraser *et al.* 1999) there is growing evidence that dysfunctions of 11beta-hydroxysteroid dehydrogenase (11β-HSD1) may be pathological. 11β-HSD1, a cortisol activating enzyme which regulates intracellular cortisol availability, will be discussed in detail in section 1.8.

Overexpression of adipose 11β-HSD1 causes visceral obesity in mouse models (Masuzaki *et al.* 2001). In human idiopathic obesity, aberrant hepatic 11β-HSD1 activity

has been demonstrated using cortisol generation curves (administration of cortisone acetate following an overnight dexamethasone suppression test) (Stewart *et al.* 1999; Rask *et al.* 2001). Global 11β-HSD1 activity, determined from urinary tetrahydrocortisols (THF+5αTHF): tetrahydrocortisone (THE) ratios, are also disrupted in the obese, with reports of increased, unaffected and reduced activity (Marin *et al.* 1992; Andrew *et al.* 1998; Rask *et al.* 2001; Reynolds *et al.* 2001). Microdialysis fluid from the subcutaneous tissue of obese patients shows enhanced 11β-HSD1 activity (Sandeep *et al.* 2005). Additionally, increased 11β-HSD1 mRNA expression has also been documented in subcutaneous (Paulmyer-Lacroix *et al.* 2002; Tomlinson *et al.* 2002; Goedecke *et al.* 2006; Li *et al.* 2007; Michailidou *et al.* 2007; Paulsen *et al.* 2007) as well as visceral fat (Desbriere *et al.* 2006; Michailidou *et al.* 2007) from obese individuals. Increased 11β-HSD1 activity in human subcutaneous adipose tissue, associated with altered lipid metabolism and insulin resistance (Veilleux *et al.* 2009), have implicated 11β-HSD1 in the development the metabolic syndrome. Recombinant mice lacking 11β-HSD1 and therapeutic inhibition of the enzyme in man improves glucose tolerance and insulin resistance (Boyle and Kowalski 2009).

These studies suggest that 11β-HSD1 is dysregulated in obesity and it is possible that dysregulation of 11β-HSD1 may contribute to IIH. Of note, weight loss has been shown to alter 11β-HSD1 activity and reduce glucocorticoid generation in human idiopathic obesity (Tomlinson *et al.* 2004b; Tomlinson *et al.* 2008) and, therefore, may represent a possible mechanism explaining the potential therapeutic effect of weight loss in IIH.

1.5.2. Gender dimorphism in IIH and 11β-HSD1

11β-HSD1 activity shows sexual dimorphism. Hepatic 11β-HSD1 activity was noted to be greater in male rats compared to female rats (Low *et al.* 1994). Studies of urinary

metabolites in humans identified higher 11β-HSD1 activity in males compared to females after puberty (Low *et al.* 1994; Dimitriou *et al.* 2003). This gender discrepancy may be due to inhibitory affects of estradiol on 11β-HSD1. Estradiol has been shown to inhibit 11β-HSD1 in rat liver, kidney and testis, although in other tissues such as the uterus and endometrium this is not the case (Arcuri *et al.* 1997; Ho *et al.* 1999; Nwe *et al.* 2000; Gomez-Sanchez *et al.* 2003). Testosterone can also inhibit 11β-HSD1 as described in the rat testis (Nwe et al. 2000). These studies indicate that sexual dimorphism in 11β-HSD1 is likely due to a more complex mechanism than simply inhibition by sex steroids, although they may well be an important factor.

Aberrant sex hormone metabolism is suggested in IIH, as patients are almost universally female (female to male ratios ranging from 4:1 to 15:1) (Durcan et al. 1988; Radhakrishnan et al. 1993) and of reproductive age (with the mean age of onset being 28 – 35) (Galvin and Van Stavern 2004; Glueck et al. 2005). It is possible that the suppression of 11β-HSD1 activity normally seen in women may be lost in IIH as a result of abnormal sex hormone metabolism.

1.6. IIH and endocrinopathies

Numerous case reports have linked IIH to endocrinopathies (Table 1-2) and glucocorticoid therapy (Table 1-3)(Kiehna *et al.* 2010). There is also a strong association with polycystic ovarian syndrome (PCOS), 39 – 57% of patients with IIH having PCOS (the background risk in the general population is 7-15% (Glueck *et al.* 2003; Tsilchorozidou *et al.* 2004; Glueck *et al.* 2005)). 27% of these patients have significant hyperandrogenism (Glueck et al. 2005) and it is possible, therefore, that hyperandrogenism may be pathological in IIH. IIH is, however, typically a disease related to females and therefore an oestrogen and progesterone dominated hormone

profile may be more important. PCOS has also been linked to an increase in 11β-HSD1, demonstrated both in mRNA expression from adipose tissue (Svendsen *et al.* 2009) as well as from urinary metabolites (Vassiliadi *et al.* 2009). Additionally, some patients have been reported to have concomitant defects in both the 11β-HSD1 and H6PDH genes (Draper *et al.* 2003) although this has not been confirmed in more recent studies (Draper *et al.* 2006; Smit *et al.* 2007). The potential relationship between PCOS and IIH will be discussed further in section 5.4.3.

Disorder	Number of cases	Reference
Cushing's disease/ syndrome	9	(Britton *et al.* 1980; Newman *et al.* 1980; Kiehna *et al.* 2010)
Adrenal hyperplasia	1	(De Campo *et al.* 1988)
Primary aldosteronism	2	(Weber *et al.* 2002)
Addison's disease	1	(Condulis *et al.* 1997)
Hypothyroidism	1	(Serratrice *et al.* 2002)
Growth Hormone	6	(Crock *et al.* 1998; Clayton and Cowell 2000; Reeves and Doyle 2002)
Hypoparathyroidism	1	(Madan Mohan *et al.* 1993)
ACTH deficiency	1	(Aanderud and Jorde 1988)
Oral contraception	2	(Janzik 1973; Ivancic and Pfadenhauer 2004)
Pregnancy	2	(Elian *et al.* 1968; Gumma 2004)

Table 1-2   Case reports of endocrinopathies associated with IIH

Treatment	Number of cases	Reference
Corticosteroid therapy	1	(Valentine 1959)
	1	(Dees and Mc 1959)
	1	(Dees and Mc 1959)
	1	(Lorenzo and Avellanal 1961)
	4	(Walker and Adamkiewicz 1964)
	1	(Ivey and Denssesten 1969)
	1	(Jewell 1972)
	1	(Vyas *et al.* 1981)
	1	(Pampapathi and Kabuubi 1987)
	1	(Lucas *et al.* 1991)
	2	(Newton and Cooper 1994)
	1	(Lorrot *et al.* 1999)
	1	(Chebli *et al.* 2004)
Chronic corticosteroid withdrawal	5	(Greer 1963)
	1	(Hosking and Elliston 1978)
	4	(Liu *et al.* 1994)
	1	(Saigusa *et al.* 2002)

Table 1-3   Case reports of IIH attributed to corticosteroid therapy

1.7. Summary

IIH, a condition of raised ICP, results from disordered CSF dynamics but detailed understanding of the role of CSF secretion and drainage are still debated. Additionally, the association between obesity, female gender and CSF balance in IIH are not understood. Dysregulation of 11β-HSD1 has been established in idiopathic obesity and may also have a role in the pathogenesis of IIH and ICP regulation at the CP and AGT.

1.8. Corticosteroids and 11B-HSD1

1.8.1. Corticosteroids

Corticosteroids, encompassing glucocorticoids and mineralocorticoids, are steroid hormones. Steroidogenesis occurs as a result of cholesterol being converted, initially, to pregnenolone by cytochrome p450 side chain cleavage enzyme (Farkash *et al.* 1986)

Chapter 1

within the mitochondrion. Pregnenolone is then converted to progesterone and thereafter

hydroxylated to either 11β-deoxycorticosterone, which is further metabolised to form

aldosterone or 17α-hydroxyprogesterone, the latter being further converted to cortisol via

21-hydroxlase and 11β-hydroxylase (

Figure 1-7). The synthesis of cortisol occurs within the middle layer of the adrenal cortex.

Cholesterol

P450scc

Pregnenolone

3β-HSD2

Progesterone ⟶ CYP17A1 ⟶ **17α-OH-Progesterone** ⟶ CYP21A2 ⟶ **11-Deoxycortisol**

CYP11B1
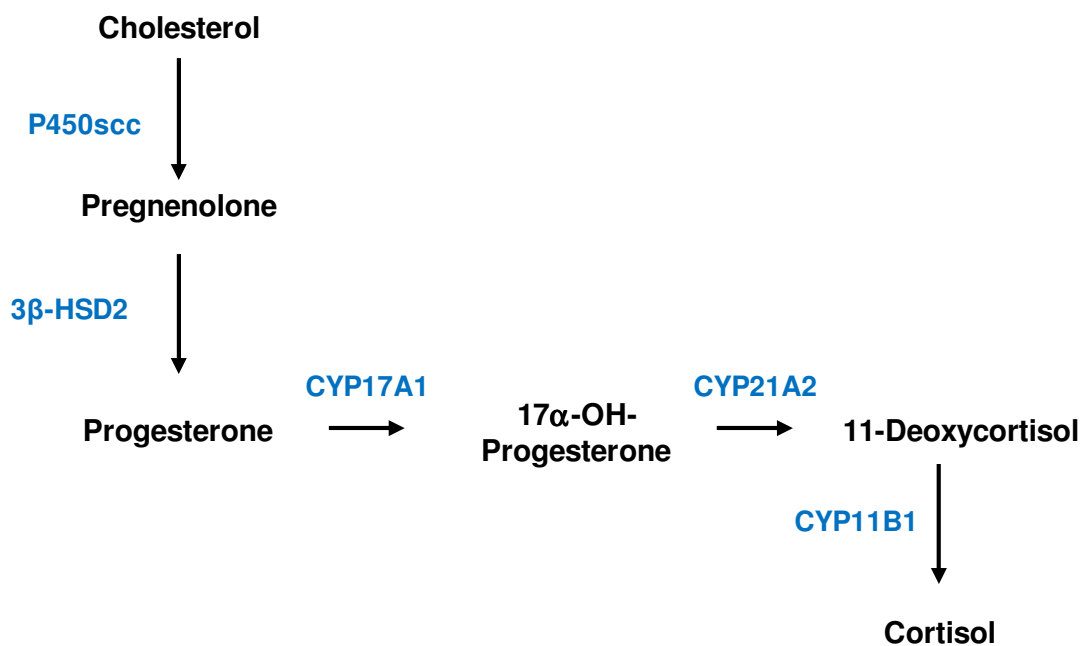
Cortisol

Figure 1-7   ***Summary of cortisol synthesis***

Cholesterol is converted to pregnenolone by P450 side chain complex (P450scc) in association with steroidogenic acute regulator protein. 3β-hydroxysteroid dehydrogenase 2 (3β-HSD2) then converts pregnenolone to progesterone which is then metabolised to 17α-hydroxyprogensterone (17α-OH-Progesterone) by 17α-Hydroxylase (CYP17A1). Further hydroxylation at carbon 21 (by 21-hydoxylase (CYP21A2)) and carbon 11 (by 11β-hydroxylase (CYP11B1)) produces cortisol.

Chapter 1

The hypothalamic pituitary adrenal (HPA) axis regulates the secretion of cortisol from the adrenal cortex (Papadimitriou and Priftis 2009). Corticotrophin releasing hormone (CRH) is released from parvocellular neurons of the paraventricular nucleus of the hypothalamus, influenced by (1) negative feedback from systemic cortisol levels, (2) cytokine signals, (3) neural signalling, including emotional responses regulated by the limbic system and (4) circadian oscillations, regulated by the suprachiasmatic nucleus (Moore and Silver 1998). CRH stimulates the release of adrenocorticotrophic hormone (ACTH) from the anterior pituitary which in turn drives cortisol synthesis in the adrenal cortex. The action of CRH is potentiated by arginine vasopressin, also produced by the hypothalamus. Circulating cortisol exerts negative feedback on the release of CRH and ACTH. The circadian secretion of cortisol ensures peak levels following a period of sleep, in preparation for a metabolically active awake period (06:00 – 08:00 am in humans). Levels then reach a nadir when returning to sleep (24:00 in humans).
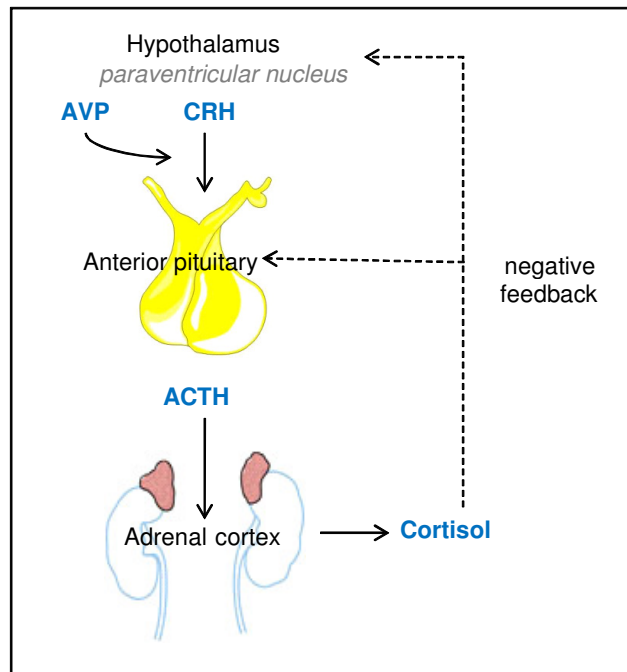
Figure 1-8 **Hypothalamic pituitary adrenal regulation of cortisol homeostasis**

Corticotropin releasing hormone (CRH), potentiated by arginine vasopressin (AVP) drives the release of adrenocorticotrophic hormone (ACTH) from the anterior pituitary gland which stimulates the synthesis and secretion of cortisol from the adrenal cortex. Cortisol, in turn, exerts negative feedback on CRH and ACTH release.

The majority of the secreted cortisol (90-95%) is transported in the blood bound to plasma protein, corticosteroid-binding globulin (CBG). Only 5-10% of cortisol remains unbound, "free", and represents the biochemically active fraction (Hammond 1990; Breuner and Orchinik 2002). Approximately 1% of free cortisol is excreted by the kidneys. Glucocorticoids have widespread effects on every system of the body and multiple mechanisms of action including potent anti-inflammatory properties, driving hepatic gluconeogenesis and regulating adipocyte differentiation (Tomlinson *et al.* 2004b).

1.8.2. Glucocorticoid signalling

Unbound glucocorticoid exerts effects via either genomic or non-genomic pathways. Genomic signalling is thought to predominate over the rapid, seconds to minutes non-genomic signalling although much controversy remain about the precise mechanisms and roles of non genomic signalling (Losel *et al.* 2003).

Glucocorticoid genomic signalling occurs predominantly via the glucocorticoid receptor (GR), but also through the mineralocorticoid receptor (MR), both members of the nuclear receptor super-family. Activation typically occurs within 15–30 minutes of ligand binding, although continuous ligand exposure can activate the receptor for days (Datson *et al.* 2008). These receptors have differing ligand binding affinity (MR has a 10-fold higher affinity for corticosteroids than the GR (Reul and de Kloet 1985), tissue localisation and effects. The GR is almost ubiquitously expressed, whereas the MR is more selectively expressed, in both epithelial and non epithelial tissues. In epithelial tissues, aldosterone predominantly binds to the MR, however, in non epithelial tissues, glucocorticoids also bind to the MR (Odermatt and Atanasov 2009). In these non epithelial tissues, such as the brain, the MR binds low concentrations (basal levels) of glucocorticoid continuously whereas the GR binds glucocorticoid only at peak circulating levels (van Steensel *et al.* 1996). The majority of glucocorticoid actions are, however, mediated via the lower affinity GR.

GR (nuclear receptor family 3, group C, class1) has two main isoforms resulting from alternate splicing of a single gene transcript (Hollenberg *et al.* 1985) although a number of other splice variant have also been described (Beck *et al.* 2009). Glucocorticoid receptor alpha (GRα) has higher affinity for exogenous dexamethasone and endogenous cortisol than for mineralocorticoids and progesterone (Beato and Klug 2000). The sparsely

expressed glucocorticoid receptor beta (GRβ) does not bind hormones evaluated thus far (Oakley *et al.* 1996) but can bind to the nuclear glucocorticoid response element and act as a dominant negative inhibitor of GC function (Bamberger *et al.* 1995). This may be important in modulating tissue sensitivity to GC's, potentially mediating GC resistance particularly in inflammatory diseases (van der Vaart and Schaaf 2009). In support of this elevated mRNA expression of GRβ has been demonstrated, in conjunction with relative glucocorticoid resistance, in patients with asthma (Goleva *et al.* 2006), ulcerative colitis (Honda *et al.* 2000), Crohn's disease (Towers *et al.* 2005) and nasal polyposis (Hamilos *et al.* 2001).

The GR is composed of a central DNA binding region (C domain), which targets the receptor to the hormone response element, and a ligand binding region (E domain), which switches the receptor's function (Beato 1989) (Figure 1-9).
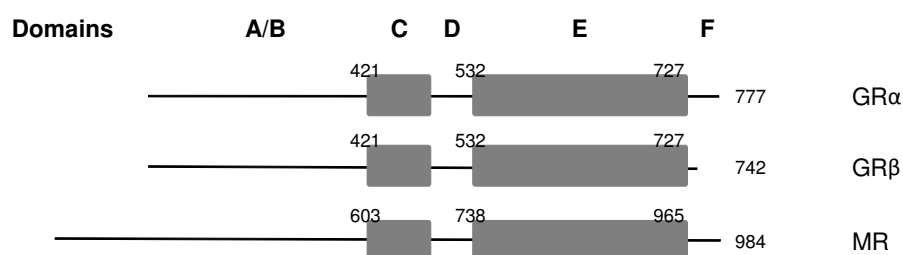
Figure 1-9 ***The domain structure of the human glucocorticoid (GR) and mineralocorticoid (MR) receptors and isoforms***

The numbers refer to amino acid positions. Domain C is the DNA binding domain, domain E the ligand binding domain. The two isoforms of the GR are identical until amino acid 727 where after they differ with GRα being longer.

The un-stimulated GR resides in the cytoplasm. The receptor is maintained in a functional but inactive state, by forming complexes with chaperones such as Heat Shock Protein

(HSP)-90KD and HSP-70 KD, as well as a multiprotein complex (p59 immunophilin, FKBP2 and p23) (Pratt and Toft 1997). Lipophilic steroid hormones pass through the plasma membrane by simple diffusion to bind the GR. A conformational change then occurs which decouples the chaperones and protein complex, exposing nuclear localisation signals which allow the GR to translocate to the nucleus. The C domain of the nuclear GR binds, as a homodimer, to a section of DNA known as the glucocorticoid response element (GRE). This process is referred to as dimerisation as the GRE has a partially pallendomic nucleotide sequence to the GR C domain. Nuclear location is stabilised by Small Ubiquitin Related Modifier-1 (SUMO-1)(Tian *et al.* 2002). Gene transcriptional activation (transactivation) then typically occurs and can be further modified following interactions with histone-modifying enzymes and cofactors (coactivators and corepressors) (Newton and Holden 2007). In addition to homodimer ligand binding, glucocorticoids can also form heterodimers by binding to both the GR and MR in tissues where the receptors co-localise, for example the hippocampus. Heterodimerisation potentially fine tunes glucocorticoid regulation (Liu *et al.* 1995).

The GR can also regulate gene transcription through binding as a monomer (Reichardt and Schutz 1998). Typically this leads to inhibition of gene transcription (transrepression). This is thought to be particularly important in driving the anti-inflammatory effects of GC's, where the effectiveness of GC's relies on their ability to reduce gene expression (Newton and Holden 2007). In this situation transrepression of the anti-inflammatory transcription factors, nuclear factor kB (NF-kB) and activator protein 1 (AP1) are thought to be important (De Bosscher *et al.* 2003) although the precise mechanism of gene repression is still debated (Glass and Ogawa 2006).

1.8.3. 11β-hydroxysteroid dehydrogenase

In peripheral tissues, corticosteroid hormone availability is regulated at a pre-receptor level by 11β-hydroxysteroid dehydrogenase (11β-HSD), a bidirectional enzyme which resides in the endoplasmic reticulum. 11β-HSD, originally identified over 50 years ago (Amelung *et al.* 1953), has two isozymes: 11β-HSD1, which acts predominantly as an oxoreductase *in vivo*, activating cortisol from cortisone, and a dehydrogenase, 11β-HSD2, which inactivates cortisol to cortisone.

1.8.3.1. 11β-HSD2

In tissues such as the kidney, salivary glands, colon and placenta, the high affinity 11β-HSD2 isozyme is abundantly expressed (Shimojo *et al.* 1997). In the renal collecting ducts 11β-HSD2 expression protects the mineralocorticoid receptor (MR) from glucocorticoid excess, mediating sodium reabsorption from the urine (Stewart and Krozowski 1999) (Figure 1-10). Inherited deficiency in 11β-HSD2 causes hyper-stimulation of the MR by cortisol with subsequent elevated sodium resorption and potassium excretion. This results in the syndrome of apparent mineralocorticoid excess which is characterised by hypertension (Stewart *et al.* 1988). Inhibitors of 11β-HSD such as liquorice, carbenoxolone and glycyrrhetinic acid have similar hypertensive effects.
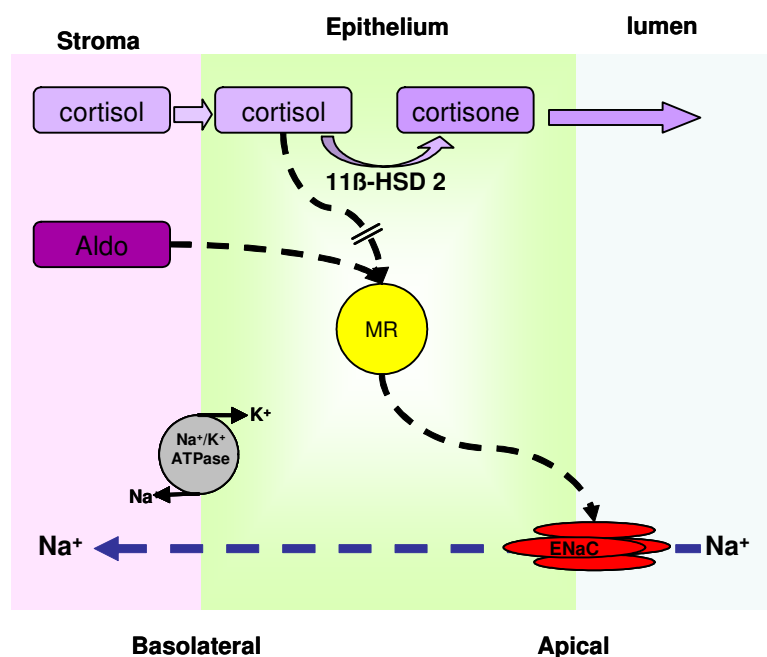
Figure 1-10 *Schematic diagram illustrating corticosteroid regulation of sodium reabsorption in the human kidney*

11β-HSD2 inactivates cortisol to cortisone allowing aldosterone (Aldo) to bind to the mineralocorticoid receptor (MR) and consequently sodium (Na$^+$) reabsorption from the urine. (ENaC, epithelial sodium channel)

1.8.3.2.   11β-HSD1

The type 1 isoform is a distinct entity to 11β-HSD2, sharing only 14% sequence homology (Stewart and Krozowski 1999). The 11β-HSD1 gene localises to Chromosome 1 (1q32.2) and is 30 Kb in size consisting of 6 exons and 5 introns (Tannin *et al.* 1991; Draper *et al.* 2002). 11β-HSD1 has a lower affinity for steroids than 11β-HSD2 and acts predominantly as an oxoreductase *in vivo* and in intact cells but can function as a dehydrogenase in cellular homogenates (Lakshmi and Monder 1988; Bujalska *et al.* 1997).

Recent work has highlighted the importance of hexose-6-phosphate dehydrogenase (H6PD) in influencing the directionality of 11β-HSD1. H6PD is an enzyme located in the

endoplasmic reticulum, which converts glucose-6-phosphate to 6-phospho-gluconolactone generating reduced nicotinamide adenine dinucleotide phosphate (NADPH) from $NADP^+$. NADPH drives 11β-HSD1 oxoreductase activity (Bujalska *et al.* 2005). There are numerous other compounds which regulate 11β-HSD1 including glucocorticoids, sex hormones, vitamin D and cytokines. The effects of these regulators are not straight forward and like the function and expression of 11β-HSD1, varies between tissues and species (Tomlinson *et al.* 2004b; Chapman and Seckl 2008). For example, oestrogen reduces rodent 11β-HSD1 activity in the liver, testis and kidney (Low *et al.* 1993; Nwe *et al.* 2000; Gomez-Sanchez *et al.* 2003) but not in the hippocampus, uterus or endometrium (Arcuri et al. 1997; Ho et al. 1999; Chapman and Seckl 2008).
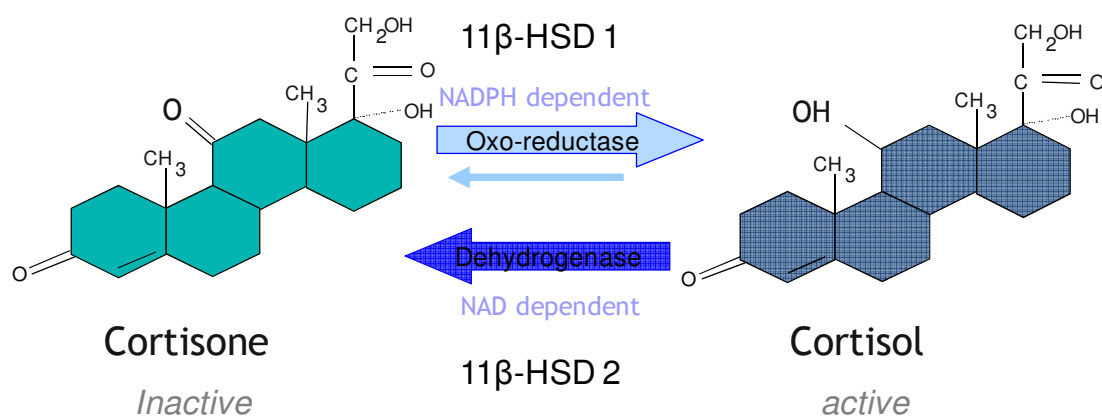
Figure 1-11   11β-hydroxysteroid dehydrogenase type 1 (11β-HSD1) metabolism

11β-HSD1 activates cortisone to cortisol while 11β-hydroxysteroid dehydrogenase type 2 (11β-HSD2) inactivates cortisol to cortisone. 11β-HSD1 activity is driven by the co factor nicotinamide adenine dinucleotide phosphate (NADPH) provided by hexose-6-phosphate dehydrogenase. NAD indicates nicotinamide adenine dinucleotide.

11β-HSD1 was originally characterised in the liver but is widely expressed in other glucocorticoid target tissues such as the adipose, lung, bone, muscle, heart, lymphoid tissues, and the central nervous system (Moisan *et al.* 1990; Whorwood *et al.* 1992; Cai *et*

al. 2001; Tomlinson *et al.* 2004b; Jang *et al.* 2009) as well as in immune cells (Thieringer *et al.* 2001; Zhang *et al.* 2005; Hardy *et al.* 2006).

In humans, the principle roles of 11β-HSD1 are in mediating hepatic gluconeogenesis and in regulating adipocyte differentiation. In humans, a defect of 11β-HSD1, known as apparent cortisone reductase deficiency (ACRD), has been described in 11 patients. These cases present with hyperandrogenism in females and precocious puberty in males as well as obesity in some cases (Phillipov *et al.* 1996; Jamieson *et al.* 1999; Tomlinson *et al.* 2004b). A recent series of four patients with ACRD were found to have inactivating mutations in H6PD, potentially preventing oxoreductase activity of 11β-HSD1 (Lavery *et al.* 2008). 11β-HSD1 knock-out mice reflect reduced glucocorticoid actions with enhanced insulin sensitivity, reduced hyperglycaemia and an improved lipid profile (Kotelevtsev *et al.* 1997; Morton *et al.* 2001). In contrast the mice over-expressing 11β-HSD1 in adipose tissue, demonstrate features of the metabolic syndrome with hyperglycaemia, dyslipideamia, hypertension and visceral obesity (Masuzaki *et al.* 2001; Masuzaki *et al.* 2003). This metabolic phenotype is less apparent in mice with hepatic over-expression of 11β-HSD1 (Paterson *et al.* 2004).

Within the CNS, research to date has focused on the importance of 11β-HSD1 in mediating mood and memory. An increase in cortisol exposure has been linked to cognitive decline and Alzheimer's disease (Meaney *et al.* 1995). In mouse models, elevated cortisol levels increase the pathological hallmarks of Alzheimer's disease (amyloid β-peptide and tau protein) (Green *et al.* 2006) and impair cognition (Issa *et al.* 1990). Adrenalectomy reduces age related cognitive decline in rats (Landfield *et al.* 1978). Glucocorticoid mediated effects on memory are thought to occur via the hippocampus, a site of high expression of 11β-HSD1, GR and MR (Moisan et al. 1990).

11β-HSD1 expression has also been demonstrated in the rodent hypothalamus, parietal cortex, anterior pituitary and cerebellum with lower levels in the brain stem, pre-optic nucleus and amygdale (Moisan *et al.* 1990; Lakshmi *et al.* 1991; Whorwood *et al.* 1995; Jellinck *et al.* 1999). In keeping with cortisol mediating memory loss through hippocampal damage, patients with Cushing's syndrome demonstrate memory deficits in the context of hippocampal shrinkage (Starkman *et al.* 1992) and primates exposed to chronic glucocorticoids develop hippocampal atrophy (Sapolsky *et al.* 1990). The role of 11β-HSD1 in mediating memory loss and hippocampal atrophy is supported by data demonstrating that inhibition of 11β-HSD1 in cultured hippocampal cells reduced glucocorticoid induced neurotoxicity (Rajan *et al.* 1996) and additionally, improved cognition in humans (Sandeep *et al.* 2004).

In line with its widespread distribution, 11β-HSD1 has multiple other physiological and pathological roles, discussion of which is beyond the limits of this thesis. This thesis will focus on the role of 11β-HSD1 in obesity and fluid dynamics.

1.8.3.3.   11β-HSD inhibitors

Most inhibitors of 11β-HSD are non specific and consequently inhibit both the type 1 and type 2 isoforms of 11β-HSD. Inhibitors include the naturally occurring bile acids (lithocholic acid and Chenodeoxycholic acid), liquorice, glycyrrhetinic acid (GE) and the anti-diabetic drug, arylsulfonamidothiazole (Tomlinson *et al.* 2004b). 11β-HSD1 inhibition, coupled with the insulin sensitising properties of arylsulfonamidothiazole derivatives highlighted the potential for 11β-HSD1 inhibitors in diabetic therapy and has lead to the development of more selective 11β-HSD1 inhibitors (Boyle and Kowalski 2009). To date, rodent studies have confirmed benefit of 11β-HSD1 inhibition in treating the metabolic syndrome (obesity, insulin resistance and hyperlipidaemia) (Lloyd *et al.*

2009) (Berthiaume *et al.* 2009) and potentially promoting weight loss (Berthiaume *et al.* 2007). Additionally, 11β-HSD1 inhibition in a mouse model of atherosclerosis, reduced aortic plaque formation (Hermanowski-Vosatka *et al.* 2005).

Study of the effect of 11β-HSD1 inhibitors in humans is currently underway (Webster *et al.* 2007; Bujalska *et al.* 2008), with a number of patents being issued in this area (Boyle and Kowalski 2009). Initial studies of the selective 11β-HSD1 inhibitor, INCB013739 (Incyte Corporation, Wilmington, DE, USA), have shown the drug to be well tolerated and safe in patients with type 2 diabetes, whilst significantly improving insulin sensitivity and lipid profiles (Rosenstock *et al.* 2009). INCB013739 is currently being studied in phase 2 clinical trials in type 2 diabetes. Although much interest has focused on the anti-metabolic and anti-obesity potential of 11β-HSD1 inhibition, there may be wider advantages in other glucocorticoid mediate conditions, including the treatment of osteoporosis, glaucoma, muscle atrophy as well as potentially enhancing wound healing and modifying the detrimental effects of elevated cortisol on cognition (Cooper *et al.* 2002; Rauz *et al.* 2003a; Sandeep *et al.* 2004; Small *et al.* 2005).

There are, however, a number of possible complications of 11β-HSD1 inhibition and consequent reduced cortisol generation (Cooper and Stewart 2009). Reduced tissue cortisol generation may induce stimulation of the HPA axis, which could in turn increase adrenal androgen secretion, potentially virilising women. Recent clinical data demonstrated that a 12 week course of the 11β-HSD1 inhibitor INCB013739, significantly elevated ACTH levels, in the context of normal salivary cortisol levels, while androgen levels only marginally increased (Rosenstock et al. 2009). There are also concerns regarding the potential pro-inflammatory actions of 11β-HSD1 inhibitors, particularly with chronic exposure (Chapman *et al.* 2009). Additionally, the clinical

impact of H6PD, a known modulator of 11β-HSD1 inhibitor efficacy, needs evaluating (Balazs *et al.* 2009).

1.9. Corticosteroids and ocular fluid dynamics

Aqueous humour (AH), a transparent fluid, circulates in the eye providing nutrition to avascular structures such as the cornea. AH is produced by the ciliary body and circulates from the posterior to the anterior segment of the eye after which it is drained via the irido-corneal angle (see section 1.9.3). The circulation of AH is vital in maintaining intraocular pressure (IOP). The dynamic balance, formed by the production and drainage of AH, is comparable to the regulation of ICP via the secretion and resorption of CSF. The ocular ciliary body is composed of two opposing apical epithelia, the pigmented epithelium (PE) and the non-pigmented epithelia (NPE) which function as a syncytium. Sodium ions are drawn across the epithelia from the PE to the NPE from where they are secreted by the $Na^+K^+ATPase$ pump. The ion shift causes an osmotic gradient which drives water into the posterior segment of the eye creating AH. This sodium dependant mechanism of fluid secretion is akin to the mechanism of CSF secretion by the embryonic-related CP (see section 1.3.2).

1.9.1. The role of corticosteroids in aqueous humour production

In the ciliary epithelium, 11β-HSD1 has been demonstrated to have a role in the control of AH production (Rauz *et al.* 2001). Cortisol generation within the ciliary body, with subsequent up-regulation of transcriptions factors such as serum and glucocorticoid regulated kinase (sgk-1) and stimulation of epithelial sodium transport, causes a net movement of Na^+ ions into the posterior chamber of the eye and production of AH.

Chapter 1

Inhibition of 11β-HSD1 at this site reduces intraocular pressure by 15-20% (Rauz *et al.* 2003a) (Figure 1-12).
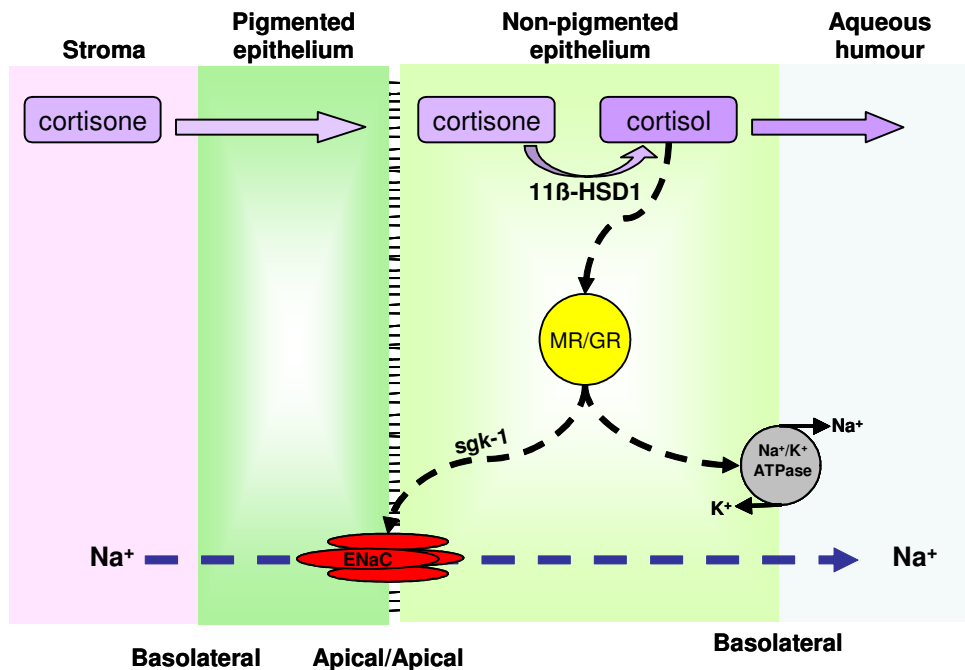
Figure 1-12 **Schematic diagram illustrating corticosteroid regulation of sodium transport in the human ocular ciliary epithelium**

> *Cortisone is converted to active cortisol in the non-pigmented epithelium by 11β-HSD1. Subsequent activation of the mineralocorticoid receptor (MR)/ glucocorticoid receptor (GR) drives epithelial sodium channels (ENaC), via the serum and glucocorticoid regulated kinase 1 (sgk-1), and Na$^+$/K$^+$ATPase pumps. The osmotic gradient consequently created across the basolateral boarder of the non-pigmented epithelium promotes aqueous humour production.*

1.9.2. Potential role of corticosteroids in CSF production

It is possible that in the CP epithelium an 11β-HSD1-dependent mechanism, akin to that occurring in the embryologically related ocular ciliary body, may regulate CSF production (Figure 1-13).
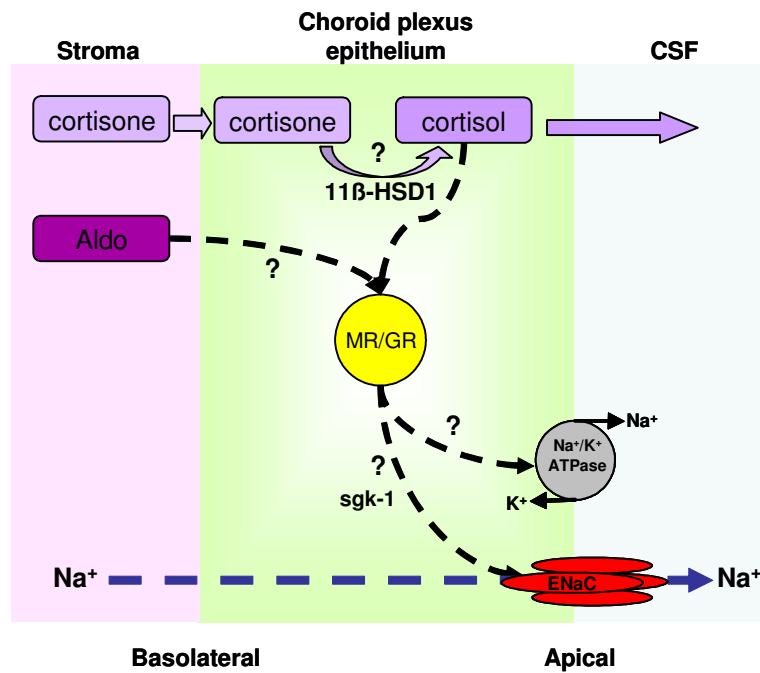
Figure 1-13 *Proposed schemata for the corticosteroid regulation of CSF secretion in the human choroid plexus epithelium*

In an analogous mechanism to the ciliary epithelium above, cortisone is converted to active cortisol in the choroid plexus epithelium by 11β-HSD1. Subsequent activation of the mineralocorticoid receptor (MR)/ glucocorticoid receptor (GR) drives epithelial sodium channels (ENaC), via the serum and glucocorticoid regulated kinase 1 (sgk-1), and $Na^+/K^+ATPase$ pumps. The osmotic gradient consequently created across the apical boarder of the choroid plexus epithelium promotes secretion of CSF.

1.9.3. The role of corticosteroids in aqueous humour drainage

In the eye, AH is drained via either the uveoscleral pathway or the trabecular meshwork (TM). The uveoscleral pathway involves fluid diffusing out of the anterior chamber of the eye between the fibres of the ciliary muscle. However, the majority of AH is thought to drain via the TM (Llobet *et al.* 2003), a reticular tissue composed of extracellular matrix. The AH then passes into Schlemm's canal and thereafter in to the aqueous veins. The TM is composed of 3 layers of connective tissue which increase in density near the canal of

Schlemm. The AH traverses the inner endothelial wall of the TM into the canal of Schlemm via intercellular or intracellular routes (Llobet et al. 2003).

Glaucoma, a condition attributed to elevated intra ocular pressure (IOP), is thought to result principally from a disruption to drainage of AH at the TM (Tan *et al.* 2006). This is likely to involve alteration of the TM extracellular matrix, increasing resistance to AH drainage. In support this , AH flow is impeded in cultured TM cells and tissue perfused with dexamethasone due to increased cross-linked actin networks in the TM (Clark *et al.* 2005). This is particularly relevant when considering the mechanism of corticosteroid induced glaucoma.

Myocilin (MYOC), also known as trabecular meshwork-induced glucocorticoid responsive protein (TIGR) is implicated in glaucoma. Mutations in the myocilin (MYOC) gene have been detected in 4% of adult onset primary open angle glaucoma (POAG) and in most cases of juvenile POAG (Wiggs *et al.* 1998). The exact mechanism of MYOC induced glaucoma is poorly defined. Dexamethasone induces the MYOC gene (Ishibashi *et al.* 2002) and TM cells are known to secrete MYOC in response to glucocorticoid stimulation. The mechanism by which MYOC obstructs ocular drainage at the TM is debated: Secreted MYOC may obstruct the TM (Polansky *et al.* 1997), the mutant MYOC may be toxic to TM cells (Zillig *et al.* 2005), myocilin may alter the function of TM cells (Jacobson *et al.* 2001), or alternatively MYOC could alters the structure of associated microfibrils in the extracellular matrix of the TM (Ueda *et al.* 2002).

In this thesis we propose that a mechanism analogous to that observed in the TM may occur in the AGT, the site of CSF drainage. Here paracrine actions of glucocorticoids on the AGT may induce MYOC expression impeding CSF drainage (Figure 1-14).
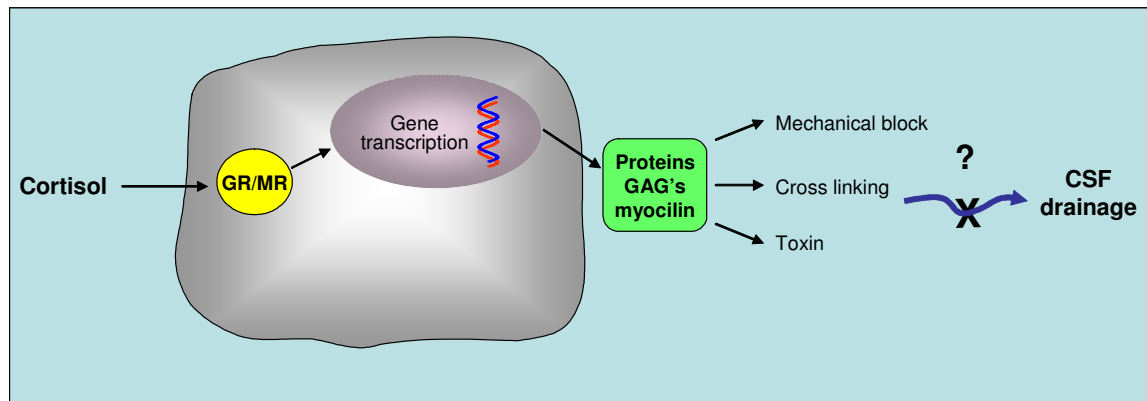
Figure 1-14 *Schematic diagram of an arachnoid granulation epithelial cell illustrating the proposed mechanism by which glucocorticoids could impede CSF drainage*

1) Secretion of soluble myocilin in the AG core could form a mechanical block. 2) Cross linking of fibres in the AG core could restrict CSF flow. 3) Toxic effects of myocilin on the AG may disrupt CSF flow. GAG's indicates glycosaminoglycans, GR/MR, the glucocorticoid /mineralocorticoid receptor.

1.10. Diagnosis of IIH

IIH is diagnosed in the setting of elevated ICP with normal neurological imaging. The diagnostic criteria were initially suggested by Dandy (Dandy 1937), but these were later revised to the modified Dandy Criteria (Smith 1985) and then to the updated modified Dandy criteria (Friedman and Jacobson 2002) (Table 1-4). These diagnostic criteria are limited as they fail to highlight the importance of universally excluding venous sinus thrombosis, using MRV or CT venography. In addition the criteria fail to define a cut-off for elevated CSF opening pressure, an issue recently addressed by Whiteley (Whiteley et al. 2006). Throughout this thesis we have used the updated modified Dandy criteria (Friedman and Jacobson 2002) to diagnose IIH with the refinements that all patients had MRV, to exclude a venous sinus thrombosis, and additionally had ICP greater than 25 cmH$_2$O.

1. If symptoms present, they may only reflect those of generalized intracranial hypertension or papilloedema.	
2. If signs present, they may only reflect those of generalized intracranial hypertension or papilledema.	
3. Documented elevated intracranial pressure measured in the lateral decubitus position.	
4. Normal CSF composition.	
5. No evidence of hydrocephalus, mass, structural, or vascular lesion on MRI or contrast-enhanced CT for typical patients, and MRI and MR venography for all others.	
6. No other cause of intracranial hypertension identified.	

Table 1-4   ***Updated modified Dandy criteria for the diagnosis of IIH***

> *Reproduced from (Friedman and Jacobson 2002). Magnetic resonance imaging (MRI), computerised tomography (CT).*

A number of other conditions can mimic IIH. These secondary forms of IIH need to be distinguished from primary IIH as the underlying pathophysiology and treatments are very different (Table 1-5). This thesis will focus solely on the primary forms of IIH.

Venous sinus thrombosis	(Karahalios *et al.* 1996)
Anaemia	(Biousse *et al.* 2003)
Obstructive sleep apnoea	(Asensio Sanchez *et al.* 2004)
Drug related (antibiotics, non–steroidal anti-inflammatory drugs, vitamin A, lithium, cimetidine)	(Ball and Clarke 2006)
Guillain Barré syndrome	(Ropper and Marmarou 1984)
CSF hyperprotinaemia or hypercullularity (spinal cord tumour, malignant meningitis)	(Ridsdale and Moseley 1978; Feldmann et al. 1986; Cremer et al. 1997)

Table 1-5   ***Secondary causes of elevated intracranial pressure***

1.11. Treatment of IIH

Effective treatment strategies in IIH have not been established and a recent Cochrane review concluded that there was insufficient evidence to determine which treatments were potentially beneficial and which were potentially harmful (Lueck and McIlwaine 2002; Lueck and McIlwaine 2005).

1.11.1.Medical therapies

Drugs used to treat IIH aim to reduce CSF production. Carbonic anhydrase inhibitors (acetazolamide) are most commonly employed although a number of other diuretics (frusemide, amiloride) can also be utilised. The clinical benefits of medical therapies have not been fully evaluated. The most recent and largest randomised controlled study to assess treatment in IIH evaluated the efficacy of acetazolamide and failed to demonstrate a beneficial effect (Ball *et al.* 2009a). Although the study was under-powered (n=50) it highlighted that acetazolamide was extremely poorly tolerated, with 48% of subjects discontinuing acetazolamide (all at doses of less than 1500 mg per day) through choice or due to side effects, typically nausea and parasthesia (Ball *et al.* 2009a). The current extensive use of acetazolamide in IIH needs to be questioned in light of these results and further studies are awaited to clarify the situation. The Neuro-Ophthalmology Research Disease Investigator Consortium (NORDIC group) began enrolment to a multi-centre US trial in January 2010, aiming to recruit 154 patients in a randomised, placebo controlled trial of acetazolamide (www.ClinicalTrials.gov identifier: NCT01003639); hopefully this study will shed further light on the area. Topiramate, is emerging as an alternative to acetazolamide (Çelebisoy *et al.* 2007) owing to multiple mechanisms of action including carbonic anhydrase inhibition (Rosenfeld 1997), weight modifying effects (reduces weight in IIH by 9.75 Kg at 12 months (Çelebisoy et al. 2007)) and efficacy in treating migraine (a frequent co morbidity in IIH).

Limited case reports have utilised therapeutic corticosteroids in IIH (Paterson *et al.* 1961; Liu *et al.* 1994; Soler *et al.* 1998) but this approach has not been substantiated (Johnston and Paterson 1974; Wall and George 1991). In fact, considerable evidence suggests a causative role for corticosteroids in the aetiology of IIH (see Table 1-3). This, coupled

with the additional problem of corticosteroid associated weight gain, has negated their use in IIH.

1.11.2. Surgical therapies

Surgical strategies are typically reserved for patients with declining visual function, despite medical therapy. Surgery may also be undertaken in cases where medical therapy is contraindicated (renal failure) or in those experiencing significant side effects from medical therapy. Occasionally, a surgical approach, typically CSF diversion, is carried out in patients with treatment refractive headaches. Surgical approaches include CSF diversion or decompressions of the optic nerve sheath with a fenestration procedure.

1.11.2.1. CSF diversion

Reducing ICP by surgical CSF diversion is performed most commonly by lumboperitoneal shunting (LPS) (87%) (Rosenberg *et al.* 1993), reflecting the less invasive nature of LPS insertion. Ventricular shunts such as ventriculoperitoneal shunts (VPS), ventriculoatrial shunts and ventriculojugular shunts are less frequently utilised (9%, 2% and 2% respectively) due to the potential difficulty of catheter placement in the small ventricles of IIH patients (Johnston *et al.* 1988; Rosenberg *et al.* 1993).

Early reports hailed CSF shunting as the treatment of choice in IIH and claimed superior efficacy to medical treatment (Johnston et al. 1988).Certainly, symptomatic improvement in IIH is invariably documented in those with functioning shunts (Eggenberger *et al.* 1996) and shunt insertion is associated with low initial morbidity (Eggenberger et al. 1996). There is, however, debate concerning the long term efficacy of CSF diversion in IIH due to shunt failure and the consequent need for revision. (Rosenberg *et al.* 1993; Burgett *et al.* 1997; Bynke *et al.* 2004). Shunt failure occurs in up to 77% of patients

(Rosenberg et al. 1993) as a consequence of shunt obstruction (65% of revisions), overdrainage and ensuing low pressure headaches (15% of revisions), and less commonly, lumbar radiculopathy, shunt migration, disconnection and abdominal discomfort (Eggenberger et al. 1996).

1.11.2.2. Optic nerve sheath fenestration

Optic nerve sheath fenestration (ONSF), reputedly first conducted by the French ophthalmologist, Louis de Wecker (1832-1906), involves an incision in the retrobulbar optic nerve dural sheath, thereby creating a fistula allowing CSF to escape the confines of the optic nerve sheath (Keltner *et al.* 1977). Decompression of the optic nerve sheath reduces ICP transmission to the optic nerve allowing papilloedema to remit and potentially reduces visual loss. The development of optic nerve sheath fibrosis following ONSF may also potentially reduce papilloedema by preventing the transmutation of CSF pressure to the optic nerve head (Davidson 1970).

The efficacy of ONSF to reduce visual loss is documented (Corbett *et al.* 1988). Delayed visual loss is, however, described up to 5 years post surgery in 10 – 32% of patients (Banta and Farris 2000). Late visual deterioration post ONSF is usually attributed to closure of the dural fistulae, however, optic nerve compression, secondary to sheath fibrosis, may also be a contributory and irreversible factor. The variable visual outcome has resulted in ONSF being rarely performed in the United Kingdom. Additionally, surgical complications are common although usually transient (diplopia, orbital apex syndrome, corneal injury, anisocoria, and traumatic optic neuropathy) (Sergott *et al.* 1990; Banta and Farris 2000). The other significant disadvantage of ONSF, is that it typically does not improve the disabling chronic headaches experienced by IIH subjects.

Chapter 1

1.11.3. Weight loss

IIH has a striking association with obesity (greater than 93%) (Glueck et al. 2005) and consequently weight loss is frequently suggested as a treatment strategy. Nevertheless, there is only one prospective weight modifying study in the published English literature, carried out over 35 years ago, which noted subjective improvement in the papilloedema in nine subjects with IIH on a low calorie rice diet (Newborg 1974). This data is supported by three further retrospective case note reviews (Johnson *et al.* 1998; Kupersmith *et al.* 1998; Wong *et al.* 2007): The first described a correlation between change in weight and resolution of papilloedema in 15 subjects and found that subjects who lost 6.2% of body weight experienced the greatest improvement in papilloedema (Johnson et al. 1998). A second, larger study (58 subjects) described improvement in the papilloedema of 74% of subjects who lost weight (mean 13.3 kg) compared to 40% of subjects whose weight remained unchanged (Kupersmith et al. 1998). The third study, a retrospective case note evaluation, demonstrated that amongst 18 patients there was a significant difference in the BMI's between those on treatment and those untreated (37.6 kg/m2 (95% confidence interval 30.6 kg/m^2 to 44.7 kg/m^2) and 30.2 kg/m^2 (95% confidence interval 25.2 kg/m^2 to 35.2 kg/m^2), respectively, p=0.05). There are also case reports describing improvement in papilloedema following weight loss achieved in the context of gastric reduction surgery (Noggle and Rodning 1986; Amaral *et al.* 1987; Sugerman *et al.* 1995; Sugerman *et al.* 1997). These studies rely on subjective measures of papilloedema and included subjects with newly diagnosed IIH, many of whom are likely to improve irrespective of any treatment given. Furthermore, these studies did not monitor concomitant changes in ICP with either weight loss or resolution of papilloedema. There is, therefore, a pressing need for dedicated, prospective research to clarify the therapeutic effect of weight reduction on IIH; this will be explored in this thesis.

1.12. Clinical evaluation in IIH

IIH is typically managed in neurology, neuro-ophthalmology, ophthalmology or less frequently in general medical clinics. In the absence of national guidelines monitoring practices vary widely.

1.12.1. Visual assessment

Visual loss in IIH can be insidious and silent (Rowe and Sarkies 1998), consequently, sensitive monitoring strategies are essential. The assessment of visual function in IIH focuses on evaluating both papilloedema severity and also the degree of visual loss.

1.12.1.1. Papilloedema

Papilloedema refers to swelling of the intra-ocular (pre-laminar) portion of the optic nerve head and in IIH occurs as a result of elevated ICP, transmitted via the CSF, in the confines of the retro-bulbar optic nerve sheath. Increased optic nerve sheath CSF pressure impedes the vascular supply (branches of the posterior ciliary artery, circle of Zinn-Haller, pial network and recurrent choroidal network (Miller *et al.* 1999)) to the optic nerve head. Vascular compromise potentiates optic nerve ischemia and visual loss.

Assessment of papilloedema is crucial in providing an indicator of disease activity and of potential visual loss. It should be noted, however, that some individuals with IIH do not develop papilloedema, despite significantly elevated ICP, likely as a result of anatomical variations in the optic nerve (Lipton and Michelson 1972; Marcelis and Silberstein 1991; Wang *et al.* 1998). The degree of papilloedema, viewed with either a direct ophthalmoscope (2-dimensional view) or via the more informative 3-dimensional views obtained from a slit lamp, is routinely recorded (Figure 1-15). Frisen grading, typically a

research tool, permits the classification of developing papilloedema but is limited by subjectivity and additionally lacks discrimination, particularly in resolving disc swelling (Frisen 1982) (Table 1-6).

Stage	Signs				
	Nasal blur	**Temporal blur**	**Peripheral TOVS***	**Central TOVS* or filled optic cup**	**Smooth dome**
0	-	-	-	-	-
1	+	-	-	-	-
2	+	+	-	-	-
3	+	+	+	-	-
4	+	+	+	+	-
5	+	+	±	±	+

Table 1-6   Frisen Grade

*The optic disc is grade according to appearance. *TOVS indicates total obscuration of major vessel segment(s) by swollen axons. + indicates present, - indicates absent.   Grading described by Frisen L.   JNNP 1982;45:13-18.*
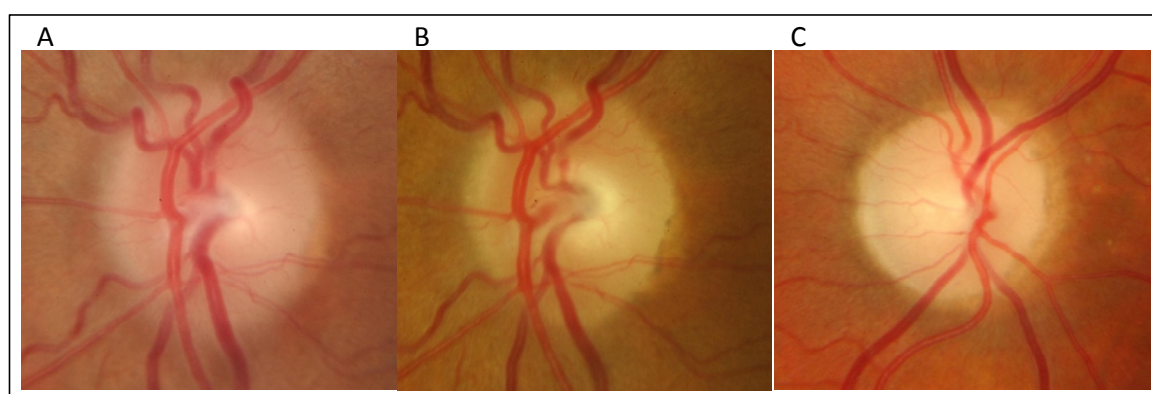
Figure 1-15   Fundus photographs

(A) Papilloedema, Frisen Grade 2, (B) resolved papilloedema in the same patient and (C) optic disc pallor (optic atrophy) a sequelae of significantly elevated ICP and subsequent optic nerve head ischaemia.

1.12.1.1.1   Objective assessment of papilloedema

Although direct visualisation of the optic disc to assess papilloedema is typical in clinical practice, the subjective assessment lacks accuracy, reproducibility and sensitivity. New techniques are emerging in visual science, primarily designed to quantify optic atrophy in

condition such as glaucoma. These techniques may also have a role in quantifying papilloedema and their role is currently being evaluated in the literature.

1.12.1.1.2   *Optical Coherence Tomography*

Optical coherence tomography (OCT) is a relatively new technique, developed in 1990, with the first *in vivo* images published in 1993 (Fercher *et al.* 1993). The echo based imaging technique utilises a broad band-width light source to penetrate tissue; the majority of the light is scattered, but a proportion will be reflected off the structure of interest. The depth and intensity of the reflected (coherent) light is measured by an optical interferometer. This enables real time, 3-dimensional imaged acquisition that has micrometer resolution (5–7 μm (Frohman *et al.* 2008)) which mirrors histological preparations (Rebolleda and Munoz-Negrete 2009). The technique is non invasive, non damaging and unlike many other imaging techniques does not utilise ionizing radiation. The depth of penetration of the light source (2 mm), limits the application of OCT to deep structures. The optical translucency of the eye, however, makes this an ideal structure to image (retinal nerve fibre layer (RNFL) thickness, macula, fovea and optic nerve).

RNFL analysis involves assessment of the peripapillary RNFL thickness using a circumferential scan of the intra-ocular optic nerve head (Figure 1-16A). The quantitative values obtained can be compared to normal population values, analysed according to disc sectors or used for monitoring progression over a time course of scans. OCT is predominantly used to accurately measure declining RNFL thickness in conditions such as glaucoma, Leber's hereditary optic neuropathy, traumatic optic neuropathy and more recently in multiple sclerosis associated optic neuritis (Medeiros *et al.* 2003; Medeiros *et al.* 2004; Barboni *et al.* 2005; Siger *et al.* 2008). Reports are however emerging, detailing the use of OCT to measure elevation (caused by axonal distension and oedema) of the

RNFL as seen in papilloedema (Savini *et al.* 2006). RNFL OCT may have a role in monitoring IIH papilloedema, as demonstrated in a study of three children with IIH (Sanchez-Tocino *et al.* 2006), as well as in an adult population (n=22) with mild papilloedema (Rebolleda and Munoz-Negrete 2009). In the latter study, RNFL was found to correlate with automated visual field perimetry. Caution however, should be employed when interpreting reductions in RNFL in IIH as this could represent either improving papilloedema or progression to optic atrophy. In these cases a discrepancy between RNFL and the automated perimetry should alert the physician to the possibility of developing optic atrophy.
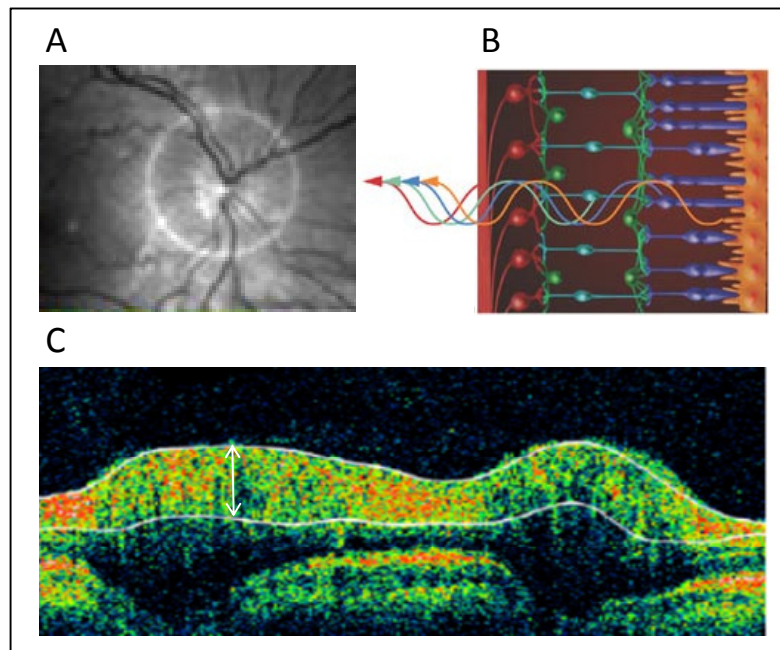
Figure 1-16   Optical coherence tomography (OCT) imaging

(A) OCT fundus image illustrating the circumferential marker for retinal nerve fiber layer (RNFL) measurement. (B) Schematic diagram illustrating light, reflected from the retina layers, which is then recorded by the optical interferometer (adapted from Frohman EM et al. Nature Clinical Practice Neurology 2008; 4: 664-675. (C) Cross sectional OCT image obtained, the arrow marks the diameter of the RNFL.

Chapter 1

1.12.1.1.3   Ultrasonography

Although the principles of USG were noted as far back as 1793 in Spallanzani's study of bat echo-navigation, it was not until the 1960's that the medical application was appreciated and images of the optic nerve obtained (Baum and Greenwood 1960). This echo technique utilised the reflection of sound waves to obtain 2-dimension, non-invasive, topographic images. Orbital USG has numerous application including evaluating ocular tumours, inflammation, vascular malformations, extra-ocular muscles, drusen and the optic nerve. Accurate optic nerve imaging has been developed (Beatty *et al.* 1998b; Beatty *et al.* 1998a) and studies are now emerging demonstrating the use of USG in IIH.

USG can facilitate the differentiation of pseudo-papilloedema (e.g. drusen) from true papilloedema in IIH subjects (Khonsari *et al.* 2009). There are also reports of ultrasonographic evaluation of papilloedema in IIH measuring either intra-ocular optic disc height (Tamburrelli *et al.* 2000) or the retro-bulbar optic nerve sheath diameter (NSD) (Stone 2009). Optic disc height is typically measured in both a horizontal and vertical plane using a high resolution real-time brightness scan (B-scan) at 10 - 20Hz pulse frequency (Tamburrelli et al. 2000) (Figure 1-17A). The optic nerve is imaged in cross-section in the retro-bulbar region, at the insertion into the optic globe. The maximal inter-pial diameter of the nerve sheath is measured with a 10Hz B-scan (Figure 1-17B). NSD is not a direct measure of papilloedema: The CSF filled subarachnoid space of the optic nerve sheath distends as a result of elevated ICP (Watanabe *et al.* 2008).

A   **B**

20MHz B-scan   *10MHz B-scan*
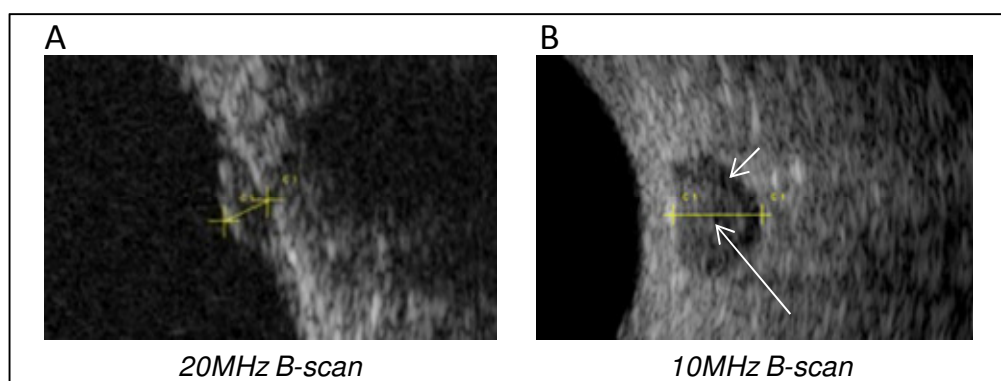
Figure 1-17   ***Ultrasonography of the optic nerve***

(A) Optic disc elevation, callipers measure from the maximal disc height to the lamina cribrosa, (B) cross section through the optic nerve (long arrow) with the callipers marking the maximal pial diameter, the short arrow marks the hypodense signal from the CSF.

In this thesis we will use OCT and USG to quantify papilloedema in IIH.

1.12.1.2.   Assessment of visual loss

There is considerable variability in the reported incidence of visual loss in IIH (Table 1-7). Current figures on the incidence of blindness in IIH are expected following the monitoring program established by The British Ophthalmic Surveillance Unit in conjunction with the Royal College of Ophthalmologists (initiated October 2005).

Number of patients in study	Number with visual loss	Study type	Author
24	1 (4%)	Prospective	(Sorensen *et al.* 1988)
34	4 (8%)	Retrospective	(Boddie *et al.* 1974)
50	5 (10%)	Prospective	(Wall and George 1991)
35	6 (17%)	Prospective	(Rowe and Sarkies 1998)
81	16 (20%)	Prospective	(Radhakrishnan et al. 1993)
57	14 (25%)	Retrospective	(Corbett et al. 1982)
68	21 (31%)	Retrospective	(Orcutt *et al.* 1984)

Table 1-7   ***Reported visual loss in IIH. Adapted from (Ball and Clarke 2006)***

Chapter 1

Despite the uncertainty of the prevalence of blindness in IIH, this area of potential morbidity is the primary focus in IIH management.

1.12.1.2.1   Visual acuity

Visual acuity, defined as spatial resolving capacity, describes the minimum angle of detail which can be resolved (Westheimer 2001) and is the most frequently used test of visual function in research and clinical practice. Acuity testing not only guides refraction but is also performed to screen and monitor disease with consequent implications for an individual's driving and occupational ability. Visual acuity testing is fundamental in monitoring IIH patients and guiding management decision.

Visual acuity testing, originally described 140 years ago (Snellen 1862) utilises charts of optotypes (symbols) commonly letters (Figure 1-18A). Variations of the original Snellen chart are widely utilised but subject to criticisms, as too many variables affect the ability to discern the optotypes. On the Snellen chart, letter selection and style affects the ability to recognise an optotype (Woodruff 1947). The number of letters per row increases in successive rows of the chart. This increases the difficulty in reading the optotypes, rather than continuing with an equivalent task further down the chart (Flom *et al.* 1963). A further consequence of varying the number of letters per row, is that missing a letter at the bottom of the chart does not have the same significance as missing a letter near the top of the chart (Williams *et al.* 2008). Finally the decrease in letter size in successive rows is not proportional (the scale is irregular and arbitrary) and this limits subsequent statistical analysis, and risks over or underestimating visual acuity (McGraw *et al.* 1995).

Alternatives to the Snellen chart have been developed to compensate for these limitations. The logarithm of the minimum angle of resolution (LogMAR) chart was designed to

ensure that the only factor which changed down the chart was the size of the letter, which

progressed logarithmically (Figure 1-18B). The letter legibility, number of letters per row,

distance between-letters and between rows was standardised (Bailey and Lovie 1976).

Each letter on the LogMAR chart is, therefore, equally weighed and equivalent to 0.02.

LogMAR charts are accurate and reliable both in clinical practice and in research (Elliott

and Sheridan 1988; Sheedy 1993.). Standardisation of test conditions (distance and

luminescence) is however, vital (Pandit 1994). The correction of the eye, whether

unaided, best corrected (accurate refraction correction used), or habitual (under everyday

conditions, with or without optical correction), must also be consistent.
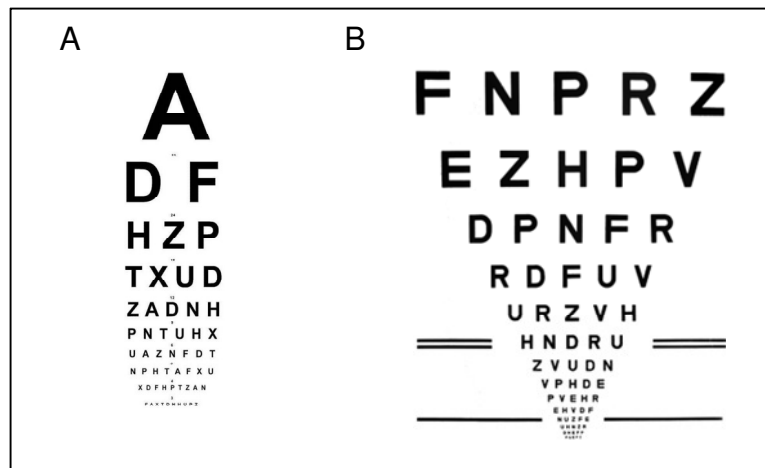
Figure 1-18 *Visual acuity measurement*

Snellen chart (A), LogMAR chart (B).

1.12.1.2.2   Colour vision

Numerous methods exist to detect deficiencies in colour vision. The most frequently used

in clinical practice are pseudoisochromatic plates. These plates consist of multiple

coloured dots of varying sizes and brightness which, in the context of normal colour

vision, display letters, numbers or shapes. Ishihara plates, which consist of either, 38, 24

or 14 plates, are commonly used and provide a quick and reliable screening test of colour

vision abnormalities. There are, however, limitations to using pseudoisochromatic plates. Principally they lack sensitivity in detecting, classifying and quantifying acquired colour vision deficiencies, particularly in the yellow-blue range.

The Farnsworth Munsell 100 Hue test permits the classification of colour deficiency and grades severity (Farnsworth 1957). The test consists of 85 different coloured caps, presented in four boxes, which the patient arranges in order of increasing hue between two reference caps. The pattern of errors varies depending on the type of colour vision defect. Standardised testing luminescence must be maintained throughout repeated assessments. A total error score can be calculated as a measure of accuracy, with the greater the number of misjudgements equating to a higher score. As colour vision varies with age, being worst at extreme ages and peaking at 19 years, the total error score is interpreted with data from a normal age matched population (Kinnear and Sahraie 2002).

Colour vision is affected in IIH (Nichols *et al.* 1997), and assessment, typically with Ishihara plates, is a standard component of visual assessment in IIH. The extent and characteristics of colour deficiency in IIH are not well described.

Figure 1-19   Farnsworth Munsell 100 Hue colour assessment

Subjects arrange randomly assorted colour discs by increasing Hue.

1.12.1.2.3   Perimetry

Focal perimetry is a mandatory component in the assessment of IIH serving to detect early abnormalities, reveal visual loss not apparent to the patient and to monitor progression and remission of visual field loss. The principle of perimetry, performed initially 150 years ago, is to determine the detection sensitivity of a target, which can vary in size and brightness, in different locations of the visual field. The loss of detection of the target indicates dysfunction in the visual pathway.

The visual field can be assessed using manual kinetic perimetry or automated perimetry. Manual perimetry (Goldman perimetry), relies on a perimetrist to move a target from an area of absent vision to a position that can be seen. This creates a map of the visual field and highlights areas that cannot be seen. The technique has the advantage of permitting a customised test, which can explore sectors of concern, whilst the technician can encourage the patient to optimise concentration. The technique is, however, time

consuming and dependant on the training of the perimetrist. Additionally, the resulting visual field map is not quantitative, merely descriptive.

Automated perimetry, such as Humphrey visual field (HVF) analysis, utilises a computer program to create a standard test procedure with defined conditions (target size and luminescence). The repeated testing of set locations within the visual field permits the assessment of false positive (trigger-happy) and false negative (potentially inattentive patient) responses. HVF analysis is sensitive and specific, and also statistically quantifiable, and consequently the preferred method in a research setting. The test is, however, time consuming, fatiguing for patients and lacks flexibility to evaluate complicated patients.

The HVF generates a numerical result which indicates the threshold of vision (the minimum intensity of light that can be detected) at each point in the visual field. This is displayed graphically (Figure 1-20A) as well as in grey scale, with black indicating that no stimulus was perceived (Figure 1-20B). The extent that the field deviates from an age matched control population is illustrated on the total deviation plot (Figure 1-20C). The mean deviation (MD), calculated from the total deviation, summarises the extent the field deviates from normal (Heijl *et al.* 1987). Negative values indicate an abnormal field. The pattern deviation takes into account any global reduction in visual sensitivity (Figure 1-20D) and, after comparison to an age matched population, the pattern standard deviation (PSD) is calculated.

Visual field analysis if frequently abnormal in IIH patients; 88% have abnormal Goldman perimetry and 92% abnormal HVF analysis at presentation (Wall and George 1991). Characteristic visual field changes in IIH patients includes enlargement of the blind spot and peripheral field constriction, often with nasal loss or arcuate deficits (Rowe and

Sarkies 1998; Galvin and Van Stavern 2004). The severity of papilloedema, however, does not correlate with the visual field loss (Wall and George 1991).

(A) Numerical result

```
            13  14 │ 18  24
         5  19  23 │ 12  27  24
      13  16  26  15 │ 26  26  <0  25
   17  19  28  30  28 │ 29  27   9  <0
30 ─┼──────────────────┼── △ ──────── ┼ 30
   14  18  23  30  29 │ 30  26   0   9
      17  28  28  30 │ 30  31  25  <0
         26  25  28 │ 26  29  27
            22  23 │ 23  25
```

(B) Greyscale diagram

(C) Total deviation

```
              -16 -15 │-11 -4
          -25 -12 -9  │-19 -3  -6
      -18 -15 -7 -18  │-7  -6 -33 -6
  -12 -12 -5  -4  -6  │-4  -6     -33
 ─────────────────────┼──────────────
  -15 -13 -9  -4  -5  │-4  -7     -22
     -14 -4  -6  -4   │-4  -2  -7 -33
          -5  -7  -5  │-6  -3  -5
              -8  -8  │-8  -6
```

(D) Pattern deviation

```
              -12 -11 │-7   0
          -21 -8  -5  │-15  1  -2
      -14 -11 -3 -14  │-3  -2 -29 -2
   -8  -8  -1   0  -2 │ 0  -2     -29
 ─────────────────────┼──────────────
  -11 -9  -5   0  -1  │ 0  -3     -18
     -10  0  -2   0   │ 0   2  -3 -29
          -1  -3  -1  │-2   1  -1
              -4  -4  │-4  -2
```

Outside normal limits
MD   -9.29 p < 0.5%
PSD   8.01 p < 0.5%

Figure 1-20   Humphrey visual field, Central 24-2 Threshold Test

> *An abnormal test from the right eye of an IIH patient showing an enlarged blind spot with superior nasal visual field loss. The abbreviated analysis illustrates the (A) numerical results, (B) the greyscale diagram, (C) the total deviation, from which the mean deviation (MD) is calculated and (D) the pattern deviation, from which the pattern standard deviation (PSD) is calculated.*

1.12.1.2.4 Contrast sensitivity

The threshold to discern low contrast optotypes can be affected by disturbance in the visual system. Deficits in contrast sensitivity may highlight pathology in the visual system before abnormalities are demonstrated by alternative tests such as visual acuity testing. One method of assessing contrast sensitivity is the Pelli Robson chart. The chart displays rows of 6 letters with letter triplets having equivalent contrast. Contrast declines in successive rows (Figure 1-21). As this chart is in a similar format to a visual acuity chart it is simple for both patients and doctors to use and is also highly reproducible (Miller et al. 1999).
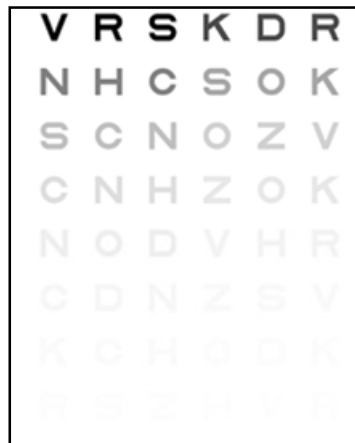
Figure 1-21   The Pelli Robson contrast sensitivity chart.

Contrast sensitivity has not been studied in detail in IIH although earlier studies have not found it to be as sensitive as HVF (Rowe and Sarkies 1998). Pelli Robson contrast sensitivity is, however, a sensitive method to identify visual dysfunction in other conditions characterised by optic nerve dysfunction such as multiple sclerosis (Balcer *et al.* 2003).

Chapter 1

1.12.2. Headache assessment

Headache is a significant cause of morbidity in IIH, affecting 68 – 97% of individuals, and frequently precipitates the initial referral to medical services (Durcan et al. 1988; Wall and George 1991; Radhakrishnan et al. 1993; Kesler and Gadoth 2001; Friedman and Rausch 2002).

Headache in IIH has been classified by the International Headache Society (IHS) (Evers 2004) (Table 1-8). The characteristics of IIH headaches are, however, more complex than this definition. Although often described as a constant headache, up to 52% of IIH headaches are episodic (Gonzalez-Hernandez *et al.* 2009). Additionally, the headache frequently has characteristics attributed to other headache types; episodic tension type headache (37%), migraine (24 - 40%) and chronic tension type headache (12%). More than one headache type is also recognised to occur in IIH patients (23% of subjects) (Friedman and Rausch 2002). It is also apparent that headaches can continue in patients despite resolving papilloedema and normalisation of the ICP (68% of subjects) (Friedman and Rausch 2002). Medication overuse may further confuse the headache phenotype. Headaches in IIH are, therefore, typically complicated and consequently challenging to monitor and treat.

There are no guidelines on headache monitoring in IIH and this area is frequently neglected despite the pain predictably representing the primary concern for the patients. There are no biological markers for headache and consequently monitoring the clinical course relies on an accurate history. Headache diaries and questionnaires, although not designed for IIH patients, are used to diagnose, quantify and characterise headaches and additionally minimise recall bias. Diary duration varies, but typically records headache frequency, severity, duration and analgesics used (Nappi *et al.* 2006). Headache diaries

have also been used as outcome measures in migraine drug trials to monitor efficacy (Sandrini *et al.* 2002; Brandes *et al.* 2004).

Numerous headache questionnaires have also been developed. The Headache Impact Test-6 (HIT-6) measures headache disability (Kosinski *et al.* 2003) and consists of 6 items which explore social functioning, role functioning, vitality, cognitive functioning, and psychological distress (see appendix 7.2). The resultant score ranges from 36-78 (interpretation in appendix, section 7.3). The questionnaire is self-administered, quick to perform (takes approximately 2 minutes to complete), validated, reliable and repeatable (Pryse-Phillips 2002; Bayliss *et al.* 2003). We will be utilising headache diaries and HIT-6 to monitor patients with IIH in this thesis.

Headache attributed to IIH
IHS 7.1.1.

A.	Progressive headache with at least one of the following characteristics and fulfilling criteria C and D:
a)	daily occurrence
b)	diffuse and/or constant (non-pulsating) pain
c)	aggravated by coughing or straining
B.	Intracranial hypertension fulfilling the following criteria:
1.	alert patient with neurological examination that either is normal or demonstrates any of the following abnormalities:
	a) papilloedema
	b) enlarged blind spot
	c) visual field defect (progressive if untreated)
	d) sixth nerve palsy
2.	increased CSF pressure (>200 mm H_2O in the non-obese, >250 mm H_2O in the obese) measured by lumbar puncture in the recumbent position or by epidural or intraventricular pressure monitoring
3.	normal CSF chemistry (low CSF protein is acceptable) and cellularity
4.	intracranial diseases (including venous sinus thrombosis) ruled out by appropriate investigations
5.	no metabolic, toxic or hormonal cause of intracranial hypertension
C.	Headache develops in close temporal relation to increased intracranial pressure
d)	Headache improves after withdrawal of CSF to reduce pressure to 120-170 mm H_2O and resolves within 72 hours of persistent normalisation of intracranial pressure

Table 1-8   IIH headache classification from the International Headache Society

1.13. Biomarkers in IIH

The diagnosis of IIH is not always straightforward (see section 1.10) and the pathogenesis remains unknown (see section 1.4). Biomarkers have the potential to facilitate diagnosis, predict prognosis, monitor disease progression and impart information on disease causality. Accurate biomarkers would, therefore, have clear advantages in the management IIH. The National Institute of Health define a biomarker as "a characteristic that is objectively measured and evaluated as an indicator of normal biological processes, pathogenic processes, or pharmacological responses to a therapeutic intervention" (2001).

Chapter 1

As a measure of disease process, biomarkers have roles in both patient care and in clinical trials. The latter are referred to as surrogate endpoints (Feigin 2004). The ideal biomarker should reflect pathogenesis and be validated in pathologically confirmed cases, as clinical diagnosis can be inaccurate in up to 15-20% of neurological patients (Stacy and Jankovic 1992). Additionally, a clinically useful biomarker must be minimally invasive, cheap, sensitive, reproducible and rapid.

The establishment of unique biomarkers for conditions affecting the brain and central nervous system have proven problematic. Traditionally, biomarkers have evolved from knowledge of the underlying disease aetiology. The pathogenesis of many neurological conditions is not fully appreciated and biomarkers have therefore remained elusive. Even in conditions where knowledge of the underlying pathology is advancing, such as MS, there is a lack of reliable biomarkers. No biomarkers have currently been identified in IIH and this likely reflects the very limited understanding of the pathogenesis.

1.13.1. Principles of metabolomics

Metabolomics is a powerful technology which has the ability to determine metabolic variations and their response to disease processes. The technique involves the quantification of the metabolic complement in a biological sample (Griffin and Shockcor 2004). As metabolites reflect both gene transcription and environmental factors, the generation of metabolite profiles are believed to have distinct advantages over genomics and proteomics in characterising biological systems (Griffin and Shockcor 2004). Metabolomics captures a snap-shot of metabolism and therefore provides information on current disease activity, rather than being informative of up-stream regulatory processes as in genomics.

Chapter 1

Although in its infancy, metabolomics has already been demonstrated to have a number of clinical applications. Ex-vivo analysis of tumour biopsies can differentiate malignant tissue from normal tissue (Griffin and Kauppinen 2007; Yang *et al.* 2007). Metabolite profiles from the serum of patients with ischemic heart disease can distinguish varying degrees of coronary artery stenosis (Brindle *et al.* 2002). Urinary metabolite profiles are able to identify patients with renal cell carcinoma from healthy controls (Kind *et al.* 2007), and partially separate MS patients from control subjects (sensitivity 65%) (t Hart *et al.* 2003).

The feasibility of CSF metabolite analysis, using NMR spectroscopy, was initially demonstrated over 20 years ago (Shinar and Navon 1986) (Petroff *et al.* 1986) and recognition that CSF metabolites were related to clinical conditions (Bell *et al.* 1987) paved the way for further research in this area (Lutz *et al.* 1996; Lutz *et al.* 1998; Lutz *et al.* 2007). Of particular relevance to the clinical application of CSF metabolomics was the identification of metabolites in MS, degenerative dementia, inflammatory spinal disease, vitamin B12 deficiency and in inborn errors of metabolism (Nicoli *et al.* 1996) (Koschorek *et al.* 1993) (Commodari *et al.* 1991) (Wevers *et al.* 1995). More recently, studies of CSF metabolite profiles have demonstrated differentiation of schizophrenia from healthy controls (Holmes *et al.* 2006a) and separation of viral, tubercular and bacterial meningitis (Subramanian *et al.* 2005). Metabolite profiles have also discriminated sporadic Parkinson's disease from that associated with the familial LRRK2 mutation (Johansen 2007), and Parkinson's disease patients from normal ageing controls (Bogdanov *et al.* 2008).

It is likely, therefore, that pathologically distinct diseases are characterised by unique metabolite profiles or fingerprints. In IIH, metabolite profiles may potentially be useful as

biomarkers and the interpretation of individual metabolite variance may also give clues to underlying pathology.

1.13.2. Metabolomic techniques

A number of techniques can be used to measure metabolites (Table 1-9), and these will be discussed in the following section.

Technique	Description	Advantage	Disadvantage
Gas chromatography/ mass spectrometry (GC/MS)	Uses gas chromatography to separate metabolites prior to mass spectrometry to identify metabolites.	Inexpensive, reproducible and highly sensitive.	Sample preparation time consuming; not all compounds suitable for GC/MS.
Liquid chromatography/ mass spectrometry	Similar to GC/MS except separation occurs during liquid chromatography.	Sample preparation less time consuming than GC/MS. Similar sensitivity to GC/MS.	More expensive than GC/MS and less reproducible.
Metabolite array	A 96-well plate is used with over 700 different assay mixtures, e.g. phenotyping Escherichia coli.	Useful screening tool when manufactured for a particular situation.	Number of metabolites measured is limited by space on the chip. Cannot screen for unknown metabolites.
Nuclear Magnetic resonance (NMR) spectroscopy	Used to screen biofluids and whole tissue *in vivo* or *ex vivo*	Automated, rapid and reproducible. Metabolite quantification and identification possible.	Lower sensitivity than mass spectrometry. Co-resonant metabolites can be difficult to quantify.
Fourier-transform infrared spectrometry	Uses vibrational frequencies of metabolites to produce spectra.	Cheap and can process a high throughput of samples.	Very difficult to identify metabolites. Poor at distinguishing metabolites within a class of compounds.
Raman spectroscopy	Extension of FT-IR relying on light scattering following irradiation with a laser.	Water only has a weak Raman spectra thus enabling observation of functional groups.	Very difficult to identify metabolites. Poor at distinguishing metabolites within a class of compounds.

Table 1-9   *Methods used in metabolite analysis.*

Adapted from Griffin 2004 (Griffin and Shockcor 2004).

1.13.2.1. Proton nuclear magnetic resonance

The Nobel Prize winning discovery of nuclear magnetic resonance (NMR) was made in 1946 (Purcell 1946) and has since been developed into many scientific fields including biochemistry and medicine. NMR relies on the principle that nuclei or electrons have spin, i.e. behave like small bar magnets, and will align themselves when placed in a magnetic field. If pulsed with radiofrequency, the aligned particles will absorb energy and resonate. Particles resonate at different frequencies depending on their atomic mass and this can provide information on the structure of the molecule (Figure 1-22).
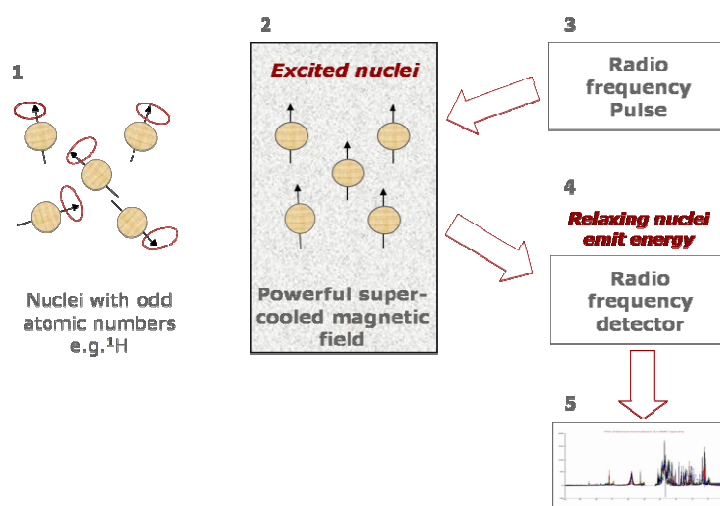
Figure 1-22   *Schematic diagram illustrating proton NMR Spectroscopy*

   Proton atoms in metabolites have spin properties (1). The particles align in a strong magnetic field (2). Radiofrequency pulses excite the particles which then resonate (3). Energy emitted (4) from the resonating particles is recorded (5).

One–dimensional (1D) Proton NMR spectroscopy is an ideal technique to assess metabolites in biofluids as it is automated and rapid: spectra are acquired in 10 minutes. After initial start up costs, samples are cheap to process, potentially enabling high throughput processing. The technique is reproducible (Lindon *et al.* 2003) and sensitive; a

cryoprobe enables the detection of metabolites in the nanogram range (Holmes *et al.* 2006b). NMR is also non destructive, allowing samples to be reused and importantly, relies on only a small sample volume (300μl), to measure multiple metabolites. If used with a reference sample, the technique can also be quantitative.

There are, however, a number of potential limitations associated with 1D ^{1}H NMR as a result of spectral peak congestion, particularly in the lower region on the spectrum (0.7 – 4.7 ppm) (Foxall *et al.* 1993). Spectral congestion, or chemical noise, occurs where multiple resonances overlap. Low concentration metabolites can potentially be obscured due to their overlap with other more prominent metabolites and thereby hinder metabolite identification. With the use of higher strength magnets (500-600 MHz), and thus the resolution of increasing numbers of metabolites, this problem is enhanced. Signal assignment is also problematic when evaluating metabolites of similar resonances, as their resonances may superimpose. The resonance congestion in 1D spectrum, therefore, limits the accuracy of metabolite identification and impairs the pattern recognition multivariate analysis.

Two-dimensional (2D) J-resolved spectroscopy (JRES) has developed to potentially ameliorate these issues. 2D JRES separates chemical shifts and the spin-spin coupling data on to different axis. The topographical "contour map" of 2D data is then projected in skyline, the appearances of which are much less congested than 1D spectrum. 2D spectral acquisition is, however, approximately three times as long as that needed for 1D spectroscopy. Additionally, interfering peaks composed of metabolites with coupled signals can be created which are problematic to interpret (Foxall et al. 1993). The analysis of proteinaceous biofluids can be difficult using 1D ^{1}H NMR, as protein signals can dominate the spectra due to their short transverse (T_2) relaxation time. 2D JRES attenuates

the protein resonances by editing the T_2 relaxation during the JRES pulse sequences (Viant 2003). Eliminating the protein signal and thus simplifying the spectra, can facilitate metabolite differentiation and identification (Foxall et al. 1993), however, potentially valuable information from protein bound metabolite may be lost.

1.13.2.2.   Gas chromatography / mass spectrometry

Gas chromatography / mass spectrometry (GC/MS) was originally used to identify metabolites in plant extracts, but since 1966 has also been used to diagnose metabolic disorders such as inborn errors in metabolism (Tanaka *et al.* 1966). The analysis of urine samples enables identification of organic acids, amino acids and glucose derivatives. The technique uses gas chromatography to separate the metabolite components of a mixture. Subsequently, mass spectrometry ionises the metabolites which are then separated according to their mass to charge ratio and are thus identified. GC/MS is more sensitive than NMR and has the advantage of potentially using a very small volume of sample (100μl), however, as metabolites cannot be uniformly ionised, metabolite identification is restricted. Additionally, sample preparation and processing are time consuming, slowing sample throughput.

Analysis of steroid pathways by urine GC/MS identifies and quantifies over 55 different metabolites or ratios of metabolites. The technique can provide an index of cortisol secretion and global 11β-HSD activity (Shackleton *et al.* 2008), estimated from renal excretion of cortisol metabolites. Assessment of 11β-HSD1 activity is made via the ratio of cortisol to cortisone metabolites i.e. tetrahydrocortisol (THF) + 5αTHF: tetrahydrocortisone (THE) ratio, and 11β-HSD2 activity is estimated from measuring urinary free cortisol: urinary free cortisone ratio (Figure 1-23). Analysis of other steroid

metabolites enables identification of alternative aberrant steroid metabolic pathways and will be discussed in more detail in section 5.3.2.1.
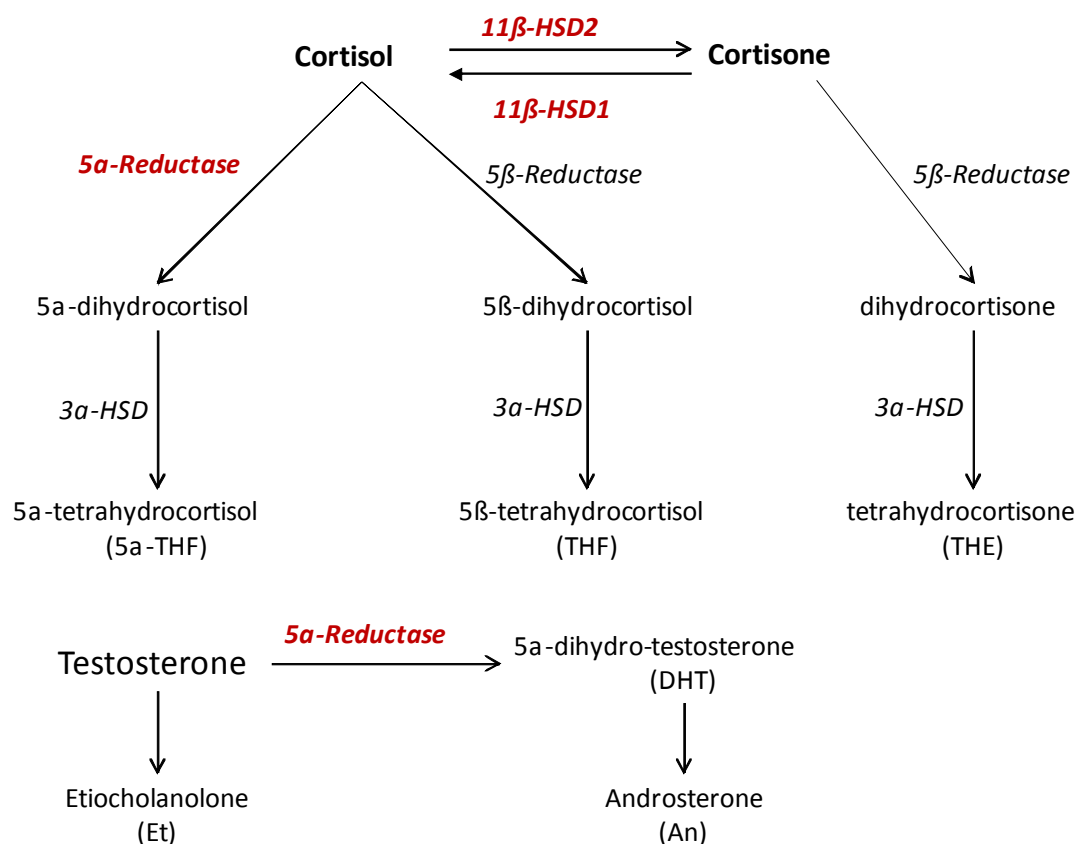
Figure 1-23   Steroid metabolites and metabolic pathways analysed by urinary GC/MS

1.13.2.3.   Liquid chromatography mass spectrometry

Liquid chromatography / mass spectrometry (LC/MS), like GC/MS can measure steroid metabolites and the intermediate products of hormone synthesis. Both techniques utilise similar techniques, however LC/MS separates samples using liquid chromatography. LC/MS offers several advantages over GC/MS. Unlike GC/MS, samples analysed by LC/MS can be non volatile and do not require extensive derivatisation. Consequently sample analysis time is reduced. The high specificity of LC/MS ensures consistent metabolite identification and quantification (Kushnir *et al.* 2009). Additionally, LC/MS is

more versatile than GC/MS allowing identification and simultaneous measurement of a greater spectrum of metabolites (Vogeser 2003). LC/MS is highly sensitive, potentially enabling smaller volumes of biofluids to be analysed (Kushnir *et al.* 2004) and additionally allowing the detection of low concentration metabolites, thereby enabling earlier diagnostic testing. The higher specificity does mean, however, that established reference levels for steroid metabolites are not transferable and need to be re-established in LC/MS.

Numerous fluids are amenable to LC/MS analysis including serum, urine, microdialysis fluids, vitreous humour, auditory perilymph and CSF (Favretto *et al.* 2009; Guitton *et al.* 2009; Jiang *et al.* 2009; Swan *et al.* 2009; Uutela *et al.* 2009). The technique is likely to be widely used in future diagnostic clinical chemistry. We aim to use LC/MS to analyse CSF glucocorticoid metabolites, an area not previously described.

1.14. Hypothesis

In summary there is no current consensus regarding the pathogenesis of IIH although disordered CSF dynamics either at the CP or AGT are likely to be key. IIH has clear endocrinological links, occurring almost exclusively (greater than 93%) in obese women. Additionally, numerous case reports document IIH in the context of corticosteroid therapy and endocrinopathies such as Cushing's syndrome. The cortisol generating enzyme 11β-HSD1 is implicated in obesity, a phenotypic characteristic of IIH and exhibits sexual dimorphism. 11β-HSD1 and glucocorticoids are also involved in IOP regulation via mechanisms which may be pertinent to CSF secretion and drainage at the CP and AGT respectively. These observations suggest that obesity and metabolic changes, particularly 11β-HSD1 activity, may play an important aetiological role in CSF dynamics and IIH.

Chapter 1

The 2005 Cochrane review highlighted that an evidence base for the treatment of IIH has not been established. Weight loss is a commonly advocated treatment as IIH patients are typically obese, however, there have been no previous prospective studies documenting the effect of weight loss on ICP in IIH. Weight loss may potentially benefit patients with IIH due to manipulation of 11β-HSD1 activity.

We hypothesis that 11β-HSD1 is important in the pathogenesis of IIH. Additionally, that 11β-HSD1 and glucocorticoids influence ICP by driving CSF secretion at the CP and drainage at the AGT. Metabolic alterations may also provide clues to the pathogenesis of IIH. Finally, we suggest that weight loss will lower ICP in obese IIH patients, via manipulation of 11β-HSD1.

This thesis aims to explore how obesity, 11β-HSD1 and metabolic changes may be involved in the pathogenesis and treatment of IIH.

1.14.1. Objectives

1. To characterise 11β-HSD1 in the CP of an animal model, the New Zealand White Albino Rabbit (NZWAR).

2. To characterise 11β-HSD1 in human CP and AGT and additionally in an untransformed human choroid plexus epithelial cell line, thereby establishing an *in vitro* model to study the role of 11β-HSD1 in CSF secretion.

3. To utilise NMR spectroscopy to identify key metabolites in the CSF and serum, specific to IIH subjects, which, in addition to facilitating diagnosis, may impart information about disease pathogenesis.

4. To define an evidence base for weight reduction in managing patients with IIH and if weight loss is beneficial in IIH to explore whether this effect occurs via modulation of 11β-HSD1 and related metabolites.

5. To characterise the obesity phenotype in IIH through examination of body composition and evaluation of the glucocorticoid, lipid and insulin profile.

Chapter 2. Methods

Chapter 2

This chapter describes the detailed methodology used in this thesis. Variations in these procedures and study designs are discussed in the appropriate chapter.

2.1. In vitro techniques

2.1.1. Haematoxylin and eosin stain

All tissue samples were initially identified using haematoxylin and eosin stain (H&E) staining. Formalin fixed tissues were embedded in paraffin and cut into 5µm sections which were mounted on electrostatically charged slides (VWR, Lutterworth, UK) to aid tissue adhesion. Sections were initially dewaxed and rehydrated (emersion in xylene, 2 x 5 minutes, and then in 100% ethanol, 2 x 5 minutes. Staining was then carried out using Meyer's haematoxylin (Surgipath-Europe Ltd, Peterborough, UK) for approximately 30 seconds. Excess haematoxylin was removed by washing in running tap water for 5 minutes and then developed, through immersion in 1% acid alcohol for 30 seconds. Counter straining was carried out with 1% eosin (Surgipath-Europe Ltd, Peterborough, UK) and again irrigated for 5 minutes in tap water. Sections were dehydrated in 100% ethanol (2 x 5 minutes) and xylene (2 x 5 minutes) prior to mounting with dibutyl-polystyrene-xylene (DPX) (BDH laboratory supplies, Poole, UK).

2.1.2. Immunohistochemistry

2.1.2.1. 11β-Hydroxysteroid dehydrogenase

Tissue sections were initially dewaxed and rehydrated by processing in xylene (2 x 5 minutes) and then in 100% ethanol (2 x 5 minutes). Antigen retrieval was achieved though immersion in citric acid buffer (pH 6) and boiling (microwaving for 2 minutes, allowing to cool for 2 minutes and then further microwaving for 2 minutes). Following

antigen retrieval, the sections were allowed to cool to room temperature and buffer removed through irrigation for 5 minutes in tap water. A 15 minute submersion in methanol hydrogenperoxide was carried out to reduce endogenous peroxidase activity. Sections were processed using a flat bed technique. Incubation with 10% normal donkey serum (NDS) in phosphate buffered saline (PBS) for 30 minutes was conducted to reduce non-specific binding. Sections were then incubated with primary antibody (Table 2-1). The anti-human polyclonal 11β-HSD1 and anti-human polyclonal 11β-HSD 2 were generated in-house (Ricketts *et al.* 1998). After washing with PBS, the sections were incubated with the secondary antibody, donkey anti-sheep immunoglobulin (Ig) G horseradish peroxidase (HRP) conjugate (The Binding Site, Birmingham, UK). The reaction was visualised using, 3,3'-diaminobenzidine tetrahydrochloride (DAB) (Sigma-Aldrich, Dorset, UK) for approximately 2 minutes. The chromagen reaction was stopped by irrigating in tap water for 5 minutes. Nuclear staining was achieved using Meyer's haematoxylin (Surgipath-Europe Ltd, Peterborough, UK) for 30 seconds. Finally the sections were dehydrated by processing through 100% ethanol (2 x 5 minutes) and xylene (2 x 5 minutes) prior to mounting with dibutyl-polystyrene-xylene (DPX). Control sections included the use of antibody pre-treated with immunising peptide and omission of primary antibody. Liver and kidney sections were used as positive control tissues for 11β-HSD1 and 2 respectively.

	Antibody	Primary		Secondary		Conditions
		Concentration	Duration (h)	Concentration	Duration (h)	
NZWAR	11β-HSD1	1:100	1.5	1:100	1	room temperature
	11β-HSD2	1:100	1	1:100	1	room temperature
Human	11β-HSD1	1:200	1.5	1:200	1	room temperature
	11β-HSD2	1:100	1	1:100	1	room temperature

Table 2-1   Antibody conditions for 11β-HSD1 and 2

2.1.2.2.   Vimentin, Factor VIII related antigen and epithelial membrane antigen

Human AGT was identified through staining with mouse monoclonal anti-human epithelial membrane antigen (EMA) IgG2a (Dako, Cambridgeshire, UK), 1:50 dilution, polyclonal rabbit anti-human Factor VIII related antigen (FVIII) (Dako, Cambridgeshire, UK), 1:1000 dilution, and mouse monoclonal anti-human vimentin IgG1, (Dako, Cambridgeshire, UK), 1:400 dilution, each incubated for 30 minutes. Positive control sections were the tonsil (EMA) and kidney (FVIII and vimentin). Negative controls were incubated with no primary antibody. This work was carried out by Charlie Shaik, Academic Unit of Ophthalmology, Division of Immunity and Infection, University of Birmingham, Birmingham, United Kingdom.

2.1.3. Cell culture

2.1.3.1.   Human choroid plexus epithelial cell line

A commercial untransformed human choroid plexus epithelial (HCPEpi) cell line (ScienCell Research Laboratories, San Diego, USA) was utilised which had been previously characterised through staining with cytokeratin-18, -19 and vimentin. These

intermediate filament proteins, from the cytoplasmic cytoskeleton, are typical markers of CP epithelial cells (Sarnat 1998). Cells were cultured in epithelial cell medium (EpiCM), supplemented with 20% foetal bovine serum (FBS), 10% epithelial growth supplement and 10% penicillin and streptomycin (P/S), (all supplied by ScienCell Research Laboratories, San Diego, USA). HCPEpi cells survive in culture for 15 population doublings.

2.1.3.1.1 *Cell recovery*

Vials of HCPEpi cells were removed from storage in liquid nitrogen and thawed at 37°C in a water bath while being gently rotated. Vials were then transferred to a sterile field and sprayed with 70% ethanol. The contents of each vial were then re-suspended in 5 ml of culture media and transferred to T25 (surface area $25cm^2$) culture plate.

2.1.3.1.2 *Cell culture*

To aid tissue adhesion and growth, cells were grown in flasks pre-coated with poly-l-lysine (ScienCell Research Laboratories, San Diego, USA). Poly-l-lysine, a positively charged synthetic amino-acid, altered the surface charge on the culture flask. Flasks were coated with poly-l-lysine ($0.2 – 2$ µg/cm^2) for a minimum of 1 hour before being washed twice with sterile water and filled with cell media suspension. A seeding density of 750,00 cells/cm^2 was used. Cells were incubated at 37°C in a humidified environment containing 5% CO_2 and 95% O_2. Cell media was replaced on the day following passage and thereafter every 48 hours unless otherwise specified.

2.1.3.1.3 *Sub-culture*

Cells were sub-cultured when they were 80-90% confluent. Media was removed and the cells irrigated with PBS. Trypsin/ ethylenediaminetetraacetic acid (EDTA) solution was added (3 ml per T25 flask) and the cells incubated at 37°C for 2 minutes. Flask agitation

aided cell detachment and when 80% of the cells were dislodged, the trypsin solution was neutralised with EpiCM supplemented with 20% FBS (3 ml per T25 flask). The cell suspension was then centrifuged at 1000 rpm and cells subsequently resuspended in fresh culture medium. Cells were passaged according to cell density and to accommodate future experiments.

2.1.3.1.4   Cell storage

Cells were collected with trypsin/EDTA as detailed above and resuspended in cell freezing media (ScienCell Research Laboratories, San Diego, USA), at a density of 500,000 cells per ml. Cells were stored at -80˚C overnight and then transferred to liquid nitrogen for long term storage.

2.1.3.2.   Arachnoid granulation primary cell line

The untransformed human arachnoid granulation primary epithelial cell line (AGEpi) was provided by collaborator Deborah Grzybowski, Ohio State University, Columbus, USA (Holman *et al.* 2005).

2.1.4. Ribonucleic acid extraction

2.1.4.1.   Ribonucleic acid extraction from human choroid plexus epithelial cells

The ribonucleic acid (RNA) yield, from HCPEpi cells, was found to be optimised by using a RNA extraction kit (Genelute mammalian total RNA extraction kit, Sigma-Aldrich Company Ltd, Dorset, UK). Briefly, the cultured cell monolayer was covered in 2-mercaptoethanol/lysis solution (10 µl:1 ml), agitated, and then transferred to a filtration column. The extraction process was then carried out according to the manufacturer's protocol. The RNA pellet was resuspended in an appropriate volume of elution solution,

depending on the size of the pellet (typically 20 ul). All elements of RNA extraction were carried out on ice in a clean environment. RNA was stored at -80˚C.

2.1.4.2.   Ribonucleic acid extraction from tissue

RNA was extracted from CP and AGT using the Genelute mammalian total RNA extraction kit (Sigma-Aldich Company Ltd, Dorset, UK) as described above. For all other tissues the RNA was extracted as follows: tissue was homogenised (approximately 100 mg) in 500 µl of Tri-reagent (Sigma-Aldich Company Ltd, Dorset, UK). The tissue suspension was centrifuged for 5 minutes at 11269 g at 4˚C and the supernatant transferred to a separate eppendorf, the cell pellet was discarded. After standing for 5 minutes the supernatant was mixed with 100 µl of chloroform. The sample was then incubated for 10 minutes at room temperature before being centrifuged for 30 minutes at 12,000 rpm to separate the RNA into the aqueous layer. Isopropanol (250 µl) (Sigma-Aldich, Dorset, UK) and glycol blue (1 µl) (Ambion, Cambridgeshire, UK) were then added to the aqueous layer prior to an overnight incubation at -20˚C. The following day, the sample was centrifuged at 11269 g for 30 minutes at 4˚C and the supernatant was then removed. The remaining RNA pellet was air dried for 5 minutes before being suspended in nuclease free water (approximately 20 µl, depending of the size of the pellet). RNA was stored at -80˚C.

2.1.4.3.   Ribonucleic acid confirmation

RNA integrity was assessed (1 µl of RNA, 2µl of loading buffer and 9 µl of nuclease free water) by electrophoresis, using a 1% agarose gel and 1 µl/ml of ethidium bromide. Intact RNA, when visualised under UV light, exhibits 2 bands corresponding to the 28S and 18S ribosomal subunits. The RNA concentration was calculated after assessing the RNA

spectrophotometrically (OD$_{260}$), 1 OD unit being equivalent to 40µg of RNA/µl. In the final year of study RNA concentration and quality were assessed using a Nanodrop spectrophotometer (Wilmington, DE, USA).

2.1.4.4.   Deoxyribonuclease treatment

Deoxyribonuclease I (DNase I), amplification grade (Invitrogen, Paisley, UK), digests single and double-stranded DNA to oligodeoxyribonucleotides. Reaction components (Table 2-2) were mixed in a 1.5 ml eppendorf on ice and then incubated for 15 minutes at room temperature. The reaction was inactivated by the addition of 1 µl of EDTA (25 mM) and the sample heated on a hot block for 10 minutes at 65˚C.

Reagent	Volume (µl)
RNA	1.0
Reaction Buffer	1.0
DNase I, Amp grade (1U/ul)	1.0
Nuclease free water	variable

Table 2-2   ***Deoxyribonuclease I reaction components***
The reaction volume was made up to a total volume of 10 µl with nuclease free water.

The RNA was then recovered through the addition of 0.1 volume of 5M ammonium acetate and 1 µl of glycol blue (Ambion, Cambridgeshire, UK). RNA was precipitated though the addition of 1 volume of isopropyl alcohol. To maximise the RNA yield, the sample was incubated overnight at -20˚C. The following day, the supernatant was removed following centrifugation at 11269 g for 15 minutes at 4˚C. The remaining RNA pellet was washed with cold, 70% ethanol and centrifuged again under the same

conditions to remove further supernatant. The RNA pellet was then allowed to air dry

before being resuspended in nuclease free water.

2.1.5. Reverse-transcriptase polymerase chain reaction

RNA was reverse transcribed to complementary DNA (cDNA) using a multiscribe reverse

transcriptase kit according to the manufacturers protocol (Applied Biosystems, Cheshire,

UK) (Table 2-3). Incubation times are listed in Table 2-4.

Reagent	Volume
RNA	1.0 µg
10 x reaction buffer	5.0 µl
MgCl$_2$ 25mM	11 µl
Deoxy-nucleotide triphosphates (NTP's)	10 µl
Random Hexamers	2.5 µl
RNase Inhibitor	1.0 µl
Multiscribe RT (500 µg/ml)	3.2 µl

Table 2-3   ***Reverse-transcriptase reaction components***

         The reaction volume was made up to 50 µl using nuclease free water.

Temperature (˚C)	Time (minutes)
25	10
37	60
48	30
95	5
4	hold

Table 2-4   ***Reverse transcriptase incubation***

2.1.6. Conventional polymerase chain reaction

The polymerase chain reaction (PCR) components (Promega, Southampton, UK) were mixed on ice, vortexed and placed in the PCR thermocycler (Table 2-5). The PCR cycle is detailed in Table 2-6. The PCR products were resolved on an agarose gel alongside a hyperladder (Bioline, London, UK) and viewed under UV light. Initially reverse transcription PCR was carried out on 18s to assess cDNA quality. Negative control reactions comprised of the above reaction mix with nuclease free water substituted for cDNA. In addition product from the reverse transcription reaction that had been carried out in the absence of multiscribe reverse transcriptase was also used as a control.

Reagent	Volume
Nuclease free water	variable
PCR buffer with dye	4.0 µl
$MgCl_2$ (25 mM)	1.6 µl (2 mM)
Deoxy-NTP's (10 mM)	0.5 µl (0.25 mM)
Taq DNA polymerase (5 µg/µl)	0.1 µl (25ng/µl)
Primer Forward (10 µM)	1.0 µl (0.5 µM)
Primer Reverse (10 µM)	1.0 µl (0.5 µM)
cDNA	2 .0µl

Table 2-5   ***Polymerase chain reaction components***

The reaction is made up to a final volume of 20 µl with nuclease free water.

Temperature (˚C)	Time (minutes)
94	5
94	0.5
60	0.5
72	0.5
72	7
4	hold

Table 2-6   ***Polymerase chain reaction incubation cycle***

Details of modifications are documented in the respective sections.

2.1.7. Real Time PCR

Real-time PCR was performed using an ABI 7500 system (Perkin-Elmer, Biosystems, Warrington, UK) in 20 μl reactions on 96-well plates in reaction buffer containing TaqMan universal PCR master mix (Applied Biosystems, Warrington, UK), 3 mM Mg, 2200 μM deoxy-nucleotide triphosphates (NTP's), 1.25 U AmpliTaq Gold polymerase (PerkinElmer, Biosystems, Warrington, UK), 1.25 U AmpErase UNG (PerkinElmer, Biosystems, Warrington, UK), 900 nmol primers, 100–200 nmol TaqMan probe and 25–50 ng cDNA. All reactions were singleplexed with primers specific for 18S RNA (provided as a pre-optimised mix; Perkin-Elmer, Beaconsfield, Bucks, UK) as an internal reference. Measurements were carried out in triplicate for each sample. All target gene probes were labelled with 6-carboxy-fluorescein FAM, and the housekeeping gene with VIC reported dye. Reactions were as follows: 50°C for 2 minutes, 95°C for 10 minutes; then 40 cycles of 95°C for 15 seconds and 60°C for 1 minute. Data were expressed as cycle threshold (Ct) values (the cycle number at which logarithmic PCR plots cross a calculated threshold line) and used to determine ΔCt values (ΔCt = Ct of the target gene

minus Ct of the housekeeping gene). All statistics were performed with ΔCt values. Relative mRNA levels are expressed as fold changes ($2^{-\Delta\Delta Ct}$).

2.1.8. Primer design

The primers for sgk-1 and MYOC were designed using the National Resource for Molecular Biology Information web site http://www.ncbi.nlm.nih.gov/. A search was carried out for the mRNA sequence of the gene of interest. The mRNA sequence was copied in FASTA (Pearson) format into an on-line primer design program (Primer3, provided by Whitehead Institute for Biomedical Research, USA), http://frodo.wi.mit.edu/. The guanine-cytosine % was limited to 40 – 60 %, and the primer annealing temperature was set at 60˚C. The primer sequences were then checked for hairpins, dimers, palindromes, repeats and runs using Net Primer (Premier Biosoft International, Canada) http://www.premierbiosoft.com/netprimer/. Primer sequences were generated by Alta Biosciences (University of Birmingham, UK).

2.1.9. 11β-HSD enzyme assay

2.1.9.1. Production of ^{3}H-cortisone

Tritiated cortisone (^{3}H-E), was generated from tritiated cortisol (^{3}H-F), using the 11β-HSD2 enzyme activity inherent in human, term, placental tissue. In a glass tube, 20 µl of ^{3}H-F, 100.0 mCi/mM (Perkin Elmer, Boston, USA) was incubated with 1000 µg of homogenised placenta using 500 µM of NAD$^+$ as a cofactor. The reaction mix was made up to 500 µl using 0.1 M phosphate buffer, pH 7.4. The reaction mix was incubated in a shaking water bath at 37˚C overnight. Steroid was then extracted and isolated as detailed below.

Chapter 2

2.1.9.2.   Steroid extraction and thin layer chromatography

This technique was used both in the production of ^{3}H-E and to extract steroid following

enzyme activity assays. Steroids were extracted using 7 ml of dichloromethane and the

reaction mixed agitated for 20 minutes. The sample was then centrifuged at 671 g for 15

minutes to separate the aqueous and organic phases. The former was then aspirated and

discarded. The organic phase was evaporated under air flow at 55°C until dry, using a

sample concentrator and Dry-Block (Techne, Staffordshire, UK). Dry steroid was then

resuspended in 80 μl of dichloromethane and 1μl of solution pipette onto individual spots

of a silica plate (Fluca, Sigma-Aldrich, UK). Unlabelled cortisol and cortisone standards

(1mg/ml) were also "spotted" onto each sample to measure the solvent front. Steroids

were separated using thin layer chromatography (TLC) in a tank containing a mobile

phase of 200 ml chloroform: ethanol (92: 8 v:v) equilibrated for 1 hour before use. The

solvent front was run to within 1 cm of the end of the silica plate (approximately 90

minutes). The silica plates were dried and scanned using a Bioscan 2000 radioimaging

detector (LabLogic, Sheffield, UK) to localise tritiated steroids. The position and activity

of ^{3}H-E and ^{3}H-F were then established.

2.1.9.3.   Steroid isolation

To harvest ^{3}H-E, the appropriate area of the silica plate was scraped into a glass tube,

eluted in 1 ml of 100% ethanol and left overnight at 4°C. Samples were then centrifuged

at 700 g for 15 minutes to remove the silica. Supernatant, containing 3H-E, was then

evaporated under air-flow at 55°C. The ^{3}H-E was re-suspended in 500 μl of 100%

ethanol, and 5 μl was then spotted onto a silica plate before again separating by TLC.

Activity and purity was then assessed using the Bioscan 2000 Radioimaging detector. [3]H-

E was diluted in ethanol and stored in glass tubes at -20°C.

Chapter 2

2.1.9.4. 11β-HSD enzyme assay protocol

11β-HSD enzyme activity was assessed in both dissected whole tissue and in cultured cells. Both oxoreductase (cortisone to cortisol) and dehydrogenase activity (cortisol to cortisone) were assessed by incubating with unlabelled cortisone (100 nM) (Sigma-Aldrich Company Ltd, Dorset, UK) and tracer amounts of ^{3}H-E (50,000 c.p.m.) (synthesised in-house section 2.1.9.1) or unlabelled cortisol (100 nM) (Sigma-Aldrich Company Ltd, Dorset, UK) and tracer amounts (1·5 nM) of ^{3}H-F (specific activity 100.0 mCi/mmol, (Perkin Elmer, Boston, USA) respectively. Reactions were diluted in serum-free medium and incubated at 37°C for 24 hours (unless stated otherwise). Assays were also incubated in the presence and absence of a 100-fold excess of glycyrrhetinic acid (GE) (5µM), a non-specific 11ß-HSD inhibitor. This concentration of GE has been previously shown to significantly reduce 11ß-HSD activity (Bujalska *et al.* 1997). After incubation, steroids were extracted and separated by TLC (detailed in section 2.1.9.2).

The conversion of substrate to product was calculated after scanning analysis, using a Bioscan 2000 radioimaging detector (LabLogic, Sheffield, UK). Enzyme activity was expressed as pmol mg^{-1} h^{-1} protein (see protein assay 2.1.10) or pmol g^{-1} h^{-1} wet weight for whole tissue explants.

2.1.10. Protein assay

Cells were washed in PBS and immersed in a minimal volume of distilled water and dislodged with a cell scraper. The cell suspension was then transferred to a 1.5 ml eppendorf and processed through 3 freeze-thaw cycles using liquid nitrogen and a 37˚C water bath. The sample was then centrifuged for 1 minutes at 11269 g after which 5 µl of supernatant was transferred to a 96 well plate, in triplicate. Bovine serum albumin (BSA) 5mg/ml was diluted in distilled water to establish a dilution series (0 mg/ml, 0.125 mg/ml

0.25 mg/ml, 0.5 mg/ml, 0.75 mg/ml, 1.0 mg/ml, 1.5 mg/ml and 2.0 mg/ml). 5 µl of each

protein standard was transferred, in triplicate, to the 96 well plates. Standard protein assay

reagents (Bio-Rad, Hemel Hempstead, UK), were added to each well using an automated

pipette. The samples were incubated at room temperature for 10 minutes to allow a

chromagen reaction. The absorbance of each well was then read for 0.1 seconds at 680 nm

using the Victor[3] 1420 multilabel counter (Perkin Elmer, Wellesley, USA). A standard

curve was plotted from the known protein concentrations and used to calculate unknown

protein concentrations.

2.2. Metabolite measurements

2.2.1. Nuclear magnetic resonance spectroscopy

Thawed samples (300µl), were centrifuged at 1000 rpm for 2 minutes prior to dilution 1:1

with deuterium oxide containing NaCl (150mM), trimethylsilyl-2,2,3,3-

tetradeuteropropionic acid (TMSP) (2.5mM) and sodium phosphate (20mM) pH 7.4. ^{1}H

NMR spectra were obtained using a DRX 500MHz spectrometer (Bruker BioSpin,

Rheinstetten, Germany) with a cryoprobe. 1D spectra were acquired using a standard

spin-echo pulse sequence (8 µs (60˚) pulse with 3 s relaxation delay, 5.3 kHz spectral

width) with 128 transients collected into 16,000 data points. Excitation sculpting was used

to suppress residual water. Samples were analysed at 20°C in 4.97 mm optical density

NMR tubes (Norell INC, Landisville, USA). 2D JRES NMR spectra were obtained as

previously described (Viant 2003). Briefly, the same conditions as that described for 1D

spectra were employed, however, a 90˚ flip angles was applied and 16 transient per

increment for 16 increments were collected into 16,000 data points. A spectral width of 50

Hz in F1, the spin-spin coupling axis, and 5.3 Hz in F2, the chemical shift axis, were used.

The operator was masked to the clinical diagnosis, and samples were processed randomly. Spectra were phased manually, baseline corrected and referenced to the TMSP resonance (0.0 ppm). To facilitate analysis, each spectrum between 0.2 and 9.0 ppm was reduced in complexity, by segmenting into 0.005 ppm bins (2.5Hz) using ProMetab (version 2) (Viant 2003) within MATLAB (version 7.0, Matworks, Cambridge, UK). Bins between 4.5 and 5.0 ppm containing residual water were removed, and the remaining bins were integrated. Each binned spectrum was normalised to a total spectral area of unity, transformed using a generalised log (glog) to increase the weighting of smaller peaks, and the peaks were aligned (Lee 2004). A data matrix was compiled with individual samples represented on rows, and chemical shifts delineated in columns.

2.2.1.1. Data processing and analysis

Data from the 2D JRES spectra were exported as 1D skyline projections, termed p-JRES. 1D and p-JRES data were analysed using an unsupervised model principal components analysis (PCA) using PLS_Toolbox (version 3.5, Eigenvector Research, Washington, USA) within MATLAB. This technique reduces the dimensionality of the binned spectra (Ramadan *et al.* 2006). This is achieved by transforming the binned spectra into new variables, termed principal components (PC), which are weighted, linear combinations of the original spectral bins (presented as weighting plots). In effect, PCA identifies the most highly variable metabolites in the NMR spectra.

Partial least squares discriminant analysis (PLS-DA) was then employed using PLS_Toolbox (version 3.5, Eigenvector Research, Washington, USA within MATLAB). This supervised analysis technique (Bijlsma *et al.* 2006; Ramadan *et al.* 2006) was used to build a model to evaluate separation between groups based on known clinical diagnosis. The PLS-DA model was cross-validated using Venetian blinds (Martens and Naes 1989;

Chauchard *et al.* 2004). This method re-assigns randomly selected blocks of data to the PLS-DA model to determine the accuracy of the model in correctly assigning class membership

Identification of the discriminating peaks in the spectra was carried out using Chenomx NMR Suite (version 4.0, Chenomx, Alberta, Canada), an NMR analysis program, in conjunction with the human metabolite database (Wishart *et al.* 2007) and published literature (Brindle et al. 2002; Subramanian et al. 2005).

Metabolomic processing and analysis was conducted with advice from Steven. P. Young, Rheumatology, School of Immunology, Infection and Inflammation, and Mark Viant School of Biosciences, University of Birmingham.

2.2.2. Gas chromatography/ mass spectrometry

GC/MS assays were carried out by Beverley Hughes at the Institute for Biomedical Research, University of Birmingham. The GC/MS assay performed was based on the method described by Palermo (Palermo *et al.* 1996). Samples of urine (1 ml of a 24 hour urine collection) and serum (1 ml) were processed.

The following isotope-labelled internal standards were used; $(9,11,12,12\text{-}^2H_4)$ cortisol and $(9,12,12\text{-}^2H_3)$ cortisone. The standards were calibrated by high-performance liquid chromatography (HPLC) analysis of solubilised, non-labelled standard of known weight. Free steroid was extracted using Sep-pak C18 cartridges (Shackleton and Whitney 1980). Labelled steroid, d_4-cortisol (0.18 µg), and d_3-cortisone (0.12 µg), as well as internal standards (stigmasterol and cholesteryl butyrate), 200 µg, were then added. The samples were then derivatised using 100 µl of 2% methoxyamine hydrochloride in pyridine and 50

µl of trimethylsilylimidazole. Lipidex chromatography was then used to purify the steroid derivative.

GC/MS was carried out using a Hewlett Packard 5970 mass spectrometer and 15 m fused-silica capillary column, 0.25 mm ID, 0.25µm film thickness (J&B Scientific, Folsom CA, and USA) using 2 µl of sample. Steroids were quantified by comparing individual peak area to the peak area of their internal standards, for cortisol fragment 605 m/z compared to 609 m/z and for cortisone fragment 531 m/z compared to 534 m/z. The relative peak area was calculated and metabolite concentration expressed as µg/24h. A quality control (QC) was analysed with each batch. The intra and inter-assay coefficient of variance was <10%.

2.2.3. Liquid chromatography / mass spectrometry

Liquid chromatography / mass spectrometry (LC/MS) was carried out on our behalf by Dr Andre van Beek and Ido Kema, (Department of Endocrinology and Department of Laboratory Medicine, University Medical Centre Groningen, University of Groningen, the Netherlands). Extraction and quantification of CSF cortisol and cortisone was performed by on- line solid phase extraction coupled with liquid chromatography and tandem mass spectrometry

100 µl of CSF was mixed directly in an autosampler vial with 20 µl internal standard solution (Cortisol-d4 , cortisone-d7 Cambridge Isotope Laboratories (Andover, MA, USA); and diluted with water to reach a final volume of 200 ul. 50 µl of the sample was injected into the XLC-MS/MS system. Sample clean-up took place by on-line SPE, using a Spark Holland Symbiosis® system (Spark Holland, Emmen, the Netherlands) as described previously (de Jong *et al.* 2007). HySphere® C18 HD 10 by 2 mm SPE cartridges (Spark Holland, Emmen, Netherlands) were used for sample extraction.

Chapter 2

Chromatographic separation was achieved by using an Xbridge C8 (particle size 3.5 μm, 2.1 mm internal diameter by 100 mm; Waters, Milford, MA).

Detection was performed with a Quattro Premier® tandem mass spectrometer equipped with a Z Spray® ion source operated in positive electrospray ionization mode (Waters, Milford, MA). Cortisol, cortisone and their deuterated internal standards were protonated to produce ions at the form $[M^+H]^+$, with m/z 363 and m/z 367, and m/z 361 and m/z 368 respectively. Upon collision-induced dissociation with argon gas, these precursor ions produced characteristic product ions of m/z 121 for both cortisol, and its deuterated internal standard. For cortisone and its internal standard, product ions were: m/z 163 and 167. The A multiple reaction monitoring mode was developed for the specific m/z transitions 363→121 and 367→121 (cortisol and internal standard cortisol) and 361→163 and 368→167 (cortisone and internal standard cortisone).

2.2.4. Commonly used buffers and reagents

Agarose gel 1%

Agarose TBE	1% (w/v)
Ethidium Bromide	1.0 µg/100ml

Tris/Borate/EDTA (TBE) [10x]

Tris	89 mM
Boric acid	89 mM
EDTA	2 mM

Citric Acid buffer 0.01M (Ph 6)

Citric acid	0.1 M
Sodium citrate	0.1 M

Make to required volume with H_2O. Adjust to Ph 6 with hydrochloric acid

Methanol Hydrogen peroxide 30%

Methanol

H_20_2 62.5:1 (v/v)

PBS

NaCl   120 mM

KCl   2.7 mM

Phosphate salt   10 mM

Trypsin

PBS

EDTA   0.5 M pH 8.0

Trypsin   0.25%

Make up with [1x] PBS and [1x] EDTA

2.3. Clinical studies

The clinical investigations carried out in this thesis were performed at the Birmingham and Midland Eye Centre, Sandwell and West Birmingham Hospitals NHS Trust or at the Wellcome Trust Clinical Research Facility, University Hospitals Birmingham NHS Trust. The majority of techniques employed to assess visual function are routinely utilised and validated (LogMAR visual acuity, Humphrey 24-2 central threshold automated perimetry, Pelli Robson contrast sensitivity and Farnsworth Munsell 100 Hue colour test). The novel techniques used to quantify papilloedema are detailed below.

2.3.1. Ultrasonography

Images were captured and measured by Dr Peter Good, visual function department, Birmingham and Midland Eye Centre. All images were obtained following application of

methylcellulose coupling gel to the closed eyelids. A high resolution scanner (Quantel Medical, Clermont–Ferrand, France) with a focal length of 25 mm and resolution of 0.01mm was used.

2.3.1.1.   Optic disc elevation

B-scan images of the optic disc were obtained at 20 MHz emission frequency. The imaging plane displaying the maximal disc height was frozen (oblique sections, which falsely represent the disc height, were not used). Measuring callipers were placed between the point of maximal optic nerve elevation and the highly reflective lamina cribrosa. Horizontal and vertical measurements were taken, and the mean established.

2.3.1.2.   Nerve sheath diameter

The optic nerve sheath was imaged using a 10 MHz B scan. A still image of the retrobulbar optic nerve was obtained and the maximal inner pial diameter measured with callipers.

2.3.2. Optical coherence tomography

Images were obtained by members of the Visual Function Department, Birmingham and Midland Eye Centre. The Stratus OCT^{TM} V4.0.1 (Carl Zeiss, Meditec, Welwyn Garden City, UK) was used to measure distension of the peripapillary RNFL. Circumferential measurements of the optic disc were made using Fast RNFL Thickness (3.4) acquisition protocol. Pupils were under normal physiological conditions. Images were re-acquired if image quality was hampered by blinking or inadequate focus (signal strength greater than six was required). The same operator collected two optimised images of each eye 10 minutes apart. The average RNFL thickness values were calculated using the "Average analysis" protocol.

2.3.3. Dual energy x-ray absorptiometry

Dual energy x-ray absorptiometry (DEXA) (QDR 4500; Hologic, Bedford, MA) measured total body composition. Fat distribution and mass was calculated using standardised software (Stewart *et al.* 1999). The fat mass coefficient of variance was less than 3%. Imaging was performed by Nicola Crabtree, Department of Nuclear Medicine, University Hospital Birmingham NHS Trust.

2.3.4. Serum measurements

Measures of total cholesterol, triglycerides and glucose were performed by the Department of Clinical Biochemistry, University Hospitals Birmingham NHS Foundation Trust Selly Oak Hospital, Birmingham, using spectrophotometric assays (Roche Diagnostics, Burgess Hill, UK). Cholesterol inter-assay coefficient of variance was 0.8% at 5.98 mmol/l (minimum sensitivity 0.08 mmol/l). Triglycerides inter-assay coefficient of variance was 1.5% at 2.28 mmol/l (minimum sensitivity 0.05 mmol/l). Glucose inter-assay coefficient of variance was 1.0% at 7.05 mmol/l (minimum sensitivity 0.11 mmol/l).

2.3.4.1. Insulin enzyme linked immunosorbant assay

Insulin was measured by enzyme linked immunosorbant assay (ELISA) (Mercodia AB, Uppsala, Sweden) in serum (25 µl). The inter-assay and intra-assay coefficient of variance was < 4% and <3.6% respectively, with a sensitivity range of 3 – 200 mU/l. The assay showed no cross reactivity with proinsulins or c-peptide. The assay was performed by Susan Hughes, Centre for Endocrinology, Diabetes and Metabolism, School of Clinical and Experimental Medicine, University of Birmingham.

Chapter 2

2.3.4.2.   The Homeostasis Model Assessment (HOMA)

The Homeostasis Model Assessment (HOMA) is based on the concept that fasting insulin levels are inversely related to insulin sensitivity. Under conditions of insulin resistance, elevated fasting glucose levels maintain the drive to the pancreatic islet B cells to secrete insulin (Turner *et al.* 1979). The HOMA score was calculated from the fasting glucose (mmol/l) and the fasting insulin (pmol/l) using software downloaded from the University of Oxford Diabetics Trials Unit (http://www.dtu.ox.ac.uk/index.php?maindoc=/homa/). The HOMA %B estimates steady state beta cell function, HOMA %S insulin sensitivity and HOMA IR (insulin resistance) as a percentage of a normal reference population, including young adults (Levy *et al.* 1998).

HOMA %B= 20 × fasting insulin (μU/ml) / fasting glucose (mmol/ml) − 3.5

HOMA %S = 1 / ((fasting insulin (μU/ml) × fasting glucose (mmol/ml)) / 22.5)

HOMA IR = fasting glucose (mmol/l) × fasting insulin (μU/ml) / 22.5

2.3.4.3.   Biochemical hyperandrogenism screening

The assays were performed by Dr Penny Clarke, Regional Endocrine Laboratory, Department of Clinical Biochemistry, University Hospitals Birmingham NHS Foundation Trust Selly Oak Hospital, Raddlebarn Road, Selly Oak, Birmingham, B29 6JD. Androstenedione was assessed by competitive radioimmunoassay using I,125-labelled D4 androstenedione (Coat-a-Count kit TKAN2, Siemens Healthcare Diagnostics, Deerfield, USA). The inter assay coefficient of variance at 7.5nmol/l was 5.2% and 6.9 % at 16.7 nmol/l, assay minimum sensitivity was 0.5 nmol/l. Dehydroepiandrosterone sulphate (DHAS) was measured by, Chemiluminescent immunometric assay (Immulite 2500, Siemens Healthcare Diagnostics, Deerfield, USA). The inter-assay coefficient of variance

at 1.79 µmol/l was 6.2% and at 13.3 µmol/L was 3.8%. Assay minimum sensitivity was 0.8 µmol/l. Sex hormone binding globulin (SHBG), was also measured by, Chemiluminescent immunometric assay (Immulite 2500, Siemens Healthcare Diagnostics, Deerfield, USA). The inter assay coefficient of variance at 19.3 nmol/l was 2.5% and at 71.0 nmol/L was 3.1%. Assay minimum sensitivity was 0.2 nmol/l. Testosterone was evaluated by liquid chromatography / tandem mass spectrometry, with testosterone-d5 used as an internal standard (Waters 2795 Quattro Premier XE system, Milford, MA). The inter-assay coefficient of variance at 1.0 nmol/l was 1.9% and at 10.0 nmol/L was 1.9%, assay minimum sensitivity was 0.03 nmol/l.

2.4. Statistical Analysis

Statistical analysis was performed using SPSS versions 14 and 15 (SPSS Inc., Chicago, USA) and Prism for Windows Version 5.0 (GraphPad Software Inc, San Diego, CA, USA) software packages. Continuous data were summarised using means and standard deviations (or medians and ranges for non-normally distributed data). Parametric data were compared using a paired t-test (Mann-Whitney for non-parametric data). Multiple comparisons were assessed using one way analysis-of-variance (ANOVA), with Kruskal-Wallis for non-parametric data. Associations between variables were analysed using Pearson correlation for parametric data and Spearman rank correlation for non-parametric data. The level at which the results were judged significant was $p < 0.05$.

Throughout the thesis statistical advice was received from Dr Peter Nightingale, Wellcome Trust Clinical Research Facility, Queen Elizabeth Hospital, University Hospitals Birmingham NHS Foundation Trust, Birmingham, B15 2TT.

95

Chapter 3. Characterisation of 11β HSD in Choroid plexus and Arachnoid Granulation tissue

3.1. Introduction

IIH is a condition of unknown aetiology characterised by elevated ICP. Improved understanding of the mechanisms which regulate ICP are consequently a vital component to enhancing our knowledge of IIH. We have discussed the potential role of 11β-HSD in modulating CSF dynamics (sections 1.9.2. and 1.9.3). To this end we characterise 11β-HSD in CP and AGT. Experiments were initially carried out in an animal model (the New Zealand White Albino Rabbit (NZWAR)) and subsequently in human tissues.

3.1.1. Animal studies

CSF secretion by the CP epithelium occurs via a similar mechanism to that which controls AH secretion in the embryologically related, ocular ciliary body. The role of 11β-HSD1 in the pre receptor regulation of AH secretion has been established (Rauz *et al.* 2001; Rauz *et al.* 2003a; Rauz *et al.* 2003b; Rauz *et al.* 2003c). We suggest, that akin to the regulation of AH, 11β-HSD1 may also have a role in modulating CSF production. We have therefore, conducted a detailed analysis of 11β-HSD isozyme expression in the NZWAR CP and compared expression of key elements of the glucocorticoid signalling pathway, to the NZWAR ciliary body. The NZWAR was chosen, as the corticosteroid profile resembles that of humans. Additionally this model has been used for a variety of *in vivo (Onyimba et al. 2006)*, CSF and intracranial pressure studies (Senay and Tolbert 1984; Greene *et al.* 1985; Uhl *et al.* 1999; Artru and Momota 2000; Taplu *et al.* 2003; Kostopoulos *et al.* 2006). The rodent was deemed to be a less suitable model as the steroid profile differs in man and rabbits (corticosterone and 11-dehydrocorticosterone in the rat) and additionally the small size impedes accurate dissection of brain structures.

3.1.2. Human Studies

11β-HSD demonstrates considerable interspecies variability (Tomlinson *et al.* 2004b) and hence we sought to characterise 11β-HSD and the glucocorticoid signalling pathway in human CP as well as in AGT.

3.2. Methods

3.2.1. Animal studies

3.2.1.1. Animal tissues

Adult (2.5 – 3.0 kg), female, New Zealand White Albino Rabbits (NZWAR) were used in this study (Charles River, Margate, UK), (n=13). The rabbits were group-housed in open floor pens, (maximum of six rabbits per pen) illuminated from 07.00 to 17.00 (10:14 hour day-night cycle). Rabbits were maintained on a standard pelleted diet (SDS-FD1, Lillico, Surrey, UK) with water *ad libitum*. The rabbits were acclimatised for a period of approximately one week before lethal injection with pentobarbital sodium 60mg/ml (J.M. Loverage p.l.c., Southampton, UK) at a dose of 1ml/kg. All animals were studied in a manner consistent with FRAME Guidelines and according to the UK Home Office Guidelines for the care and use of laboratory animals.

CSF was collected via puncture of the cisterna magna. CP and ciliary body were surgically dissected and stored in either sterile eppendorfs containing Hams F12 Dulbecco's Modified Eagle's Medium (DMEM – Invitrogen, Paisley, UK) for enzyme assay, or in RNA Later (Sigma-Aldrich, Dorset, UK) for RNA extraction. In four rabbits, the brain was dissected from the skull en bloc, following perfusion fixation with 50ml of

10% formalin. The whole brains were then immersed in 10% formalin for a further three days, prior to paraffin embedding and sectioning.

3.2.1.2. Immunohistochemistry

Histological conformation was carried out using H&E staining (section 2.1.1). Immunohistochemical analyses were performed on 5 µm thick coronal sections of NZWAR whole brain (four) mounted on coated slides (VWR, Lutterworth, UK). 11β-HSD immunolocalisation was carried out as described (section 2.1.2.1), using primary antibody concentrations of 1:100 for both 11β-HSD1 and 11β-HSD2.

3.2.1.3. 11β-HSD activity assay

The rabbit CP was divided into five, of which four pieces were placed whole into individual wells of a 24-well plate. The fifth piece of tissue was fixed in formalin and embedded in paraffin for confirmatory histology with H&E staining. Tissue was incubated with 100 nM cortisol and 100 nM cortisone (Sigma-Aldrich Company Ltd, Dorset, UK) with tracer amounts (1·5 nM) of tritiated steroids at 37˚C for 24 hours, as previously described (2.1.9.4 and 2.1.9.2). 100-fold excess of GE (5µM) was used as a non-specific 11ß-HSD inhibitor.

3.2.1.4. Real Time polymerase chain reaction

RNA was extracted and reverse transcribed from CP and ciliary body explants from three rabbits as described (section 2.1.4.2 and 2.1.5). As the intron exon boundaries were not defined for our genes of interest, total RNA was DNase I treated to remove any genomic DNA contamination (Deoxyribonuclease I, Invitrogen, Paisley, UK) (section 2.1.4.4). Quantity and quality of mRNA was assessed (section 2.1.4.3) prior to real time PCR (methodology detailed in section 2.1.5).

Chapter 3

Primers and probes used for defining 11β-HSD1, GRα and sgk-1 mRNA levels were designed using Primer Express software (Applied Biosystems, Warrington, UK) (Table 3-1). cDNA (50 ng) was used for real-time PCR, to define expression of the three genes of interest (section 2.1.7). All statistics were performed with ΔCt and relative mRNA levels expressed as fold changes ($2^{-\Delta\Delta Ct}$).

Target Gene	Primer Sequence
GRα	Forward 5'-AGAAAGCATCGCGAGCCTC
	Reverse 5'-AGCAGGCGCTGTGCTCC
	Probe - TCGGCTAGTGGTGCAGACAACCCC
11β-HSD1	Forward 5'-CCCACTGCCTGAAGCTGG
	Reverse 5'-GCAAAGGTCATGTCCTCCATG
	Probe - CCTCCGCACACTACATTGCTGGCA
sgk-1	Forward 5'-AGAAAGCATCGCGAGCCTC
	Reverse 5'-AGCAGGCGCTGTGCTCC
	Probe - TCGGCTAGTGGTGCAGACAACCCC

Table 3-1   ***Real time PCR primer sequences***

Primers and probes used in real time PCR. GRα indicates the glucocorticoid receptor α; 11β-HSD1, 11β-hydroxysteroid dehydrogenase type 1; sgk-1, serum and glucocorticoid-regulated kinase1

3.2.1.5.   Cerebrospinal fluid cortisol measurements

The CSF from nine female rabbits was centrifuged at 176g for 2 minutes to remove any contaminating cells, and the CSF supernatant was stored at -80˚C until analysis. The CSF

cortisol was analysed using an ELISA technique according to manufacturer's protocol (Assay Design's Incorporated, Michigan).

3.2.2. Human studies

3.2.2.1. Human tissues and cells

Human tissue and cells were obtained from four sources: (1) Surgically acquired tissue specimens of CP and AGT obtained from the neurosurgical department (University Hospital Birmingham NHS Foundation Trust, UK) from patients undergoing tumour excision; (2) Formalin fixed, snap frozen, and fresh tissue specimens of CP and AGT from the Parkinson's Disease Society Tissue Bank at Imperial College, London, UK (funded by the Parkinson's Disease Society of the United Kingdom, registered charity 948776); (3) A commercial untransformed primary HCPEpi cell line; and (4) An untransformed primary AGEpi cell line established by collaborator Deborah Grzybowski (Grzybowski *et al.* 2006b). Ethical approval was in place for all aspects of the study (Dudley Local Research Ethics Committee (LREC) 06/Q2702/19). Tissue specimens were transported in three different ways; 1) fixed in 10% formalin, 2) fresh frozen, after snap freezing in liquid nitrogen and 3) in sterile pots containing DMEM (Invitrogen, Paisley, UK) supplemented with 1% penicillin and streptomycin (P/S).

3.2.2.2. Immunohistochemistry

Formalin fixed human CP and AGT (n=6) were embedded in paraffin and 5µm sections mounted on electrostatically charged slides (VWR, Lutterworth, UK). Tissue identification was facilitated using H&E staining. AGT was further characterised through staining with vimentin, FVIII and EMA (section 2.1.2.2). Immunolocalisation for 11β-HSD1 and 2 was then conducted as described (sections 2.1.2.1) on CP and AGT. Primary

and secondary antibody dilutions were 1:200 for 11β-HSD1, and 1:100 for 11β-HSD2. Human liver and kidney was utilised as positive control tissues for 11β-HSD1 and 2 respectively, and antibody pre-treated with immunising peptide as a negative control.

3.2.2.3.   Reverse transcriptase polymerase chain reaction

RNA was extracted from fresh frozen CP and AGT as well as from HCPEpi and AGEpi cells using the Genelute mammalian total RNA extraction kit (Sigma-Aldich Company Ltd, Dorset, UK), and reverse-transcribed using Multiscribe reverse transcriptase according to the manufacturer's protocol (Applied Biosystems, Warrington, UK) (section 2.1.4). RNA concentration and quality were confirmed, and standardised mRNA expression was monitored through comparison to housekeeping gene 18s. PCR was carried out using GoTaq DNA polymerase (section 2.1.6).   Primer sequence (Alta Biosciences, Birmingham, UK) and cycle details are listed in Table 3-2.

Gene	Primer	cDNA, bp	Annealing temp	PCR cycles	Accession number
11β-HSD1	5'ACCAGAGATGCTCCAAGGAA 3' 5'ATGCTTCCATTGCTCTGCTT 3'	411	60	30	NM 005525
11β-HSD2	5'TGGAGGTGAATTTCTTTGGC 3' 5'GGATTCTTTAGGCCAGGGTC 3'	774	60	30	U27318
GRα	5'TCGACCAGTGTTCCAGAGAAC 3' 5'TTTCGGAACCAACGGGAATTG 3'	693	60	30	NM 001024094
MR	5'AACTTGCCTCTTGAGGACCAA 3' 5'AGAATTCCAGCAGGTCGCTC 3'	450	60	30	NM 000901
H6PD	5'AGAAGCGAGACAGCTTCCAC 3' 5'GCTGCTGGGAAAAGAACAAC 3'	603	60	30	NM 004285
sgk-1	5'AGGGCAGTTTTGGAAAGGTT 3' 5'GCTTTGTCCTGTCCTTCTGC 3'	699	60	34	NM 005627
Myocilin	5' CTGCCTACAGCAACCTCCTC 3' 5'CTCGCATCCACACACCATAC 3'	399	60	34	NM 000261
5α Reductase 1	5'CAGATCCCCGTTTTCTAATAGG 3' 5'AAACGTGAAGAAAGCAAAAGC 3'	239	60	30	NM 001047.2
5α Reductase 2	5' CTGGAGAAATCAGCTACAGG 3' 5' GCTTTCCGAGATTTGGGGTA 3'	226	60	30	NM 000348.3
AR	5'CGGAAGCTGAAGAAACTTGG 3' 5'ATTTTTCAAGCCCATCCACTG 3'	584	60	34	NM 000044.2
ERα	5'AGACATGAGAGCTGCCAACC 3' 5'GCCAGGCCATTCTAGAAGG 3'	299	55	34	NM 000125.3
ERβ	5'TCACATCTGTATGCGGAACC 3' 5'CGTAACACTTCCGAAGTCGG 3'	346	55	34	NM 001437.2

Table 3-2   *Primer sequences used for PCR*

temp indicates temperature.

3.2.2.4.   11β-HSD assay

Human CP (n = 5) and AGT (n = 2), within 30 hours of post-mortem, were washed in PBS, surgically dissected from surrounding tissue and divided into equal sized pieces (approximately 100 mg). Activity assays were conducted in an identical manner to that described in rabbit tissues (section 3.2.1.3). Enzyme activities were expressed as pmol h^{-1} g^{-1} wet weight.

11β-HSD activity assays were also conducted on HCPEpi and AGEpi cell cultured to 90% confluence in 12 well plates. Cells were washed twice with sterile PBS prior to 24 hour enzyme assay, which was carried out using serum free media. 24 hour incubation was chosen as 11β-HSD oxoreductase reaction kinetics were assessed over a time course (4, 6, 8, 10, 12, 16, 24 h, n = 3) with a linear reaction phase demonstrated between 10 and 24 hours (data not shown). Additionally, enzyme assays carried out on HCPEpi cells of varying passage (range 3-8, n = 6) demonstrated non significant variation with cell passage. However, the HCPEpi cells, at passages greater than 8, altered in morphology and were therefore no longer deemed to be truly representative of epithelial cells and so not utilised.

3.3. Results

3.3.1. Animal studies

3.3.1.1.   Immunohistochemistry

Cross-species reactivity of the 11β-HSD1 anti-human antibody was confirmed using sections of rabbit liver as previously described (Onyimba *et al.* 2006). The rabbit liver probed with the 11β-HSD1 antibody, revealed intracellular staining surrounding the

central vein (Figure 3-1A), a pattern typical of human liver (Ricketts et al. 1998). A pre-adsorbed antibody specifically removed the staining (Figure 3-1B). Sections of whole NZWAR brain demonstrated immunoreactivity confined to the epithelial layer of the CP (Figure 3-1C) that was reduced after prior treatment of the antibody with immunising peptide (Figure 3-1D). Kidney cortical collecting ducts, an area of high 11β-HSD2 expression in the human, stained intensely for 11β-HSD2 in the rabbit (Figure 3-1E), compared to a section incubated with no primary antibody (Figure 3-1F). CP tissue probed with 11β-HSD2 antibody revealed no staining (Figure 3-1G and H).
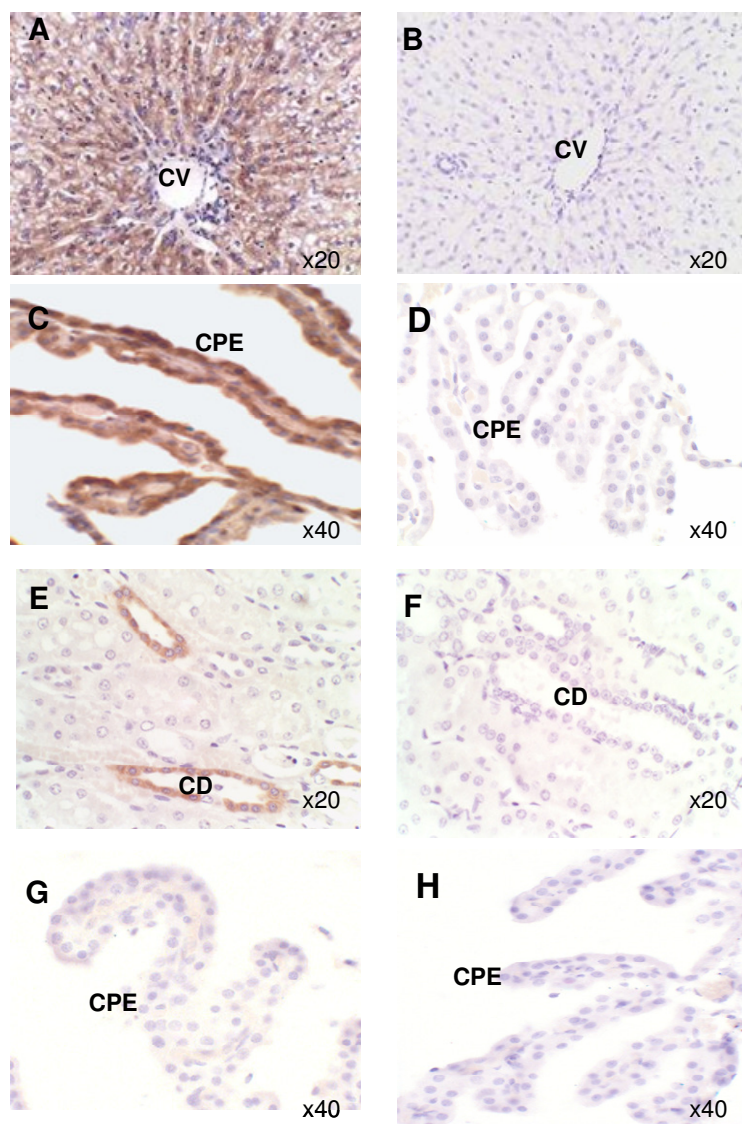
Figure 3-1   Immunohistochemistry using anti- human 11β-HSD1 antibody

Characteristic distribution of 11β-HSD1 staining in the rabbit liver surrounding the central vein (CV) (A). No staining was detected using the pre-adsorbed antibody (B). 11β-HSD1 staining was seen in the choroid plexus epithelial cells (CPE), (C) and was specifically removed with pre-adsorbed immunising peptide (D). Immunohistochemistry using anti-human 11β-HSD2 antibody demonstrated intense staining of the rabbit kidney collecting ducts (CD) confirming cross-species reactivity (E), which was absent when the section was incubated with no primary antibody (F). There was no expression of 11β-HSD2 in the CPE (G), when compared to a section incubated with no primary antibody (H).

3.3.1.2. 11β-HSD activity assays

11β-HSD activity assays confirmed predominant oxoreductase activity in dissected CP (Figure 3-2), and indicated a significantly higher substrate conversion of cortisone to cortisol versus cortisol to cortisone (median conversion 5.0 (range 4.1- 5.6) pmol $h^{-1}mg^{-1}$ versus 1.1 (range 0.7 -1.6) pmol $h^{-1}mg^{-1}$ respectively; $p<0.001$)). Co-incubation with GE reduced both oxoreductase activity and dehydrogenase activity (median conversion 0.2 pmol $h^{-1}mg^{-1}$; $p<0.001$) versus 0.3 pmol $h^{-1}mg^{-1}$; $p<0.05$ respectively).
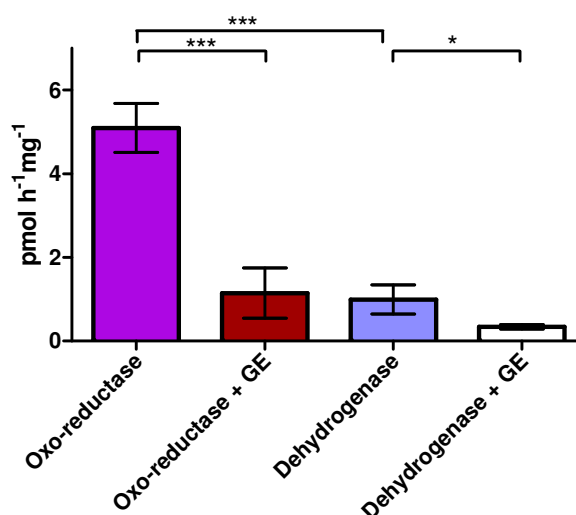
Figure 3-2   ***11β-HSD activity in rabbit choroid plexus***

> *Range plots (median, full range; n=6) show oxoreductase activity was significantly higher than dehydrogenase activity (*** p<0.001). Oxo-reductase and dehydrogenase activities were significantly inhibited when co-incubated with 100-fold excess of glycyrrhetinic acid (GE) (oxoreductase *** p<0.001; dehydrogenase * p<0.05).*

3.3.1.3. Real time polymerase chain reaction

Real time PCR analyses of CP and ciliary body whole tissue revealed comparable expression of 11β-HSD1, GRα and sgk-1 genes in both tissues (Figure 3-3); n=3, ciliary

body:CP ratios: 11β-HSD1, 1:0.9; GRα, 1:0.8; sgk-1, 1:1.2. sgk-1 is a glucocorticoid regulated transcription factor which drives epithelial sodium transport.

ΔCt 16.8 16.6 15.2 14.9 13.4 13.7
SEM 0.1   0.9   0.9   1.0   0.4   0.9
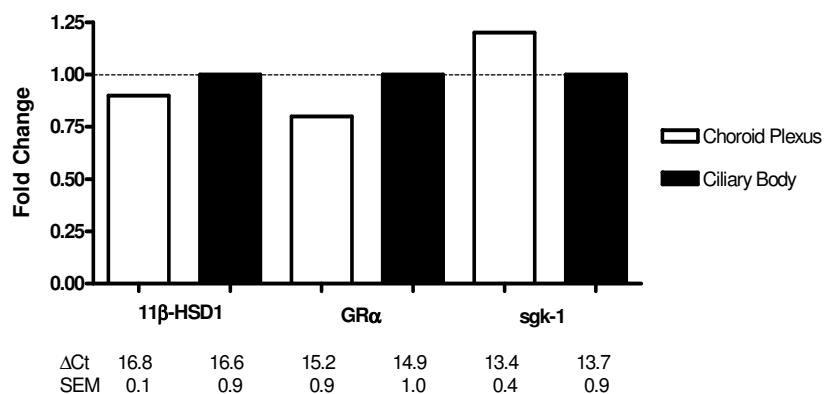
Figure 3-3   Real time (Taq Man) PCR in rabbit choroid plexus and ciliary body

Expression of 11β-HSD1, GRα and sgk-1 in choroid plexus compared to levels in the ocular ciliary body,(n=3). Relative mRNA expression is documented as fold change, ($2^{-\Delta\Delta Ct}$), with ΔCt's and standard error of the mean (SEM).

3.3.1.4.   CSF cortisol enzyme linked immunosorbant assay

Cortisol was detected in rabbit CSF in 6 out of the 9 rabbits, median 1.7 (range 1.4 – 4.3) nmol/l. CSF and cortisol levels were undetectable in 3 rabbits due to the haemolysed nature of the samples.

3.3.2. Human studies

3.3.2.1.   Immunohistochemistry

H&E staining provided confirmatory histology of human CP and AGT (Figure 3-4). Immunohistochemistry in the AGT, confirmed characteristic staining for vimentin in the AG core and cap cell cluster (Kida et al. 1988), compared to a section incubated with no

primary antibody. FVIII specifically stained the AG endothelium but did not stain the cap cell cluster when compared to a section incubated with no primary antibody (Kida et al. 1988). The epithelial cells of the arachnoid cap stained positively for EMA, while the section incubated with no primary antibody did not (Figure 3-5).

11β-HSD 1 antibody showed a characteristic distribution of staining around the liver central vein, which was specifically removed when incubated with a pre-adsorbed antibody (Figure 3-6A and B). The CP epithelium stained positively for 11β-HSD1, this was specifically removed with a pre-absorbed antibody (Figure 3-6C, D, E and F). In the AGT, 11β-HSD1 stained the arachnoid cap cell cluster, compared to sections incubated with a pre-absorbed antibody (Figure 3-4G, H, I and J). No staining was seen when sections of CP or AGT were incubated with anti-human 11β-HSD2 antibody, although kidney collecting ducts stained in a characteristic distribution (data not shown).

3.3.2.2. Reverse transcriptase polymerase chain reaction

Reverse transcriptase PCR of HCPEpi cells, AGEpi cells, human CP tissue and human AGT tissue identified mRNA expression for key elements of the glucocorticoid pathway and sex hormone receptors. 11β-HSD2 was not expressed in tissues or cell lines (Figure 3-7). The HCPEpi cells differed from the human CP tissue in that it did not express oestrogen receptor α or MYOC. 5α Reductase 1 expression was noted in both the HCPEpi and AGEpi cell lines but expression was very weak in the AGT and not seen in the CP tissue. 5α Reductase 2 was not expressed in either tissues or cell lines.
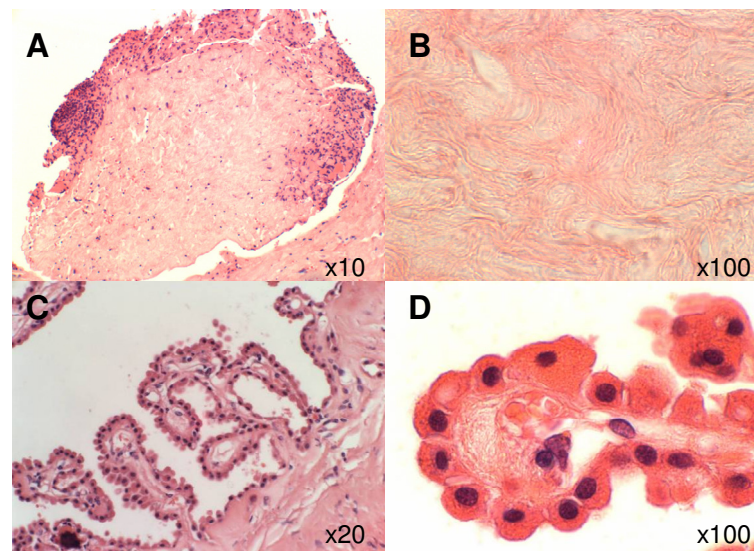
Figure 3-4   ***Haematoxylin and eosin staining***

Confirmatory histology of (A) arachnoid granulation tissue, (B) arachnoid granulation tissue core, (C) choroid plexus and (D) single choroid plexus villus.
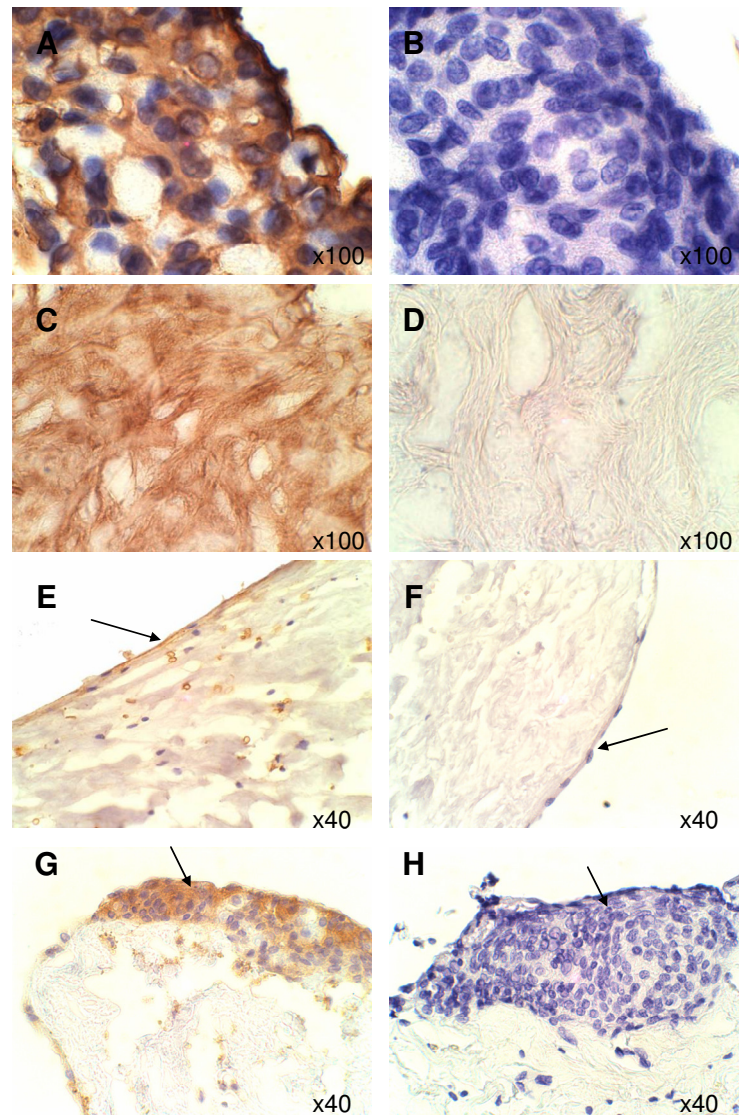
Figure 3-5 *Immunohistochemistry in human arachnoid granulation (AG) tissue*

Anti human vimentin shows characteristic staining in the AG cap cell cluster (A) and core (C) compared to sections incubated with no primary antibody (B) and (D). Anti-human FVIII stained the AG endothelium (arrow, E) compared to a control section with no primary antibody (F). Anti-human EMA stained the arachnoid cells in the AG cap cell cluster (arrow, G) compared to a control incubated with no primary antibody (H).
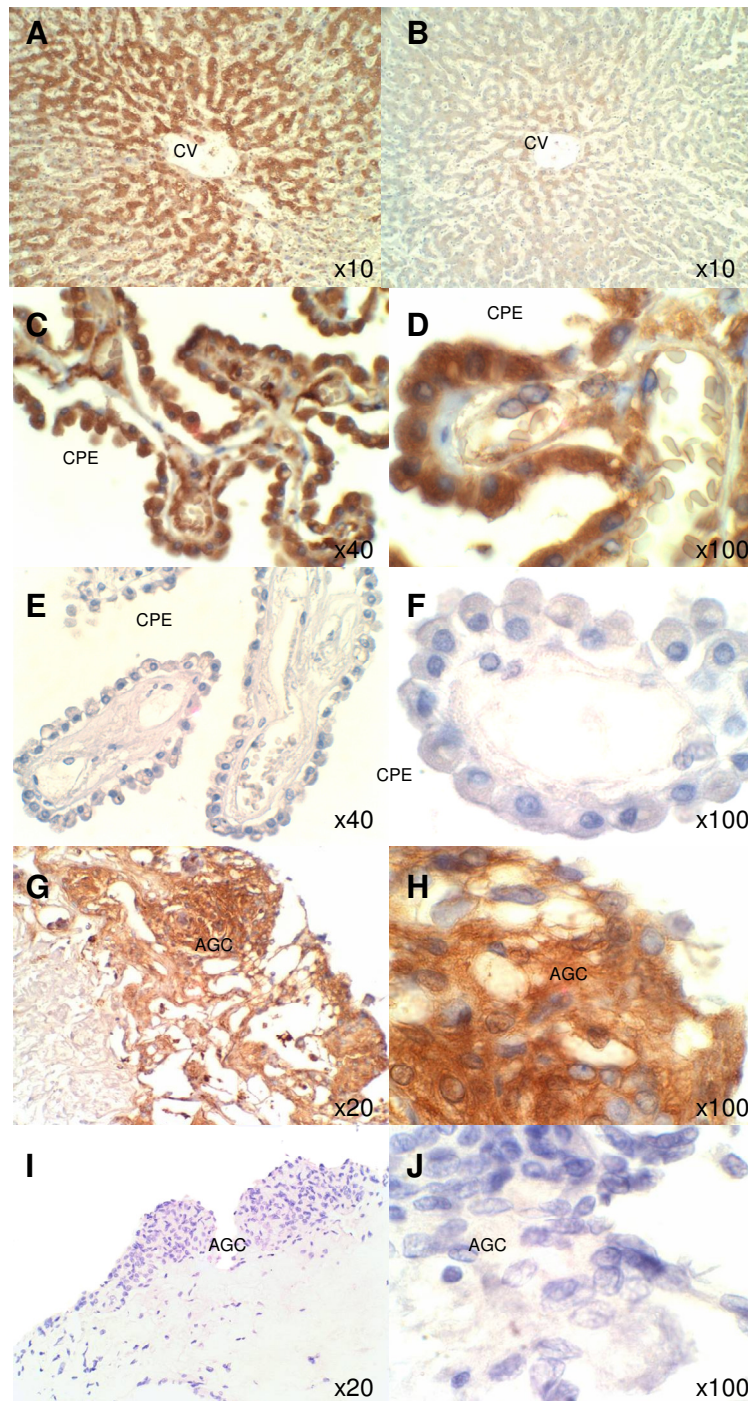
Figure 3-6 ***11β-HSD immunohistochemistry in human choroid plexus and arachnoid granulation tissue***

Characteristic distribution of 11β-HSD1 staining in the human liver surrounding the central vein (CV) (A). Minimal staining when the primary antibody was pre-absorbed with immunising peptide (B). 11β-HSD1 staining in the choroid plexus epithelial cells (CPE) (C, D), specifically removed with pre-adsorbed immunising peptide (E, F). 11β-HSD1 staining in the arachnoid granulation cap cell cluster (AGC) (G, H,) which was specifically removed with pre-adsorbed immunising peptide (I, J).

411 bp						11β-HSD 1
774 bp						11β-HSD 2
693 bp						GRα
450 bp						MR
603 bp						H6PD
699 bp						sgk
399 bp						Myo
239 bp						5α Reductase 1
226 bp						5α Reductase 2
584 bp						AR
299 bp						ER α
346 bp						ER β

HCPEpi AGEpi CP AGT +ve -ve
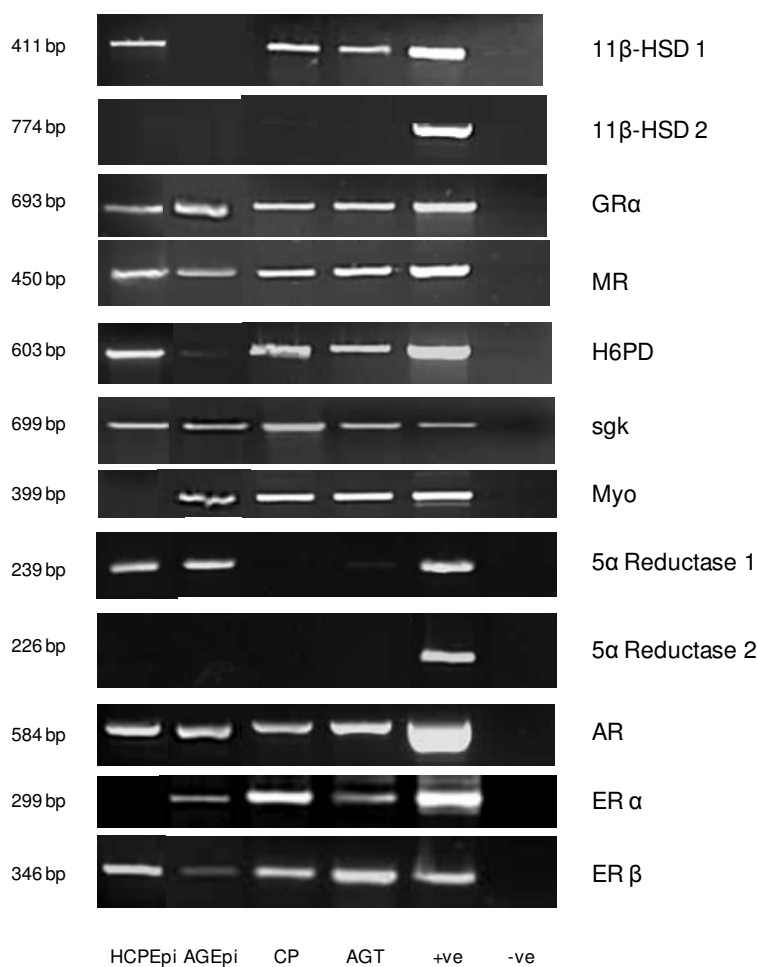
Figure 3-7   Polymerase chain reaction mRNA expression in human choroid plexus and arachnoid granulation primary cells and tissue

Expression of 11β-HSD1, glucocorticoid receptor alpha (GRα), mineralocorticoid receptor (MR), hexose-6-phosphate dehydrogenase (H6PD), serum and glucocorticoid-regulated kinase isoform 1 (sgk),myocilin (myo), 5α reductase 1 and 2, androgen receptor (AR), oestrogen receptor alpha & beta (ERα & β) in a human choroid plexus epithelial cell line (HCPEpi), human arachnoid granulation epithelial cell line (AGEpi), human choroid plexus (CP) and human arachnoid granulation tissue (AGT). Positive controls (+ve) were liver (11β-HSD1, GR, H6PD, sgk-1, 5α reductase 1 and 2); kidney (MR); differentiated adipocyte cell line (11β-HSD2); heart (myocilin); testis (AR) and placenta (ER α & β). Negative control (-ve) no cDNA template.

Chapter 3

3.3.2.3.   11β-HSD assay

3.3.2.3.1   Tissue

11β-HSD assays were performed on CP tissue explants (n=4), all donors were male

patients with Parkinson's disease, none of which had used glucocorticoid therapy, with a

mean age 75 ± 7.4 years. Activity assays were initiated at 23 ± 6 hours (range 16 – 29

hours) post mortem. 11β-HSD activity decreased dramatically after 30 hours post mortem

(data not shown). Activity assays demonstrated predominant oxoreductase (cortisone to

cortisol; 19.0 (range 9.6-29.3) pmol $h^{-1}g^{-1}$ (wet weight)) versus dehydrogenase activity

(cortisone to cortisol; 2.0 (range 0.7-3.1) pmol $h^{-1}g^{-1}$; p<0.001). Oxoreductase activity was

significantly inhibited (0.5 (range 0.0 – 1.0) pmol $h^{-1}g^{-1}$) when co-incubated with 100-fold

excess of GE (p<0.001) (Figure 3-8). No 11β-HSD activity was detected in the AGT.
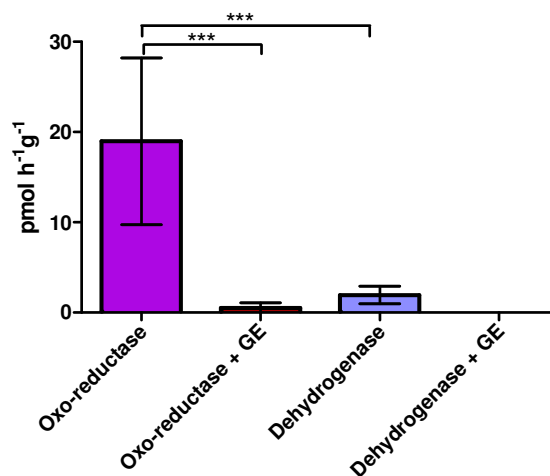
Figure 3-8   11β-HSD activity enzyme assays conducted on whole choroid plexus tissue

Explants (n=4) demonstrated predominant oxoreductase versus dehydrogenase activity (*** p<0.001). Oxoreductase activity was significantly inhibited when co-incubated with 100-fold excess of glycyrrhetinic acid (GE) a non-specific inhibitor of the 11β-HSDs (*** p<0.001).

3.3.2.3.2   Cell lines

Activity studies in HCPEpi cells demonstrated significantly higher oxoreductase activity

(8.7, range 3.5 – 16.2 pmol $h^{-1}mg^{-1}$, n=6) compared to dehydrogenase activity (0.0, range

0.0 – 0.5 pmol $h^{-1}mg^{-1}$, p=0.01, n=4) that was reduced in the presence of GE (Figure

3-9A).
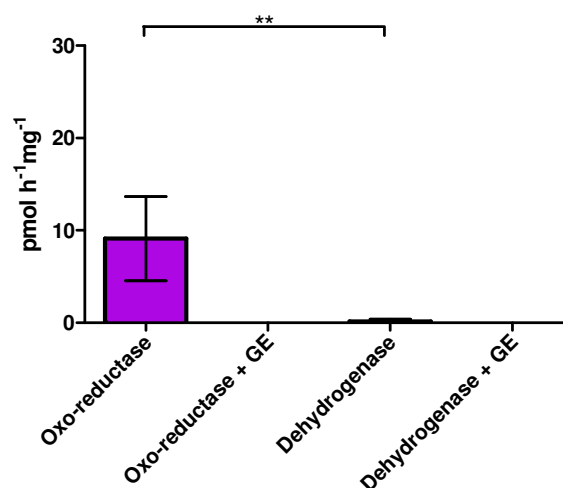
Figure 3-9   11β-HSD activity enzyme assays conducted on a primary choroid plexus cell line

HCPEpi cells incubated with 100nM of cortisol or cortisone in the presence and absence of an 11β-HSD inhibitor (glycyrrhetinic acid) demonstrated predominant oxoreductase activity compared to dehydrogenase (8.7 pmol $h^{-1}mg^{-1}$, n=6 and 0.0 pmol $h^{-1}mg^{-1}$, n=4 respectively, $^{**}p= 0.01$).

3.4. Discussion

3.4.1. Animal studies

Previously, work within the group has shown expression of 11β-HSD1 and epithelial

sodium channels within the ciliary body epithelium, and corticosteroid regulation of sgk-1

via the GR and MR. These data indicate that 11β-HSD1 may be a feature of sodium

transport in the human ocular ciliary epithelium, capable of manipulating IOP (Rauz *et al.* 2001; Rauz *et al.* 2003a; Rauz *et al.* 2003b; Rauz *et al.* 2003c). In our current study, immunohistochemistry localised 11β-HSD1 to the NZWAR CP epithelial cells. This mirrors the localisation of 11β-HSD1 in the NZWAR NPE, the secretary epithelia of the ciliary body (Onyimba et al. 2006).The localisation of 11β-HSD1 to the CP secretary cells is unusual as, with the exception of the ocular ciliary body epithelial cells, most other secretory epithelia express 11β-HSD2 (Burton and Anderson 1983; Rusvai and Naray-Fejes-Toth 1993). We have also shown that the rabbit CP and ciliary body epithelium express similar levels of 11β-HSD1, GRα and sgk-1 mRNA.

The 11β-HSD activity assays demonstrate predominant oxoreductase activity, compared to dehydrogenase activity in the CP tissue, (median conversion 5.0 (range 4.1- 5.6) pmol h^{-1} mg^{-1} versus 1.1 (range 0.7 -1.6) pmol h^{-1} mg^{-1} respectively; p<0.001)) indicating 11β-HSD1 activity. As this is a bi-directional enzyme, it is also likely to have resulted in the minimal dehydrogenase activity demonstrated. 11β-HSD1 mediated dehydrogenase activity possibly reflects cell disruption following dissection of the CP tissue, as has been noted in other systems (Lakshmi and Monder 1988). Since 11β-HSD2 was not localised to the CP by immunohistochemistry, the dehydrogenase activity is unlikely to reflect activity of this isozyme. The level of 11β-HSD activity in the NZWAR CP was comparable to that of the NZWAR ciliary body (oxoreductase median conversion 2.1 (range 1.3- 2.8) pmol $h^{-1}mg^{-1}$ versus dehydrogenase 0.9 (range 0.5-2.0) pmol $h^{-1}mg^{-1}$) (Onyimba et al. 2006).

These data highlight the potential for the NZWAR CP to act as a glucocorticoid target tissue capable of regulating local cortisol availability through 11β-HSD1. 11β-HSD1 may therefore, be involved in regulating sodium transport in the CP, as well as in the ciliary

body, with the potential to influence CSF production and consequently ICP. AGT, through restriction of CSF drainage, is also vital in ICP balance. Unfortunately, it was not possible to study the AGT in the NZWAR as, despite considerable preliminary work dissecting rabbit meninges, AGT could not be reliably identified.

Classically, 11β-HSD1 is not associated with sodium transport. This bidirectional isozyme functions *in vivo* as an oxoreductase, facilitating glucocorticoid mediated responses in key peripheral tissues including liver, adipose and bone (Tomlinson *et al.* 2004b). Hence, within the CNS, it is exciting to speculate that in addition to mediating CSF production, 11β-HSD1 may have a role in regulating CSF cortisol bioavailability. It would be interesting to assess the activity of CP 11β-HSD1 in a variety of neuro-physiological processes associated with elevated CSF cortisol, for example memory loss (Lupien *et al.* 1999; Wolf 2003), CNS ageing (Guazzo *et al.* 1996; Arroyo *et al.* 2005), immune-modulation (Elenkov 2004), and pathological processes such as Alzheimer's disease (Hoogendijk *et al.* 2005).

Traditionally, the origins of CSF cortisol have been attributed to the activation of the HPA axis and diffusion from systemically circulating cortisol across the blood-brain-barrier (BBB) into the CSF (Marynick *et al.* 1976; Marynick *et al.* 1977; Poisson *et al.* 1984). Within the CNS, cortisol binds to the GR, expressed in the hippocampus, amygdala, pre-frontal cortex and hypothalamus (Holmes and Seckl 2006; Nishi and Kawata 2006). These sites also express 11β-HSD1, which may serve to augment intracranial cortisol (Harris *et al.* 2001). CSF cortisol has a degree of self regulation via negative feedback on the HPA axis (Harris et al. 2001; Holmes and Seckl 2006) and according to our data, the CP could act as an alternative local source of cortisol. As many of the other glucocorticoid responsive tissues in the brain (Harris et al. 2001) modulate their own local cortisol

generation via 11β-HSD1, it is likely that the CP cortisol produced, acts in an autocrine fashion. In addition, the identification of key elements of the glucocorticoid response cascade (GR and sgk-1) in the CP, suggest a local mechanism of action for cortisol within the CP.

We measured total CSF cortisol in the rabbit to be 1.7 (range 1.4 - 4.3) nmol/l whilst that in human CSF is reported to range from 4.0 – 8.8 nmol/l (Baker *et al.* 2005). No studies have accurately demonstrated the percentage of CSF cortisol originating from the circulation versus the percent synthesised from within the CNS. In primates and in humans, at low serum cortisol concentrations, the level of CSF cortisol mirrors unbound serum cortisol. This suggests diffusion of unbound serum cortisol across the blood brain barrier (BBB) into the CSF whereas other sources have alluded to a blood-brain cortisol-barrier, possibly mediated by P-glycoprotein, preventing cortisol equilibrating between the serum and CSF (Ueda *et al.* 1992; Karssen *et al.* 2001). This is highlighted by the finding that increased plasma cortisol levels (greater than 300-400 nmol/l) in human adults, are not mirrored by a corresponding rise in CSF cortisol (Guazzo et al. 1996). In addition, CSF cortisol levels vary due to a number of factors such as (i) diurnal variation - this is opposite to that of serum (Kling *et al.* 1994) (ii) stage of the menstrual cycle (Parry *et al.* 2000), (iii) gender - serum cortisol is 19% higher in females (Laughlin and Barrett-Connor 2000) and (iv) age - CSF cortisol levels increase with age (Guazzo *et al.* 1996; Van Cauter *et al.* 1996; Arroyo *et al.* 2005). Isolated measures of CSF cortisol are therefore prone to inaccuracy. Future studies quantifying CSF cortisone, or radiolabelling free circulating cortisol will help define the source of the cortisol within the cerebral ventricles. It is, however, clear that intracranial cortisol levels are not merely a function of systemic cortisol generation by the adrenal glands. Thus, this novel mechanism of cortisol generation by the CP may prove important in CNS neuroendocrine function.

In summary, this is the first description of a cortisol generating system in the CP epithelial cells mediated by 11β-HSD1. Here 11β-HSD1 oxoreductase activity potentiates levels of the biologically active corticosteroid, cortisol. This isozyme is likely to be integral to CP physiology and may be involved in regulating CSF production as well as possibly influencing CSF cortisol levels. Modulation of CSF secretion by CP 11β-HSD1 may have pathogenic implication in IIH. These findings provide a rationale for further characterisation of 11β-HSD and glucocorticoids in human tissue and CSF.

3.4.2. Human studies

3.4.2.1. Expression of 11β-HSD in human choroid plexus compared to rabbit CP

Immunohistochemistry revealed an identical pattern of expression of 11β-HSD isozymes in human tissue sections compared to sections from the NZWAR. 11β-HSD1 localised to the CP epithelial cells in both species. There was no evidence of 11β-HSD2 expression in rabbit or human CP. Previous studies have shown that 11β-HSD2 expression in the brain rapidly declines after birth (Holmes *et al.* 2006c), remaining only in proliferating tissue such as the cerebellar external granular layer and thalamus (Roland *et al.* 1995; Robson *et al.* 1998). In these tissues, 11β-HSD2 inactivation of cortisol is thought to protect the proliferating tissue from cortisol stimulated neuronal damage (Diaz *et al.* 1998; Holmes *et al.* 2006c). MR's in the adult brain are generally not protected by 11β-HSD2, and due to their high affinity for glucocorticoids (ten times that of the glucocorticoid receptor), bind cortisol at basal concentrations potentially mimicking GR action (Funder *et al.* 1988; Funder 1996).

Activity assays in human CP tissue demonstrated predominant 11β-HSD1 activity in keeping with activity in the NZWAR CP. 11β-HSD1 is a bi-directional enzyme and could

therefore have been responsible for the low levels of dehydrogenase activity observed. 11β-HSD1 mediated dehydrogenase activity likely reflects cell disruption following dissection of the CP tissue, as has been noted in other systems (Lakshmi and Monder 1988). Since 11β-HSD2 was not expressed in the CP by immunohistochemistry, the dehydrogenase activity is unlikely to reflect activity of this isozyme.

3.4.2.2.   Characterisation of 11β-HSD in a human choroid plexus epithelial cell line

HCPEpi cells demonstrated a comparable pattern of 11β-HSD activity to human tissue with predominant oxoreductase activity (8.7 (range 3.5-16.2) pmol h$^-$1mg^{-1}) compared to dehydrogenase activity (0.0 (range 0.0-0.5) pmol h$^-$1mg^{-1}, p=0.01) although the level of activity was lower than that established in CP tissue. These differences might be explained by the differences in cell types contained within the CP tissue (epithelial cell as well as CP stroma and capillaries) compared to the HCPEpi cells (exclusively epithelial cells). However, immunohistochemical characterisation did not demonstrate 11β-HSD1 in the CP stroma or capillary network suggesting these components of the CP tissue are unlikely to have significantly contributed to oxoreductase activity. The HCPEpi cells, expressed 11β-HSD1, H6PD, GR, MR and sgk-1 mRNA.

The results from the HCPEpi cells are in keeping with the data from the human CP tissue and further endorse the potential role of glucocorticoids and 11β-HSD1 in the human CP. Additionally, the similarities between HCPEpi cells and CP tissue suggests that the HCPEpi cells may provide a useful model for future *in vitro* work to clarifying the functional role of 11β-HSD1 in the secretion of CSF.

3.4.2.3. Characterisation of 11β-HSD in human arachnoid granulation tissue

We were able to successfully identify human AGT using H&E staining in addition to immunolocalisation with vimentin, FVIII and EMA. The AGT did not demonstrate oxoreductase or dehydrogenase activity. This was surprising as immunohistochemistry localised 11β-HSD1 to the epithelial arachnoid cap cells. It is possible that 11β-HSD activity in the AGT declined rapidly after postmortem. Alternatively the enzyme may be expressed but not active or expressed at very low levels. The AGT did, however, express key elements of the glucocorticoid pathway (GR, MR and MYOC). These results highlight the potential for the AGT to function as a glucocorticoid target tissue. In the ocular environment MYOC induction by glucocorticoids restricts the drainage of AH and elevates IOP (Rozsa *et al.* 2006). It is possible that an analogous mechanism may occur in the AGT, influencing drainage of CSF.

3.4.3. Conclusion

The precise role of CP 11β-HSD1 has yet to be determined. As initially hypothesised, it may have a role in regulating CSF secretion, however, the ramifications of CSF cortisol generation are potentially diverse. CNS glucocorticoids have detrimental effects on the developing foetal cerebellum (Holmes, 2006) as well as anti-inflammatory and immune regulatory properties with the potential to modulate diseases such as Multiple Sclerosis, Behçet's Disease and CNS vasculitis (Sellebjerg *et al.* 2000; Siva *et al.* 2004; Younger 2004). There are also a variety of neuro-physiological processes associated with elevated CSF cortisol, such as memory loss (Lupien et al. 1999; Wolf 2003; Miller and O'Callaghan 2005; Chapman and Seckl 2008), CNS ageing (Guazzo et al. 1996; Arroyo et al. 2005), immune-modulation (Elenkov 2004), and other pathological processes such as Alzheimer's disease (Hoogendijk et al. 2005; Green et al. 2006). Hence, within the CNS,

one could speculate, that in addition to mediating CSF production, CP 11β-HSD1 may have a role in regulating CSF cortisol bioavailability, and thus influence a diverse range of physiological and pathological processes.

In summary, 11β-HSD1 activity is likely to be integral to CP physiology, potentiating levels of biologically active cortisol within the choroid plexus itself and secretion of cortisol into the CSF. 11β-HSD1 driven cortisol generation in the CP may represent an underlying mechanism mediating CSF secretion and ICP dynamics. Inhibition of 11β-HSD1 may, consequently, represent a therapeutic strategy to modulate CSF secretion and ICP.

Chapter 4. NMR-Based Metabolomic Analysis of Cerebrospinal Fluid and Serum in Idiopathic Intracranial Hypertension

Chapter 4

4.1. Introduction

One approach to improving our understanding of disease aetiology, is through defining disease specific, metabolite biomarkers. The study of metabolites (metabolomics) reflects both genetic and environmental factors and consequently has the potential to accurately delineate a disease process. Metabolite biomarkers have the additional advantage of potentially facilitating disease diagnosis and monitoring. The knowledge of disease specific metabolites is particularity important in conditions such as IIH, where disruption of normal metabolic processes, manifesting as obesity and elevated ICP, are key factors in the disease process. Identification of IIH specific metabolites may enhance our understanding of the pertinent, metabolic processes in this condition.

In this study, we aimed to establish a profile of disease specific metabolites in IIH. We also aimed to define metabolite profiles in two control conditions: MS and cerebrovascular disease (CVD). These control conditions were chosen as they represented distinct patho-physiological processes commonly admitted to the neurology unit for diagnostic evaluation. We evaluated whether the metabolite profiles of these conditions, IIH, MS and CVD, could be distinguished from a heterogeneous group of patients who attended for investigation of neurological diseases, using CSF and serum metabolic profiling. In addition, we aimed to validate the metabolite biomarker profiles, by demonstrating that the profiles identified, could be used to predict diagnosis in a second cohort of patients (prospectively collected in succession) whose diagnosis were masked.

4.2. Method

4.2.1. Patients

Patients were recruited from University Hospital Birmingham NHS Foundation Trust and Sandwell & West Birmingham Hospitals NHS Trust, UK. Cohort 1 study subjects consisted of a heterogeneous group of patients under investigation for neurological symptoms. All patients underwent lumbar puncture (LP) as part of their routine investigations. Subjects were excluded if aged less than 16 years or if unable to give written, informed consent. Patients with IIH were recruited at the time of initial presentation or following a clinical deterioration. They were diagnosed according to the updated modified Dandy Criteria (Friedman and Jacobson 2002). Subjects with MS were recruited during remission following a presenting, clinically isolated syndrome. Only those who went on to fulfil the McDonald criteria (McDonald *et al.* 2001), were included in the MS cohort. To avoid confounding effects of acute illness, patients with CVD were recruited during convalescence, after imaging confirmation of a cerebrovascular accident. All patient notes were reviewed at one year to confirm diagnosis. Those subjects having no neurological diagnosis and normal neurological investigations one year after recruitment were classified as "no diagnosis identified". Clinical details including medical history, investigations, current medication and time of last meal were noted for each subject. Anthropological measures were recorded; BMI was calculated as weight in kg/ height in m^2. Permission for the study was obtained from the local research ethics committee (Solihull LREC 04/Q2706/65 approved 15/01/2005), all participants gave written informed consent.

4.2.2. Samples

All LPs were carried out with the patient in the left lateral position, whilst breathing regularly (Neville and Egan 2005) and CSF opening pressure was measured by direct manometry. CSF and blood samples were collected at the time of LP and transported on ice, before being promptly centrifuged at 176 g for 10 minutes and aliquoted. All samples were stored at -80°C and analysed after a maximum of one freeze-thaw cycle. Thawed samples (300μl) were centrifuged at 1000 rpm for 2 minutes, prior to dilution 1:1 with deuterium oxide containing NaCl (150mM), TMSP (2.5mM) and sodium phosphate (20mM) pH 7.4.

4.2.3. Experimental outline

CSF and serum samples were processed and analysed separately. 1D and 2D JRES spectra were acquired from patients with IIH, MS, CVD as well as from those subjects under investigation for other neurological diseases (see section 2.2.1). Multivariate pattern recognition analysis was used to evaluate the NMR spectra and determine disease specific metabolite biomarkers (cohort 1). A second cohort of CSF and serum samples with unknown diagnosis were then prospectively collected (cohort 2) from consecutive patients, using the same technique and inclusion and exclusion criteria as for cohort 1. The ability of metabolite biomarker profiles, defined in cohort 1, to identify undiagnosed patients in cohort 2, were then assessed (Figure 4-1).

4.2.4. Evaluation of disease specific metabolite profiles in matched cohorts

Phenotypic features are known to influence metabolite profiles (Holmes *et al.* 2008). To reduce the effects of phenotype (gender, age, BMI) influencing the metabolite profile, the

disease groups were also compared to control subjects, matched for gender, age (± 5 yr) and BMI (± 2 kgm^{-2}).

4.2.5. Evaluation of experimental technical variance

Five patients evaluated in cohort 1 were re-analysed at the start of cohort 2 processing, to evaluate technical variance between cohort 1 and 2. These five patients were further analysed at the end of cohort 2 to evaluate technical variance within cohort 2.
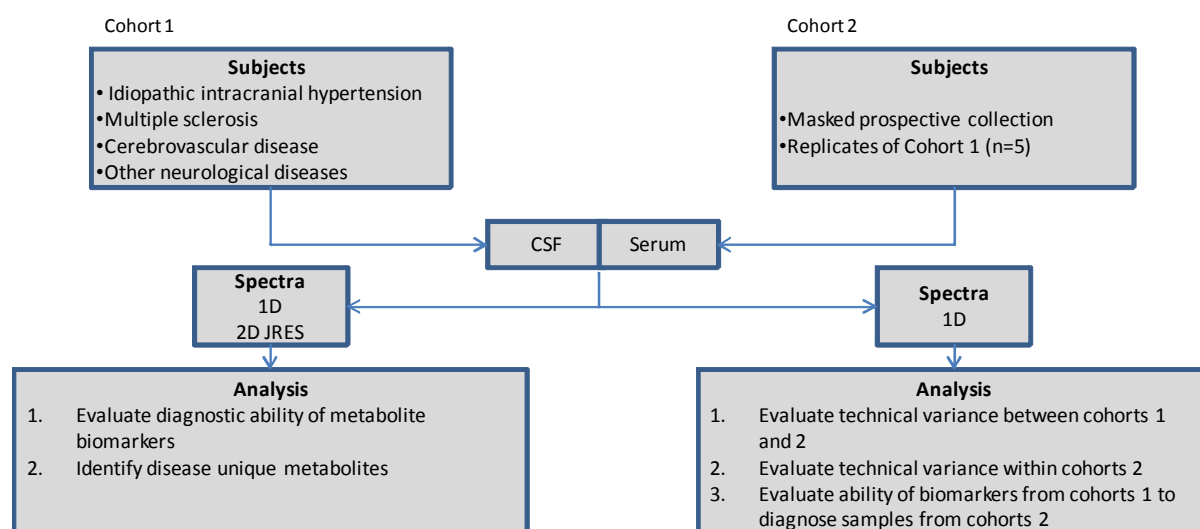
Figure 4-1   NMR metabolomics experimental design

4.2.6. Statistical analysis

Data were analysed using cluster modelling techniques, PCA and PLS-DA using PLS_Toolbox (version 3.5, Eigenvector Research, Washington, USA) within MATLAB (see section 2.2.1.1). The PLS-DA model was cross-validated using Venetian blinds. Disease specific metabolite profiles were identified in IIH, MA and CVD for cohort 1 from the PLS-DA model. The cohort 1 metabolite profiles were then used to predict the diagnosis of patients from cohort 2.Results are expressed as sensitivity (the proportion of

positive (diseased) subjects who test positive with the biomarker profile) and specificity (the proportion of negative (control) subjects who test negative with the biomarker profile) (Loong 2003). Positive and negative predictive values are not quoted, as they are dependent on the underlying prevalence of disease in a population. Thus they would not be appropriate in our study, as the disease cohorts are not representative of population prevalence. We quote the positive likelihood ratios (the increased probability of disease if the test is positive) and negative likelihood ratios (the decreased probability of disease if the test is negative). Continuous data were summarised using means and standard deviations, or medians and ranges for non-normally distributed data.

4.3. Results

4.3.1. Patient characteristics

CSF (n = 87) and matching serum (n = 72) samples were collected from the study population (cohort 1). The number of serum samples processed was less than that of CSF due to sample loss. Patient characteristics for cohort 1 are shown in Table 4-1. The diagnoses of the patients in the "other diseases" group are given in Table 4-2, which included 11 patients with no neurological diagnosis. The IIH patients were significantly younger (p < 0.001), had higher BMIs (p = 0.02) and higher LP opening pressures (p < 0.001) than subjects in the other groups. There were no consistent medication trends in the diagnostic groups (in the IIH cohort only one patient was taking acetazolamide).

The prospective patient cohort (cohort 2), comprised CSF and serum samples from twenty five consecutively collected patients whose diagnoses were masked. Following NMR spectral acquisition and processing, patient diagnosis was established from medical records. Eight patients were diagnosed with IIH (Friedman and Jacobson 2002) and three

with MS (McDonald et al. 2001), while there were no patients with CVD in this cohort. The remaining subjects, comprised a group with mixed neurological diseases (Table 4-2). The patient characteristics of cohort 2 are shown in (Table 4-3). The IIH patients had higher BMIs (p< 0.001) and opening pressures (p< 0.001) than patients in other diagnostic groups.

Characteristic		**IIH**	**MS**	**CVD**	**Other**
Number	CSF	25	12	9	41
	Serum	17	11	9	35
Age [a]	CSF	$29.3 \pm 7.5^{***}$	38.0 ± 10.4	58.9 ± 7.6	48.9 ± 13.3
	Serum	$28.2 \pm 7.7^{***}$	37.6 ± 10.8	58.1 ± 7.5	50.1 ± 13.8
Female (%)	CSF	100^{**}	75.0	50.0	66.7
	Serum	100^{*}	81.8	44.4	65.7
BMI [a] (kgm^{-2})	CSF	$34.8 \pm 5.4^{**}$	27.2 ± 5.9	26.7 ± 5.2	29.1 ± 8.1
	Serum	$34.9 \pm 6.1^{**}$	27.3 ± 6.2	26.7 ± 5.2	28.9 ± 8.0
Opening pressure [a] (cm CSF)	CSF	$35.9 \pm 6.2^{***}$	17.1 ± 3.5	18.3 ± 4.6	19.3 ± 8.5
	Serum	$35.8 \pm 7.3^{***}$	17.1 ± 3.8	17.3 ± 5.3	19.6 ± 9.2
CSF Glucose [a]	CSF	3.6 ± 1.0	3.3 ± 0.4	3.7 ± 0.8	3.5 ± 0.6
	Serum	3.7 ± 1.2	3.3 ± 0.4	3.7 ± 0.8	3.6 ± 0.7
CSF Protein [a]	CSF	0.3 ± 0.1	0.4 ± 0.2	0.4 ± 0.1	0.6 ± 0.8
	Serum	0.3 ± 0.1	0.4 ± 0.1	0.5 ± 0.4	0.6 ± 0.9

Table 4-1   Subject characteristics for cohort 1

a Mean ± standard deviation. Characteristics of each diagnostic group are compared to all other groups including the "other" controls. The IIH group was significantly younger, more obese and had a higher opening pressure than all other groups including "other" controls. *** p < 0.001, ** p <0.01, * p < 0.05. IIH = idiopathic intracranial hypertension, MS = multiple sclerosis and CVD = cerebrovascular disease.

Clinical diagnosis	Number of cases	
	Cohort 1	Cohort 2
No diagnosis identified	11	
Headache or migraine	6$^{\#\#}$	4
Motor neurone disease	2	1
Peripheral neuropathy	2	2
Dementia/Alzheimer's disease	1$^{\#}$	1
Aseptic meningitis	1	
Cervical myelopathy	1	
Cerebral vasculitis	2	1
Secondary intracranial hypertension	1	
CNS tumour	1$^{\#}$	2
Mixed connective tissue disease	1	
Subarachnoid haemorrhage	1$^{\#}$	
Spastic paraparesis	1	
Uveitis	1	
Unexplained optic neuropathy	1	
CNS Inflammation	1	
Parkinson's Disease	1	
Spinal cord infarct	1	
other	5$^{\#}$	4
Total	**41**	**14**

Table 4-2   ***Clinical diagnoses in patients comprising the "Other diseases" group***

$^{\#}$ *indicates that a single serum sample was lost and subsequently not processed,* $^{\#\#}$ *refers to two lost samples.*

Characteristic	IIH	MS	Other
Number	8	3	14
Age [a]	32.0 ± 8.1	50.7 ± 19.1	47.4 ± 16.9
Female (%)	87.5	100	64.3
BMI [a] (kgm^{-2})	$38.2 \pm 6.7^{***}$	21.0 ± 2.3	26.1 ± 4.8
Opening pressure [a] (cm CSF)	$34.1 \pm 6.2^{***}$	13.0 ± 1.0	16.6 ± 3.7
CSF Glucose [a]	3.6 ± 0.7	3.3 ± 0.4	3.5 ± 0.8
CSF Protein [a]	0.3 ± 0.1	0.5 ± 0.2	0.7 ± 0.5

Table 4-3   ***Subject characteristics cohort 2***

> *[a] Mean ± standard deviation. Characteristics of each diagnostic group are compared to all other groups including the "other" controls. The IIH group was significantly more obese and had a higher opening pressure than MS patients and "other" controls. *** p < 0.001. IIH indicates idiopathic intracranial hypertension and MS indicates multiple sclerosis.*

4.3.2. Cohort 1 CSF metabolomics

NMR spectra were excluded from further analysis if they displayed poor data quality, such as distorted baselines or unusually broad peak widths or had T2 Hotellings and Q residuals outside a 95 % confidence interval. Those with outlying metabolite profiles due to disease diversity were maintained in the analysis.

4.3.2.1. Cohort 1, 1D CSF spectra- whole cohort analysis

Eighty-seven CSF spectra were acquired. A glog $1x10^{-6}$ was applied to transform the spectra. Eleven samples were excluded from further analysis due to technically abnormal spectra (Figure 4-2A, B). The PCA scores plots illustrate partial clustering of data, particularly in the IIH and MS cohorts (Figure 4-2C). Data were then used to build a PLS-

DA model to distinguish those spectra based on prior knowledge of the diagnostic groups (Figure 4-2D).
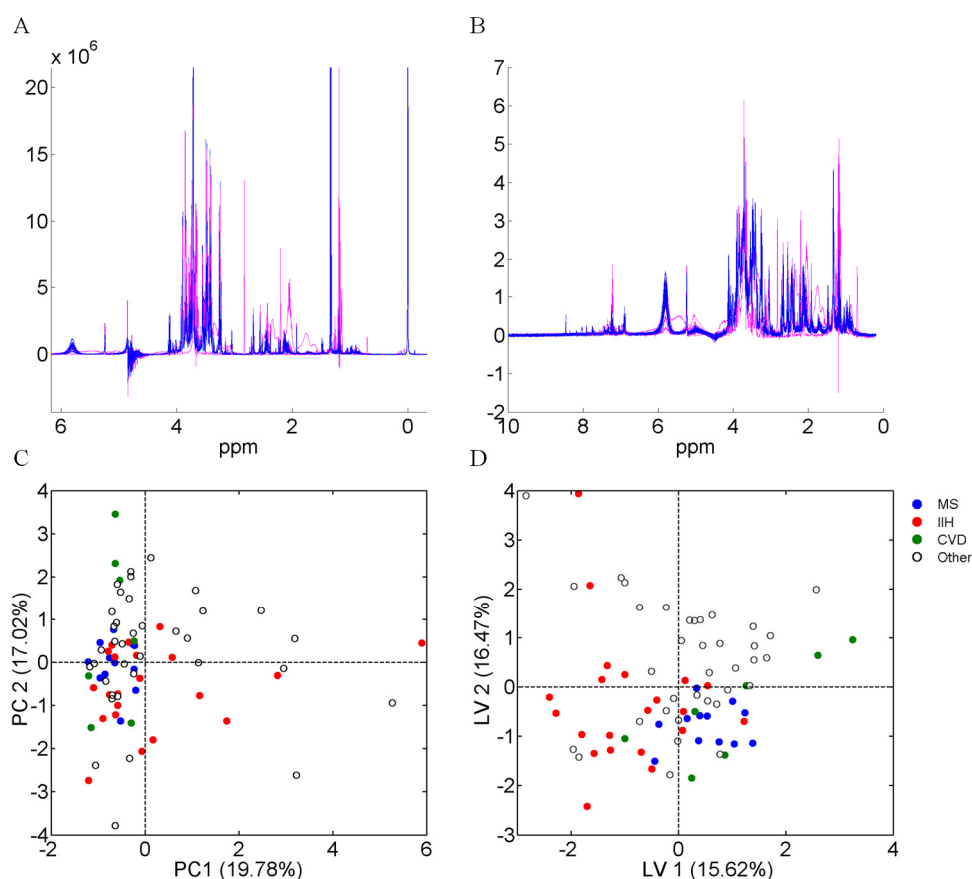
Figure 4-2   ***Cohort 1, 1D CSF spectra whole cohort analysis***

> *Raw CSF spectra (A) and glog transformed, normalised, binned NMR spectra (B). Outlying spectra are shown in pink and have been excluded from further analysis. The PCA scores plot show the CSF spectra acquired (C) This unsupervised analysis illustrates partial clustering of spectra for the diagnostic groups. PLS-DA scores plot show CSF spectra acquired (D).*

Following cross-validation with Venetian blinds, the sensitivity and specificity of the PLS-DA model for predicting diagnosis of each diagnostic group was; 71% and 70% respectively for IIH, 83% and 53% respectively for MS, and 57% and 67% respectively for CVS (Figure 4-3A,B and C).
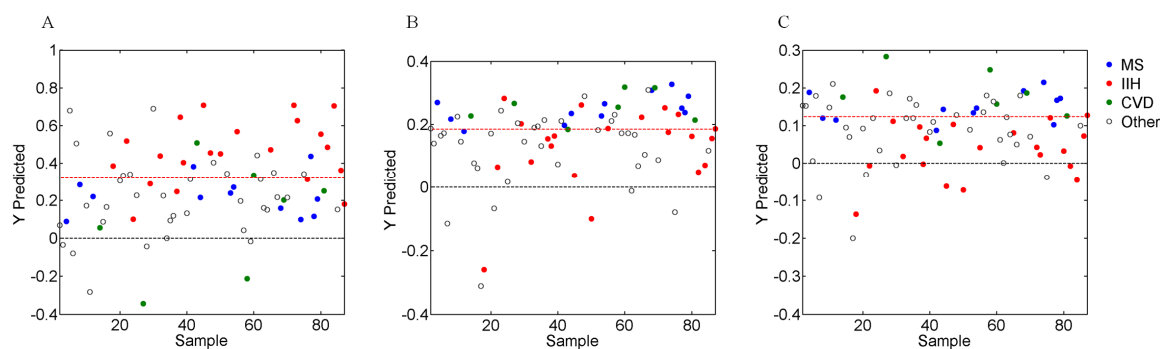
Figure 4-3   ***Cohort 1, 1D CSF spectra whole cohort prediction plots***

> *The PLS-DA model identifies subjects with (A) IIH (sensitivity 71% and specificity 70%) using a prior cut-off of 0.32 for class membership. (B) Subjects with multiple sclerosis (MS) were identified (sensitivity 83% and a specificity 53%) using a prior cut-off of 0.19 for class membership. (C) Subjects with cerebrovascular disease were identified (sensitivity 57% and specificity 67%) using a prior cut-off of 0.11 for class membership.*

4.3.2.2. Cohort 1, 1D CSF spectra- matched analysis

Diagnostic groups (IIH, MS and CVD) were further compared to a matched cohort with mixed neurological diseases, to eliminate bias in the regression model due to phenotype. PCA illustrated clustering of IIH patients (n=10) and matched controls (n=10) which was enhanced in the PLS-DA model (Figure 4-4A, B and C). Cross validation of the PLS-DA model confirmed a sensitivity of 80% and a specificity of 80%, using a cut-off of 0.41 for class membership. Patients with MS (n=10) were compared to matched controls (n=10) (Figure 4-4D, E and F). Clear discrimination was seen between classes using PLS-DA modelling, sensitivity 80% and specificity 80%, using a cut-off of 0.50 for class membership. Patients with CVD (n=7) were not as clearly separated from matched controls (n=7) (Figure 4-4G, H and I), sensitivity 57% and specificity 71% (cut-off for class membership of 0.50).
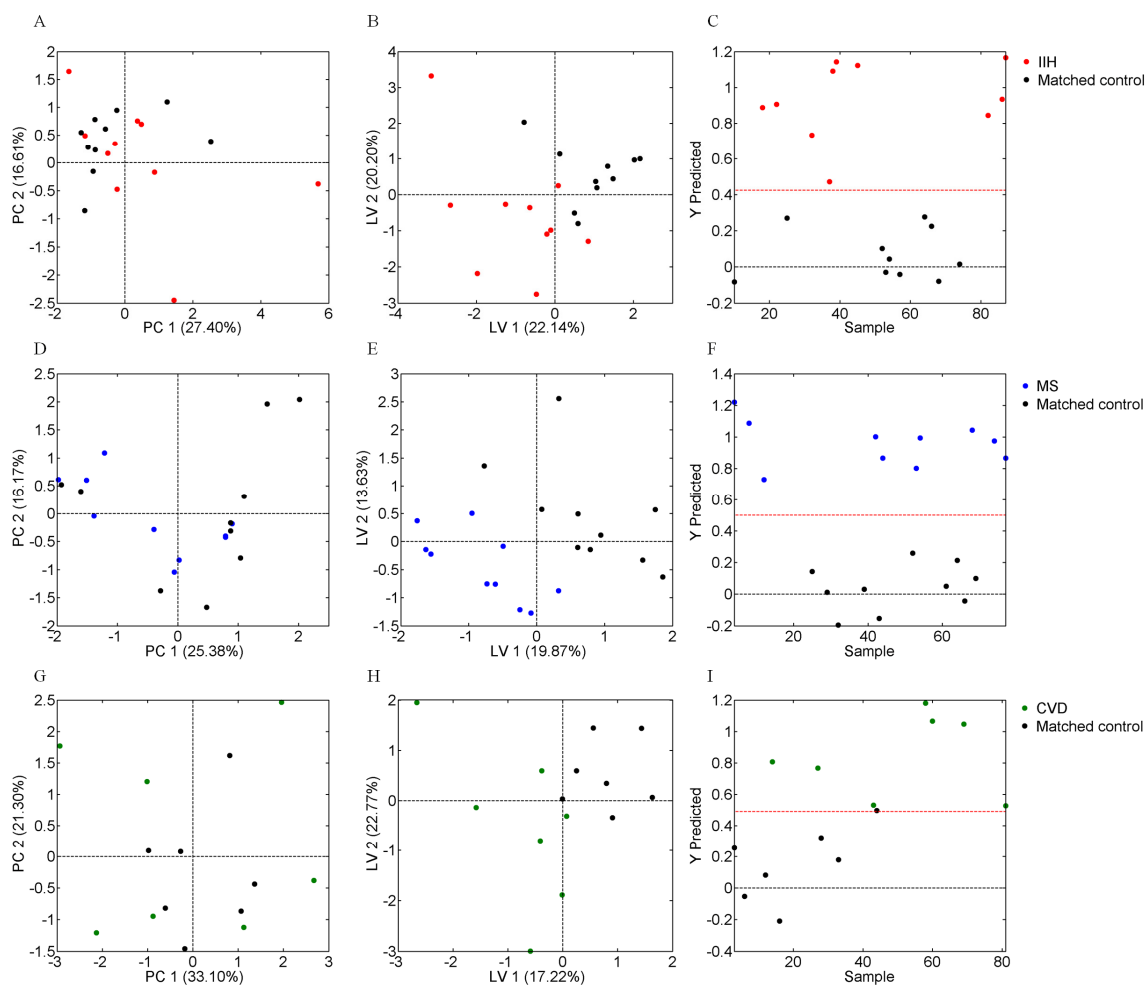
Figure 4-4   Cohort 1, 1D CSF spectra matched analysis

IIH compared to a matched control group, PCA (A), PLS-DA (B) and prediction plot (80% sensitivity and 80% specificity) (C). MS compared to a matched control group, PCA (D), PLS-DA (E) and prediction plot (80% sensitivity and 80% specificity) (F). CVD compared to a matched control population, PCA (G), PLS-DA (H) and prediction plot (57% sensitivity and 71% specificity) (I).

4.3.2.3.   Cohort 1, 2D CSF spectra- whole cohort analysis

Eighty-seven 2D CSF spectra were acquired; a glog $1x10^{-5}$ was applied to transform the spectra. Nine samples were excluded from further analysis due to technically abnormal

spectra (Figure 4-5A, B). The PCA scores plot showed limited clustering of data (Figure 4-5C) but separation was improved in the PLS-DA model (Figure 4-5D).
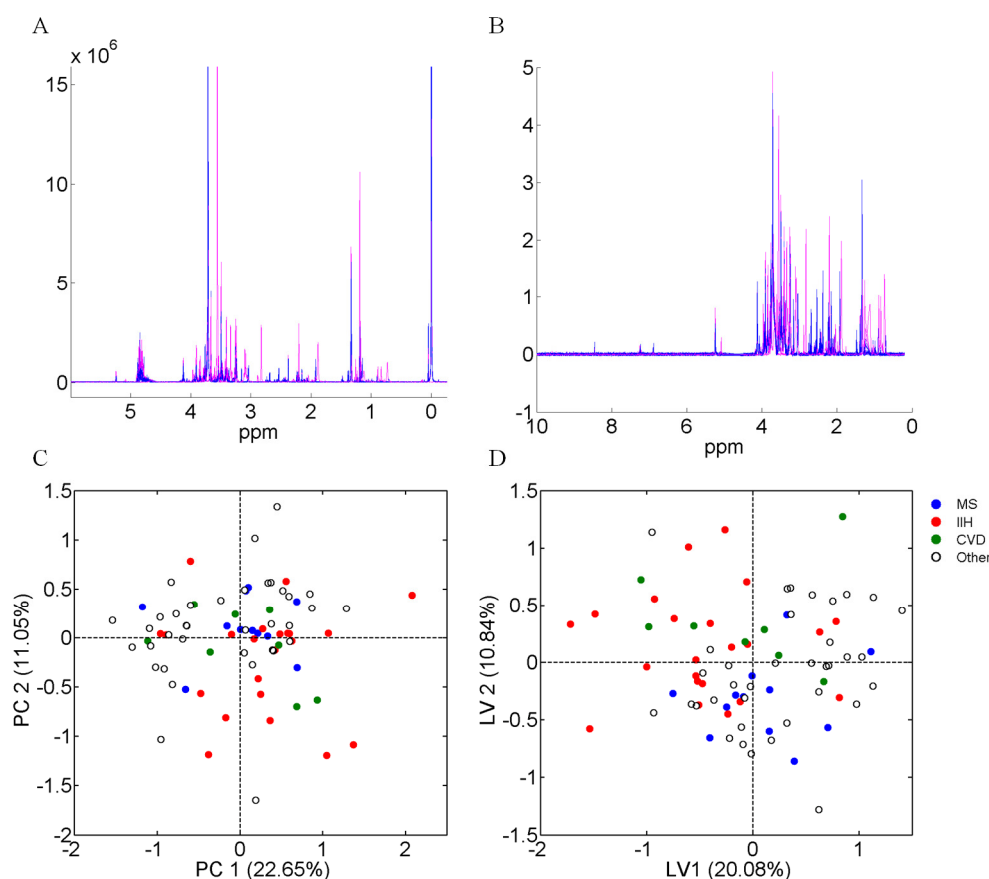
Figure 4-5   Cohort 1, 2D CSF spectra whole cohort analysis

Raw CSF spectra (A) and glog transformed normalised binned NMR spectra (B). Outlying spectra, shown in pink, have been excluded from further analysis. PCA scores plot showing the CSF spectra acquired (C) This unsupervised analysis illustrates limited clustering of spectra for the diagnostic groups. PLS-DA scores plot showing CSF spectra acquired (D).

Following cross-validation with Venetian blinds, the sensitivity and specificity of the PLS-DA model for predicting diagnosis of each diagnostic group was 64% and 75% respectively for IIH, 67% and 44% respectively for MS, and 0% and 66% respectively for CVD.
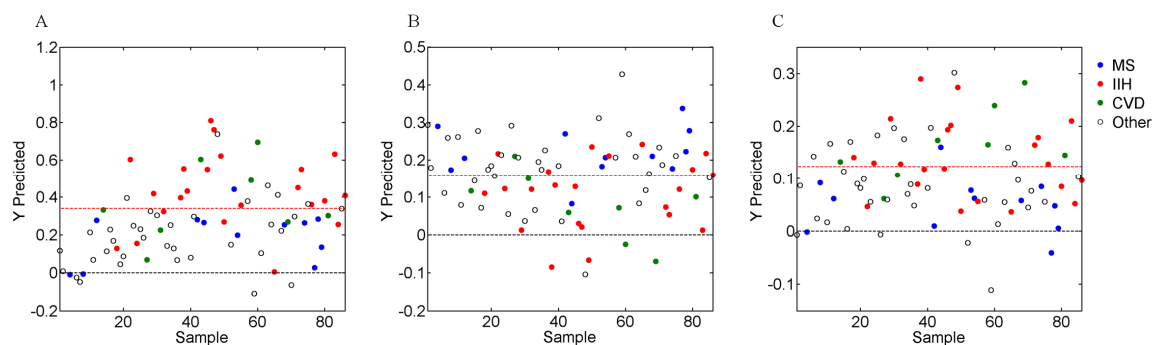
Figure 4-6   ***Cohort 1, 2D CSF spectra whole cohort prediction plots***
The PLS-DA model identifies subjects with (A) IIH (sensitivity 64% and specificity 75%) using a prior cut-off of 0.33 for class membership. (B) Subjects with multiple sclerosis (MS) were identified (sensitivity of 67% and a specificity of 44%) using a prior cut-off of 0.16 for class membership. (C) Subjects with cerebrovascular disease were identified (sensitivity 0% and specificity 66%) using a prior cut-off of 0.13 for class membership.

4.3.2.4.   Cohort 1, 2D CSF spectra- matched analysis

The 2D spectra of the diagnostic groups were compared to a matched (age, gender and BMI) control cohort with mixed neurological diseases. PCA and PLS-DA models were used to distinguish the IIH patients from matched controls (n=10) (Figure 4-7A, B). The PLS-DA model was found to have a sensitivity of 60% and a specificity of 80%, using a cut-off of 0.48 for class membership (Figure 4-7C). The PCA and PLD-DA model of the MS cohort was separated from the matched control population (n=10) with a sensitivity of 50% and a specificity of 80%, 0.59 was the cut-off for class membership (Figure 4-7D, E and F). The model was not accurate in distinguishing patients with CVD from matched controls (n=8) (sensitivity 88% and specificity 13%), prior cut-off of 0.62 for class membership (Figure 4-7G, H and I).
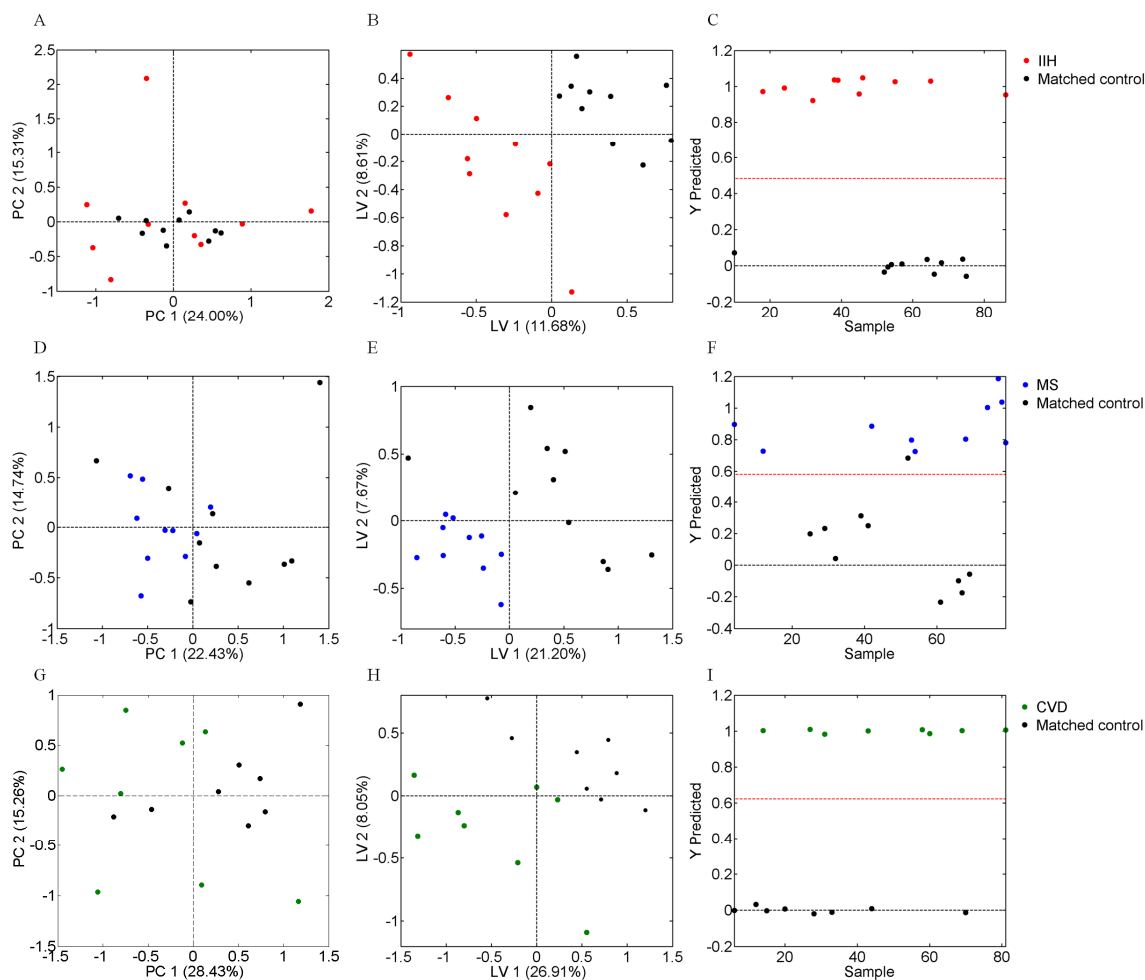
Figure 4-7   ***Cohort 1, 2D CSF spectra matched analysis***

> *IIH compared to a matched control group, PCA (A), PLS-DA (B) and prediction plot (60% sensitivity and 80% specificity) (C). MS compared to a matched control group, PCA (D), PLS-DA (E) and prediction plot (50% sensitivity and 80% specificity) (F). CVD compared to a matched control population, PCA (G), PLS-DA (H) and prediction plot (88% sensitivity and 13% specificity) (I).*

4.3.3. Cohort 1 serum metabolomics

4.3.3.1. Cohort 1, 1D serum spectra- whole cohort analysis

Analysis of the serum spectra (n= 72), identified two technically anomalous spectra which were excluded. A glog $1x10^{-6}$ was used to transform the spectra (Figure 4-8A, B). PCA of

the serum spectra revealed limited clustering for each diagnostic group (Figure 4-8C).

PLS-DA revealed modest data clustering (Figure 4-8D), but this was not as prominent as

that observed for the 1D CSF spectra.
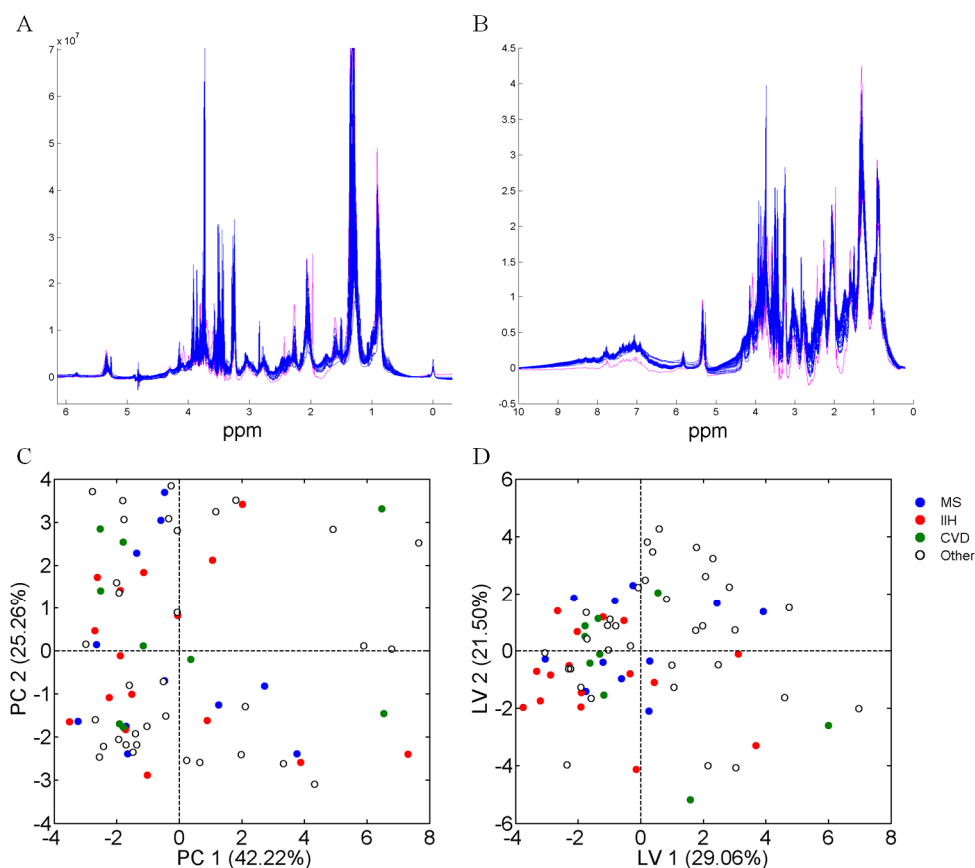
Figure 4-8   Cohort 1, 1D serum spectra whole cohort analysis

Raw CSF spectra (A) and glog transformed, normalised, binned NMR spectra (B). Outlying spectra are shown in pink and have been excluded from further analysis. Serum PCA scores plot (C) and PLS-DA scores plot (D).

Using Venetian blinds to cross-validate the PLS-DA model, the sensitivity and specificity

in predicting the diagnosis of each group were 50% and 83% respectively for IIH, 27%

and 70% respectively for MS, and 27% and 69% respectively for CVD (Figure 4-9A,B

and C).
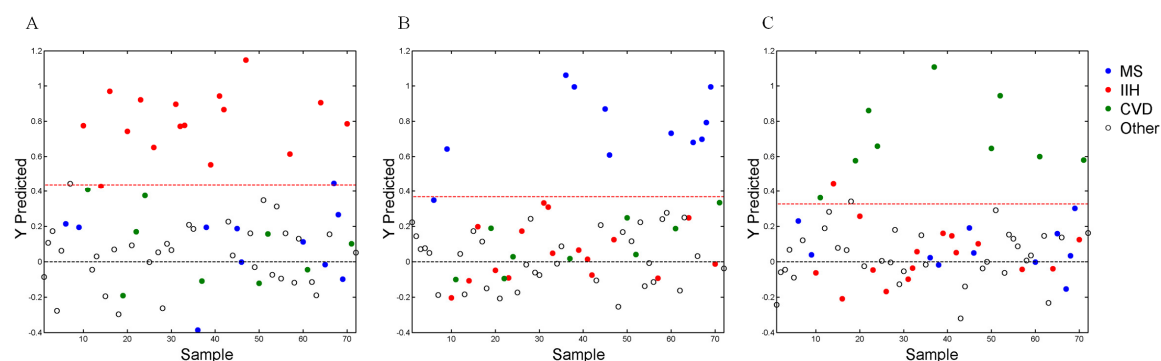
Figure 4-9   Cohort 1, 1D serum spectra- whole cohort prediction plots

The PLS-DA model identified subjects with (A) IIH (sensitivity 50% and specificity 83%) using a prior cut-off of 0.42 for class membership. (B) Subjects with multiple sclerosis (MS) were identified (sensitivity of 27% and a specificity of 70%) using a prior cut-off of 0.38 for class membership. (C) Subjects with cerebrovascular disease (CVD) were identified (sensitivity 27% and specificity 69%) using a prior cut-off of 0.33 for class membership.

4.3.3.2.   Cohort 1, 1D serum spectra- matched analysis

The diagnostic groups were compared to a matched (age, gender and BMI) control cohort with mixed neurological diseases. Discrimination of the IIH cohort (n=10) from matched controls (n=10) was not as pronounced as that observed with 1D CSF spectra. The PLS-DA model was able to identify patients with IIH (sensitivity 70% and specificity 78%, using a cut-off of 0.39 for class membership) (Figure 4-10A, B and C). The MS cohort (n=10) was not clearly distinguished from a matched cohort with PCA or PLS-DA modelling, with validation of the PLS-DA model exhibiting a sensitivity of 70% but a specificity of 20% (cut-off for class membership of 0.19) (Figure 4-10D,E and F). Of note, however, patients with CVD were clearly distinguished from matched controls (n=7) using PCA and PLS-DA models. The PLS-DA model revealed a sensitivity of 75% and a

specificity of 75% when cross validated and using a cut-off of 0.50 for class membership

(Figure 4-10G,H and I).
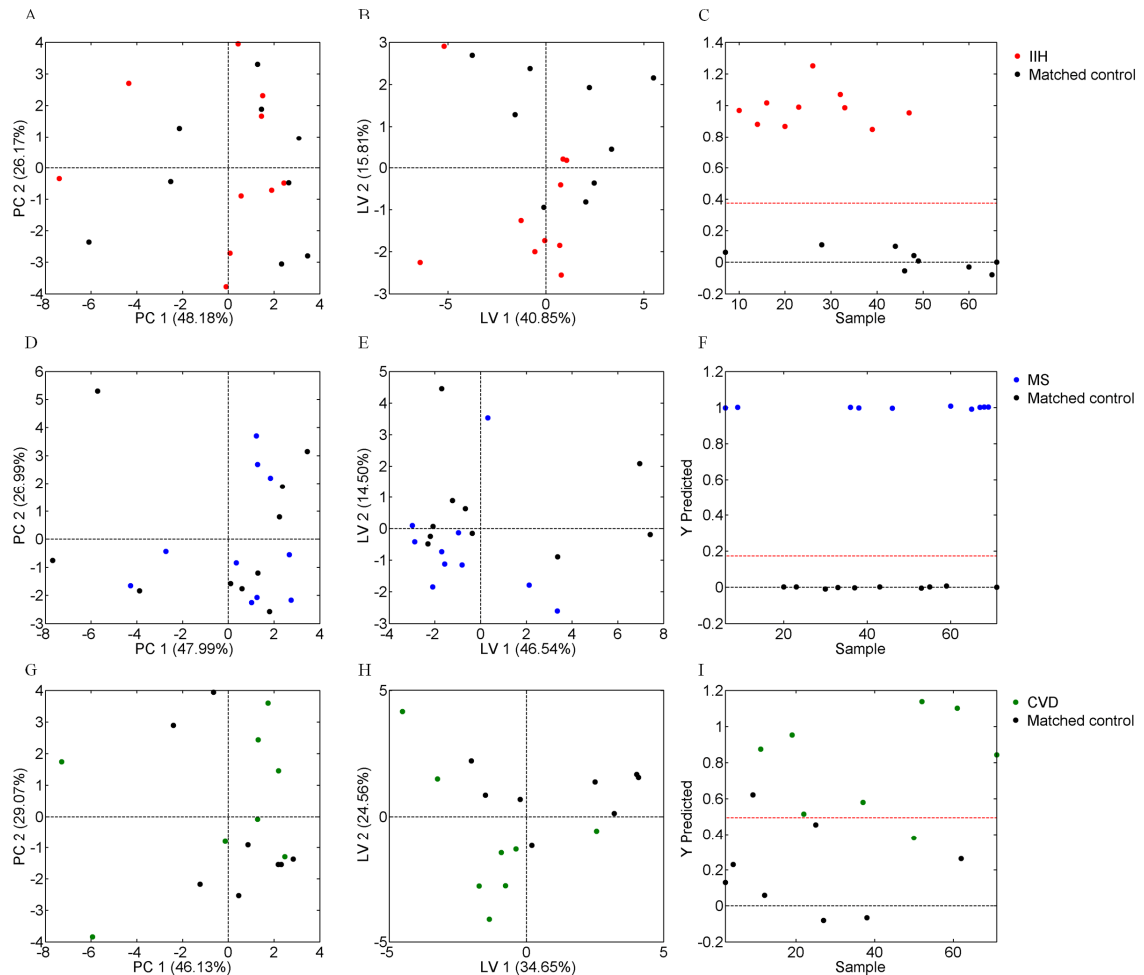
Figure 4-10   Cohort 1, 1D serum spectra matched analysis

IIH compared to a matched control group, PCA (A), PLS-DA (B) and prediction plot (70% sensitivity and 78% specificity) (C). MS compared to a matched control group, PCA (D), PLS-DA (E) and prediction plot (70% sensitivity and 20% specificity) (F). CVD compared to a matched control population, PCA (G), PLS-DA (H) and prediction plot (75% sensitivity and 75% specificity) (I).

4.3.3.3.   Cohort 1, 2D serum spectra- whole cohort analysis

Analysis of the serum spectra (n= 72) identified eight technically anomalous spectra which were excluded, glog $1x10^{-5}$ was used to transform the spectra (Figure 4-11A, B). The PCA and PLS-DA model for the 2D serum spectra was less discriminating than that observed for 1D serum spectra (Figure 4-11C, D).
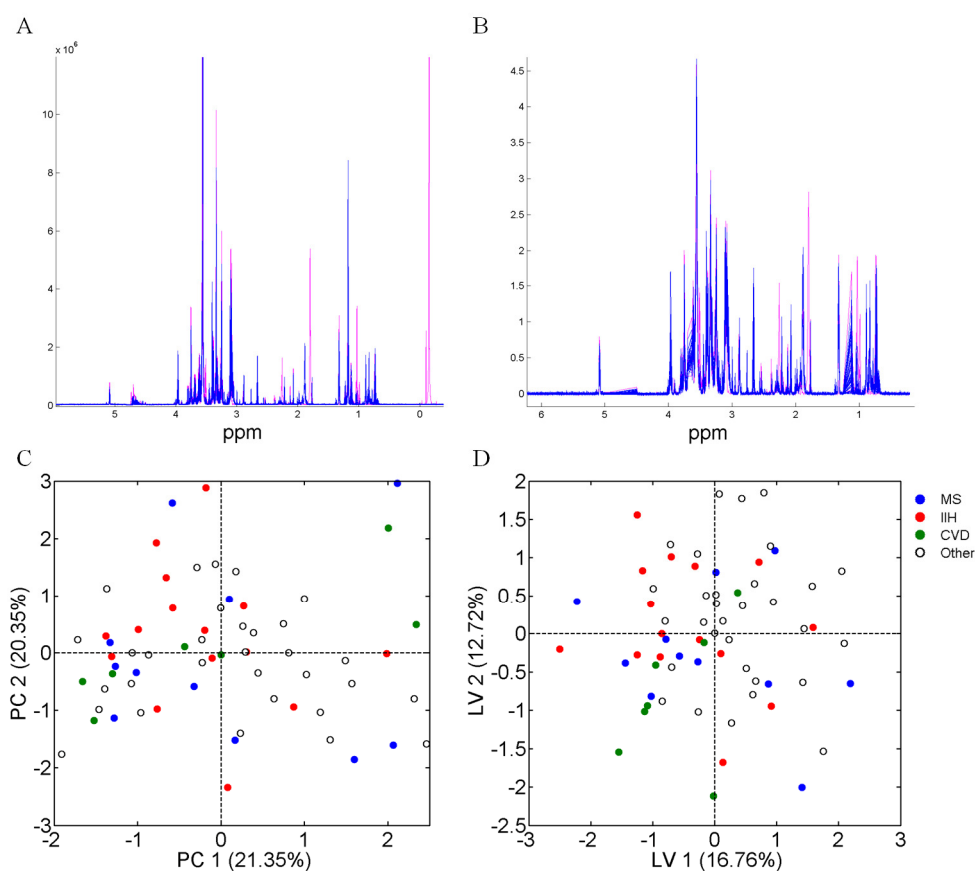

Figure 4-11   Cohort 1, 2D serum spectra whole cohort analysis

Raw CSF spectra (A) and glog transformed normalised binned NMR spectra (B). Outlying spectra are shown in pink and have been excluded from further analysis. Serum PCA scores plots (C) and PLS-DA scores plots (D).

The lack of clustering on the PCA and PLS-DA scores plots are reflected in the limited accuracy of the model to identify diagnostic groups following cross validation. In the IIH

patients, the sensitivity was 20% and specificity 80%, whereas the MS patients were identified with a sensitivity of only 18% and specificity of 72%. For the CVD patients, the sensitivity of the model was 14% and specificity 90% (Figure 4-12).
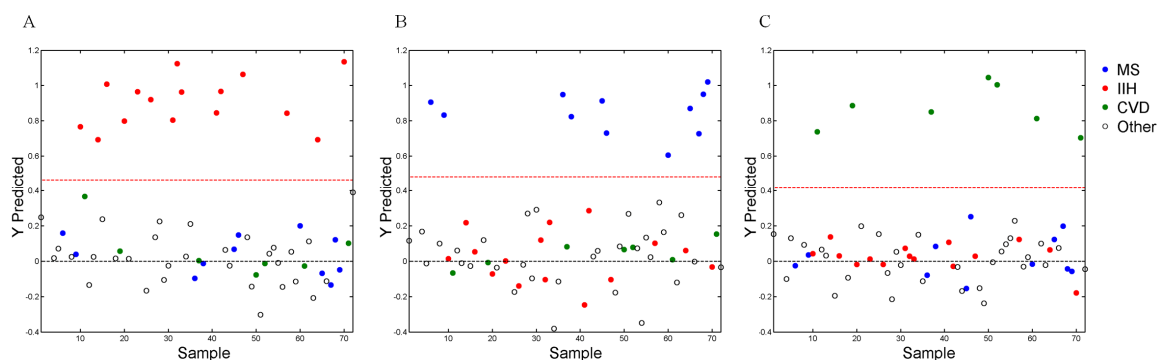

Figure 4-12   Cohort 1, 2D serum spectra- whole cohort prediction plots

The PLS-DA model identified subjects with (A) IIH (sensitivity 20% and specificity 80%) using a prior cut-off of 0.48 for class membership. (B) Subjects with multiple sclerosis (MS) were identified (sensitivity of 18% and a specificity of 72%) using a prior cut-off of 0.49 for class membership. (C) Subjects with cerebrovascular disease (CVD) were identified (sensitivity 14% and specificity 90%) using a prior cut-off of 0.42 for class membership.

4.3.3.4.   Cohort 1, 2D serum spectra- matched analysis

The diagnostic groups were compared to a matched (age, gender and BMI) control cohort, with mixed neurological diseases. The IIH cohort was discriminated from matched controls (n=10) with similar accuracy to that observed with 2D CSF spectra, with clustering of diagnostic groups was observed in the PCA and PLS-DA model. Cross validation of this model was 60% sensitive and 80% specific, with a cut-off of 0.48 for class membership (Figure 4-13A, B and C). Modelling MS patients against matched controls (n=10) revealed very poor discrimination compared to both CSF and 1D serum spectra (sensitivity 50% and specificity 10%, with a cut-off of 0.21 for class membership) (Figure 4-13D,E and F). The CVD cohort (n=8) was discriminated more accurately than

that observed in the CSF models, with clustering of patients particularly identified in the

PLS-DA model. The validated PLS-DA model was 63% sensitive and 75% specific

(using a cut-off of 0.42 for class membership) (Figure 4-13G, H and I).
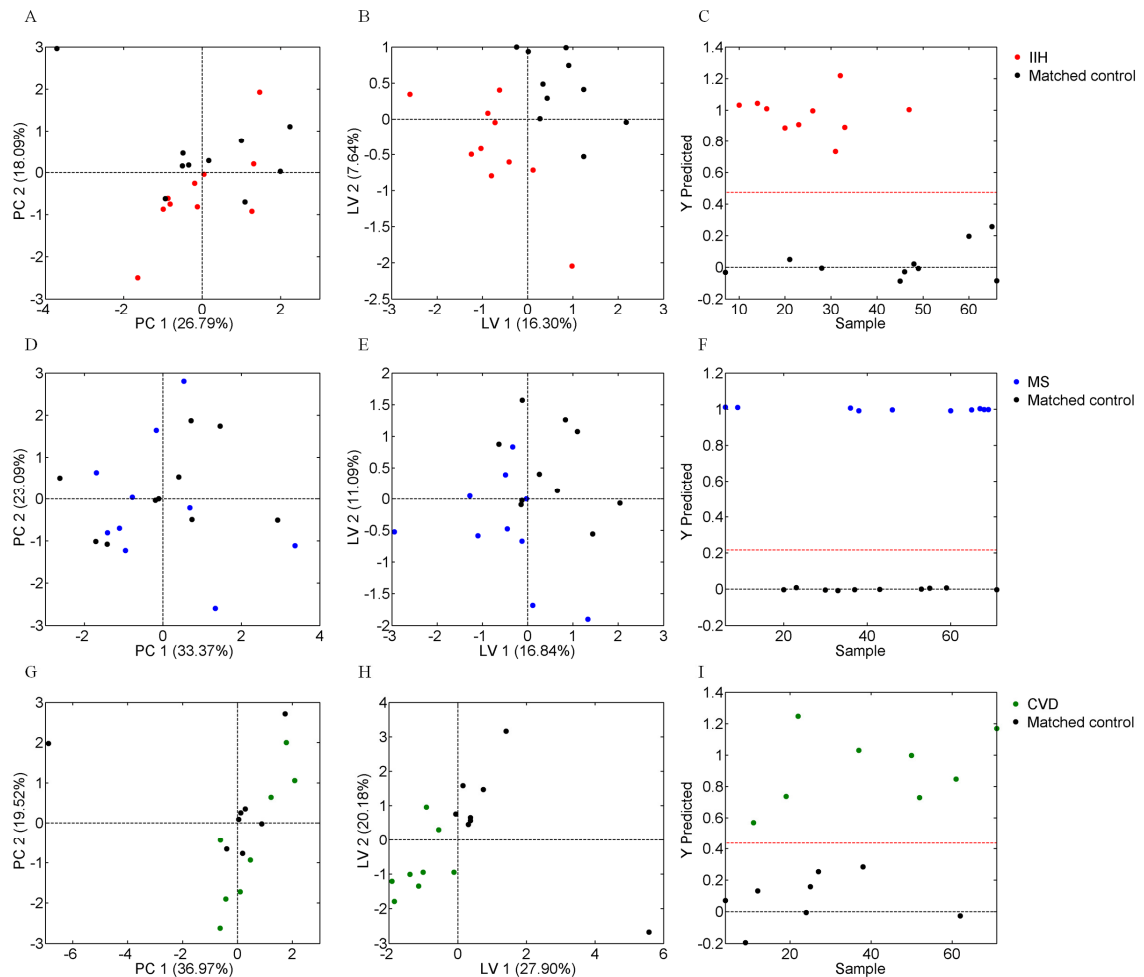
Figure 4-13   Cohort 1, 2D serum spectra matched analysis

> *IIH compared to a matched control group, PCA (A), PLS-DA (60% sensitivity and 80% specificity) (B) and prediction plot (C). MS compared to a matched control group, PCA (D), PLS-DA (E) and prediction plot (50% sensitivity and 10% specificity) (F). CVD compared to a matched control population, PCA (G), PLS-DA (H) and prediction plot (63% sensitivity and 75% specificity) (I).*

4.3.4. Cohort 1 modelling summary

The metabolite profiles were more accurate when derived from the 1D, rather than from the 2D spectra. Although phenotype is known to influence metabolite profiles (Holmes et al. 2008), we only found evidence of a weak (yet significant), correlation between the PC2 scores of the CSF dataset with age (r = 0.24, p = 0.025) and the PC1 scores of the serum dataset with BMI (r = -0.24, p = 0.04). It is likely, therefore, that in our cohorts, the relationship between age, BMI and principal components is more complex than a linear relationship. The matched analysis, did however, greatly enhance the accuracy of the metabolite biomarker profiles. No significant correlation was found between the principal component scores for the CSF and serum metabolite profiles. Amongst the IIH patient, the 1D matched metabolite profiles were sensitive and specific, in both CSF (80% and 80% respectively) and serum (70% and 78%). Spectral data are summarised in Table 4-4. MS metabolites were more accurately identified from 1D, matched CSF profiles (80% sensitivity and specificity). CVD metabolite profiles were most accurate when derived from the 1D serum matched analysis (75% sensitivity and specificity).

Cohort 1 1D CSF spectra				
	%	IIH	MS	CVD
Whole cohort	Sensitivity	71	83	57
	Specificity	70	53	67
	PLR:NLR	2.4:0.4	1.8:0.3	1.7:0.6
Matched cohort	Sensitivity	80	80	57
	Specificity	80	80	71
	PLR:NLR	4.0:0.3	4.0:0.3	2.0:0.6
Cohort 1 1D serum spectra				
	%	IIH	MS	CVD
Whole cohort	Sensitivity	50	27	27
	Specificity	83	70	69
	PLR:NLR	3.0:0.6	0.9:1.0	0.9:1.1
Matched cohort	Sensitivity	70	70	75
	Specificity	78	20	75
	PLR:NLR	3.2:0.4	0.9:1.5	3.0:0.3
Cohort 1 2D CSF spectra				
	%	IIH	MS	CVD
Whole cohort	Sensitivity	64	67	0
	Specificity	75	44	66
	PLR:NLR	2.6:0.5	1.2:0.8	0.0:1.5
Matched cohort	Sensitivity	60	50	88
	Specificity	80	80	13
	PLR:NLR	3.0:0.5	2.5:0.6	1.0:0.9
Cohort 1 2D serum spectra				
	%	IIH	MS	CVD
Whole cohort	Sensitivity	20	18	14
	Specificity	80	72	90
	PLR:NLR	1.0:1.0	0.6:1.1	1.4:1.0
Matched cohort	Sensitivity	60	50	63
	Specificity	80	10	75
	PLR:NLR	3.0:0.5	0.56:5.0	2.5:0.5

Table 4-4   *Summary of cohort 1 1D & 2D NMR multivariate modelling.*

Idiopathic intracranial hypertension (IIH), multiple sclerosis (MS), cerebrovascular disease (CVD), cerebrospinal fluid (CSF), positive likelihood ratio (PLR), negative likelihood ratio (NLR).

4.3.5. Cohort 2

The technically abnormal spectra from cohort 2 (CSF, n=2 and serum, n =0) were excluded from the analysis. The patient characteristics of cohort 2 subjects were not a direct match to those of patients analysed in cohort 1. This necessitated the use of the less

diagnostically accurate, whole cohort (i.e., unmatched), disease specific metabolite biomarker profiles, to predict the diagnoses of patients in cohort 2.

The CSF IIH metabolite profile was used to build both PCA and PLS-DA scores plots which illustrated clustering of IIH patients from cohort 1 and 2 (Figure 4-14A,B). The cohort 1 (whole cohort, unmatched) PLS-DA prediction model for IIH (Figure 4-14C) was then applied to the cohort 2 data (Figure 4-14D). The CSF IIH metabolite profile from cohort 1 was able to predict the diagnosis of IIH in cohort 2 patients (sensitivity 63% and specificity 75%). This was similar to the accuracy observed in the cohort 1 (whole cohort, unmatched) IIH CSF profile (71% sensitivity and 70% specificity). The accuracy of the unmatched serum IIH PLS-DA metabolite profile from cohort 1, although not useful diagnostically (sensitivity 50% and specificity 83%), was replicated when applied to the cohort 2 patients (sensitivity 50% and specificity 83%).

The CSF metabolite profiles for MS subjects generated from cohort 1 and 2 data were analysed by PCA (Figure 4-15A) and PLS-DA (Figure 4-15B). The PLS-DA prediction model from cohort 1 (Figure 4-15C) was used to identify patients with MS in cohort 2 (sensitivity 67% and specificity 75%) (Figure 4-15D).The sensitivity and specificity of the original cohort 1 MS biomarker profile was 83% and 53% respectively. The MS serum metabolite profile generated by the PLS-DA of cohort 1 predicted the diagnosis of MS in cohort 2 subjects, with a sensitivity of 67% and a specificity of 73%.

There were no patients with CVD in cohort 2. Table 4-5 summarises the sensitivity and specificity of the PLS-DA, whole cohort (unmatched), metabolite biofluid profiles from cohort 1, in predicting the diagnosis of IIH and MS in cohort 2. No significant difference was identified between the diagnostic accuracy of the metabolite profiles when applied to

cohort 1 or 2 (IIH CSF profile p=0.673, IIH serum profile p=1.0, MS CSF profile p=0.078

and MS serum profile p=0.054).

Cohort 2 *1D* CSF spectra				
%		IIH	MS	CVD
Whole cohort	Sensitivity	63	67	-
	Specificity	75	75	-
	PLR:NLR	*2.5:0.5*	*2.7:0.4*	
Cohort 2 *1D* serum spectra				
%		IIH	MS	CVD
Whole cohort	Sensitivity	50	67	-
	Specificity	83	73	-
	PLR:NLR	*3.0:0.6*	*2.5:0.5*	

Table 4-5 **Summary of accuracy of cohort 2 1D unmatched metabolite profiles in predicting diagnosis of cohort 2 patients.**

Idiopathic intracranial hypertension (IIH), multiple sclerosis (MS), cerebrovascular disease (CVD), cerebrospinal fluid (CSF), positive likelihood ratio (PLR), negative likelihood ratio (NLR).
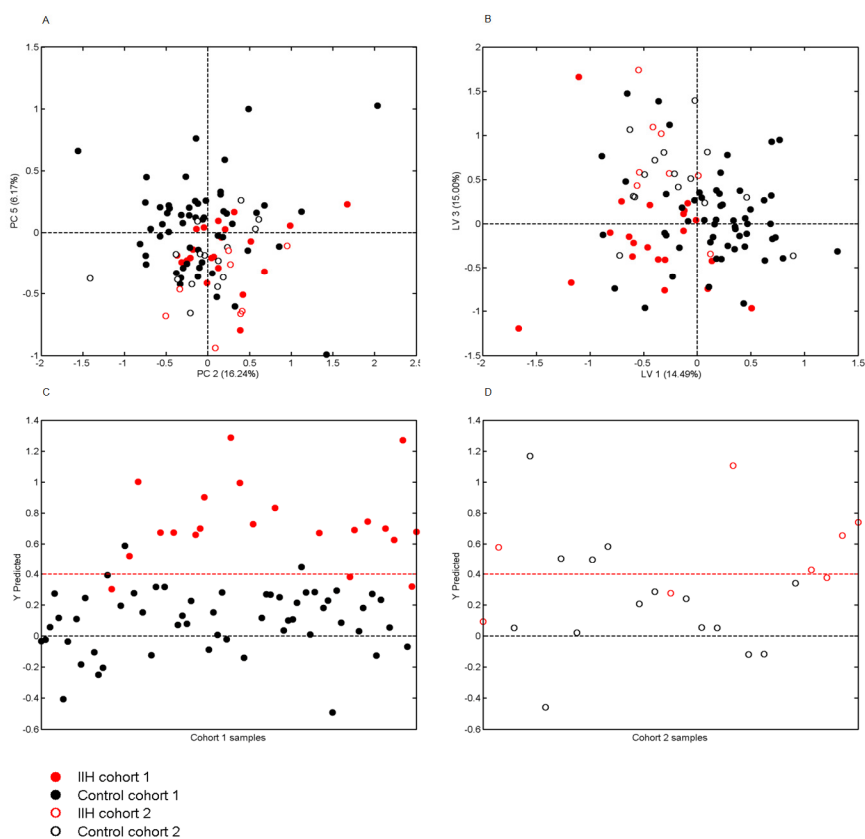
Figure 4-14 ***The cerebrospinal fluid PLS-DA models constructed with cohort 1 data were used to predict those patients with IIH in cohort 2***

(A) PCA, (B) PLS-DA, (C) prediction plot from cohort 1 and (D) prediction plot applied to cohort 2 (sensitivity 63% and specificity 75%). The principal component (PC) and latent variable (LV) represent variance in the spectra, with contribution to the variance shown in brackets. Cohort membership threshold is indicated by the red dotted lines on the prediction plots.
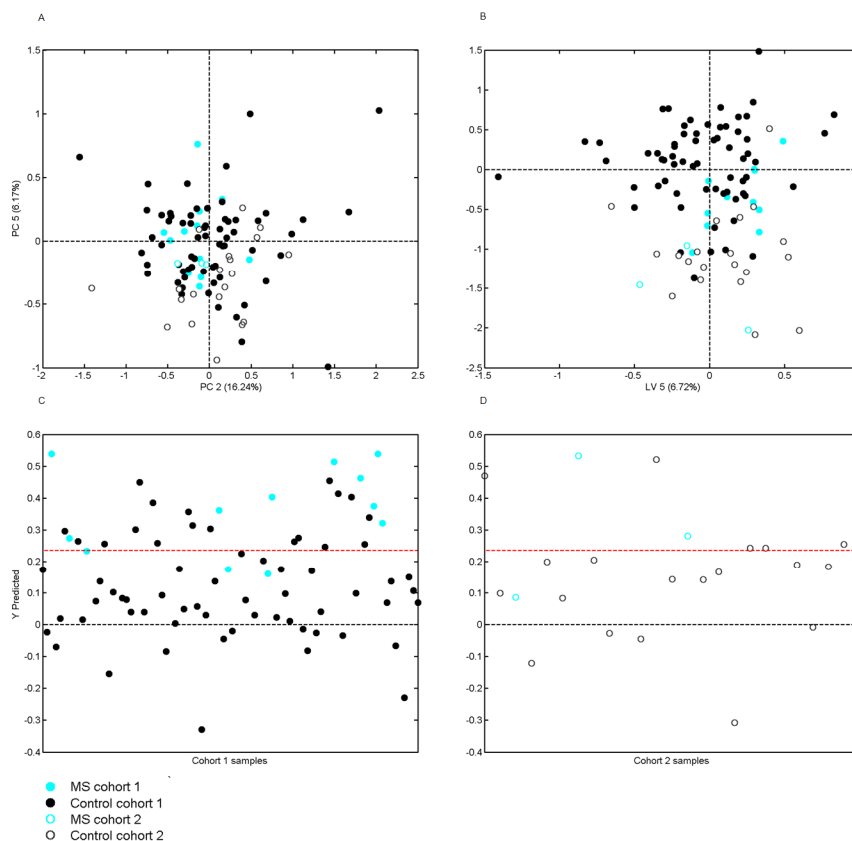
Figure 4-15 **The cerebrospinal fluid PLS-DA models constructed with cohort 1 data were used to predict those patients with MS in cohort 2**

(A) PCA, (B) PLS-DA, (C) prediction plot from cohort 1 and (D) prediction plot applied to cohort 2 (sensitivity 67% and specificity 75%). The principal component (PC) and latent variable (LV) represent variance in the spectra, with contribution to the variance shown in brackets. Cohort membership threshold is indicated by the red dotted lines on the prediction plots.

4.3.6. Technical variance

The technical variance between the whole of cohort 1 and 2 are illustrated (Figure 4-16 A&B). The variance was due to inconsistent resolution of ethanol (a contaminant) and urea. These areas were therefore excluded from analysis of cohort 2 (ethanol, 3.635 – 3.695 and 1.13 – 1.35 ppm and urea, 5.5 – 6.0 ppm). The five CSF samples from cohort 1 which were also analysed as part of cohort 2 showed a positive shift in PC1. Of the five serum replicates, one was technically anomalous and excluded, the remaining four

showed a negative shift in PC2 between cohorts 1 and 2. These PCA shifts were similarly

explained by differing resolution of ethanol and urea. The CSF and serum samples run at

the start and end of cohort 2 showed very similar principle components and thus there was

little technical variance between the start and end of cohort 2 processing (Figure 4-16

C&D).
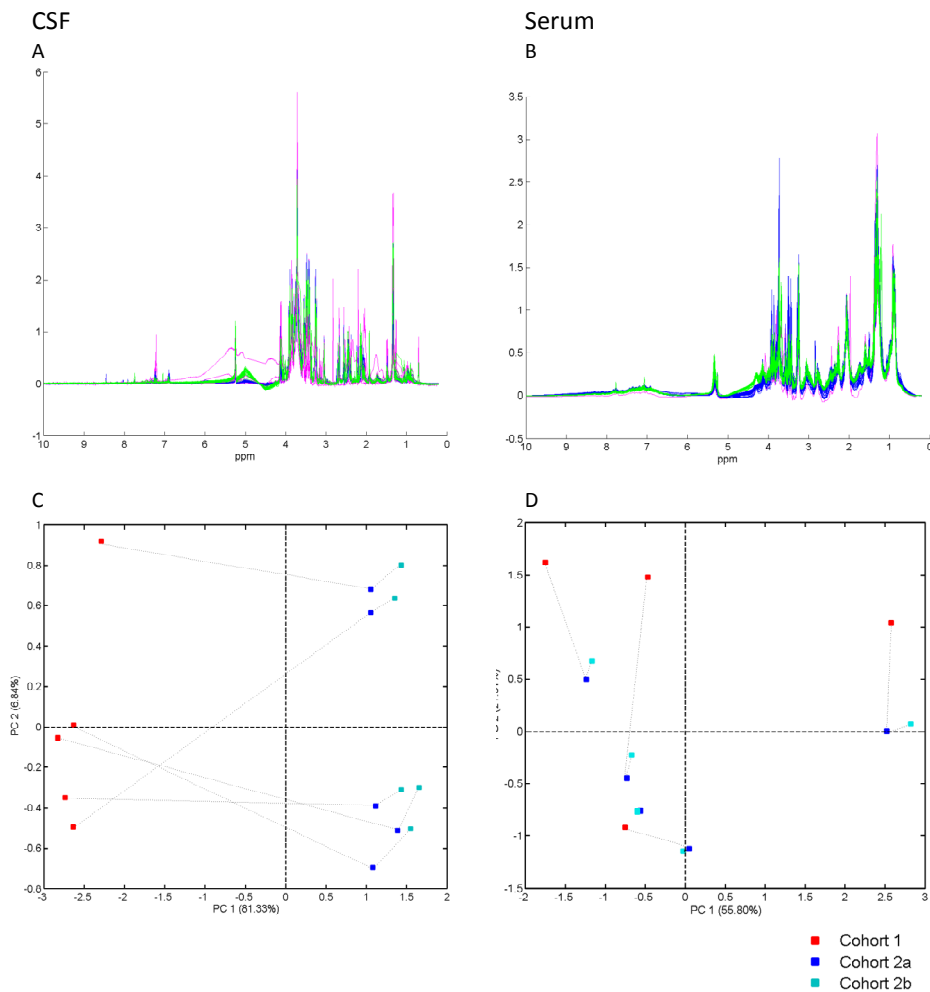
Figure 4-16   Technical variance of cohorts 1 and 2

The 1D normalised, glog transformed, binned spectra are shown for cohorts 1 and 2 (blue and green respectively) with anomalous spectra illustrated in pink (A) CSF and (B) serum. PCA plots are shown for five identical samples run in cohort 1, at the start of cohort 2 (Cohort 2a) and end of cohort 2 (Cohort 2b), (C) CSF and (D) serum.

4.3.7. Metabolite identification

Identification of the primary spectral peaks involved in diagnostic discrimination was approached using weightings plots from the PLS-DA models. Metabolites were identified from the most diagnostically predictive biofluid. IIH and MS metabolites were therefore identified in the CSF while the CVD metabolites were identified in the serum (Figure 4-17). Individual metabolites identified from the matched disease metabolite profiles were similar to those identified from the whole cohort (unmatched) profiles (data not shown).
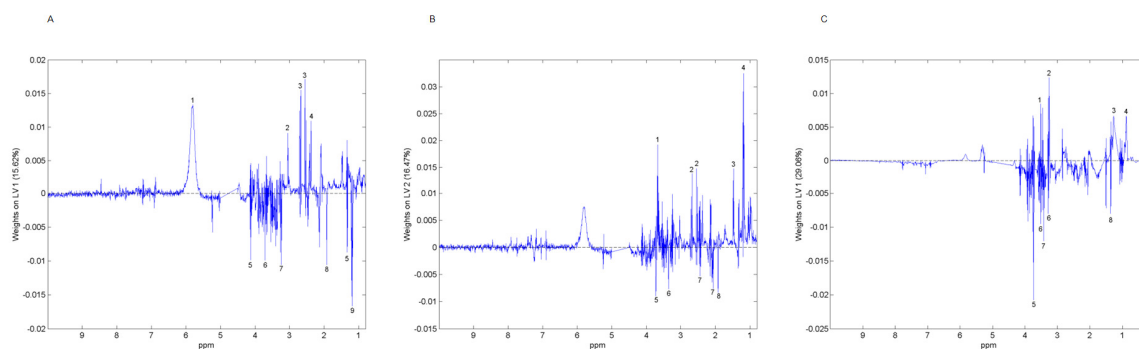
	IIH	MS	CVD
Reduced	1) Urea (5.83)	1) Oxaloacetate (3.70)	1) Glycine (3.52)
	2) Creatinine (3.05)	2) Citrate (2.55 & 2.69)	2) Betaine (3.23)
	3) Citrate (5.55 & 2.69)	3) Alanine (1.48)	3) Methylmalonate (1.27)
	4) 3-hydroxyisovalarate (2.38)	4) 3-hydroxybutyrate (1.20)	4) Butyrate (0.89)
Elevated	5) Lactate (4.13 & 1.33)	5) 2-aminobutyrate (3.72)	5) Oxaloacetate (3.73)
	6) Oxaloacetate (3.71)	6) 1,3-dimethylurate (3.36)	6) Glucose (3.91 & 3.24)
	7) Glucose (3.24)	7) Glutamate (2.07 & 2.45)	7) 1,3-dimethylurate (3.36)
	8) Acetate (1.93)	8) Acetate (1.93)	8) Lactate (4.13 & 1.33)
	9) 3-hydroxybutyrate (1.20)		

Figure 4-17 *Metabolite identification from weightings plots*

Plots illustrate the key peaks contributing to the differentiation between diagnostic groups identified in the cohort 1 PLS-DA models. (A) Principal IIH metabolites are characterized by low CSF LV1 scores, (B) Principal MS metabolites are characterized by low CSF LV2 scores, (C) Principal CVD metabolites are characterized by low serum LV1 scores. NMR chemical shifts (ppm), which describe the location of the peaks in the spectra, are shown in brackets for each metabolite.

Assessment of spectral peak areas, which are proportional to metabolite concentration, revealed that urea was significantly reduced in the CSF of patients with IIH compared to subjects with other neurological conditions (IIH median concentration 29.7 (range 14.2-37.5 arbitrary units (au)), MS median concentration 34.2 (range 25.1-42.1 au), CVD median concentration 32.3 (range 25.0-50.1 au) and other median concentration 34.8 (range 15.6-46.0 au), $p<0.05$). Acetate was found to be significantly elevated in the CSF of IIH patients compared to with other neurological conditions (IIH median concentration 34.9 (range 14.4-61.1 au), MS median concentration 31.3 (range 15.6-45.1 au), CVD median concentration 39.0 (range 16.3-45.5 au) and other median concentration 27.5 (range 14.8-52.4 au), $p<0.05$) (Figure 4-18).
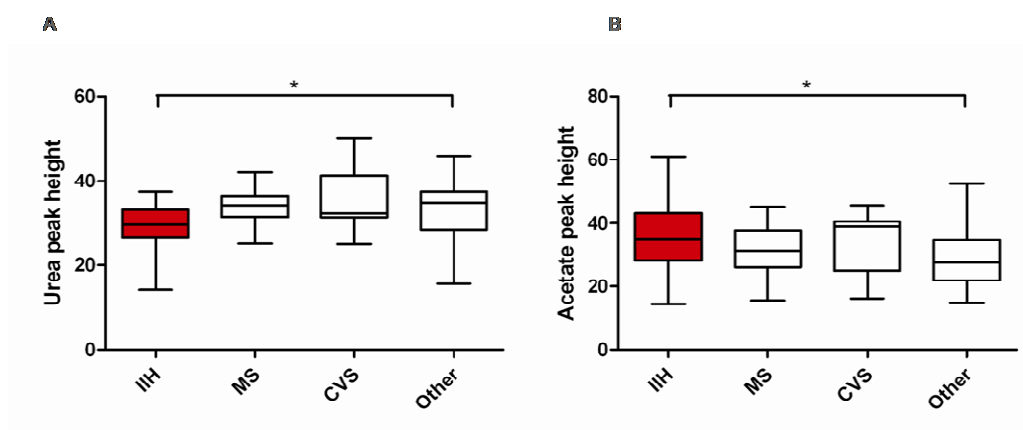
Figure 4-18   Significant metabolites in the IIH spectra

Box and whiskers plots with median and ranges showing (A) reduced CSF urea in the IIH cohort compared to subjects with other neurological diseases, (B) elevated CSF acetate in the IIH cohort compared to subjects with other neurological diseases.

4.4. Discussion

^{1}H NMR is a powerful technique for measuring multiple metabolites in a biofluid, thus providing a vast amount of information on both the high and low concentration constituents of a sample. Metabolomics provides an overview of a biofluid that represents the end-products of gene transcription, protein translation and environmental effects, all factors known to influence disease state. Additionally, the technique is automated, rapid (spectra are acquired in 10 minutes), reproducible and relatively sensitive (detection of metabolites in the nanogram range) (Holmes *et al.* 2006b). The data from this study, and others, (Nicoli *et al.* 1996; Subramanian *et al.* 2005; Holmes *et al.* 2006a; Holmes *et al.* 2006b; Lutz *et al.* 2007) suggests that different neurological conditions are represented by unique biofluid metabolic fingerprints which may reflect distinct variations in underlying pathology. We have demonstrated that there are distinct differences in the spectra acquired from CSF and serum of patients with IIH, MS and CVD.

The study used multivariate regression analysis to identify metabolite biomarker profiles in the CSF and serum of patients with IIH, MS and CVS. Our analysis has shown that 1D spectra were more discriminating than 2D spectra for all diagnostic groups. Although 2D JRES reduce spectral congestion, the resonance from large macromolecules such as proteins can be lost (Viant 2003). Consequently, the signals from potentially discriminating protein bound metabolites may be lost, thus possibly reducing the sensitivity of the spectra.

Despite the heterogeneity of the neurological patients analysed, we have demonstrated that there are distinct differences in the spectra acquired from the CSF and serum of patients with IIH, MS and CVD. We were able to identify patterns of metabolite variance in individual diagnostic groups and using statistical modelling we identified age, gender

and BMI specific disease biofluid metabolite profiles. These predicted diagnosis with a sensitivity and specificity of 80% in IIH and MS (CSF profiles) and 75% in CVD (serum profiles). The heterogeneity of the control group was likely to have impaired the biomarker discovery and thus sensitivity and specificity of the metabolite profiles. Our approach, however, would yield biomarkers which could be transferred to a clinical setting, where we would aim to use biomarkers to help distinguish between different neurological diseases. Phenotypic features, such as gender and age (own unpublished data) are known to influence NMR spectra and our data highlights the importance of accounting for these variables when establishing metabolite profiles. Dietary factors, in the 24 hours preceding sample collection, are known to impact upon the metabolite profiles, even in fasted patients (Maher *et al.* 2007). Nutrition, however, was unlikely to have led to false biomarker discovery in our analysis, as each disease cohort represented a spectrum of dietary habits.

Discrimination of patients with IIH was observed to be optimal using 1D CSF spectra (sensitivity 71% and specificity 70% when modelled against the whole control cohort and 80% sensitivity and specificity when modelled against a matched control cohort). The 1D serum profile was also of value in IIH (sensitivity 70% and specificity 78%). This possibly implicates both CNS and systemic factors in IIH disease aetiology. This is the first identification of biomarkers specific to IIH and is thus an important step in defining the condition and advancing knowledge regarding the aetiology. A diagnostic test has not been previously documented for IIH and the identification of potentially diagnostic CSF and serum biomarker profiles may have important clinical implications in terms of expediting accurate diagnosis and monitoring disease progression. It will now be important to confirm that the metabolic biomarkers in IIH are distinct from other causes of elevated intracranial pressure. The single patient with secondary intracranial

hypertension, resulting from anaemia, did have a different biomarker profile to the IIH patients.

Biomarker profiles in the MS patients were most accurately identified using 1D CSF spectra (sensitivity 83% but a specificity of 53%). The accuracy of the profile increased when the MS patients were compared to a matched control population (sensitivity and specificity 80%). Serum metabolite biomarkers in MS were not as discriminatory as that observed in the CSF. Although patients with MS can demonstrate systemic biochemical features, such as an inflammatory cytokine profile, this is usually during disease relapse (Carrieri *et al.* 1998). The samples in this study were collected during disease remission, and this may account for the absence of a systemic serum metabolite profile.

Regression analysis of CSF metabolites did not discriminate patients with CVD from control subjects with sufficient sensitivity or specificity. Disease unique serum metabolite biomarker profiles however, were more accurate in identifying patients with CVD from matched controls (sensitivity and specificity 75%). The pathological heterogeneity in the CVD cohort is a likely explanation for the reduced diagnostic precision e.g. patients with atherosclerotic and embolic CVD were grouped for analysis, but have differing aetiology.

It is not possible to compare the accuracy of diagnostic metabolomics with other diagnostic tests for IIH, MS and CVD, as they do not exist. Numerous studies have evaluated the accuracy of the "Revised McDonald Criteria" in predicting which patients will progress from a clinically isolated syndrome to clinically definite MS, but these studies have not evaluated the ability of the criteria to exclude alternative diagnoses (Polman *et al.* 2005; Swanton *et al.* 2007). In addition, the McDonald criteria use a spectrum of clinical and para-clinical tests to define MS. The advantages of a single biofluid diagnostic test are clear. Further evaluation to define metabolite biomarker

profiles at different stages of MS would be of additional value. The diagnosis of CVD is less challenging. The differentiation of patients with MS from those with CVD in the context of an ambiguous MRI scan can, however, be problematic. In these situations, a combined approach using CSF and serum metabolomic profiles may facilitate diagnosis. Although we have identified disease unique metabolite profiles, the future use of metabolite biomarkers in the clinical environment will require optimisation to improve accuracy. In our study, the accuracy of disease-unique metabolite profiles may have been affected by inherent inaccuracies in clinical diagnosis (Stacy and Jankovic 1992), co-morbidities such as the possible coexistence of MS and CVS, and pathological heterogeneity in the disease cohorts (e.g. classification of both embolic and atherosclerotic CVD in the same cohort). Confirmation of diagnosis at post-mortem may ultimately improve disease classification.

Technical advances in metabolomics are rapidly progressing as this approach moves from the field of analytical chemistry, into medicine. The interpretation of serum spectra is a particular problem due to variable protein binding of metabolites. Techniques to protein deplete samples prior to spectral acquisition, such as filtration and protein suppression during analysis, may be of benefit, and need to be validated in clinical metabolomics (Tiziani *et al.* 2008). Analytical techniques which eliminate phenotypic features such as gender and drug metabolites may also have a role and will need evaluation (Tiziani et al. 2008). Ideally, accurate metabolomic profiles in non invasive biofluids such as urine, will need to be developed to negate the requirement for diagnostic LP.

Disease treatment in neurology is predicted to advance over the next decade with the development of genetic, stem cell and immunomodulatory therapies. Biomarkers will be essential in the development and deployment of these therapies, to facilitate diagnosis,

guide prognosis and therapy, evaluate experimental pharmacotherapy and in addition provide surrogate endpoints and markers for clinical research (Feigin 2004; Lolli *et al.* 2006; Staner 2006). Ideally, clinical biomarkers need to be highly sensitive and specific, generalisable, representative of disease pathology and reflect the diversity of clinical outcomes. Single biomarkers will rarely achieve these ideals and it is likely that composite endpoints will be required. There are, therefore, clear advantages to using metabolic biomarker profiles which represent multiple differentiating metabolites. The diagnostic ability of metabolite biomarkers will clearly need optimising and evaluating in larger patient cohorts, with a greater spectrum of more diagnostically challenging diseases.

4.4.1. Metabolite interpretation

Individual metabolites, highlighted in the weightings plot, warrant further evaluation to establish if they reflect pathogenic disease mechanisms or are, in fact, the consequence of the disease process. Interpretation of CSF metabolites is complex, as the origin of these metabolites is not established (metabolites may reflect systemic metabolism and subsequent transfer across the blood brain barrier or local CNS generation). As little is known about the pathogenesis of IIH (Sinclair *et al.* 2008), we were interested to note elevated levels of lactate in the CSF of these patients. Predominant lactate peaks have been identified in inflammatory CNS disease (Simone *et al.* 1996) possibly implicating an inflammatory component in IIH (Sinclair et al. 2008). Additionally, elevated levels of lactate have been identified in vitreous humour of rabbits with elevated intraocular pressure and are thought to reflect anaerobic metabolism (Ngumah *et al.* 2006). In IIH, anaerobic metabolism may be attributed to reduced blood supply due to compressed vasculature from the elevated ICP. Additionally, elevated oxaloacetate levels, in

conjunction with reduced citrate levels in IIH, may represent impaired action of citrate synthase in the citric acid cycle. This, in conjunction with elevated ketone bodies (3-hydroxybutyrate, an enantiomer of the ketone β-hydroxybutyric acid), may suggest a predominantly anaerobic environment, deficient in carbohydrate substrate in patients with IIH. The findings of low urea and elevated acetate in the CSF of patients with IIH are of interest. Both of these compounds have been previously identified in the CSF (Commodari et al. 1991; Subramanian et al. 2005) but their significance is unclear. Further exploration of the role of urea and acetate in IIH is needed.

In the MS cohort, elevation of CSF glutamate, a known CNS neurotoxic trigger (Choi *et al.* 1987), compounded by low levels of oxaloacetate (an inhibitor of neuronal cell death) may contribute to axonal loss (Berry and Toms 2006) and represents an area for further study. Elevated levels of CSF acetate and reduced citrate are in keeping with previous studies (Lynch *et al.* 1993) (Simone et al. 1996). The implication of these metabolite alterations is unclear, although deranged CSF citrate has also been noted in Alzheimer's disease (Ghauri *et al.* 1993).

The reduced levels of serum betaine in patients with cerebrovascular disease is intriguing and may indicate a population at high risk of stroke, as betaine, a methyl donor, reduces levels of homocysteine, a known risk factor for cerebrovascular disease (Spence 2006). Additionally, elevated serum glucose is likely to reflect impaired insulin sensitivity in these patients, another established risk factor for stroke (Prakash and Matta 2008). Elevated lactate levels, also noted in earlier NMR studies (Hiraoka *et al.* 1994), and a proposed shift from aerobic to anaerobic cerebral glycolysis following a cerebrovascular event, have been previously documented in patients following cerebrovascular events (Meyer *et al.* 1968; Zupping *et al.* 1971).

4.4.2. Conclusion

In summary, we have illustrated and validated the use of metabolomics to identify differences in metabolite profiles in patients with IIH, MS and CVD. Metabolomics offers great potential in establishing neurological biomarkers and efforts should concentrate on optimising spectral processing to increase diagnostic accuracy, evaluating the accuracy of urinary metabolite profiles and establishing a national neurological metabolite database. The novel identification of IIH specific metabolites is of particular importance, as understanding of disease aetiology is so limited. Absolute confirmation, by mass spectrometry, of the disease specific metabolites, is now required prior to detailed *in vitro* assessment.

Chapter 5. The role of weight loss in idiopathic intracranial hypertension

Chapter 5

5.1. Introduction

The following chapter details the effect of weight loss on IIH. To facilitate interpretation of the data, each section of the chapter has been divided into 3 sections. The first section addresses the therapeutic effect of weight loss on intracranial pressure, headache and visual parameters in patients with IIH. The second section describes the metabolic consequences of weight loss, particularly the effects on glucocorticoids and 11β-HSD1. Finally, the metabolic profile of patients with IIH has been compared to a population of healthy control subjects matched for age, gender and BMI.

5.1.1. The clinical consequences of weight loss in idiopathic intracranial hypertension

Introduction

Evidence to guide therapeutic strategies in IIH is limited, as highlighted in the 2005 Cochrane review which found insufficient evidence as to which treatments were potentially beneficial and which were harmful (Lueck and McIlwaine 2005). The condition has a striking association with obesity (greater than 93%) (Glueck et al. 2005) and, consequently, weight loss is frequently suggested as a critical treatment strategy. Nevertheless, there is only one prospective weight modifying study published in the English literature. This study was carried out over 35 years ago and noted subjective improvement in the papilloedema in nine subjects with IIH, on a low calorie rice diet (Newborg 1974); data supported by retrospective case note reviews (Johnson et al. 1998; Kupersmith et al. 1998; Wong et al. 2007) (discussed in section 1.11.3). These studies, however, relied upon subjective measures of papilloedema and included subjects with newly diagnosed IIH, many of whom are likely to improve, irrespective of any treatment

given. Furthermore, these studies did not monitor concomitant changes in ICP with either weight loss, or resolution of papilloedema. In this context, we initiated a detailed examination of the interplay between weight loss in IIH with objective measures of papilloedema, visual function, headache scores and crucially, changes in ICP.

5.1.2. Effect of weight loss on the metabolic phenotype and 11β-HSD1, in idiopathic intracranial hypertension

Introduction

11β-HSD1 dysregulation in obesity has been previously established (Andrew *et al.* 1998; Stewart *et al.* 1999; Rask *et al.* 2001; Reynolds *et al.* 2001) and may be an important factor in obesity and disordered CSF dynamics in IIH patients (see section 1.5.1). Weight loss is know to modulate 11β-HSD1 activity in obese subjects (Tomlinson *et al.* 2004a; Tomlinson *et al.* 2008) and may underlie the therapeutic advantage demonstrated in IIH patients on a weight reduction program (section 5.3.1).

Obesity is frequently associated with hyperlipidaemia, hypertension, glucose intolerance and fatty liver. Collectively, these features are known as the Metabolic syndrome, a state of impaired insulin sensitivity, predisposing to type 2 diabetes and atherosclerotic vascular disease, noted particularly in individuals with centrally distributed adiposity (Ginsberg 2000). Obesity is characterised by an enlarged white adipose tissue mass, which not only provides an energy store, but additionally represents an important endocrine organ that has the ability to secrete over a hundred factors, including proteins, cytokines, fatty acids and prostaglandins (Mercer *et al.* 1996; Fain 2006). The endocrine properties of adipose tissue enable communication with numerous other organs facilitating appetite regulation, energy homeostasis, insulin sensitivity, reproductive function, bone metabolism and immune modulation (Fantuzzi 2005). Adipose

distribution and insulin sensitivity have not been previously investigated in IIH and may have important implications for the risk of metabolic syndrome these patients.

In summary, we suggest that 11β-HSD1 may be involved in the pathogenesis of IIH and that therapeutic weight loss may be beneficial, due to manipulation of local glucocorticoids concentrations and 11β-HSD1. Additionally, we suggest that obesity in IIH may predispose IIH patients to the metabolic syndrome. We aim to characterise 11β-HSD1, fasted metabolites and body composition in a cohort of patients with IIH before and after weight loss.

5.1.3. Comparison of metabolic phenotype and 11β-HSD1 in idiopathic intracranial hypertension and control patients

Introduction

We have previously described the association between IIH and obesity, and have suggested that patients with IIH, akin to obese individuals, may be susceptible to the metabolic syndrome. In this section, we aim to further characterise the metabolic phenotype of IIH patients, compared to obese control subjects.

5.2. Methods

5.2.1. The clinical consequences of weight loss in idiopathic intracranial hypertension

5.2.1.1. Study population

Subjects with IIH were identified from the Birmingham and Midland Eye Centre, Sandwell and West Birmingham Hospitals NHS Trust, University Hospitals Birmingham

Chapter 5

NHS Foundation Trust and University Hospitals of Leicester NHS Trust, following informed written consent (ethical approval from Dudley Local Research Ethics Committee (LREC) 06/Q2702/64). IIH was diagnosed according to the modified Dandy Criteria (Friedman and Jacobson 2002) with all patients having normal MRI, MRV, papilloedema (confirmed on slit lamp examination by a neuro-ophthalmologist), ICP greater than 25cmH$_2$O and disease duration greater than 3 months at enrolment. Subjects were excluded if they had undergone previous CSF diversion or optic nerve sheath fenestration, were pregnant or planning to conceive, had significant co-morbidity (cardiac disease, unstable diabetes, alcohol or drug dependence) or were less than 16 years of age. All subjects meeting the inclusion and exclusion criteria were invited to take part in the study.

5.2.1.2.   Study design

Twenty five IIH subjects were prospectively recruited into a three stage study: Stage 1 consisted of a three month period of no new intervention (control phase); Stage 2 comprised a three month intensive diet; and in Stage 3 subjects were followed for a further three months after completion of the diet (Figure 5-1). Weight loss was achieved using a previously validated (Tomlinson *et al.* 2004a), nutritionally complete, very low calorie total meal replacement liquid diet (VLCD) (Lipotrim, Howard Foundation, Cambridge, UK) which provided subjects with a total of 425 Kcal/day. No additional food was consumed and patients were advised to consume at least 2 litres of fluid per day. During Stage 2, subjects were weighed weekly and given dietetic advice.

Subjects were evaluated at baseline and at the end of stages 1, 2 and 3. Anthropometric data were collected and BMI was calculated from the weight divided by the square of the

height (kgm^{-2}). The presence of symptoms (tinnitus, visual loss, diplopia, visual obscurations and headache) was noted. Medication use was also recorded.

Assessment of visual function, under standardised luminescence, was carried out using a LogMAR chart to assess visual acuity, automated perimetry (Humphrey 24-2 central threshold) to measure the visual field mean deviation, a Pelli Robson chart to evaluate contrast sensitivity and a Farnsworth Munsell 100 Hue test to appraise colour vision.

Papilloedema was evaluated using ultrasonography of the optic disc elevation and nerve sheath diameter (maximal retrobulbar pial diameter), using a high resolution brightness scan (B-scan), with emission frequency 20MHz and 10MHz respectively (Quantel Medical, Clermont–Ferrand, France). Additionally, average axonal distention around the optic disc (a marker of papilloedema) was measured from the distension of the peripapillary RNFL thickness (vitreoretinal interface to photoreceptors) using OCT (Stratus OCT^{TM} V4.0.1, Carl Zeiss, Meditec, Welwyn Garden City, UK). Masked papilloedema grading (Frisen rating scale with grade 5 most severe) of fundus photographs was also conducted at each visit by a neuro-ophthalmologist (Frisen 1982) (Table 1-6). Disc ranking was also applied to each photograph by a masked neuro-ophthalmologist: pairs of fundal photographs at the start and end of each stage were randomly ordered and labelled; the disc which appeared most swollen was selected. If no difference in the appearance of the disc was perceived, this was also noted.

Headache phenotype (according to the International Headache Society (IHS) criteria) (Evers 2004) was assessed at baseline. A daily headache diary, completed in the week prior to each visit, evaluated headache severity using a visual analogue pain scale (VAS), headache frequency (days/week) and analgesia use (days/week). A headache

questionnaire, HIT-6, (score range 36 – 78) was also completed (questionnaire illustrated in the appendix, section 7.2) (Kosinski et al. 2003).

ICP was measured by LP by the same physician (Alex Sinclair) at baseline, 3 and 6 months after all listed outcome measures had been assessed. Measurements were taken with the patient breathing steadily in the left lateral position, legs extended greater than 90° at the hip, allowing adequate time to ensure a stable ICP reading.
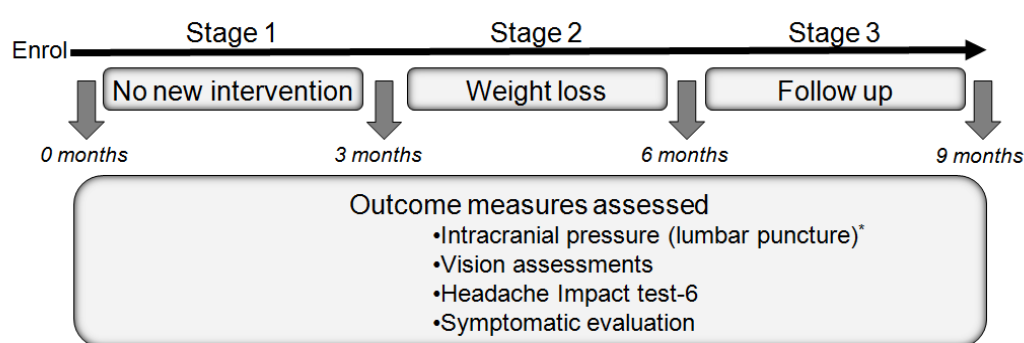
Figure 5-1   Schematic diagram of weight loss study design

Visual assessments include measurement of: (1) papilloedema by ultrasonographic evaluation of optic disc elevation and nerve sheath diameter, as well as optical coherence tomography measurement of retinal nerve fibre layer; (2) LogMAR visual acuity; (3) Humphrey visual field 24-2 mean deviation; (4) Pelli Robson contrast sensitivity; (5) Farnsworth Munsell 100 Hue colour assessment. Symptoms evaluated include headache, tinnitus, visual loss, obscurations and diplopia. *lumbar puncture is only carried out at baseline, 3 and 6 months.

5.2.1.3.   Statistical analysis

Statistical analysis was performed as described (section 2.4). Additionally serial measurements were analysed using repeated measures ANOVA (for parametric or log transformed data) or Friedman's test, with *post hoc* evaluation achieved using a Wilcoxon Signed-Rank test (for non-parametric data). Analysis of dichotomous variables was conducted using a Cochran's Q test, and the Sign test was used to evaluate changes in

categorical data. Associations between clinical parameters and objective outcome measures were analysed using Pearson correlation for parametric data and Spearman rank correlation for non-parametric data. Missing data were excluded from analysis and data analysed only if present at all time points. The level at which the results were judged significant was $p < 0.05$ (or $p < 0.017$ for Wilcoxon signed rank test and Sign test as three pairwise comparisons were being made per variable). Right and left eye data correlated significantly and yielded analogous results. Right eye data are therefore quoted.

5.2.2. Effect of weight loss on the metabolic phenotype and 11β-HSD1, in idiopathic intracranial hypertension

Methods

5.2.2.1.   Study population

The study population detail in section 5.2.1.1 were utilised for this study. Additional exclusion criteria included, hormone manipulating medication, significant co-morbidity including unstable diabetes and known endocrinopathies.

5.2.2.2.   Study design and sample collection

The study was conducted according to that described in section 5.2.1.2; briefly, a three month observation period (stage 1) was followed by a three month VLCD (stage 2) (Lipotrim, Howard Foundation, Cambridge, UK). At baseline, and the end of stages 1 and 2, anthropological measures (BMI and waist circumference, measured at the level of the umbilicus), blood pressure (Dynamap, Critikon, Tampa, FL) and biofluid samples (blood, CSF and urine) where collected. Blood and CSF samples, were collected in a fasted state between midday and 14:00h. After collection, blood and CSF samples were promptly centrifuged at 176g for 10 minutes, aliquoted, stored at -80˚C and analysed after

a maximum of one freeze-thaw cycle. Blood samples were evaluated for total cholesterol, triglycerides, glucose, insulin and HOMA scores calculated (section 2.3.4.). Cortisol and cortisone was measured in the serum and CSF using LC/MS (2.2.3). 24h urine samples were also collected (collection from first void of the day and thenceforth for 24h), the total volume noted and aliquots stored at -80˚C before analysis for steroid metabolites by GC/MS (section 2.2.2). A DEXA total body scanner (QDR 4500; Hologic, Bedford, MA) analysed body composition including fat distribution at the start and end of stage 2. Finally, evaluation for polycystic ovarian syndrome (PCOS), according to the Rotterdam ESHRE 2004 criteria (REA-SPCW 2004) was conducted at baseline (Table 5-1). PCOS biochemical investigation for hyperandrogenism included serum androstenedione, DHAS, SHBG and testosterone (section 2.3.4.3).
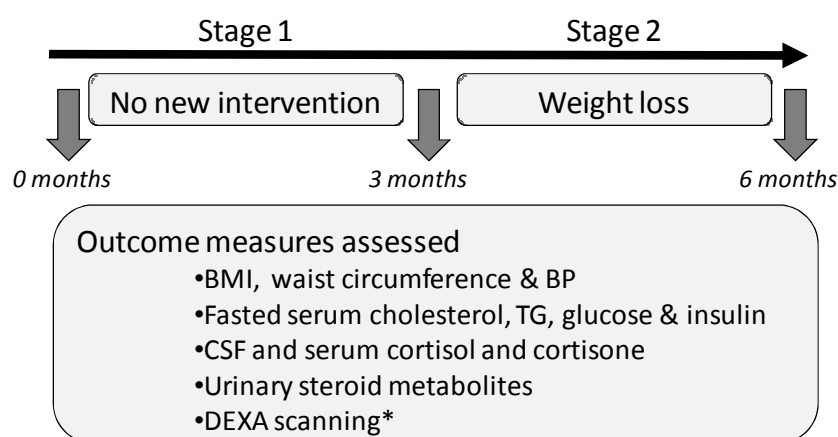
Figure 5-2   Schematic diagram of study design for metabolic phenotyping during weight loss

*Body mass index (BMI), blood pressure (BP), triglycerides (TG), cerebrospinal fluid (CSF). *Dual energy x-ray absorptiometry (DEXA) was only performed at 3 and 6 months.*

Rotterdam PCOS Criteria (2 out of 3) (REA-SPCW 2004)
1. Oligo (cycle length > 45 days) - or amenorrhoea (no menstrual period for the past 6 months).
2. Clinical (hirsutism, acne & male pattern balding) and/or biochemical signs of hyperandrogenism.
3. Polycystic ovaries and exclusion of other aetiologies (congenital adrenal hyperplasia, androgen-secreting tumours, Cushing's syndrome).

Table 5-1   Revised Rotterdam criteria for diagnosis of polycystic ovarian syndrome (PCOS)

5.2.2.3.   Comparison of weight loss in IIH, with non IIH obese subjects

Non IIH obese subjects were previously investigated, using an identical study design (Tomlinson *et al.* 2004a; Tomlinson *et al.* 2008). In an exploratory analysis, which was not the primary aim of this study, the effect of weight loss on glucocorticoids, fasting metabolites, and body composition was compared between the IIH and non IIH obese patients (matched for gender, BMI ± 2 kgm^{-2} and age ± 5 years). The non-IIH obese patients represented a historical control cohort recruited following local advertisement.

5.2.2.4.   Statistical analysis

Data were analysed as described in section 5.2.1.3. The level at which the results were judged significant was $p < 0.05$ (or $p < 0.025$ for Wilcoxon signed rank test, as two pairwise comparisons were being made per variable).

5.2.3. Comparison of metabolic phenotype and 11β-HSD1 in idiopathic intracranial hypertension and control patients

Methods

Chapter 5

5.2.3.1. Study population

Subjects with IIH were identified as described in section 5.2.2.1, using identical inclusion and exclusion criteria. A proportion of these patients were subsequently recruited into the weight loss study (sections 5.2.1.1). Participants were fully informed and written consent was taken (ethical approval from Dudley Local Research Ethics Committee (LREC) 06/Q2702/64). Control obese subjects were provided by Dr Jeremy Tomlinson (Birmingham Prospective Obesity, Diabetes Steroid metabolism study (BPODS cohort), South Birmingham LREC 04/q2707/278, approved 22/12 2004). Controls were recruited as part of a previous study (Tomlinson *et al.* 2004a; Tomlinson *et al.* 2008) following local advertisement. Those control subject using hormone manipulating medication or with significant past medical history (including diabetes) were excluded.

5.2.3.2. Study design and sample collection

The IIH and control subjects were matched for gender and BMI ($\pm$ 2 kgm^{-2}). For both the IIH and control subjects, anthropological measures, sample collection and processing (serum and urine), and DEXA scanning were conducted in an identical manor using the same equipment / assays techniques (described in section 5.2.2.2) (Figure 5-3). Screening for PCOS, was however, rigorously conducted in the IIH cohort, whilst control subjects were not formally screened (all control subjects with an existing diagnosis of PCOS were, however, excluded).

171
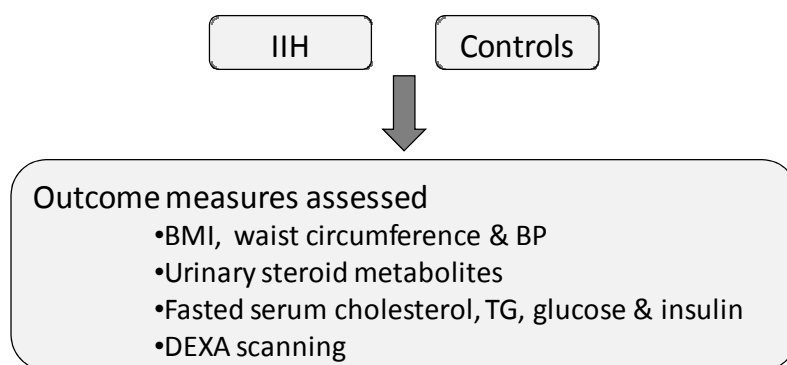
Figure 5-3   Schematic diagram of study design comparing IIH and control subjects

Idiopathic intracranial hypertension (IIH), body mass index (BMI), blood pressure (BP), triglycerides (TG), dual energy x-ray absorptiometry (DEXA).

5.2.3.3.   Statistical analysis

Statistical methodology is described in detail in section 2.4. Data were summarised using means and standard deviations. The IIH and control groups were compared using a two-tailed, non-parametric t-test (Mann-Whitney). Where a significant correlation was noted between a variable and age, multivariable regression models were used to control for the effect of age. Missing data were excluded from analysis.

5.3. Results

5.3.1. The clinical consequences of weight loss in idiopathic intracranial hypertension

Results

Twenty-five patients were recruited, while 12 patients declined the invitation to participate in the study due to concerns about LP. The recruited subjects, and those declining study entry, had homogeneous characteristics. Amongst the recruited patients,

one was subsequently excluded as they were found to have anaemia, a secondary cause of raised ICP. Upon treatment of the anaemia, all signs and symptoms of IIH resolved. Two patients did not complete Stage 2 of the study, as they were unable to tolerate the diet, and a further two patients were lost to follow-up at the final study visit (9 months). Subjects dropping out of the study had similar clinical and anthropometric characteristics to those remaining in the study. Patient demographics are shown in Table 5-2. During the study 44% of patients received an unchanging dose of acetazolamide. No other medications for IIH were used by study subjects. There were minimal side effects associated with the VLCD; 3 patients complained of constipation, 2 of light headed feelings (ameliorated by increased fluid intake) and one described halitosis. No subjects proceeded to CSF diversion, or optic nerve sheath fenestration, during the study.

Characteristic	
Number	25
Age	34.4 ± 9.2
Female gender	25 (100%)
Ethnicity	
Caucasian	20 (80%)
African-Caribbean	3 (12%)
South West Asians (Indo-Pakistanis)	2 (8%)
Disease duration to enrolment (months)	39.0 ± 49.2
Acetazolamide therapy	11 (44%)

Table 5-2   ***Baseline demographics***

Mean and standard deviations are quoted.

At baseline (Table 5-3), mean weight was 101.5 ± 16.0 kg (BMI 38.2 ± 5.0 kgm^{-2}) and ICP was 39.8 ± 5.1 cmH_2O. Universal papilloedema was confirmed using USG and OCT and graded most frequently as Frisen grade 2 (83% of cases) with the remainder grade 1 (17%) (Figure 5-4A). At baseline, there was minimal evidence of visual loss, with LogMAR acuity recorded as -0.02 ± 0.10 and the average HVF mean deviation recorded

as -3.8 ± 4.1 (i.e. a low deviation from the variance observed in the general population). Eight subjects (40%) described symptoms of visual loss (e.g. blurred vision and blind spots). Visual obscurations were reported by 3 patients (15%), tinnitus by 10 patients (50%) and diplopia, which, due to subject understanding was not described at baseline, occurred in 7 patients (35%) at the diet onset. Headache was almost universally reported (19 patients, 95%) and represented a major source of morbidity (HIT-6 scores 57.5 ± 9.0). Baseline headache phenotyping identified that 60% of patients (12 out of 20) had migraineous headache (IHS 1.1, 1.2 and 1.5.1), in addition to headache attributed to IIH (IHS 7.1.1) and 35% described medication overuse (Evers 2004).

As expected, none of the parameters measured altered significantly during Stage 1 (no intervention). Weight significantly reduced following the VLCD (Stage 2) by 15.7 ± 8.0 kg, p<0.001 (-15.3 ± 7.0% of weight) (Figure 5-5A). In conjunction with the weight reduction (Stage 2), there was a clinically and statistically significant drop in ICP (-8.0 ± 4.2 cmH_2O, p<0.001) (Figure 5-5B).

All three techniques used to objectively evaluate different aspects of papilloedema showed significant improvement following weight loss (stage 2): Optic disc elevation measured by USG p=0.002 (Figure 5-6A), optic nerve sheath diameter p=0.004 (Figure 5-6B) and peripapillary RNFL thickness p=0.001 (Figure 5-6C). There was, however, no significant improvement in the less discriminating Frisen grade during stage 1, 2 or 3 (14% improved during stage 1 and 5% improved following stage 2, stage 3 and from the start of the diet to the final follow up, no deterioration in the disc was detected) (Figure 5-4B). Disc ranking was more discriminating at detecting changes in papilloedema; improved: deteriorated 43:19%, p=0.267 for stage 1, 55:23%, p=0.143 for stage 2,

45:25%, p=0.224 for stage 3 and 50:10%, p=0.039 from the start of the diet to the final follow up (Figure 5-4C).

The actual LogMAR visual acuity score improved significantly (p<0.001), but this equated to an improvement by only one line (0.1) in 25.0% of subjects and was not deemed clinically significant. We did note a significant improvement in the Pelli Robson contrast sensitivity following weight loss (following stage 1, 16% improved and 13% deteriorated while following stage 2 (diet stage) 46% improved and 4% deteriorated, p=0.003). During the course of the study, small improvements were noted in HVF mean deviation (0.4 ± 1.6 for stage 1 (p=0.110) and 0.7 ± 2.4 for stage 2 (p=0.162)) and Farnsworth Munsell colour assessment (-21.4 ± 49.7 for stage 1 (p=0.012) and -23.6 ± 45.3 for stage 2 (p=0.027)) (Table 5-3). This is likely to reflect a subject-related learning effect and not a response to weight reduction (Castro *et al.* 2008).

Headache (HIT-6) significantly improved, following weight loss, to a score of 46.9 ± 10.1 (p=0.004) (Figure 5-7A). Additionally, significant improvements were noted in headache severity (VAS from 4.2 ± 2.8 to 1.9 ± 2.8, p=0.015) (Figure 5-7B), headache frequency (from 4.4 ± 2.9 to 2.1 ± 2.8 days per week, p=0.011) (Figure 5-7C) and weekly analgesic use from 2.2 ± 2.5 to 0.2 ± 0.4 days per week, p=0.007) (Figure 5-7D and Table 5-3). Patient symptoms (headache, tinnitus, obscurations and diplopia) showed significant improvement following VLCD (stage 2) (p<0.001, p=0.004, p=0.025 and p=0.008 respectively) (Table 5-3).

Change in ICP during the VLCD did not correlate with change in weight (r=0.280, p=0.209) (Figure 5-5C), or with changes in any of the other outcome measures. Interestingly, if one outlying patient, in whom the start diet LP pressure appears falsely

low (51 cmH$_2$O at baseline, 36 cmH$_2$O at diet onset and 33.5 cmH$_2$O after the diet), is removed, the correlation becomes significant (r=0.440, p=0.046). All outcome measures including weight change (0.2 ± 2.5 kg, p=0.894) were unaltered at the final three months post-diet visit (end of Stage 3, Table 5-3), with the exception of headache symptoms (present in 50% of individuals at the final visit, compared to 58% at the end of the diet, p=0.002), the USG evaluation of papilloedema (nerve sheath diameter -0.4 ± 0.8, p=0.035 and disc elevation -0.07 ± 0.15, p=0.059) and HVF mean deviation (-1.2 ± 2.0, p=0.009) which continued to improve.

Data for the intention to treat analysis (25 patients at baseline, 24 patients at the start of the diet, 22 patients at the end of the diet and 20 patients at the end of the follow-up period) are illustrated in appendix 7.4. This analysis does not alter the overall meaning or significance of the results.

Study characteristics and symptom chronology at each assessment

Characteristic	Baseline	Start Diet	End Diet	Final	P value
Patient numbers	20	20	20	20	
Weight (kg)	101.5 ± 16.0	102.5 ± 16.8	86.8 ± 15.6	87.0 ± 12.9	<0.001
BMI (kgm^{-2})	38.2 ± 5.0	38.6 ± 5.3	32.6 ± 4.7	32.8 ± 4.4	<0.001
Intracranial pressure (cm CSF)	39.8 ± 5.1	38.0 ± 5.0	30.0 ± 4.9	N/A	<0.001
Vision					
Ultrasonographic optic disc elevation (mm)	1.02 ± 0.30	0.97 ± 0.31	0.82 ± 0.28	0.75 ± 0.26	0.002
Ultrasonographic optic nerve sheath diameter (mm)	4.5 ± 1.0	4.7 ± 1.0	4.0 ± 1.2	3.6 ± 1.2[a]	0.004
Optical coherence tomography (Average optic disc elevation) (microm) [#]	144.1 ± 45.5	135.0 ± 48.0	109.3 ± 27.9	108.2 ± 28.6	0.001
LogMAR visual acuity[‡]	-0.02 ± 0.10	0.01 ± 0.11	-0.06 ± 0.09	-0.07 ± 0.08	<0.001[a]
Pelli Robson contrast sensitivity[‡]	1.58 ± 0.17	1.61 ± 0.11	1.67 ± 0.05	1.68 ± 0.10	0.003
Humphrey visual field 24-2 mean deviation[‡]	-3.8 ± 4.1	-3.4 ± 3.7	-2.7 ± 3.0	-1.5 ± 1.8[a]	ns
Farnsworth Munsell 100 Hue colour assessment[#]	110.7 ± 86.5	89.3 ± 84.6[b]	65.7 ± 54.9[b]	61.3 ± 62.0[b]	ns
Headache					
Headache Impact Test (HIT-6)[‡]	57.5 ± 9.0	54.5 ± 1.0	46.9 ± 10.1	48.4 ± 9.6	0.004
Headache severity (VAS 0-10)[‡]	3.8 ± 2.4	4.2 ± 2.8	1.9 ± 2.8	2.6 ± 2.7	0.015
Headache Frequency (days/wk)[‡]	3.8 ± 2.9	4.4 ± 2.9	2.1 ± 2.8	2.6 ± 3.1	0.011
Analgesic use (days/wk) [‡]	2.2 ± 2.7	2.2 ± 2.5	0.2 ± 0.4	1.0 ± 2.1	0.007
Symptoms					
Headache[†] (n (%))	19 (95)	19 (95)	12 (60)	10 (50)	<0.001
Tinnitus[†] (n (%))	10 (50)	10 (50)	4 (20)	4 (20)	0.004
Visual loss[†] (n (%))	8 (40)	7 (35)	3 (15)	1 (5)	0.063
Obscurations[†] (n (%))	3 (15)	4 (20)	0 (0)	0 (0)	0.025
Diplopia[†] (n (%))	0 (0)	7 (35)	0 (0)	0 (0)	0.008

Table 5-3   ***Study characteristics and symptom chronology at each assessment***

Summary statistics represent values for cohort completing study (n=20). p values indicates significant changes following weight reduction (start diet versus end diet; stage 2). No significant changes were noted from baseline to start diet (stage 1) or from end diet to final visit (stage 3) unless indicated. ^{A} significant improvement noted but this was not found in the left eye. ^{b} significant change noted after each stage, therefore weight loss stage did not significantly improve variable. All data analysed (at four time points, except ICP which was analysed at three time points) using repeated measures ANOVA unless stated otherwise. $^\#$ indicates data was logged prior to analysis. ‡ indicates that a Friedman's test was used for analysis and if significant a Wilcoxon Signed rank test was subsequently carried out, results of the latter are quoted in the table. † indicates that a Cochran's Q test revealed a significant improvement in all variables and subsequently a Sign test was used to evaluate differences at each study stage. Abbreviations: CSF, cerebrospinal fluid; NS, not significant; VAS, Visual analogue score; wk, week.
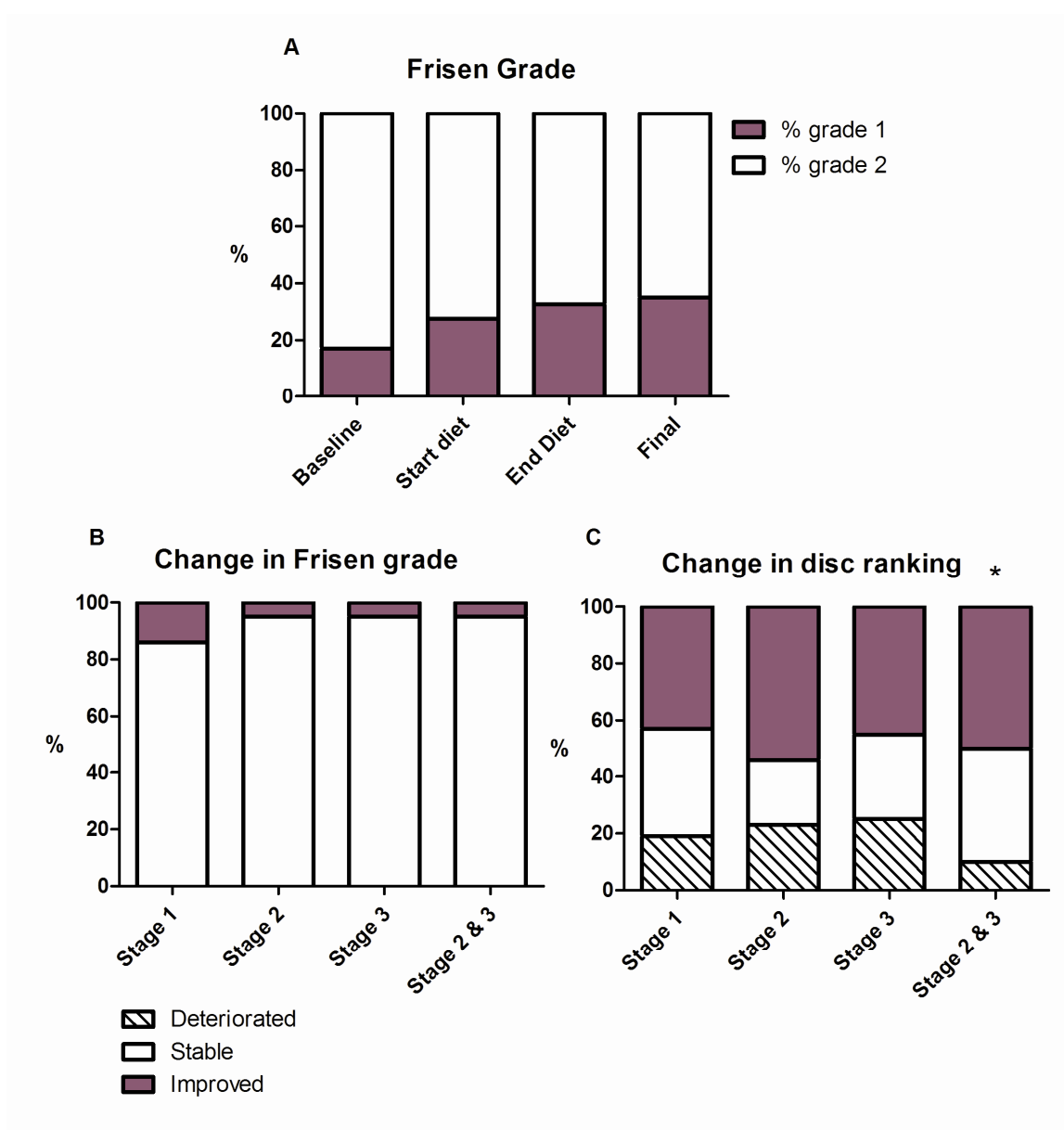
Figure 5-4   ***Evaluation of fundal photography***

(A) The majority of discs were classified as Frisen grade 2 (83% at baseline, 73% start diet, 68% end diet and 65% at the final time point, all other discs were classified as grade 1). (B) There was no significant change in the Frisen grade during the study. (C) Disc analysed by ranking did reveal a significant improvement from the start of the diet to the end of follow up (10% deteriorated, 40% stable and 50% improved, p=0.039). (*p<0.05).Intention to treat analysis.

A Weight

B Intracranial pressure

C Relationship between weight and intracranial pressure

$r=0.280$
$p=0.209$
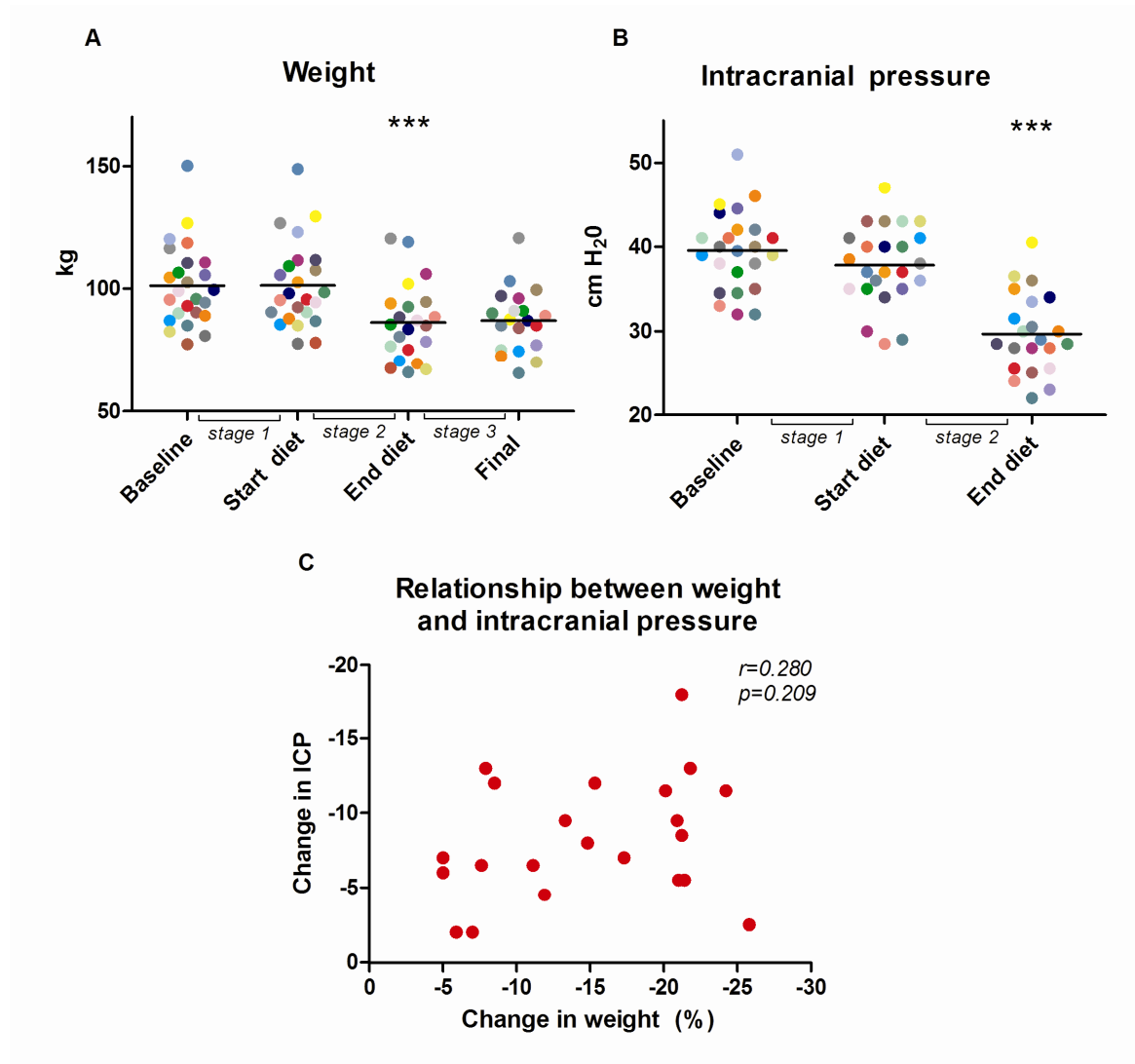
Figure 5-5 ***Weight and intracranial pressure assessment***

Scatter plots with means showing (A) weight loss, (B) intracranial pressure (ICP) change, (C) relationship between change in ICP and weight. *** indicates significant change from previous time point (p<0.001).
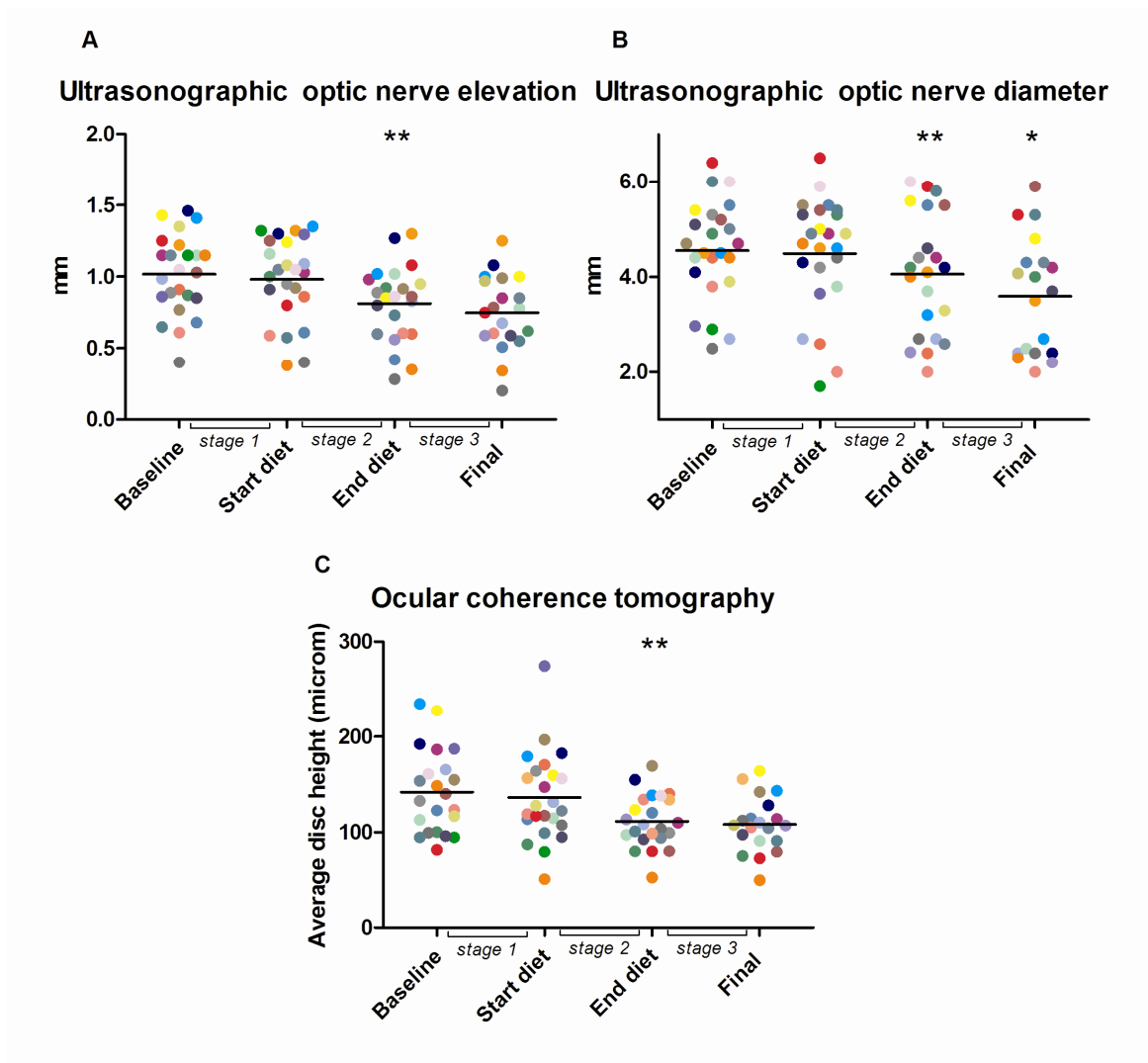
Figure 5-6 **Quantification of papilloedema**

> *Scatter plots with means (A) ultrasonographic optic nerve elevation, (B) ultrasonographic optic nerve diameter, (C) optical coherence tomography retinal nerve fibre layer average distension. Significant changes are from previous time point (** p<0.01 and *p<0.05).*
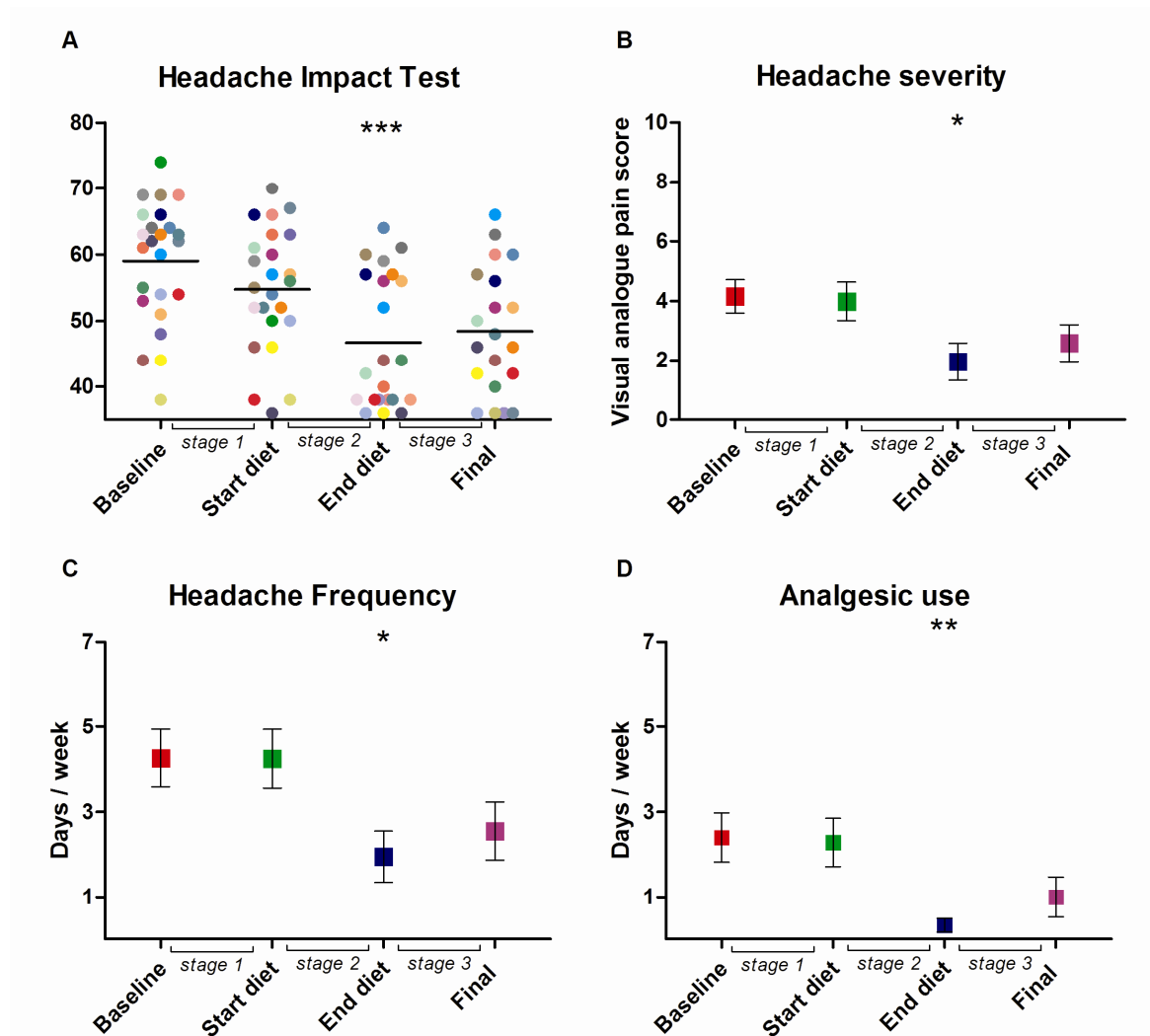
Figure 5-7   Headache assessment

(A) Scatter plot with means showing Headache Impact Test-6 scores. Headache diary assessment of (B) headache severity, using a visual analogue pain score where 0 indicates no pain and 10 maximum pain, (C) headache frequency (number of days per week with headache) and (D) analgesic use (number of days analgesia used per week). Plots illustrate means and standard error of the mean. Significant changes are from previous time point (*** p<0.001, ** p<0.01 and * p<0.05).

5.3.2. Effect of weight loss on the metabolic phenotype and 11β-HSD1, in idiopathic intracranial hypertension

Results

25 subjects were enrolled and 22 completed the study (one was excluded, due to a secondary cause of IIH, and two were lost to follow-up). Results are analysed on an intention to treat basis and baseline demographics are shown in Table 5-2 and represent data for the whole cohort at each time point (25 patients at baseline, 24 patients at the start of the diet and 22 patients at completion of the study), consequently data quoted for changes between time points will reflect the differences noted in the cohort present at the end of the time period. Five IIH subjects (20%) had PCOS. As described in the previous section, weight remained stable during the observation period (Stage 1) (0.8 ± 3.1 kg) and there were no significant changes in any of the outcome measures. The VLCD (Stage 2) caused a significant reduction in weight (14.2 ± 7.8 kg, p<0.001), equivalent to loss of 15.2 ± 7.8% of weight (BMI fell by 5.8 ± 3.0 kgm^{-2}). The waist circumference also fell significantly (9.8 ± 5.4 cm, p<0.001).

5.3.2.1.   Urinary steroid metabolites

No changes in the urinary steroid metabolites were noted over the observation period (Stage 1). Following the VLCD (Stage 2), there was a significant reduction in the THF+5α-THF: THE ratio (from 0.95 ± 0.30 start diet *vs.* 0.81 ± 0.25 end diet, p=0.001) (Figure 5-8A) (Table 5-4). The urinary free cortisol: cortisone ratio, an indicator of 11β-HSD2 activity, did not change during the study suggesting that the change in THF+5α-THF: THE reflected reduced 11β-HSD1 activity. In keeping with reduced 11β-HSD1 activity, the total cortisol (Fm) to total cortisone (Em) metabolite ratio also fell (0.73 ±

0.22 *vs*. 0.63 ± 0.19, p=0.001). The change in global 11β-HSD1 activity correlated significantly with the fall in ICP (r=0.504, p=0.028) (Figure 5-9A). Total glucocorticoid metabolites, reflecting daily cortisol secretion rate, also fell following weight loss (p=0.013) (Figure 5-8B). Measures of 5α-reductase activity decreased following the VLCD (5α-THF, p=0.002; 5α-THF:THF ratio, p=0.005; An, p=0.006; An:Et ratio, p=0.002; Table 2) (Figure 5-8C,D,E&F). The intra and inter-assay coefficient of variance was <10%.

5.3.2.2.   CSF and serum cortisol and cortisone

Cortisol and cortisone levels in the CSF were lower than that observed in the serum (baseline cortisol 9.5 ± 5.0 nmoles/l vs 239 ± 116 nM/l   and cortisone 5.0 ± 2.0 nmoles/l vs 39.2 nmoles/l for CSF and serum respectively). Cortisol: cortisone ratios were lower in the CSF compared to the serum (1.9 ± 0.4 vs 6.0 ± 2.0 respectively), although in the absence of measuring free steroid levels, these ratios should be interpreted with caution. Absolute CSF and serum steroid concentrations did not change following weight loss (Table 5-4), but the change in CSF cortisone negatively correlated with change in weight (r= -0.512, p=0.018) (Figure 5-9B) and BMI (r= -0.444, p=0.044). Interestingly the CSF cortisol, measured at all time points (baseline, end of Stage 1 and 2) correlated significantly with subject age (baseline, r=0.533, p=0.006; start diet, r=0.487, p=0.016; end diet, r=0.663, p<0.001; all time points r=0.584, p<0.001 (Figure 5-9C).

Characteristic		Baseline	Start diet	End diet	p value
Patient numbers		25	24	22	
Clinical features	Weight (kg)	101.3 ± 16.5	101.3 ± 17.4	86.3 ± 15.5	**<0.001**
	BMI (kgm^{-2})	37.9 ± 4.9	38.1 ± 5.3	32.4 ± 4.9	**<0.001**
	Waist (cm)	111.1 ± 10.4	111.1 ± 10.0	101.0 ± 12.0	**<0.001**
Urine (µg/24 h)	THF+5αTHF:THE	0.89 ± 0.23	0.95 ± 0.30	0.81 ± 0.25	**0.001**
	Cortisol: cortisone	0.70 ± 0.19	0.75 ± 0.19	0.69 ± 0.30	0.456
	5αTHF:THF	1.18 ± 0.62	1.20 ± 0.64	0.93 ± 0.47	**0.005**
	5αTHF	1883.0 ± 1502.0	1868.9 ± 1370.0	1031.3 ± 925.3	**0.002**
	THF	1586.8 ± 971.2	1553.6 ± 659.2	1053.0 ± 648.5	**0.020**
	Total GC metabolites	10745.1 ± 5902.6	10826.2 ± 5804.5	6995.4 ± 4480.2	**0.013**
	An	2424.0 ± 2121.1	2579.7 ± 2273.8	1536.7 ± 1609.6	**0.006**
	An:Et	1.42 ± 0.69	1.48 ± 0.90	1.16 ± 0.68	**0.002**
	An+Et+DHEA	5361.3 ± 4849.2	5352.3 ± 4920.2	3679.8 ± 4004.8	**0.010**
	Fm	4401.7 ± 2872.9	4384.9 ± 2372.3	2660.1 ± 1837.3	**0.004**
	Em	6343.5 ± 3144.6	6441.3 ± 6567.0	4335.3 ± 2730.9	**0.022**
	Fm:Em	0.68 ± 0.14	0.73 ± 0.22	0.63 ± 0.19	**0.001**
CSF (nmoles/l)	Cortisol	9.52 ± 5.00	8.36 ± 3.66	8.60 ± 3.56	0.852
	Cortisone	5.04 ± 1.99	4.67 ± 1.69	4.88 ± 1.56	0.944
	Cortisol: Cortisone ratio	1.85 ± 0.44	1.81 ± 0.37	1.76 ± 0.39	0.619
Serum (nmoles/l)	Cortisol	239.03 ± 115.66	194.48 ± 82.41	190.27 ± 92.63	0.708
	Cortisone	39.19 ± 15,78	37.66 ± 15.36	35.39 ± 10.64	0.932
	Cortisol : cortisone ratio	6.01 ± 1.95	5.15 ± 1.01	5.15 ± 1.67	0.614
Serum: CSF ratio	Cortisol	26.33 ± 9.43	24.00 ± 7.49	24.61 ± 11.86	0.754
	Cortisone	8.20 ± 3.00	8.23 ± 1.92	7.69 ± 1.43	0.509
	Cortisol: cortisone ratio	3.31 ± 0.95	2.94 ± 0.72	3.15 ± 1.24	1.00

Table 5-4   ***Study characteristics and steroid metabolite changes during study***

Data summary statistics represent complete cohort at each time point. Mean and standard deviations shown. No significant changes were noted between baseline and start diet. p values represent changes from start diet to end diet. CSF indicates cerebrospinal fluid; BMI, body mass index; THF, tetrahydrocortisol; THE, tetrahydrocortisone; GC, glucocorticoids; An, androstenedione; Et, etiocholanolone; DHEA, dehydroepiandrosterone; Fm, total cortisol metabolites; Em, total cortisone metabolites.
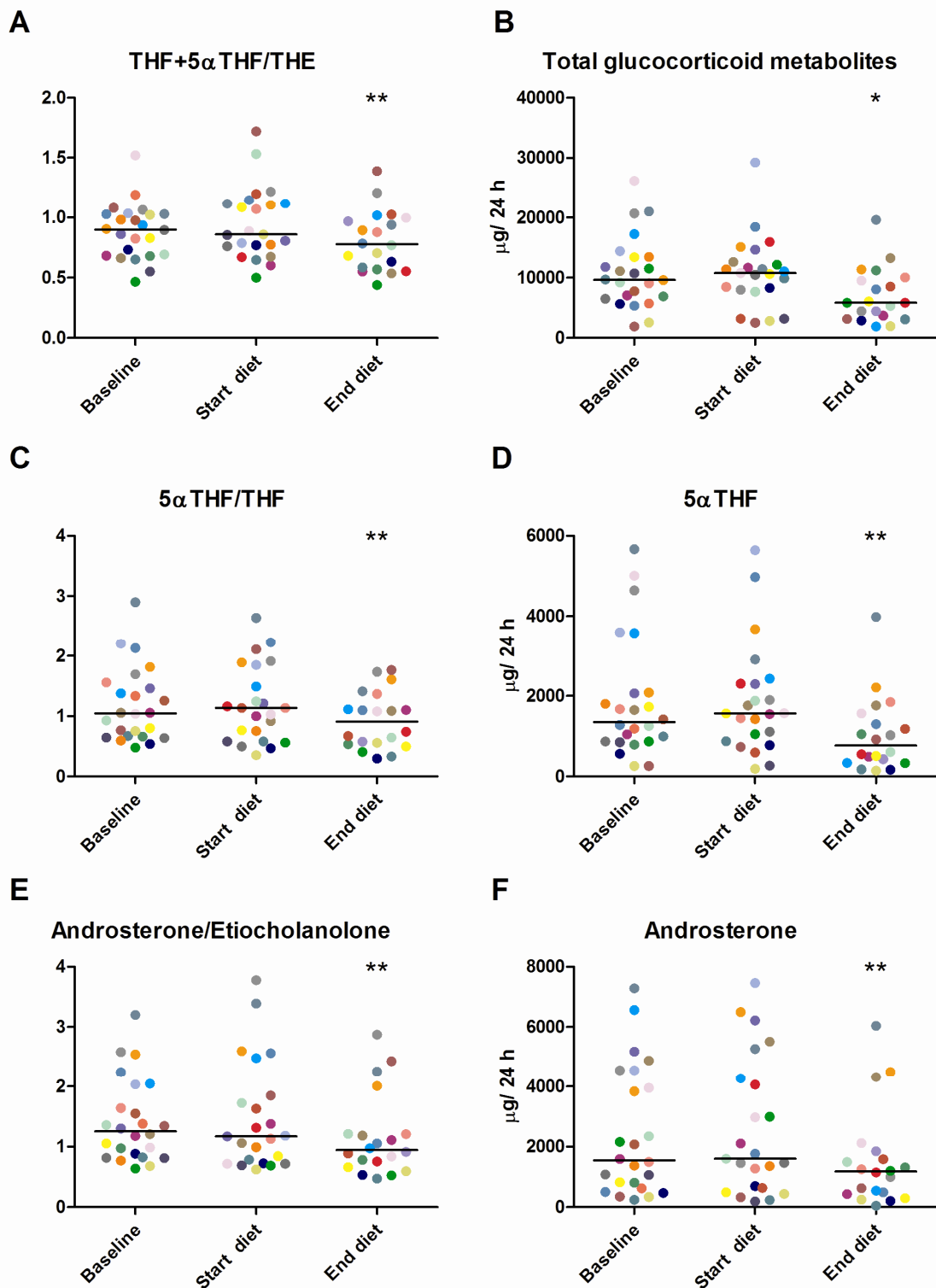
Figure 5-8   ***Urinary steroid metabolite changes following weight loss***

Scatter plots with median and ranges illustrating significant reductions in: (A) 11β-HSD 1 activity (tetrahydrocortisol (THF) and 5αTHF) to tetrahydrocortisone (THE) ratio); (B) total glucocorticoid metabolites and 5α reductase activity indicated by the (C) 5αTHF:THF ratio, (D) 5αTHF, (E) androsterone: etiocholanolone ratio and (F) androsterone. p values indicate change from previous time point (** p<0.01, *p<0.05).

186
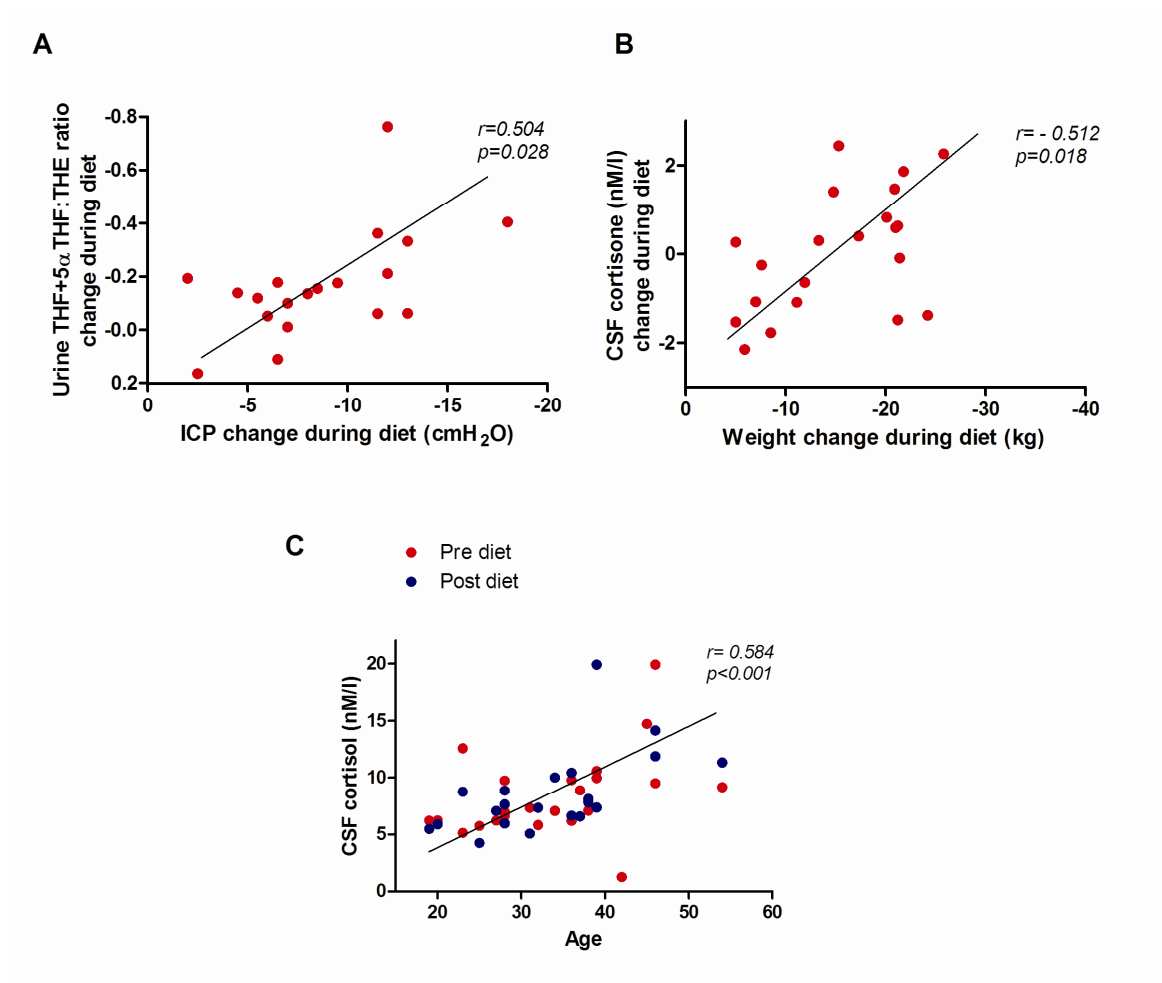
Figure 5-9   *Correlations of metabolic changes with clinical parameter*

(A) The change in urine 11β-HSD 1 activity correlated with change in intracranial pressure (ICP) following the diet. (B) The extent of weight loss inversely correlated with change in cerebrospinal fluid (CSF) cortisone following the diet. (C) Age demonstrated a linear correlation with CSF cortisol. THF indicates tetrahydrocortisol and THE tetrahydrocortisone.

5.3.2.3.   Fasted metabolite profiles

The fasting serum cholesterol was observed to significantly reduce (0.62 ± 0.86 mmol/l, p=0.007) although the triglycerides did not significantly alter. BP was noted to fall with weight loss, although this showed considerable patient variability and did not reach the level of statistical significance (reduction of 2.9 ± 17.9 mmHg in stage 1 and 5.3 ± 17.5

Chapter 5

mmHg in stage 2). The fasting glucose and insulin fell significantly (reduction of 0.13 ± 0.95 mmol/l, p=0.021 and 6.6 ± 6.3 µU/ml, p<0.001 respectively). In keeping with the changes in glucose and insulin, the HOMA %B, %S and IR significantly improved (p=0.002, p=0.001 and p=0.001 respectively). The results are summarised in Table 5-5.

Characteristic	Baseline	Start diet	End diet	p value
Systolic BP (mmHg)	134.5 ± 15.9	130.4 ± 15.2	124.8 ± 13.7	0.135[a]
Cholesterol (mmol/l)	4.9 ± 0.9	5.0 ± 1.0	4.5 ± 1.0	**0.007**
Triglycerides (mmol/l)	1.57 ± 0.95	1.56 ± 1.11	1.24 ± 0.62	0.185[a]
Glucose (mmol/l)	4.5 ± 0.7	4.7 ± 0.9	4.3 ± 0.5	**0.021[a]**
Insulin (µU/ml)	14.8 ± 8.7	17.4 ± 11.7	10.7 ± 9.3	**<0.001**
HOMA %B	191.2 ± 81.0	201.5 ± 108.9	158.0 ± 94.0	**0.002**
HOMA %S	65.3 ± 30.7	61.3 ± 38.1	114.8 ± 78.8	**0.001**
HOMA IR	1.88 ± 1.00	2.54 ± 2.37	1.30 ± 1.07	**0.001**
Glucose : Insulin ratio	0.36 ± 0.15	0.37 ± 0.22	0.67 ± 0.49	**<0.001[a]**

Table 5-5 ***Fasted metabolic profile before and after weight loss***

> [a] *significance level is p<0.025 as two pair-ways comparisons are being made per variable. Blood pressure (BP), Homeostasis Model Assessment (HOMA), percent beta cell function (%B), percent insulin sensitivity (%S), insulin resistance (IR).*

5.3.2.4.   Dual energy x-ray absorptiometry

In keeping, with the weight loss observed following the VLCD (stage 2), fat mass was noted to reduce in both the trunk and limbs (p<0.001), although the fat was predominantly lost from the trunk (4.7 ± 3.7 % lost from the trunk with a relative increase in limb fat, 1.1 ± 2.1 %). The trunk: limb fat mass ratio was correspondingly noted to significantly decrease (p=0.014). Lean mass also fell with weight loss (p<0.001). Results are

summarised in Table 5-6. There was no correlation between ICP and measures of fat

mass.

Characteristic	Start diet	End diet	Change	p
Total fat mass (kg)	45.0 ± 9.8	36.1 ± 10.1	-9.10 ± 4.7	**<0.001**
Total fat (%)	44.7 ± 3.9	40.6 ±5.3	-4.1 ± 2.7	**<0.001**
Total lean mass (kg)	52.4 ± 6.1	49.1 ± 6.3	-3.9 ± 2.3	**<0.001**
Total lean (%)	52.8 ± 3.6	56.6 ± 4.9	3.7 ± 2.6	**<0.001**
Total BMC (g)	2417.5 ± 314.7	2415.2 ± 338.3	-12.6 ± 63.6	0.526
Total BMC (%)	2.5 ± 0.4	2.8 ± 0.5	0.4 ± 0.2	**<0.001**
Trunk fat mass (kg)	22.2 ± 5.0	17.6 ± 5.4	-5.0 ± 2.8	**<0.001**
Trunk fat (%)	44.9 ± 4.4	40.5 ± 6.0	-4.7 ±3.7	**<0.001**
Trunk lean mass (kg)	26.2 ± 0.3	24.3 ± 0.4	0.2 ± 0.1	**<0.001**
Trunk lean (%)	53.6 ± 4.3	57.8 ± 5.9	4.4 ± 3.6	**<0.001**
Trunk BMC (g)	692.3 ± 96.5	675.4 ± 107. 7	-20.2 ± 54.5	0.179
Trunk BMC (%)	1.4 ± 0.3	1.6 ± 0.3	0.2 ± 0.1	**<0.001**
Limb fat mass (kg	21.8 ± 5.5	17.6 ± 5.1	-4.1 ± 2.1	**<0.001**
Limb fat (%)	48.2 ± 4.9	48.7 ± 4.5	1.1 ± 2.1	**<0.001**
Limb lean mass (kg)	23.0 ± 3.0	21.4 ± 2.9	-2.0 ± 1.5	**<0.001**
Limb lean (%)	50.5 ± 4.3	53.9 ± 4.8	2.8 ± 2.5	**<0.001**
Limb BMC (g)	1191.3 ± 143.8	1200.5 ± 151.4	5.9 ± 30.1	0.455
Limb BMC (%)	2.7 ± 0.4	3.1 ± 0.5	0.4 ± 0.3	**<0.001**
Trunk: limb fat mass ratio	1.04 ± 0.23	1.01 ± 0.20	-0.06 ± 0.10	**0.014**

Table 5-6   *Dual energy x-ray absorptiometry body composition analysis following weight loss.*

BMC indicates bone mineral content.

5.3.2.5.   Comparison of glucocorticoid, metabolic, and body composition changes in

IIH and non IIH obese subjects following weight loss

After matching the IIH and non IIH obese patients, all subjects were female and there

were no significant difference in BMI (p=0.369) or age (p=0.224) (Table 5-7).

Characteristic	IIH	Control	p
Number	22	13	
Gender (% female)	100	100	
Age (years)	34.4 ± 9.2	40.4 ± 13.5	0.224
Weight (kg)	101.3 ±16.5	100.4 ± 12.5	0.863
BMI (kgm^{-2})	37.9 ± 4.9	36.5 ± 4.8	0.369
Waist (cm)	111.1 ± 10.4	104.3 ± 7.8	0.043

Table 5-7   *Baseline demographics of the IIH and non IIH obese control subjects embarking on a weight loss regimen*

The extent of weight loss, following the three months VLCD, was very similar between the two groups (IIH lost 15.2 ± 3.0 kg and controls lost 13.3 ± 4.4 kg). There was no statistically significant difference in the fasting metabolite changes (Table 5-8). Similarly, changes in the fat mass distribution were not statistically different (Table 5-8). The urinary steroid metabolites showed greater reduction in 11β-HSD1 activity (demonstrated by the THF + 5αTHF: THE ratio) in the IIH cohort, although this did not reach the level of statistical significance (IIH 0.23 ± 0.26 and controls 0.13 ± 0.14, p=0.667) (Figure 5-10A). The GC metabolites also showed a trend towards a greater increase in the IIH subjects (IIH 3476.8 ± 52531.1 and controls 1669.8 ± 5139.4, p=0.250) (Figure 5-10B).

Characteristic	IIH	Control	p
Weight (kg)	-15.2 ± 3.0	-13.3 ± 4.4	0.775
BMI (kgm^{-2})	-5.8 ± 3.0	-4.8 ± 1.5	0.555
Waist (cm)	-9.4 ± 5.9	-10.4 ± 5.5	0.649
BP systolic	-6.4 ± 19.6	-1.9 ± 8.9	0.568
Fasting metabolites			
Cholesterol (mmol/l)	-0.6 ± 0.9	0.6 ± 1.9	0.118
TG (mmol/l)	-0.3 ± 0.7	0.2 ± 0.7	0.087
Glucose (mmol/l)	-0.3 ± 0.6	0.1 ± 1.3	0.408
Insulin (µU/ml)	-6.7 ± 6.9	-6.2 ± 4.1	0.917
HOMA %B	-49.3 ± 63.8	-39.0 ± 44.4	0.709
HOMA %S	51.8 ± 60.5	67.3 ± 64.7	0.500
HOMA IR	-1.3 ± 2.3	0.9 ± 0.6	0.862
Glucose : Insulin ratio	0.29 ± 0.37	0.39 ± 0.32	0.110
DEXA			
Total fat mass(kg)	-9.10 ± 4.7	-9.3 ± 3.4	0.957
Total Fat (%)	-4.1 ± 2.7	-4.0 ± 2.4	0.986
Trunk fat mass (kg)	-5.0 ± 2.8	-4.9 ± 2.4	0.870
Urinary steroid metabolites			
THF +5αTHF:THF	-0.23 ± 0.26	-0.13 ± 0.14	0.667
5αTHF:THF	-0.30 ± 0.40	-0.33 ± 0.38	0.672
Total GC metabolites (µg/24h)	-3476.8 ± 52531.1	-1669.8 ± 5139.4	0.250

Table 5-8   *Changes with weight loss noted in the idiopathic intracranial hypertension (IIH) and non IIH obese patients.*

TG indicates triglycerides, blood pressure (BP), Homeostasis Model Assessment (HOMA), percent beta cell function (%B), percent insulin sensitivity (%S), insulin resistance (IR), tetrahydrocortisol (THF), tetrahydrocortisone (THE) and glucocorticoids (GC).
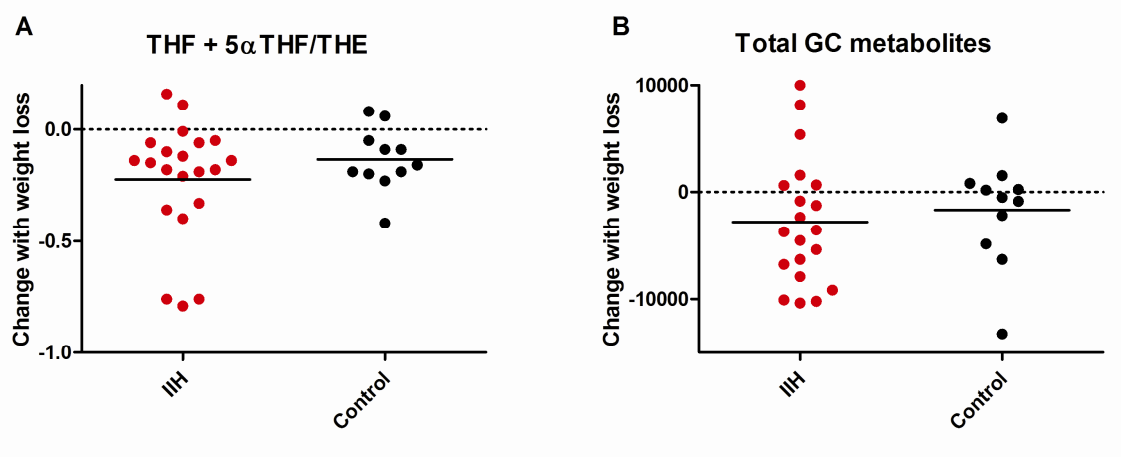
Figure 5-10   Metabolite changes in IIH and idiopathic obesity

Changes in 11β-HSD1 activity (tetrahydrocortisol (THF) + 5α THF/ tetrahydrocortisone (THE) ratio) and total glucocorticoid metabolites (GC) following a three months very low calorie diet in IIH and non IIH obese controls.

5.3.3. Comparison of metabolic phenotype and 11β-HSD1 in idiopathic intracranial hypertension and control patients

Results

29 IIH and 47 control subjects were recruited. Baseline demographics are shown in Table 5-9. There was no significant difference in the gender, weight, BMI or waist between IIH and control subjects ($p=1.00$, $p=0.125$, $p=0.078$ and $p=0.343$). The IIH patients were, however, significantly younger than the control subjects (32.8 ± 8.6 years compared to 49.1 ± 6.9 years, $p<0.001$). Six (20.7%) of the IIH patients had coexisting PCOS.

	IIH	Control	p
Female gender ((number (%))	29 (100)	47 (100)	1.00
Weight (kg)	96.1 ± 12.6	91.1 ± 14.4	0.125
BMI (kgm^{-2})	36.2 ± 3.7	34.5 ± 4.3	0.078
Waist (cm)	106.5 ± 10.2	104.2 ± 9.7	0.343
Age (years)	32.8 ± 8.6	49.1 ± 6.9	<0.001
BP systolic	130.3 ± 14.9	125.3 ±15.0	0.273
Coexisting PCOS (number (%))	6 (20.7)	0	

Table 5-9   *Demographics of the idiopathic intracranial hypertension (IIH) and control subjects*

PCOS indicated polycystic ovarian syndrome

5.3.3.1. Urinary steroid metabolites

Global 11β-HSD1 activity, as indicated by the THF+5αTHF: THE ratio, did not significantly differ between the IIH patients and the obese controls (0.96 ± 0.36 and 0.94 ± 0.35 respectively, p=0.869). The 11β-HSD2 activity (free cortisol: cortisone ratio) was higher in IIH patients (0.71 ± 0.19 and 0.64 ± 0.45 respectively, p=0.005), however, this difference was lost following multivariate regression analysis to adjust for age (p=0.590). The total glucocorticoid metabolites, a determinant of HPA axis activity, were greater in the IIH than the control cohort (10396.9 ± 5227.3 µg24^{-1} and 8417.3 ± 4075.0 µg24^{-1} respectively, p=0.027) and were independent of age.

Cortisol inactivation by 5α reductase, which was independent of age, was significantly greater in the IIH than control patents (5αTHF: THF ratio, 1.15 ± 0.19 and 0.82 ± 0.38, p=0.009; 5αTHF, 1727.7 ± 1139.4 µg24^{-1} and 1162.4 ± 697.5 µg24^{-1}, p=0.014 respectively). Reduced 5β-reductase activity is unlikely to explain these results, as excretion of THF did not differ between groups. Androgen metabolism by 5α reductase was also higher in the IIH than control patients (An, 2377.6 ± 2119.0 µg24^{-1} and 1134.9 ± 820.9 µg24^{-1}, p=0.015; An+Et+DHEA, 5265.7 ± 4472.3 µg24^{-1} and 2519.0 ± 1727.9 µg24^{-1}, p=0.003, respectively). The differences in androgen metabolites were, however,

not maintained following multivariate regression analysis to adjust for the age differences between the groups (An, p=0.553 and An+Et+DHEA, p=0.736). The androgen metabolites negatively correlated with age in both IIH and control subjects even after adjustment for BMI (An, r=-0.418, p=0.030 and r=-0.411, p=0.005; An+Et+DHEA, r=-0.474, p=0.001 and r=-0.376, p=0.010 respectively). The urinary metabolite changes are summarised in Table 5-10. None of the urinary steroid metabolites, or ratios, demonstrated a linear relationship with ICP.

Characteristic	IIH	Control	p
THF+5αTHF:THE	0.96 ± 0.36	0.94 ± 0.35	0.869
F:E	0.71 ± 0.19	0.64 ± 0.45	**0.005**
5αTHF:THF	1.15 ± 0.19	0.82 ± 0.38	**0.009**
5αTHF	1727.7 ± 1139.4	1162.4 ± 697.5	**0.014**
THF	1525.1 ± 612.2	1520.9 ± 946.5	0.303
Total GC	10396.9 ± 5227.3	8417.3 ± 4075.0	**0.027**
An	2377.6 ± 2119.0	1134.9 ± 820.9	**0.015**
An: Et	1.38 ± 0.70	1.15 ± 0.52	0.200
An+Et+DHEA	5265.7 ± 4472.3	2519.0 ± 1727.9	**0.003**
Fm	4200.4 ± 2081.8	3435.2 ± 1765.5	0.055
Em	6196.5 ± 3300.3	4982.2 ± 2442.5	0.060
Fm: Em	0.74 ± 0.25	0.70 ± 0.20	0.677

Table 5-10   Urinary steroid metabolite profiles in idiopathic intracranial hypertension (IIH) and control subjects

Tetrahydrocortisol (THF), tetrahydrocortisone (THE), glucocorticoids (GC), androstenedione (An), etiocholanolone (Et), dehydroepiandrosterone (DHEA), total cortisol metabolites (Fm) and total cortisone metabolites (Em) ($\mu g24^{-1}$).

5.3.3.2.   Fasted metabolite profiles

The fasting serum cholesterol, triglycerides and glucose did not differ between groups (p=0.481, p=0.971 and p=0.328 respectively). The fasting insulin was higher in the IIH

subjects than controls (14.3 ± 6.4 and 10.8 ± 7.8 µU/ml, p=0.036 respectively). This was in keeping with a lower glucose: insulin ratio in the IIH patients (IIH, 0.4 ± 0.2 and controls, 0.8 ± 0.9, p=0.027). The HOMA scores showed a trend towards increased insulin resistance in the IIH cohort (HOMA IR 2.1 ± 2.1 in IIH and 1.6 ± 1.1 in controls) but this did not reach the level of statistical significance (p=0.147) (Table 5-11).

Characteristic	IIH	Control	p
Cholesterol (mmol/l)	4.9 ± 1.1	5.1 ± 1.0	0.481
Triglycerides (mmol/l)	1.5 ± 1.1	1.3 ± 0.6	0.971
Glucose (mmol/l)	4.8 ± 0.9	4.7 ± 0.6	0.328
Insulin (µU/ml)	14.3 ± 6.4	10.8 ± 7.8	**0.036**
HOMA %B	170.0 ± 63.8	141.7 ± 55.6	0.073
HOMA %S	67.8 ± 35.8	102.9 ± 76.3	0.140
HOMA IR	2.1 ± 2.1	1.6 ± 1.1	0.147
Glucose: Insulin ratio	0.41 ± 0.20	0.83 ± 0.87	**0.027**

Table 5-11   ***Fasting metabolite profiles in idiopathic intracranial hypertension (IIH) and control subjects***

Blood pressure (BP), Triglycerides (TG), Homeostasis Model Assessment (HOMA), percent beta cell function (% B), percent insulin sensitivity (% S) and insulin resistance (IR).

5.3.3.3.   Dual energy x-ray absorptiometry

Fat mass distribution did not differ between IIH and control subjects (Table 5-12). The total fat mass correlated with the total glucocorticoid metabolites measured by urinary GC/MS (IIH, r=0.691, p=0.001 and controls r=0.361, p=0.014). Trunk bone mineral content mass was higher in IIH subjects (IIH, 676.8 ± 92.0 and controls 582.8 ± 105.2, p<0.001), however, the difference was lost following multivariate regression analysis which accounted for age differences between the groups (p=0.138). Other differences in body composition noted between the groups were lost following correction for age.

Characteristic	IIH	Control	p
Total fat mass (kg)	42.0 ± 7.5	39.3 ± 9.2	0.125
Total fat (%)	43.9 ± 3.5	43.4 ± 4.4	0.655
Total lean mass (kg)	50.9 ± 4.8	48.5 ± 6.4	0.100
Total lean (%)	53.6 ± 3.3	54.2 ± 4.2	0.615
Total BMC mass (kg)	23.7 ± 2.5	21.4 ± 3.3	**0.004**
Total BMC (%)	2.5 ± 0.4	2.4 ± 0.4	0.494
Trunk fat mass (kg)	20.5 ± 3.2	19.9 ± 5.2	0.194
Trunk fat (%)	43.8 ± 3.4	43.4 ± 5.1	0.812
Trunk lean mass (kg)	25.5 ± 2.8	25.1 ± 3.5	0.655
Trunk lean (%)	54.7 ± 3.2	5.4 ± 5.0	0.558
Trunk BMC mass (g)	676.8 ± 92.0	582.8 ± 105.2	**<0.001**
Trunk BMC (%)	1.5 ± 0.3	1.3 ± 0.2	**0.008**
Limb fat mass (kg)	20.5 ± 5.0	18.3 ± 4.3	0.139
Limb fat (%)	46.3 ± 4.7	45.7 ± 5.0	0.791
Limb lean mass (kg)	22.2 ± 2.5	20.4 ± 3.3	**0.014**
Limb lean (%)	51.0 ± 4.4	516 ± 4.8	0.845
Limb BMC mass (g)	1170.9 ± 104.1	1079.1 ± 241.3	**0.030**
Limb BMC (%)	2.7 ± 0.4	2.7 ± 0.4	0.410
Trunk: limb ratio	1.0 ± 0.2	1.1 ± 0.2	0.135

Table 5-12   Dual energy x-ray absorptiometry (DEXA) body composition in idiopathic intracranial hypertension (IIH) and control subjects

BMC indicates bone mineral content.

5.3.3.4.   Influence of polycystic ovarian syndrome

The IIH patients with PCOS were removed, leaving 23 patients in the IIH cohort and 47 in the control cohort (Table 5-13).

	IIH (no PCOS)	Control	P
Female gender ((number (%))	23 (100)	47 (100)	
Weight (kg)	93.9 ± 12.5	91.1 ± 14.4	0.419
BMI (kgm^{-2})	35.4 ± 3.5	34.5 ± 4.3	0.367
Waist (cm)	104.6 ± 10.4	104.2 ± 9.7	0.342
Age (years)	33.6 ± 8.8	49.1 ± 6.9	<0.001
BP systolic	131.4 ± 14.9	125.3 ±15.0	0.192

Table 5-13   Demographics following exclusion of those IIH patients with coexisting polycystic ovarian syndrome (PCOS)

Chapter 5

Following exclusion of the IIH patients with PCOS, there were no differences in the

fasting serum metabolites (Table 5-14), or body composition between the groups.

Differences in the 24 hour urinary steroid profiles between IIH and BMI matched controls

were lost, with the exception of 5αTHF:THF (Table 5-15). This metabolite ratio, a

reflection of 5α reductase activity, remained higher in the IIH cohort (IIH, 1.15 ± 0.61 and

controls 0.82 ± 0.38, p=0.028) and did not correlate with age.

Characteristic	IIH (no PCOS)	Control	P
Cholesterol (mmol/l)	4.9 ± 1.0	5.1 ± 1.0	0.543
Triglycerides (mmol/l)	1.5 ± 1.2	1.3 ± 0.6	0.967
Glucose (mmol/l)	4.8 ±0.9	4.7 ± 0.6	0.486
Insulin (μU/ml)	16.6 ± 6.2	10.8 ± 7.8	0.116
HOMA %B	159.5 ± 66.1	141.7 ± 55.6	0.395
HOMA %S	73.1 ± 37.4	102.9 ± 76.3	0.432
HOMA IR	2.1 ± 2.3	1.6 ± 1.1	0.451
Glucose: Insulin Ratio	0.45 ± 0.20	0.83 ± 0.87	0.185

Table 5-14 *Fasting metabolite ratios following exclusion of those IIH patients with coexisting polycystic ovarian syndrome (PCOS)*

Characteristic	IIH (no PCOS)	Control	P
THF+5αTHF:THE	1.01 ± 0.38	0.94 ± 0.35	0.511
F:E	0.69 ±0.20	0.64 ± 0.45	**0.033**
5αTHF:THF	1.15 ± 0.61	0.82 ± 0.38	**0.028**
5αTHF	1635.7 ± 1184.5	1162.4 ± 697.5	0.066
THF	1461.2 ± 664.8	1520.9 ± 946.5	0.699
Total GC	9726.0 ±5556.7	8417.3 ± 4075.0	0.172
An	1799.2 ±1808.3	1134.9 ± 820.9	0.236
An: Et	1.38 ± 0.73	1.15 ± 0.52	0.297
An+Et+DHEA	4030.0 ± 3540.6	2519.0 ± 1727.9	0.076
Fm	4014.9 ± 2211.1	3435.2 ± 1765.5	0.212
Em	5711.1 ± 3489.8	4982.2 ± 2442.5	0.374
Fm: Em	0.77 ±0.26	0.70 ± 0.20	0.279

Table 5-15   *Urinary steroid metabolite profiles following exclusion of those IIH patients with coexisting polycystic ovarian syndrome (PCOS)*

Differences in the F:E ratio were lost following multivariate regression to correction for age. Tetrahydrocortisol (THF), tetrahydrocortisone (THE), glucocorticoids (GC), androstenedione (An), etiocholanolone (Et), dehydroepiandrosterone (DHEA), total cortisol metabolites (Fm) and total cortisone metabolites (Em) ($\mu g24^{-1}$).

5.4. Discussion

5.4.1. The clinical consequences of weight loss in idiopathic intracranial hypertension

Discussion

This is the first prospective longitudinal study to demonstrate that weight loss is effective in reducing not only headaches and papilloedema, but also ICP in IIH. The study results provide an evidence base for therapeutic weight reduction in IIH.

Whilst we acknowledge that LP only records a snap-shot assessment of ICP and does not reflect diurnal fluctuations, the minimal changes in ICP reported over Stage 1 (no intervention; -1.8 ± 5.5 cmH$_2$O) indicate that the variability in ICP did not significantly

influence our data. The absence of a direct relationship between weight loss and change in ICP, suggests a more complex relationship which may be influenced by a patient-specific weight threshold for raised ICP. ICP fell to a "normal" level (below 25 cmH$_2$O) in 4 patients (20%). In those patients whose ICP remained above 25 cmH$_2$O, 81% (13 out of 16 patients) had become asymptomatic for tinnitus, visual loss, diplopia and visual obscurations after weight loss, compared with 25% (4 out of 16) of these subjects at baseline. These data highlight that it might not be necessary for IIH subjects to reduce their ICP to below defined normal levels (25cmH$_2$O) in order to achieve significant symptomatic relief. This may, however, be an overly simplistic concept as obesity is known to marginally increase ICP (Whiteley et al. 2006) and it is possible that the CSF dynamics equilibrium in resolving IIH is re-set, such that apparent normality occurs at higher pressures.

Papilloedema improved significantly following weight loss, as demonstrated using OCT (p<0.001), USG optic disc elevation (p=0.002) and optic nerve sheath diameter (p=0.004). The Frisen grade, designed to classify developing papilloedema (Frisen 1982), was found not to be sensitive enough to detect changes in resolving papilloedema. Disc ranking, was more discriminating than Frisen grading, but was only able to detect a significant change in the disc appearance from the start of the diet to the final follow up (start stage 2 to end stage 3). Delayed resolution of papilloedema, following reduction in ICP, has been previously reported post ventriculoperitoneal shunting in IIH (resolution over 0.6 to 7.0 months) (Bynke et al. 2004) and is in keeping with the observation that USG measures of papilloedema continued to improve during the 3 months following the VLCD (stage 3). Evaluation of papilloedema in previous IIH therapeutic studies has relied upon subjective observation. Our use of objective imaging measures to quantify papilloedema marks an important advance in gauging optic disc swelling that will enhance IIH research and

contribute to future clinical trial design. Although the potential application of USG and OCT in IIH monitoring has been previously described (Tamburrelli *et al.* 2000; Rebolleda and Munoz-Negrete 2009), the sensitivity in detecting changes in mild papilloedema (Frisen grade 1 (17%) and 2 (83%)) noted in our study suggests they are likely to have a seminal role in influencing future clinical practice and research.

Symptoms (headache, tinnitus, obscurations and diplopia) all significantly improved following weight loss. Headache impact, which was substantial at baseline (57.5 ± 9.0), significantly improved following weight loss ($p<0.001$) to a level which had no or little impact on daily life (46.9 ± 10.1) (disability quantification from www.headachetest.com/HIT6translations.html (Shin *et al.* 2008) (section 7.3). It is important to note that a subgroup continued to have severe HIT-6 scores following the diet, despite an equivalent weight and ICP reduction to that of the whole study cohort (Figure 5-7A). Alternative headache phenotypes may account for the headache morbidity in this subgroup. Headaches have been described in 68% of patients with IIH following resolution of the signs of IIH, typically episodic tension type headache or migraine (Friedman and Rausch 2002).

The extent of weight reduction (loss of 15.3% of body weight) is of considerable importance, as this cohort of patients had all previously failed numerous weight loss strategies. The success of the VLCD is likely to reflect a combination of diet tolerability, ketosis (which enhanced hypothalamic satiety), weekly substantial weight loss (a powerful motivator for diet compliance and persistence), as well as individual weekly review sessions to monitor, motivate and provide nutritional counselling.

The struggle for patients to achieve and maintain weight reduction is universally recognised. Dietary weight loss, through VLCDs, gradual calorie restriction or

macronutrient exclusion (fat, carbohydrates or protein) may be as little as 2–4 kg at 2 years (Sacks *et al.* 2009). Other non-diet strategies to encourage weight loss include pharmacological and surgical interventions. Obesity pharmacological therapies, are unlikely to achieve sufficient weight loss to significantly modify IIH; Orlistat reduces weight by a mean of 2.89 kg and Sibutramine reduces weight by 4.45 kg, at 12 months (Li *et al.* 2005). Additionally, the prescribing licence for Sibutramine has recently been withdrawn by the European Medicines Agency due to concerns about cardiovascular risk (Williams 2010). A more useful weight modifying drug may be Topiramate (reduces weight by 9.75 kg at 12 months in IIH (Çelebisoy et al. 2007)) with additional potential to reduce CSF secretion via carbonic anhydrase inhibition (Rosenfeld 1997) and efficacy in treating coexisting migraine. Gastric weight reduction surgery may be effective and resolving papilloedema has been reported in a series of 8 patients (Sugerman et al. 1995). Although the advantage of this approach has been limited by unacceptable morbidity (6 of the 8 patients), recent studies indicate safety and efficacy of laparoscopic bariatric surgery, and provide rationale for the re-evaluation of this technique in IIH (Flum *et al.* 2009).

We recognise that the non-randomised controlled study design needs to be taken into account when evaluating our data. Patient acceptability and ethical considerations prevented recruitment to a control cohort (which would need to undergo serial lumbar puncture). However, a major strength of this study is that all patients had chronic stable IIH (disease duration 39.0 ± 49.2 months). This reduced the risk of bias due to the possibility of rapid spontaneous resolution of IIH, which is a recognised phenomenon in some patients with acute IIH. A consequence of selecting a chronic IIH cohort was that visual impairment was minimal and papilloedema mild (Frisen grades all 2 or less) in the majority of patients at enrolment. Patients with a history of declining vision, requiring

CSF diversion surgery, or other aggressive treatment, were not included in our study. Visual function (LogMAR score and HVF) was preserved at baseline in this IIH cohort and a clinically significant improvement was not noted or expected. We did note a significant improvement in the Pelli Robson contrast sensitivity. Repeated measurements in contrast sensitivity identify variability of one triplet (3 letters) (Lovie-Kitchin and Brown 2000) and although the mean values changed very little during our study, significantly more patients show an improvement following weight loss than after the baseline observation period. Contrast sensitivity may consequently represent a useful tool to monitor visual changes in IIH. The statistically significant improvement noted in the LogMAR score was not deemed clinically significant, as only 25.0% improved by greater than one line and, consequently, the changes noted may merely reflected inherent variability when repeatedly taking measurements (Gibson and Sanderson 1980). It is, however, noteworthy that, despite studying a chronic IIH cohort with little visual impairment, we observed clinically and statistically significant improvements in symptoms and papilloedema.

Our study is the first to confirm the relationship between weight loss and reduction in ICP. Weight loss is also effective in reducing headaches and papilloedema in patients with IIH. It provides an evidence base for clinicians to advise and encourage IIH patients to embark upon and maintain a weight reducing diet. Our data suggests that weight loss clinics may have a role in the management of IIH. The long term effectiveness and health economics of this approach will require critical evaluation in a further study comparing weight reduction using NHS dieticians with specially designated weight reduction clinics in IIH.

5.4.2. Effect of weight loss on the metabolic phenotype and 11β-HSD1, in idiopathic intracranial hypertension

Discussion

The pathogenesis of IIH is not established, however, the association with obesity and ICP dysregulation is well recognised (Sinclair et al. 2008). We suggest that IIH, like obesity, may result from dysregulation of 11β-HSD1 activity and that therapeutic weight loss may be beneficial due to manipulation of 11β-HSD1. We have, therefore, characterised glucocorticoid metabolism in IIH subjects before and after significant weight reduction (loss of $15.2 \pm 7.8\%$ of body weight).

We observed a reduction in global 11β-HSD1 activity, as assessed by the urinary THF+5α-THF: THE ratio, but unchanged free cortisol: cortisone ratio, following weight loss. The greatest reduction in global 11β-HSD1 activity occurred in IIH subjects who experienced the largest fall in ICP ($r=0.504$, $p=0.028$). Previous studies of weight loss in non IIH obese subjects, do not report significant changes in urinary 11β-HSD1 activity (Tomlinson *et al.* 2004a; Tomlinson *et al.* 2008). Interestingly, however, unpublished sub-analysis of females from the idiopathic obesity cohort indicate a trend towards decrease in 11β-HSD1 activity. It is possible therefore, that following weight loss, there are gender differences in 11β-HSD1 activity. Weight loss may also cause tissue specific changes in 11β-HSD1, as indicated by elevated adipocyte 11β-HSD1 mRNA expression in obese patients following weight reduction (Tomlinson *et al.* 2004a; Tomlinson *et al.* 2008). Adipose expression of 11β-HSD1 would be an avenue for future research in IIH.

When comparing the weight induced changes in urinary steroid metabolites, in IIH and non IIH obese subjects, we found no significant difference. This study was not, however, designed for this sub-analysis, the analysis was carried out using historical obese controls,

and additionally, it is likely that the low numbers of patients, particularly in the control group (n=13), lead to the analysis being insufficiently powered to detect significant changes. It is interesting, however, that the fall in global 11β-HSD1 activity in IIH subject was nearly double that noted in non IIH subjects. A dedicated and appropriately powered study is needed to investigate this area further.

Reduced 5α-reductase activity, as assessed by the urinary 5α-THF:THF and An:Et ratio, was demonstrated in the IIH subjects following weight loss and has also been noted in obese cohorts (Tomlinson et al. 2008). The precise role of 5α-reductase (a cortisol inactivating enzyme) which is highly expressed in liver and adipose tissue, is under investigation (Andrew et al. 1998). Decreased 5α-reductase activity, with consequent reduced inactivation of cortisol, may account for the diminished HPA axis drive, indicated by the reduced total urinary metabolite excretion noted in the IIH cohort. The observed reduction in 5α-reductase activity is not solely a reflection of cortisol metabolism, as 5α-reductase also has a key role in activating testosterone to 5α dihydrotestosterone (Bruchovsky and Wilson 1968). Changes in androgen metabolism may have therapeutic implications in the female biased condition of IIH. Interestingly, both 5α-reductase and 11β-HSD1 are regulated by oestrogen with higher levels demonstrated in females (Mode and Norstedt 1982) (Low et al. 1994). Five of the IIH subjects (20%) met the diagnostic criteria for PCOS (REA-SPCW 2004), a condition with a similar obese female phenotype associated with enhanced 5α reductase activity (Vassiliadi et al. 2009). The role of 5α reductase activity in PCOS, and the potential for dysregulation in IIH, will be discussed further in section 5.4.3.

To further analyse 11β-HSD1 expression in the CP, we carried out the novel quantification of both cortisol and cortisone in CSF using LC/MS. CSF cortisol and

cortisone levels were observed to be much lower in the CSF than serum with concentrations mirroring those observed in aqueous humour (Rauz et al. 2001), although much lower than that demonstrated in other fluids such as synovial fluid (Hardy *et al.* 2008). These results pose many questions, not least the impact of cortisol binding globulin (CBG) on free glucocorticoid levels in the CSF. Previous studies suggest that free cortisol levels in the CSF mirror that observed in the serum, with 20% of CSF cortisol bound to protein (Carroll *et al.* 1976). CSF cortisone concentrations have, to our knowledge, not been previously evaluated. As serum cortisone has limited binding to CBG, and thus total levels are a close approximation to free cortisone levels (Cooper *et al.* 2005), equilibration across the blood brain barrier (BBB) would be predicted. However, CSF levels are notably lower than those measured in serum (serum: CSF cortisone ratio 8.2) suggesting local conversion of cortisone to cortisol by 11β-HSD1. Neither the CSF nor serum cortisol or cortisone levels significantly changed with weight loss. However, it is likely that this approach to measuring *in vivo* changes in CP 11β-HSD1 activity is too simplistic as CSF glucocorticoids will reflect both local tissue steroid metabolism as well as glucocorticoid transfer across the BBB. Future study of BBB function and free CSF steroid levels in IIH may shed light on this area. The lack of significant change in serum glucocorticoid levels mirrors findings in non IIH obese subjects and is in keeping with decreased cortisol secretion (mediated by reduced 11β-HSD1) offset by increased adrenal cortisol secretion driven by the HPA axis (Tomlinson et al. 2008).

Weight loss correlated with CSF cortisone levels (r= -0.512, p=0.018) in that those individuals who lost the most weight had the highest CSF cortisone. Whilst we did not see changes in CSF cortisol, these observations may reflect a reduction in 11β-HSD1 activity. The significant correlation of age with CSF cortisol noted in our study is of interest as elevated CSF cortisol has been linked to memory deficits and Alzheimer's disease

(Lupien *et al.* 1998; Popp *et al.* 2009). In this context CSF cortisol levels require further study in larger mixed age cohort.

We acknowledge that a stress effect of the VLCD may have impacted on our results, however, as there was no significant difference in the serum cortisol levels from baseline to that measured following the diet, we feel this is unlikely. We also accept that the benefits of therapeutic weight loss in IIH may not relate exclusively to 11β-HSD1 as changes in adipose tissue, an active endocrine organ, with subsequent alterations on the inflammatory cytokine and adipokine profiles, particularly leptin (Ball *et al.* 2009b), may have impacted on CSF dynamics.

Features of the metabolic syndrome, including fasting serum cholesterol, glucose and insulin resistance (measured by the HOMA %B, %S, IR and glucose: insulin ratio), significantly improve following weight reduction. The degree of change was mirrored in the non IIH obese cohort (Table 5-8). The precise mechanism by which weight loss improves insulin resistance is unknown. In both our study and others, decreased global glucocorticoids are associated with improved insulin sensitivity and the significant reduction noted in 5α reductase activity may be crucial (Tomlinson et al. 2008). 11β-HSD1 inhibitors also have insulin sensitising effects (Bhat *et al.* 2008; Lloyd *et al.* 2009; Zhang *et al.* 2009a) suggesting that the decreased global 11β-HSD1 activity noted following weight loss in the IIH cohort may have impacted on insulin sensitivity. Further characterisation of metabolic features in IIH compared to control subjects will be considered in the next section of the chapter (section 5.4.3).

Changes in body composition were also seen before and after weight loss in IIH subjects. Both the fat and lean mass were noted to reduce following the diet and we observed that the proportion of fat lost from the trunk was greater than that lost from the limbs. It is

interesting to speculate that loss of abdominal fat is key in therapeutic weight reduction in IIH. As this study does not directly compare the therapeutic effects of loss of abdominal fat to loss of limb fat, firm conclusions cannot be drawn.

In summary, this study describes global reduction in 11β-HSD1 activity with weight loss which correlates with improved ICP in IIH patients. The CSF glucocorticoid studies represent an approach to determining CP 11β-HSD1 activity but further investigation to disentangle the effects of serum steroid dialysis across the BBB relative to CP steroid generation are needed. The use of LC/MS does, however, utilise a novel technique to quantify CSF glucocorticoids. Our previous *in vitro* characterisation of 11β-HSD1 in CP and AGT highlights the potential for glucocorticoid manipulation of CSF dynamics (Chapter 3). These studies raises the possibility that elevated 11β-HSD1 may represent a pathogenic mechanism in IIH. Future work will need to investigate the functional consequence of 11β-HSD1 manipulation on CSF secretion and IIH. Inhibition of 11β-HSD1 activity may, however, represent a therapeutic strategy for the treatment of IIH.

5.4.3. Comparison of metabolic phenotype and 11β-HSD1 in idiopathic intracranial hypertension and control patients

Discussion

We sought to evaluate the metabolic phenotype in IIH patients by comparing the urinary steroid profiles, fasting metabolites and body composition with a cohort of BMI matched, healthy control subjects.

11β-HSD1 activity, inferred from the THF+5αTHF:THE ratio, and 11β-HSD2 activity, inferred from the free cortisol: cortisone ratio, were found to be similar in IIH patients

compared to obese healthy control subjects. This does not exclude the potential for 11β-HSD dysregulation in IIH, as urine metabolites estimate global 11β-HSD activity, but do not necessarily reflect tissue specific or pathogenic 11β-HSD activity. The assessment of other markers of 11β-HSD, such as hepatic 11β-HSD activity, estimated from cortisol generation curves, and adipose 11β-HSD mRNA expression, have proven useful in establishing 11β-HSD1 dysregulation in obesity and maybe of interest in IIH (Stewart *et al.* 1999; Rask *et al.* 2001; Paulmyer-Lacroix *et al.* 2002; Tomlinson *et al.* 2002; Li *et al.* 2007). Comparing the cortisol and cortisone levels in the CSF of IIH and healthy obese patients would also be valuable, although ethical considerations are likely to prevent the collection of CSF from healthy obese controls.

The novel finding of enhanced 5α reductase activity in patients with IIH is of interest. The 5αTHF: THF ratio and 5αTHF were significantly higher in IIH patients compared to obese controls (p=0.009, p=0.014 respectively). It is unlikely that the differences noted in 5α reductase activity were a result of age differences between the cohorts, as age did not have a significant relationship with either variable. This is in keeping with other studies, which found no significant relationship between 5α reductase and age (Vassiliadi et al. 2009). Androgen metabolites, also indicative of increased 5α reductase activity, were higher in the IIH patients (An, p=0.015 and An+Et+DHEA, p=0.003). Of note, six of the IIH cohort described symptoms of hyperandrogenism (hirsutism, acne and male pattern balding). Of these, 3 were confirmed as having PCOS. Elevated 5α reductase activity has been linked to hirsutism (both idiopathic and that noted in PCOS) (Serafini and Lobo 1985; D'Amico and Roehrborn 2007) and may explain the hirsutism noted in the IIH patients. The elevated androgen metabolism in the IIH patients likely reflects the younger age of this cohort as the significant differences noted between groups was lost following multivariate regression analysis accounting for age. The androgen metabolites correlated

significantly with age, reflecting the established pattern of androgen levels increasing until menopause and falling thereafter (Sowers *et al.* 2009).

Elevated 5α reductase activity in IIH patients has not been previously described. 5α reductase is a pivotal enzyme in both cortisol and androgen metabolism. There are two isoforms of 5α reductase (Russell and Wilson 1994). The type 1 isoform is localised to chromosome 5 (Jenkins *et al.* 1991) and is located predominantly in the liver, adipose, non-genital skin, cerebellum and hypothalamus, as well as in the sebacceous glands and scalp following puberty. The type 2 isoform is localised to chromosome 2 (Jenkins et al. 1991) and is expressed in high levels in the prostate, androgen sensitive tissue and liver (Thigpen *et al.* 1993). Deficiency of 5α reductase type 2, an autosomal recessive disorder, manifests as male pseudohermaphroditism. This is due to impaired activation of testosterone to DHT, which is essential for the development of male genitalia (Andersson *et al.* 1991). 5α reductase type 1 deficiency has not been described in humans.

Enhanced 5α reductase activity has been demonstrated in obesity (Andrew et al. 1998) and, additionally, adipose tissue demonstrates 5α reductase activity (Andrew et al. 1998), but the precise role in obesity is not established. 5α reductase activity is also known to be regulated by oestrogen, with sexual dimorphism (higher levels in females) demonstrated in rodents (Mode and Norstedt 1982). BMI and gender are unlikely to account for the elevated 5α reductase activity noted in IIH, as the control cohort was gender and BMI matched.

PCOS is also associated with elevated 5α reductase activity. PCOS affects approximately 10-15% of women and is a heterogeneous condition, comprising of clinical and biochemical hyperandrogensism, oligo/amenorrhoea and metabolic syndrome (Tsilchorozidou et al. 2004). Increased 5α reductase activity has been demonstrated in

urinary metabolites in PCOS (Stewart *et al.* 1990; Chin *et al.* 2000; Fassnacht *et al.* 2003; Tsilchorozidou *et al.* 2003; Vassiliadi *et al.* 2009). Additionally, elevated levels of 5α reductase are found in ovarian tissue of PCOS patients (Jakimiuk *et al.* 1999). Since the description "diabetes of bearded women" nearly a century ago (Achard 1921), there has been growing interest in the association of PCOS to insulin resistance, defined as a reduced glucose response to a given amount of insulin (Tsilchorozidou et al. 2004). This association occurs in both the lean and obese PCOS patients (Dunaif *et al.* 1989). The potential role of 5α reductase and cortisol metabolism, in insulin resistance, is not yet defined, but remains an area of interest (Horton *et al.* 1993; Vassiliadi *et al.* 2009). Of note, finasteride (an inhibitor of 5α reductase type 2) is effective in treating hirsutism (Petrone *et al.* 1999), and altering ovarian morphology (Arie *et al.* 2004) in PCOS, but long term effects on insulin resistance have not been studied.

In this study, enhanced 5α reductase activity was demonstrated in IIH patients and, as PCOS and IIH share a similar phenotype (both groups of patients are typically obese women of childbearing age), it is possible that the increased 5α reductase activity seen in the IIH patients reflected coexisting PCOS. We, therefore, reanalysed the IIH cohort without the six PCOS patients. 5α reductase activity, indicated by the 5αTHF: THF ratio, (the most representative of 5α reductase activity (Stewart et al. 1990)), was still significantly higher in the IIH patients following exclusion of the PCOS patients (p=0.028). It is possible, therefore, that 5α reductase activity is important in the pathogenesis of IIH.

20.7% of the IIH cohort met the diagnostic criteria (REA-SPCW 2004) for PCOS. Although the small size of the IIH cohort limits interpretation, this figure is greater than the background incidence of PCOS (10-15%) (Tsilchorozidou et al. 2004). The incidence

of coexisting PCOS and IIH may in fact be greater than the figure suggested in our study; one centre reported that between 39 and 57% of IIH patients were found to have PCOS (Glueck et al. 2003; Glueck et al. 2005). This raises the possibility that, together, IIH and PCOS represent a spectrum of disorders in obese female patients which are characterised by enhanced 5α reductase activity. The nature of this relationship clearly needs further clarification; particularly the possible role of 5α reductase in ICP dynamics. Of interest, initial characterisation of human CP and AGT epithelial cells confirmed expression of 5α reductase 1 (Figure 3-7).

The total glucocorticoid metabolites, an indicator of HPA axis drive were higher in the IIH cohort (p=0.027) than in obese controls. Enhanced HPA axis activity (following both stimulation by ACTH and suppression by dexamethasone) has been noted in obesity and PCOS (Pasquali *et al.* 1993; Duclos *et al.* 2001), particularly amongst those with central obesity (Pasquali et al. 1993; Duclos et al. 2001). The mechanism for HPA axis activation in obesity is debated although considerable evidence is accumulating to suggest that dysregulation of peripheral cortisol metabolism by 11β-HSD1 and 5α reductase is crucial (Stewart *et al.* 1990; Andrew *et al.* 1998; Stewart *et al.* 1999; Rask *et al.* 2001; Reynolds *et al.* 2001; Tomlinson *et al.* 2008). It is interesting to speculate that the increased HPA axis activity in IIH patients, which was more than what would be expected from their BMI alone, reflects pathogenic cortisol dysregulation.

Study of the fasting serum metabolites revealed that IIH patients had elevated HOMA IR scores at baseline (2.1 ± 2.1), indicative of insulin resistance (normal scores are less than 1 (Wallace *et al.* 2004)). The IIH patients had significantly higher insulin and glucose: insulin ratio than control subjects (insulin 14.3 ± 6.4 µU/ml in IIH and 10.8 ± 7.8 µU/ml in controls, p=0.036 and glucose: insulin ratios 0.41 ± 0.20 in IIH and 0.83 ± 0.87 in

controls, p=0.027). The HOMA %B, %S and IR scores were also indicative of inferior insulin sensitivity in the IIH, compared with the control group, although differences did not reach the level of statistical significance. Following removal of the IIH patient with PCOS from the IIH cohort absolute values for insulin, HOMA %B, %S, IR and glucose: insulin ratio remained very similar and continue to showed a trend towards increased insulin resistance in the IIH patients compared to controls, however, differences were no longer significant (insulin 16.6 ± 6.2 µU/ml in IIH and 10.8 ± 7.8 µU/ml in controls, p=0.116 and glucose: insulin ratio 0.45 ± 0.20 in IIH and 0.83 ± 0.87 in controls, p=0.185). It is possible that the PCOS patient in the IIH cohort contributed to the insulin resistance noted, however, it is also very likely that exclusion of the PCOS patients, and consequently reduction in the IIH cohort size, meant that the comparison was no longer adequately powered to elicit a significant difference. It is important to note that although diabetic patients were excluded from the control cohort, identification of PCOS was not undertaken. Consequently, the control cohort may have contained patients with PCOS. In summary, the IIH patients, both with and without PCOS, had elevated HOMA IR scores (greater than two) indicating impaired insulin sensitivity and consequently may be at increased risk of developing diabetes (Costa *et al.* 1998). Longitudinal evaluation of insulin sensitivity in IIH will shed light on this area.

DEXA scanning did not identify a difference in fat mass distribution between IIH and control subjects. It is, therefore, unlikely that fat distribution dictates which obese patients develop IIH. Centrally distributed obesity has been previously suggested as causative in IIH (Sugerman et al. 1995) and although this is unlikely in light of these DEXA results, it remains possible that preferential loss of abdominal fat may be of therapeutic benefit (section 5.3.2.4). The BMC was lower in the control subjects in keeping with their increased age and consequent tendency to osteopenia.

Chapter 5

It is suggested that the results of this study are interpreted with caution as the control population, whilst universally female and matched for BMI, were not matched for age. Although careful analysis and the use of multivariate regression should have eliminated bias, due to the age differences of the cohorts, this cannot be completely excluded. Additionally, interpretation of the study was compromised through the use of a historical obese control cohort. The obese controls may have had underlying methodological differences to the IIH cohort, despite all attempts to standardised collection of anthropometric and DEXA data through the use of similar techniques and equipment, as well as processing the urine and serum samples using identical assays methodologies. The analysis of IIH patients, carried out following the exclusion of the PCOS patients, is particularly likely to be prone to bias as the obese control cohort were not rigorously screened for PCOS, consequently impairing the reliability of these analyses. It will be important to replicate these results in a large gender, BMI and age matched study using contemporary obese control subjects screened for PCOS.

In summary, this study suggests that IIH patients have enhanced 5α reductase activity and elevated total glucocorticoid metabolites (reflecting HPA axis activity), in conjunction with greater insulin resistance, compared with BMI matched control subjects. Although a difference in global 11β-HSD1 activity was not noted between IIH and control subjects, alterations in tissue specific activity may exist. It is possible that regulation of cortisol by both 5α reductase and 11β-HSD1 is important in IIH and ICP dynamics. Further evaluation of the interplay between these two enzymes and their potential role in CSF secretion and drainage would be of interest. These studies also suggest that IIH patients have a degree of insulin resistance that is at least that expected from their BMI and is greater in those with coexisting PCOS. Insulin resistance in the IIH patients, akin to obese individuals, may increase their risk of developing future metabolic complications.

Longitudinal evaluation of insulin sensitivity, diabetes and vascular events, would further clarify the risk of metabolic syndrome in IIH subjects.

Chapter 6. Conclusions & future work

Chapter 6

6.1. Conclusions

The pathogenesis of IIH, a condition of raised ICP in obese women, has not been established. This thesis examined the role of obesity, 11β-HSD1 and metabolic changes in the pathogenesis and treatment of IIH. Initial *in vitro* studies explored the role of 11β-HSD in the regulation of CSF dynamics. We confirmed 11β-HSD1 expression and activity in the CP of an animal model, the NZWAR, and subsequently in human tissue. Together, these finding highlight the capability of the CP to generate cortisol and possibly influence CSF cortisol levels. Autocrine effects of CP cortisol on the glucocorticoid signalling pathway may in turn influence CSF secretion. In order to further examine CSF secretion, a HCPEpi cell line was analysed. This was found to have a comparable pattern of 11β-HSD1 expression and activity to human CP tissue and was consequently deemed a representative model for future study of CP function.

Study of the AGT, the CSF drainage structure, was not possible in the NZWAR due to the microscopic nature of the granulations preventing reliable identification. Characterisation of post mortem human AGT identified 11β-HSD1 in the epithelial cap cells of the granulation. Although enzyme activity was not demonstrated, key elements of the glucocorticoid signalling cascade (including GRα and MYOC) were identified, highlighting the potential of the AGT to act as a glucocorticoid target tissue, influenced by paracrine actions of cortisol. Characterisation of a human AGEpi cell line, established by our collaborators (Holman et al. 2005), mirrored that of AGT and, therefore, may represent a suitable model for future evaluation of the functional consequences of cortisol on CSF drainage.

Chapter 6

We suggested that IIH, a condition almost exclusively found in the obese population (Giuseffi et al. 1991; Wall and George 1991), was characterised by a deranged metabolic profile and consequently utilised a metabolomics approach to define a unique metabolite profile in the CSF and serum. Proton NMR spectroscopy, coupled with computer modelling (PCA and PLS-DA), were therefore used to identify those metabolites which most accurately defined IIH, as well as two control conditions (MS and CVD). We found that phenotypic features influenced the metabolite profile. Consequently, evaluation of metabolite profiles from disease populations matched for gender, age and BMI, revealed diagnostic metabolites with highest accuracy (80% sensitivity and sensitivity in IIH CSF). Defining disease specific, diagnostic metabolite biomarkers was a novel use for metabolomics (Sinclair *et al.* 2009). This will require further evaluation, comparison between centres and ultimately standardisation, particularly as current techniques for data processing vary widely. In the setting of IIH, identification of potentially diagnostic metabolites may ultimately prove useful in a clinical setting, particularly if profiles are evaluated in non invasive fluids such as urine. Additionally, longitudinal evaluation of IIH metabolite profiles will indicate the utility of biomarker profiles in disease monitoring. We have however, established proof of concept of this technique, and suggest that the application of metabolomics to other more diagnostically challenging diseases may well be of value.

To enhance our understanding of the pathogenesis of IIH the metabolite profile was also used to identify the predominant metabolites in the CSF of IIH patients (lactate, oxaloacetate, glucose, acetate and 3-hydroxybutyrate). Interpretation of these metabolites is complicated, as they may reflect the cause or the consequence of disease. Additionally, the precision of our metabolite identification is dependent on the accuracy of established metabolite libraries. Thus, before detailed investigation of the association between

metabolites and IIH aetiology, metabolite identity should be confirmed using mass spectroscopy. It was interesting to note, that although the CSF metabolite profiles most accurately defined IIH (sensitivity and specificity 80%), the serum profiles were also acceptable (sensitivity 70% and specificity 78%), potentially implicating both CNS and systemic factors in the aetiology of IIH. Further exploration of the role of both the CSF and serum metabolites may augment our knowledge of the underlying disease process in IIH.

To more accurately define the role of obesity, metabolic changes and 11β-HSD1 in IIH, clinical studies were conducted. Through the use of a VLCD, we were able to evaluate the effect of weight loss on: 1) ICP, and treatment of IIH and 2) metabolic changes. We demonstrated that weight reduction is of therapeutic value in IIH, significantly reducing ICP, papilloedema and headaches. Ideally the study would have utilised a randomised control design, but ethical considerations, regarding the acceptability of performing three LP's on control patients who were not undergoing a potentially beneficial intervention, prevented this more robust method of study. A large, multicentered, randomised study of the effect of weight loss is, however, being initiated in the United Sates and we await the results. Our IIH cohort suffered no significant side effects as a result of weight reduction, a recent report of cerebellar tonsillar herniation following weight loss in IIH (Graber *et al.* 2009) is, however, noted. The extent of this problem will need to be monitored in future clinical studies. This study was the first to use objective assessment of papilloedema in a trial setting. The utility of USG measurement of optic disc elevation and nerve sheath diameter, as well as OCT in quantifying papilloedema, was demonstrated. These novel techniques may be useful in both a clinical and research setting to aid identification of papilloedema and monitor disease progression. The techniques now require evaluation over a greater range of Frisen grades (most of the discs evaluated in our study had mild

papilloedema with Frisen grade 1 or 2), and inter and intra observer variability needs to be closely scrutinised.

Having established the role of therapeutic weight loss in IIH, we sought to evaluate whether the benefits noted, related to alterations in metabolism and 11β-HSD1. The urinary, serum and CSF metabolite profiles were, therefore, assessed using GC/MS and LC/MS both before and after weight reduction. A reduction in global 11β-HSD1 activity was identified following weight reduction, which correlated significantly, with reduction in ICP. Assessment of CSF and serum glucocorticoids did not identify reduced cortisol, as one might have expected in the setting of reduced 11β-HSD1 activity. There was, however, a significant correlation between increased levels of cortisone (potentially indicating reduced 11β-HSD1 activity) and weight loss. The interpretation of serum and CSF glucocorticoids were complicated by the regulatory effects of the HPA axis correcting the serum glucocorticoid levels as well as the potential for transfer of steroids across the BBB.

Our final comparison of IIH subjects, with a cohort of gender and BMI matched controls, did not identify divergent urinary 11β-HSD1 activity between the groups. Tissue specific differences in 11β-HSD1 were not investigated but would be of future interest. We found evidence of activation of the HPA axis (elevated total glucocorticoid metabolites) in the IIH patients which was significantly higher than that identified in matched control subjects. Additionally, HPA axis activation fell following therapeutic weight loss in IIH. Increased HPA axis drive is recognised in obesity (Pasquali et al. 1993; Duclos et al. 2001), but it is interesting to note that the elevation in HPA axis activity seen in IIH was greater than that noted in subjects with idiopathic obesity. Dysregulation of 11β-HSD1 may be a factor contributing to HPA axis activation, although the influence of 5α

reductase may also be important. Our results also indicated increased 5α reductase activity in IIH subjects compared to matched controls. Additionally, levels of 5α reductase fell following therapeutic weight loss. Inactivation of cortisol by 5α reductase has been implicated in driving the HPA axis (Stewart et al. 1990). The role of 5α reductase in IIH and CSF dynamics has not been previously explored, but may well be important.

Idiopathic obesity is associated with the development of the metabolic syndrome and consequent increased mortality and morbidity. As IIH patients are phenotypically obese, we suggested that they may also have an increased risk of developing the metabolic syndrome. We demonstrated evidence of insulin resistance (HOMA IR score greater than 2) in the IIH subjects and additionally elevated insulin levels and glucose: insulin ratios, when compared to subjects with idiopathic obesity (BMI matched). The BP and lipid profiles were, however, similar in IIH and idiopathic obese subjects. These results suggest that IIH subjects have reduced insulin sensitivity, although interestingly, this was primarily related to those with coexisting PCOS. The long term consequences of insulin resistance in this relatively young cohort of IIH subjects will require prospective evaluation.

Despite the almost ubiquitous association of obesity with IIH, not all obese subjects develop IIH. Centrally distributed adiposity has been previously cited as causative, due to pressure effects elevating intra-abdominal pressure, which subsequently elevates intra-thoracic pressure and cerebral venous pressure and finally ICP (Sugerman et al. 1995). A recent study however, evaluated waist: hip ratios in IIH and obese individuals and found lower ratios in IIH subjects. They concluded that fat preferentially accumulated in the lower body in IIH subjects (Kesler *et al.* 2009). We assessed body composition using

DEXA scanning in IIH and matched subjects with idiopathic obesity and found no difference in the distribution of fat mass. DEXA scanning before and after weight loss did however indicate that preferential loss of central fat mass may be most therapeutically beneficial. Our data suggested that it was unlikely that fat distribution was causative in IIH. The explanation as to why a proportion of obese subjects develop IIH remains unknown.

In summary, our *in vitro* studies suggested that both the CP and AGT express 11β-HSD1 and have the potential, to act as glucocorticoid target tissues, which may be important in CSF dynamics and ICP regulation in IIH. We have demonstrated the therapeutic efficacy of weight loss in IIH and provided evidence that the beneficial effects may relate to alterations in the glucocorticoid profile driven 11β-HSD1 and potentially, 5α reductase.

6.2. Future directions

6.2.1. *In vitro* studies

The *in vitro* studies confirmed expression of 11β-HSD1 and key element of the glucocorticoid signalling pathway in human CP and AGT, with the potential for cortisol generation by 11β-HSD1 demonstrated in the CP. A progression to this work would be to investigate the functional consequences of glucocorticoids and 11β-HSD1 on CSF secretion and drainage. Monolayers of HCPEpi cells grown on a permeable supports designed to measure a volumetric readout (Haselbach *et al.* 2001; Speake *et al.* 2001), would provide a suitable model to explore the ability of CP cells to produce CSF under a variety of conditions (cortisol, cortisone, dexamethasone, aldosterone, GE, RU38486 (a GR inhibitor) and RU26752 (a MR inhibitor)) defining the functional impact of glucocorticoids on CSF secretion. Functional studies using real-time RT-PCR could also

be used to define the induction of expression of putative target genes involved in CSF production (αENaC, βENaC, sgk-1, Na$^+$K$^+$ATPase subunits) following incubation of CP cells with corticosteroid receptor agonists (cortisol, dexamethasone, and aldosterone). The permeability of AGEpi cells could be similarly investigated in conjunction with the regulation of MYOC by glucocorticoids.

Further work using animal models would also be of value. Using intraventricular pressure recording in mice (Nawashiro *et al.* 2002), we could explore the effect of 11β-HSD1 inhibitors on ICP. Within the secretory cells of the CP epithelium, 11β-HSD1 is unlikely to represent the only regulator of CSF secretion, as numerous ion channels are involved in CSF secretion (Figure 1-6). Through the use of intraventricular monitoring, in conjunction with intraventricular administration of selective ion channel and 11β- HSD1 inhibitors, we could start to unravel the extent to which 11β-HSD1 influences total CSF secretion. ICP has not been studied in the 11β-HSD1 knockout or over-expression mouse. This area may also be worthy of further assessment, although these mice appear to have no overt CSF phenotype.

The measures of CSF cortisol, as a reflection of tissue specific (CP) 11β-HSD1 activity, were difficult to interpret, due to the influence of steroid dialysis across the BBB. Study of systemic and CSF radio-labelled cortisol in animal models, with normal and elevated ICP, may improve our understanding of this area.

In addition to unravelling the role of 11β-HSD1 in IIH, the studies have demonstrated elevated 5α reductase in IIH patients. 5α reductase levels were also demonstrated to fall with therapeutic weight loss. It is possible therefore, that in addition to 11β-HSD1, cortisol regulation by 5α reductase may have a role in IIH. 5α reductase has not been previously investigated in the context of CSF dynamics, although our work demonstrated

expression of 5α reductase1 in HCPEpi and AGEpi. A detailed examination of the localisation, activity and function of 5α reductase in CP and AGT is therefore warranted.

6.2.2. Clinical studies

The clinical studies have confirmed the therapeutic benefit of weight loss in IIH. Global 11β-HSD1 activity fell in conjunction with weight reduction and ICP, supporting our hypothesis that the pathogenesis of IIH is influenced by elevated 11β-HSD1. To further explore the role of systemic dysregulation of 11β-HSD1, analysis of adipose tissue 11β-HSD1 expression and hepatic 11β-HSD1 activity in IIH subjects and matched controls, would be of interest. Evaluation of CP and AGT cortisol and cortisone concentrations in IIH subjects would be very interesting; however, the low morbidity associated with IIH has meant that postmortem brain tissue is not currently available in European brain banks.

11β-HSD1 inhibitors, used in the context of obesity and the metabolic syndrome, are currently the focus of considerable research (Boyle and Kowalski 2009). A randomised control study examining the therapeutic potential of 11β-HSD1 inhibitors in IIH is ultimately required to establish proof of concept. We also acknowledge that this thesis has not explored the potential contribution of H6PD in the pathogenesis of IIH. This area will need exploring in light of recent studies demonstrating the ability of H6PD to regulate 11β-HSD1 (Zhang *et al.* 2009b) and additionally modulate the effect of 11β-HSD1 inhibition (Balazs et al. 2009).

Recent work describing familial cases of IIH (Corbett 2008), highlight the potential for a genetic influence in IIH. Polymorphisms in the 11β-HSD1 gene have been described, which influence the function of 11β-HSD1 (Malavasi *et al.* 2009), although it is not clear if these polymorphisms have pathogenic implications for the metabolic syndrome

(Robitaille *et al.* 2004; Ku *et al.* 2009; Miyamoto *et al.* 2009). Further characterisation and DNA banking of familial IIH cases would be of value, particularly in relation to identifying polymorphisms in 11β-HSD1.

The use of objective measures (USG and OCT) to quantify papilloedema, mark an important step in optic disc monitoring. Although not included in this thesis, additional disc measurements were taken using Heidelberg Retina Tomography alongside the USG and OCT measurement. We plan to compare these techniques to ascertain the most accurate, consistent, and cost effective technique. Discriminatory, clinically relevant, objective outcome measures have been lacking in previous IIH studies. Our successful utilisation of objective papilloedema measures in conjunction with headache diaries, disability scales (HIT-6), as well as visual contrast sensitivity measures, will impact on the planning of future IIH studies. Pelli Robson contrast sensitivity was noted to be a sensitive technique to monitor changes in vision in the IIH subjects, despite clinically insignificant changes in acuity. The use of low contrast, letter acuity charts, which have been noted as discriminatory in MS associated optic neuritis (Mowry *et al.* 2009), would be worthy of investigation in the setting of IIH.

In the future, we aim to accurately characterise the clinical and metabolic phenotype of a longitudinal cohort of IIH patients. This will involve the establishment a bio-bank of blood, urine and CSF samples with corresponding clinical data. Large studies of this nature are essential to determine much needed information on disease progression, remission, and severity in the context of metabolic changes. Epidemiological data may well reveal subtypes of disease, with differing disease courses. It is interesting to speculate that these disease subtypes may have differing aetiologies, which will require tailored investigation of pathogeneses, and potentially individualised treatment.

Chapter 7. Appendix

7.1. Ethical approval

Permission for all aspects of this study was obtained from the local research ethics committees and all participants gave written informed consent.

1. Evaluation of Hormones and Obesity Mediators on Cerebrospinal Fluid (Solihull LREC 04/Q2706/65. Approved 15/01/2005)

2. Evaluation of 11Beta-HSD in Human Choroid Plexus and Arachnoid Granulation tissue (Dudley LREC 06/Q2702/19. Approved 20/03/2006)

3. The Impact of Weight Loss on Idiopathic Intracranial Hypertension (Dudley LREC 06/Q2702/64. Approved 06/09/06)

7.2. Headache Impact Test-6

Headache Impact Test- 6
This questionnaire was designed to help you describe the way you feel and what you cannot do because of your headache.   To complete, please circle one answer for each   question
1   **When you have headaches, how often is the pain severe?**   Never   Rarely   Sometimes   Very Often   Always
2   **How often do headaches limit your ability to do usual daily activities including household work, work, school, or social activities?**   Never   Rarely   Sometimes   Very Often   Always
3   **When you have a headache, how often do you wish you could lie down?**   Never   Rarely   Sometimes   Very Often   Always
4   **In the past 4 weeks, how often have you felt too tired to do work or daily activities because of your headaches?**   Never   Rarely   Sometimes   Very Often   Always
5   **In the past 4 weeks, how often have you felt fed up or irritated because of your headaches?**   Never   Rarely   Sometimes   Very Often   Always
6   **In the past 4 weeks, how often did your headache limit your ability to concentrate on work or daily activities?**   Never   Rarely   Sometimes   Very Often   Always
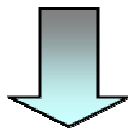
Column 1
(6 points each)
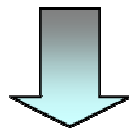
Column 2
(8 points each)
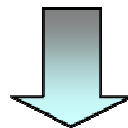
Column 3
(10 points each)
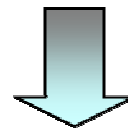
Column 4
(11 points each)
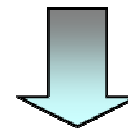
Column 5
(13 points each)

Total Score

Higher scores indicate greater impact on your life.
Score range is 36 - 78.

7.3. Interpretation of Headache Impact Test-6

If You Scored 60 or More
Your headaches are having a very severe impact on your life. You may be experiencing disabling pain and other symptoms that are more severe than those of other headache sufferers.

If You Scored 56 – 59
Your headaches are having a substantial impact on your life. As a result you may be experiencing severe pain and other symptoms, causing you to miss some time from family, work, school, or social activities.

If You Scored 50 – 55
Your headaches seem to be having some impact on your life.

If You Scored 49 or Less
Your headaches seem to be having little to no impact on your life at this time.

http://www.headachetest.com/HIT6/PDFS/English.pdf (Shin et al. 2008)

7.4. Intention to treat analysis of the IIH patients in the weight loss study

Characteristic	Baseline	Start Diet	End Diet	Final	P value
Patient numbers	25	24	22	20	
Weight (kg)	101.3 ± 16.5	101.3 ± 17.4	86.3 ± 15.5	87.0 ± 12.9	<0.001
BMI (kgm^{-2})	37.9 ± 4.9	38.1 ± 5.3	32.4 ± 4.9	32.8 ± 4.4	<0.001
Intracranial pressure (cm CSF)	39.5 ± 4.6	37.8 ± 4.7	29.7 ± 4.7	N/A	<0.001
Vision					
Ultrasonographic optic disc elevation (mm)	1.02 ± 0.27	0.98 ± 0.29	0.81 ± 0.26	0.75 ± 0.26	0.002
Ultrasonographic optic nerve sheath diameter (mm)	4.6 ± 1.0	4.5 ± 1.2	4.1 ± 1.3	3.6 ± 1.2[a]	0.004
Optical coherence tomography (average optic disc elevation) (microm) [#]	142.2 ± 43.6	136.3 ± 46.3	111.4 ± 27.4	108.2 ± 28.6	0.001
LogMAR visual acuity[‡]	0.04 ± 0.28	0.09 ± 0.42	-0.02 ± 0.23	$-.07 \pm 0.08$	<0.001[a]
Pelli Robson contrast sensitivity[‡]	1.56 ± 0.17	1.57 ± 0.14	1.66 ± 0.08	1.68 ± 0.10	0.003
Humphrey visual field 24-2 mean deviation[‡]	-4.5 ± 4.3	-3.4 ± 3.4	-2.8 ± 2.9	-1.5 ± 1.8[a]	ns
Farnsworth Munsell 100 Hue colour assessment[#]	114 ± 78.1	88.5 ± 76.8[b]	71.6 ± 54.3[b]	59.2 ± 61.1b	ns
Headache					
Headache Impact Test (HIT-6)[‡]	59.2 ± 9.0	54.8 ± 9.3	46.7 ± 10.1	48.4 ± 9.6	0.004
Headache severity (VAS 0-10)[‡]	4.2 ± 2.4	4.0 ± 2.9	1.9 ± 2.7	2.6 ± 2.7	0.015
Headache Frequency (days/wk)[‡]	4.3 ± 2.9	4.3 ± 3.1	2.0 ± 2.7	2.6 ± 3.1	0.011
Analgesic use (days/wk) [‡]	2.4 ± 2.6	2.3 ± 2.6	0.3 ± 0.7	1.0 ± 2.1	0.007
Symptoms					
Headache[†] (n (%))	24 (96)	23 (96)	14 (58)	10 (50)	<0.001
Tinnitus[†] (n (%))	15 (60)	14 (58)	4 (17)	4 (20)	0.004
Visual loss[†] (n (%))	11 (44)	9 (38)	3 (13)	1 (5)	0.063
Obscurations[†] (n (%))	5 (20)	6 (26)	0 (0)	0 (0)	0.025
Diplopia[†] (n (%))	2 (8)	9 (38)	0 (0)	0 (0)	0.008

Table 7-1   *Intention to treat analysis showing the study characteristics and symptom chronology at each assessment during the weight loss study*

Data summary statistics represent complete cohort at each time point (intention to treat analysis). p values indicates significant changes following weight reduction (start diet versus end diet; (stage 2). No significant changes were noted from baseline to start diet (stage 1) or from end diet to final visit (stage 3) unless indicated. ^A significant improvement noted but this was not found in the left eye. ^b significant change noted after each stage, therefore weight loss did not significantly improve variable. All data analysed using repeated measures ANOVA (at four time points, except ICP which was analysed at 3) unless stated otherwise. [#] indicates data was logged prior to analysis. [‡] indicates that a Friedman's test was used for analysis and if significant a Wilcoxon Signed rank test was subsequently carried out, results of the latter are quoted in the table. [†] indicates that a Cochran's Q test revealed a significant improvement in all variables and subsequently a Sign test was used to evaluate differences at each study stage. Abbreviations: CSF, cerebrospinal fluid; NS, not significant; VAS, Visual analogue score; wk, week.

Chapter 8. References

Aanderud, S. and Jorde, R. (1988). "ACTH deficiency, hyperprolactinemia and benign intracranial hypertension. A case report." Acta Endocrinol (Copenh) **118**(3): 346-50.

Achard, C. T., J (1921). "Le virilisme pilaire et son association a l'insuffisance glucolytique (diabetes des femmes a barb). ." Bulletin of the Academy of National Medicine **86**: 51-64.

Adams, J. H. and Graham, D. I. (1988). "An Introduction to Neuropathology." Churchill Livingstone, New York, 2nd Ed: 34 - 36.

Amaral, J. F., Tsiaris, W., Morgan, T., et al. (1987). "Reversal of benign intracranial hypertension by surgically induced weight loss." Arch Surg **122**(8): 946-9.

Amelung, D., Hubener, H. J., Roka, L., et al. (1953). "Conversion of cortisone to compound F." J Clin Endocrinol Metab **13**(9): 1125-6.

Andersson, S., Berman, D. M., Jenkins, E. P., et al. (1991). "Deletion of steroid 5 alpha-reductase 2 gene in male pseudohermaphroditism." Nature **354**(6349): 159-61.

Andrew, R., Phillips, D. I. and Walker, B. R. (1998). "Obesity and gender influence cortisol secretion and metabolism in man." J Clin Endocrinol Metab **83**(5): 1806-9.

Arcuri, F., Battistini, S., Hausknecht, V., et al. (1997). "Human endometrial decidual cell-associated 11 beta-hydroxysteroid dehydrogenase expression: its potential role in implantation." Early Pregnancy **3**(4): 259-64.

Arie, W. M., Bagnoli, V. R. and da Fonseca, A. M. (2004). "Effects of finasteride on the morphology of polycystic ovaries." Int J Gynaecol Obstet **87**(1): 52-3.

Arroyo, A., Rosel, P. and Marron, T. (2005). "Cerebrospinal fluid: postmortem biochemical study." J Clin Forensic Med **12**(3): 153-6.

Artru, A. A. and Momota, T. (2000). "Rate of CSF formation and resistance to reabsorption of CSF during sevoflurane or remifentanil in rabbits." J Neurosurg Anesthesiol **12**(1): 37-43.

Asensio Sanchez, V. M., Merino Angulo, J. and Narros Gimenez, A. (2004). "[Apnea syndrome: risk factors for pseudotumor cerebri]." An Med Interna **21**(10): 520.

Atkinson, A., Colburn, W., DeGruttola, V., et al. (2001). "Biomarkers and surrogate endpoints: preferred definitions and conceptual framework." Clin Pharmacol Ther **69**(3): 89-95.

Bailey, I. L. and Lovie, J. E. (1976). "New design principles for visual acuity letter charts." Am J Optom Physiol Opt **53**(11): 740-5.

Baker, D. G., Ekhator, N. N., Kasckow, J. W., et al. (2005). "Higher levels of basal serial CSF cortisol in combat veterans with posttraumatic stress disorder." Am J Psychiatry **162**(5): 992-4.

Balazs, Z., Nashev, L. G., Chandsawangbhuwana, C., et al. (2009). "Hexose-6-phosphate dehydrogenase modulates the effect of inhibitors and alternative substrates of 11beta-hydroxysteroid dehydrogenase 1." Mol Cell Endocrinol **301**(1-2): 117-22.

Balcer, L. J., Baier, M. L., Cohen, J. A., et al. (2003). "Contrast letter acuity as a visual component for the Multiple Sclerosis Functional Composite." Neurology **61**(10): 1367-73.

Ball, A. K. and Clarke, C. E. (2006). "Idiopathic intracranial hypertension." Lancet Neurol **5**(5): 433-42.

Ball, A. K., Mathews, T., Burdon, M. A., et al. (2009a). "A Randomised Controlled Trial of Treatments for Idiopathic Intracranial Hypertension (The IIH Pilot Trial)." North American Neuro-Ophthalmology Society **Poster 91**.

Ball, A. K., Sinclair, A. J., Curnow, S. J., et al. (2009b). "Elevated cerebrospinal fluid (CSF) leptin in idiopathic intracranial hypertension (IIH): evidence for hypothalamic leptin resistance?" Clin Endocrinol (Oxf) **70**(6): 863-9.

Bamberger, C. M., Bamberger, A. M., de Castro, M., et al. (1995). "Glucocorticoid receptor beta, a potential endogenous inhibitor of glucocorticoid action in humans." J Clin Invest **95**(6): 2435-41.

Banta, J. T. and Farris, B. K. (2000). "Pseudotumor cerebri and optic nerve sheath decompression." Ophthalmology **107**(10): 1907-12.

Barboni, P., Savini, G., Valentino, M. L., et al. (2005). "Retinal nerve fiber layer evaluation by optical coherence tomography in Leber's hereditary optic neuropathy." Ophthalmology **112**(1): 120-6.

Baum, G. and Greenwood, I. (1960). "Ultrasonography-an aid in orbital tumor diagnosis." Arch Ophthalmol **64**: 180-94.

Bayliss, M. S., Bjornerm, J. B., Kosinski, M., et al. (2003). "Development of HIT-6, a paper-based short form for measuring headache impact." In: Olesen J, Steiner TJ, Lipton RB. Frontiers in Headache Research. Reducing the Burden of Headache. New York: Oxford University Press-USA **11**: 386–90.

Beato, M. (1989). "Gene regulation by steroid hormones." Cell **56**(3): 335-44.

Beato, M. and Klug, J. (2000). "Steroid hormone receptors: an update." Hum Reprod Update **6**(3): 225-36.

Beatty, S., Good, P. A., McLaughlin, J., et al. (1998a). "Correlation between the orbital and intraocular portions of the optic nerve in glaucomatous and ocular hypertensive eyes." Eye **12 (Pt 4)**: 707-13.

Beatty, S., Good, P. A., McLaughlin, J., et al. (1998b). "Echographic measurements of the retrobulbar optic nerve in normal and glaucomatous eyes." Br J Ophthalmol **82**(1): 43-7.

Beck, I. M., Vanden Berghe, W., Vermeulen, L., et al. (2009). "Crosstalk in inflammation: the interplay of glucocorticoid receptor-based mechanisms and kinases and phosphatases." Endocr Rev **30**(7): 830-82.

Bell, J. D., Brown, J. C., Sadler, P. J., et al. (1987). "High resolution proton nuclear magnetic resonance studies of human cerebrospinal fluid." Clin Sci (Lond) **72**(5): 563-70.

Berry, E. V. and Toms, N. J. (2006). "Pyruvate and oxaloacetate limit zinc-induced oxidative HT-22 neuronal cell injury." NeuroToxicology **27**(6): 1043-1051.

Berthiaume, M., Laplante, M., Festuccia, W., et al. (2007). "Depot-specific modulation of rat intraabdominal adipose tissue lipid metabolism by pharmacological inhibition of 11beta-hydroxysteroid dehydrogenase type 1." Endocrinology **148**(5): 2391-7.

Berthiaume, M., Laplante, M., Festuccia, W. T., et al. (2009). "Additive action of 11beta-HSD1 inhibition and PPAR-gamma agonism on hepatic steatosis and triglyceridemia in diet-induced obese rats." Int J Obes (Lond) **33**(5): 601-4.

Bhat, B. G., Hosea, N., Fanjul, A., et al. (2008). "Demonstration of proof of mechanism and pharmacokinetics and pharmacodynamic relationship with 4'-cyano-biphenyl-4-sulfonic acid (6-amino-pyridin-2-yl)-amide (PF-915275), an inhibitor of 11 - hydroxysteroid dehydrogenase type 1, in cynomolgus monkeys." J Pharmacol Exp Ther **324**(1): 299-305.

Bijlsma, S., Bobeldijk, I., Verheij, E. R., et al. (2006). "Large-scale human metabolomics studies: a strategy for data (pre-) processing and validation." Anal Chem **78**(2): 567-74.

Biousse, V., Rucker, J. C., Vignal, C., et al. (2003). "Anemia and papilledema." Am J Ophthalmol **135**(4): 437-46.

Boddie, H. G., Banna, M. and Bradley, W. G. (1974). ""Benign" intracranial hypertension. A survey of the clinical and radiological features, and long-term prognosis." Brain **97**(2): 313-26.

Bogdanov, M., Matson, W. R., Wang, L., et al. (2008). "Metabolomic profiling to develop blood biomarkers for Parkinson's disease." Brain **131**(Pt 2): 389-96.

Boyle, C. D. and Kowalski, T. J. (2009). "11beta-hydroxysteroid dehydrogenase type 1 inhibitors: a review of recent patents." Expert Opin Ther Pat **19**(6): 801-25.

Brandes, J. L., Saper, J. R., Diamond, M., et al. (2004). "Topiramate for migraine prevention: a randomized controlled trial." JAMA **291**(8): 965-73.

Breuner, C. W. and Orchinik, M. (2002). "Plasma binding proteins as mediators of corticosteroid action in vertebrates." J Endocrinol **175**(1): 99-112.

Brindle, J. T., Antti, H., Holmes, E., et al. (2002). "Rapid and noninvasive diagnosis of the presence and severity of coronary heart disease using 1H-NMR-based metabonomics." Nat Med **8**(12): 1439-44.

Britton, C., Boxhill, C., Brust, J. C., et al. (1980). "Pseudotumor cerebri, empty sella syndrome, and adrenal adenoma." Neurology **30**(3): 292-6.

Bruchovsky, N. and Wilson, J. D. (1968). "The conversion of testosterone to 5-alpha-androstan-17-beta-ol-3-one by rat prostate in vivo and in vitro." J Biol Chem **243**(8): 2012-21.

Bujalska, I., Draper, N., Michialidou, Z., et al. (2005). "Hexose-6-phosphate dehydrogenase confers oxo-reductase activity upon 11β-hydroxysteroid dehydrogenase type 1." Journal of Molecular Endocrinology **35**: 675-684.

Bujalska, I., Shimojo, M., Howie, A., et al. (1997). "Human 11 beta-hydroxysteroid dehydrogenase: studies on the stably transfected isoforms and localization of the type 2 isozyme within renal tissue." Steroids **62**(1): 77-82.

Bujalska, I. J., Gathercole, L. L., Tomlinson, J. W., et al. (2008). "A novel selective 11beta-hydroxysteroid dehydrogenase type 1 inhibitor prevents human adipogenesis." J Endocrinol **197**(2): 297-307.

Burgett, R. A., Purvin, V. A. and Kawasaki, A. (1997). "Lumboperitoneal shunting for pseudotumor cerebri." Neurology **49**(3): 734-9.

Burton, A. F. and Anderson, F. H. (1983). "Inactivation of corticosteroids in intestinal mucosa by 11 beta-hydroxysteroid: NADP oxidoreductase (EC 1.1.1.146)." Am J Gastroenterol **78**(10): 627-31.

Bynke, G., Zemack, G., Bynke, H., et al. (2004). "Ventriculoperitoneal shunting for idiopathic intracranial hypertension." Neurology **63**(7): 1314-6.

Cai, T. Q., Wong, B., Mundt, S. S., et al. (2001). "Induction of 11beta-hydroxysteroid dehydrogenase type 1 but not -2 in human aortic smooth muscle cells by inflammatory stimuli." J Steroid Biochem Mol Biol **77**(2-3): 117-22.

Carrieri, P. B., Provitera, V., De Rosa, T., et al. (1998). "Profile of cerebrospinal fluid and serum cytokines in patients with relapsing-remitting multiple sclerosis: a correlation with clinical activity." Immunopharmacol Immunotoxicol **20**(3): 373-82.

Carroll, B. J., Curtis, G. C. and Mendels, J. (1976). "Cerebrospinal fluid and plasma free cortisol concentrations in depression." Psychol Med **6**(2): 235-44.

Castro, D. P. E., Kawase, J. and Melo Jr, L. A. S. (2008). "Learning effect of standard automated perimetry in healthy individuals." Arquivos Brasileiros de Oftalmologia **71**: 523-528.

Çelebisoy, N., Gökçay, F., Eirin, H., et al. (2007). "Treatment of idiopathic intracranial hypertension: topiramate vs acetazolamide, an open-label study." Acta Neurologica Scandinavica **116**(5): 322-327.

Chandra, V., Bellur, S. N. and Anderson, R. J. (1986). "Low CSF protein concentration in idiopathic pseudotumor cerebri." Ann Neurol **19**(1): 80-2.

Chapman, K. E., Coutinho, A. E., Gray, M., et al. (2009). "The role and regulation of 11beta-hydroxysteroid dehydrogenase type 1 in the inflammatory response." Mol Cell Endocrinol **301**(1-2): 123-31.

Chapman, K. E. and Seckl, J. R. (2008). "11beta-HSD1, inflammation, metabolic disease and age-related cognitive (dys)function." Neurochem Res **33**(4): 624-36.

Chauchard, F., Cogdill, R., Roussel, S., et al. (2004). "Application of LS-SVM to non-linear phenomena in NIR spectroscopy: development of a robust and portable sensor for acidity prediction in grapes." Chemometrics and Intelligent Laboratory Systems **71**(2): 141-150.

Chebli, J. M., Gaburri, P. D., de Souza, A. F., et al. (2004). "Benign intracranial hypertension during corticosteroid therapy for idiopathic ulcerative colitis: another indication for cyclosporine?" J Clin Gastroenterol **38**(9): 827-8.

Chin, D., Shackleton, C., Prasad, V. K., et al. (2000). "Increased 5alpha-reductase and normal 11beta-hydroxysteroid dehydrogenase metabolism of C19 and C21 steroids in a young population with polycystic ovarian syndrome." J Pediatr Endocrinol Metab **13**(3): 253-9.

Choi, D. W., Maulucci-Gedde, M. and Kriegstein, A. R. (1987). "Glutamate neurotoxicity in cortical cell culture." J Neurosci **7**(2): 357-68.

Clark, A. F., Brotchie, D., Read, A. T., et al. (2005). "Dexamethasone alters F-actin architecture and promotes cross-linked actin network formation in human trabecular meshwork tissue." Cell Motil Cytoskeleton **60**(2): 83-95.

Clayton, P. E. and Cowell, C. T. (2000). "Safety issues in children and adolescents during growth hormone therapy--a review." Growth Horm IGF Res **10**(6): 306-17.

Commodari, F., Arnold, D. L., Sanctuary, B. C., et al. (1991). "1H NMR characterization of normal human cerebrospinal fluid and the detection of methylmalonic acid in a vitamin B12 deficient patient." NMR Biomed **4**(4): 192-200.

Condulis, N., Germain, G., Charest, N., et al. (1997). "Pseudotumor cerebri: a presenting manifestation of Addison's disease." Clin Pediatr (Phila) **36**(12): 711-3.

Cooper, M. S., Rabbitt, E. H., Goddard, P. E., et al. (2002). "Osteoblastic 11beta-hydroxysteroid dehydrogenase type 1 activity increases with age and glucocorticoid exposure." J Bone Miner Res **17**(6): 979-86.

Cooper, M. S. and Stewart, P. M. (2009). "11Beta-hydroxysteroid dehydrogenase type 1 and its role in the hypothalamus-pituitary-adrenal axis, metabolic syndrome, and inflammation." J Clin Endocrinol Metab **94**(12): 4645-54.

Cooper, M. S., Syddall, H. E., Fall, C. H., et al. (2005). "Circulating cortisone levels are associated with biochemical markers of bone formation and lumbar spine BMD: the Hertfordshire Cohort Study." Clin Endocrinol (Oxf) **62**(6): 692-7.

Corbett, J. J. (2008). "The first Jacobson Lecture. Familial idiopathic intracranial hypertension." J Neuroophthalmol **28**(4): 337-47.

Corbett, J. J., Nerad, J. A., Tse, D. T., et al. (1988). "Results of optic nerve sheath fenestration for pseudotumor cerebri. The lateral orbitotomy approach." Arch Ophthalmol **106**(10): 1391-7.

Corbett, J. J., Savino, P. J., Thompson, H. S., et al. (1982). "Visual loss in pseudotumor cerebri. Follow-up of 57 patients from five to 41 years and a profile of 14 patients with permanent severe visual loss." Arch Neurol **39**(8): 461-74.

Costa, A., Rios, M., Casamitjana, R., et al. (1998). "High prevalence of abnormal glucose tolerance and metabolic disturbances in first degree relatives of NIDDM patients.

A study in Catalonia, a mediterranean community." Diabetes Res Clin Pract **41**(3): 191-6.

Cremer, P. D., Johnston, I. H. and Halmagyi, G. M. (1997). "Pseudotumour cerebri syndrome due to cryptococcal meningitis." J Neurol Neurosurg Psychiatry **62**(1): 96-8.

Crock, P. A., McKenzie, J. D., Nicoll, A. M., et al. (1998). "Benign intracranial hypertension and recombinant growth hormone therapy in Australia and New Zealand." Acta Paediatr **87**(4): 381-6.

D'Amico, A. V. and Roehrborn, C. G. (2007). "Effect of 1 mg/day finasteride on concentrations of serum prostate-specific antigen in men with androgenic alopecia: a randomised controlled trial." Lancet Oncol **8**(1): 21-5.

Dandy, W. (1937). "Intracranial pressure without brain tumour: diagnosis and treatment." Ann Surg **106**: 492-513.

Datson, N. A., Morsink, M. C., Meijer, O. C., et al. (2008). "Central corticosteroid actions: Search for gene targets." Eur J Pharmacol **583**(2-3): 272-89.

Davidson, S. I. (1970). "A surgical approach to plerocephalic disc oedema." Trans Ophthalmol Soc U K **89**: 669-90.

Davson, H. and Segal, M. B. (1970). "The effects of some inhibitors and accelerators of sodium transport on the turnover of 22Na in the cerebrospinal fluid and the brain." J Physiol **209**(1): 131-53.

De Bosscher, K., Vanden Berghe, W. and Haegeman, G. (2003). "The interplay between the glucocorticoid receptor and nuclear factor-kappaB or activator protein-1: molecular mechanisms for gene repression." Endocr Rev **24**(4): 488-522.

De Campo, C., Pocecco, M., Bouquet, F., et al. (1988). "[Recurrent iatrogenic benign intracranial hypertension in a case of congenital adrenogenital syndrome with loss of salts]." Pediatr Med Chir **10**(3): 323-6.

de Jong, W. H., Graham, K. S., van der Molen, J. C., et al. (2007). "Plasma free metanephrine measurement using automated online solid-phase extraction HPLC tandem mass spectrometry." Clin Chem **53**(9): 1684-93.

Dees, S. C. and Mc, K. H., Jr. (1959). "Occurrence of pseudotumor cerebri (benign intracranial hypertension) during treatment of children with asthma by adrenal steroids; report of three cases." Pediatrics **23**(6): 1143-51.

Deng, Q. S. and Johanson, C. E. (1989). "Stilbenes inhibit exchange of chloride between blood, choroid plexus and cerebrospinal fluid." Brain Res **501**(1): 183-7.

Desbriere, R., Vuaroqueaux, V., Achard, V., et al. (2006). "11beta-hydroxysteroid dehydrogenase type 1 mRNA is increased in both visceral and subcutaneous adipose tissue of obese patients." Obesity (Silver Spring) **14**(5): 794-8.

Diaz, R., Brown, R. W. and Seckl, J. R. (1998). "Distinct ontogeny of glucocorticoid and mineralocorticoid receptor and 11beta-hydroxysteroid dehydrogenase types I and II mRNAs in the fetal rat brain suggest a complex control of glucocorticoid actions." J Neurosci **18**(7): 2570-80.

Dimitriou, T., Maser-Gluth, C. and Remer, T. (2003). "Adrenocortical activity in healthy children is associated with fat mass." Am J Clin Nutr **77**(3): 731-6.

Donaldson, J. O. (1979). "Cerebrospinal fluid hypersecretion in pseudotumor cerebri." Trans Am Neurol Assoc **104**: 196-8.

Draper, N., Echwald, S. M., Lavery, G. G., et al. (2002). "Association studies between microsatellite markers within the gene encoding human 11beta-hydroxysteroid dehydrogenase type 1 and body mass index, waist to hip ratio, and glucocorticoid metabolism." J Clin Endocrinol Metab **87**(11): 4984-90.

Draper, N., Powell, B. L., Franks, S., et al. (2006). "Variants implicated in cortisone reductase deficiency do not contribute to susceptibility to common forms of polycystic ovary syndrome." Clin Endocrinol (Oxf) **65**(1): 64-70.

Draper, N., Walker, E. A., Bujalska, I. J., et al. (2003). "Mutations in the genes encoding 11beta-hydroxysteroid dehydrogenase type 1 and hexose-6-phosphate dehydrogenase interact to cause cortisone reductase deficiency." Nature Genetics **34**: 434-439.

Duclos, M., Gatta, B., Corcuff, J. B., et al. (2001). "Fat distribution in obese women is associated with subtle alterations of the hypothalamic pituitary adrenal axis activity and sensitivity to glucocorticoids." Clinical Endocrinology **55**(4): 447-454.

Dunaif, A., Segal, K. R., Futterweit, W., et al. (1989). "Profound peripheral insulin resistance, independent of obesity, in polycystic ovary syndrome." Diabetes **38**(9): 1165-1174.

Durcan, F. J., Corbett, J. J. and Wall, M. (1988). "The incidence of pseudotumor cerebri. Population studies in Iowa and Louisiana." Arch Neurol **45**(8): 875-7.

Eggenberger, E. R., Miller, N. R. and Vitale, S. (1996). "Lumboperitoneal shunt for the treatment of pseudotumor cerebri." Neurology **46**(6): 1524-30.

Elenkov, I. J. (2004). "Glucocorticoids and the Th1/Th2 balance." Ann N Y Acad Sci **1024**: 138-46.

Elian, M., Ben-Tovim, N., Bechar, M., et al. (1968). "Recurrent benign intracranial hypertension (pseudotumor cerebri) during pregnancy." Obstet Gynecol **31**(5): 685-8.

Elliott, D. B. and Sheridan, M. (1988). "The use of accurate visual acuity measurements in clinical anti-cataract formulation trials." Ophthalmic Physiol Opt **8**(4): 397-401.

Ernst, S. A., Palacios, J. R., 2nd and Siegel, G. J. (1986). "Immunocytochemical localization of Na+,K+-ATPase catalytic polypeptide in mouse choroid plexus." J Histochem Cytochem **34**(2): 189-95.

Evers, S. (2004). "[The new IHS classification. Background and structure]." Schmerz **18**(5): 351-6.

Fain, J. N. (2006). "Release of interleukins and other inflammatory cytokines by human adipose tissue is enhanced in obesity and primarily due to the nonfat cells." Vitam Horm **74**: 443-77.

Fantuzzi, G. (2005). "Adipose tissue, adipokines, and inflammation." J Allergy Clin Immunol **115**(5): 911-9; quiz 920.

Farb, R. I., Vanek, I., Scott, J. N., et al. (2003). "Idiopathic intracranial hypertension: the prevalence and morphology of sinovenous stenosis." Neurology **60**(9): 1418-24.

Farkash, Y., Timberg, R. and Orly, J. (1986). "Preparation of antiserum to rat cytochrome P-450 cholesterol side chain cleavage, and its use for ultrastructural localization of the immunoreactive enzyme by protein A-gold technique." Endocrinology **118**(4): 1353-65.

Farnsworth, D. (1957). "The FarnsworthMunsell 100Hue Test for the examination of color discrimination." Maryland: Munsell Color Company, Inc.

Fassnacht, M., Schlenz, N., Schneider, S. B., et al. (2003). "Beyond adrenal and ovarian androgen generation: Increased peripheral 5 alpha-reductase activity in women with polycystic ovary syndrome." J Clin Endocrinol Metab **88**(6): 2760-6.

Favretto, D., Nalesso, A., Frison, G., et al. (2009). "A novel and an effective analytical approach for the LC-MS determination of ethyl glucuronide and ethyl sulfate in urine." Int J Legal Med **124**(2): 161- 4.

Feigin, A. (2004). "Evidence from biomarkers and surrogate endpoints." NeuroRx **1**(3): 323-30.

Feldmann, E., Bromfield, E., Navia, B., et al. (1986). "Hydrocephalic dementia and spinal cord tumor. Report of a case and review of the literature." Arch Neurol **43**(7): 714-8.

Fercher, A. F., Hitzenberger, C. K., Drexler, W., et al. (1993). "In vivo optical coherence tomography." Am J Ophthalmol **116**(1): 113-4.

Feschenko, M. S., Donnet, C., Wetzel, R. K., et al. (2003). "Phospholemman, a single-span membrane protein, is an accessory protein of Na,K-ATPase in cerebellum and choroid plexus." J Neurosci **23**(6): 2161-9.

Flom, M. C., Heath, G. G. and Takahashi, E. (1963). "Contour Interaction and Visual Resolution: Contralateral Effects." Science **142**: 979-80.

Flum, D. R., Belle, S. H., King, W. C., et al. (2009). "Perioperative safety in the longitudinal assessment of bariatric surgery." N Engl J Med **361**(5): 445-54.

Foxall, P. J., Parkinson, J. A., Sadler, I. H., et al. (1993). "Analysis of biological fluids using 600 MHz proton NMR spectroscopy: application of homonuclear two-dimensional J-resolved spectroscopy to urine and blood plasma for spectral simplification and assignment." J Pharm Biomed Anal **11**(1): 21-31.

Fraser, R., Ingram, M. C., Anderson, N. H., et al. (1999). "Cortisol effects on body mass, blood pressure, and cholesterol in the general population." Hypertension **33**(6): 1364-8.

Friedman, D. I. and Jacobson, D. M. (2002). "Diagnostic criteria for idiopathic intracranial hypertension." Neurology **59**(10): 1492-5.

Friedman, D. I. and Rausch, E. A. (2002). "Headache diagnoses in patients with treated idiopathic intracranial hypertension." Neurology **58**(10): 1551-3.

Frisen, L. (1982). "Swelling of the optic nerve head: a staging scheme." J Neurol Neurosurg Psychiatry **45**(1): 13-8.

Frohman, E. M., Fujimoto, J. G., Frohman, T. C., et al. (2008). "Optical coherence tomography: a window into the mechanisms of multiple sclerosis." Nat Clin Pract Neurol **4**(12): 664-75.

Funder, J. W. (1996). "Mineralocorticoid receptors in the central nervous system." J Steroid Biochem Mol Biol **56**(1-6 Spec No): 179-83.

Funder, J. W., Pearce, P. T., Smith, R., et al. (1988). "Mineralocorticoid action: target tissue specificity is enzyme, not receptor, mediated." Science **242**(4878): 583-5.

Galvin, J. A. and Van Stavern, G. P. (2004). "Clinical characterization of idiopathic intracranial hypertension at the Detroit Medical Center." J Neurol Sci **223**(2): 157-60.

Ghauri, F. Y., Nicholson, J. K., Sweatman, B. C., et al. (1993). "NMR spectroscopy of human post mortem cerebrospinal fluid: distinction of Alzheimer's disease from control using pattern recognition and statistics." NMR Biomed **6**(2): 163-7.

Gibson, S. A. and Sanderson, H. F. (1980). "Observer variation in ophthalmology." Br J Ophthalmol **64**: 457-460.

Gideon, P., Sorensen, P. S., Thomsen, C., et al. (1994). "Assessment of CSF dynamics and venous flow in the superior sagittal sinus by MRI in idiopathic intracranial hypertension: a preliminary study." Neuroradiology **36**(5): 350-4.

Gideon, P., Sorensen, P. S., Thomsen, C., et al. (1995). "Increased brain water self-diffusion in patients with idiopathic intracranial hypertension." AJNR Am J Neuroradiol **16**(2): 381-7.

Gilles, F. H. and Davidson, R. I. (1971). "Communicating hydrocephalus associated with deficient dysplastic parasagittal arachnoidal granulations." J Neurosurg **35**(4): 421-6.

Ginsberg, H. N. (2000). "Insulin resistance and cardiovascular disease." J Clin Invest **106**(4): 453-8.

Giuseffi, V., Wall, M., Siegel, P. Z., et al. (1991). "Symptoms and disease associations in idiopathic intracranial hypertension (pseudotumor cerebri): a case-control study." Neurology **41**(2 (Pt 1)): 239-44.

Glass, C. K. and Ogawa, S. (2006). "Combinatorial roles of nuclear receptors in inflammation and immunity." Nat Rev Immunol **6**(1): 44-55.

Glueck, C. J., Aregawi, D., Goldenberg, N., et al. (2005). "Idiopathic intracranial hypertension, polycystic-ovary syndrome, and thrombophilia." J Lab Clin Med **145**(2): 72-82.

Glueck, C. J., Iyengar, S., Goldenberg, N., et al. (2003). "Idiopathic intracranial hypertension: associations with coagulation disorders and polycystic-ovary syndrome." J Lab Clin Med **142**(1): 35-45.

Goedecke, J. H., Wake, D. J., Levitt, N. S., et al. (2006). "Glucocorticoid metabolism within superficial subcutaneous rather than visceral adipose tissue is associated with features of the metabolic syndrome in South African women." Clin Endocrinol (Oxf) **65**(1): 81-7.

Goleva, E., Li, L. B., Eves, P. T., et al. (2006). "Increased glucocorticoid receptor beta alters steroid response in glucocorticoid-insensitive asthma." Am J Respir Crit Care Med **173**(6): 607-16.

Gomez-Sanchez, E. P., Ganjam, V., Chen, Y. J., et al. (2003). "Regulation of 11 beta-hydroxysteroid dehydrogenase enzymes in the rat kidney by estradiol." Am J Physiol Endocrinol Metab **285**(2): E272-9.

Gonzalez-Hernandez, A., Fabre-Pi, O., Diaz-Nicolas, S., et al. (2009). "[Headache in idiopathic intracranial hypertension]." Rev Neurol **49**(1): 17-20.

Goodwin, J. (2003). "Recent developments in idiopathic intracranial hypertension (IIH)." Semin Ophthalmol **18**(4): 181-9.

Graber, J. J., Racela, R. and Henry, K. (2009). "Cerebellar Tonsillar Herniation After Weight Loss in a Patient With Idiopathic Intracranial Hypertension." Headache: Epub ahead of print.

Green, K. N., Billings, L. M., Roozendaal, B., et al. (2006). "Glucocorticoids increase amyloid-beta and tau pathology in a mouse model of Alzheimer's disease." J Neurosci **26**(35): 9047-56.

Greene, C. S., Jr., Lorenzo, A. V., Hornig, G., et al. (1985). "The lowering of cerebral spinal fluid and brain interstitial pressure of preterm and term rabbits by furosemide." Z Kinderchir **40 Suppl 1**: 5-8.

Greer, M. (1963). "Benign intracranial hypertension. II. Following corticosteroid therapy." Neurology **13**: 439-41.

Griffin, J. L. and Kauppinen, R. A. (2007). "A metabolomics perspective of human brain tumours." Febs J **274**(5): 1132-9.

Griffin, J. L. and Shockcor, J. P. (2004). "Metabolic profiles of cancer cells." Nat Rev Cancer **4**(7): 551-61.

Grzybowski, D. M., Hererick, E. E., Kapoor, K. G., et al. (2006a). "Human arachnoid granulation probability of occurrence and surface area quantification." Cerebrospinal Fluid Res **3** (suppl 1): S13.

Grzybowski, D. M., Holman, D. W., Katz, S. E., et al. (2006b). "In vitro model of cerebrospinal fluid outflow through human arachnoid granulations." Invest Ophthalmol Vis Sci **47**(8): 3664-72.

Guazzo, E. P., Kirkpatrick, P. J., Goodyer, I. M., et al. (1996). "Cortisol, dehydroepiandrosterone (DHEA), and DHEA sulfate in the cerebrospinal fluid of man: relation to blood levels and the effects of age." J Clin Endocrinol Metab **81**(11): 3951-60.

Guitton, J., Coste, S., Guffon-Fouilhoux, N., et al. (2009). "Rapid quantification of miglustat in human plasma and cerebrospinal fluid by liquid chromatography coupled with tandem mass spectrometry." J Chromatogr B Analyt Technol Biomed Life Sci **877**(3): 149-54.

Gumma, A. D. (2004). "Recurrent benign intracranial hypertension in pregnancy." Eur J Obstet Gynecol Reprod Biol **115**(2): 244.

Gutierrez, Y., Friede, R. L. and Kaliney, W. J. (1975). "Agenesis of arachnoid granulations and its relationship to communicating hydrocephalus." J Neurosurg **43**(5): 553-8.

Halmi, P., Parkkila, S. and Honkaniemi, J. (2006). "Expression of carbonic anhydrases II, IV, VII, VIII and XII in rat brain after kainic acid induced status epilepticus." Neurochemistry International **48**(1): 24-30.

Hamilos, D. L., Leung, D. Y., Muro, S., et al. (2001). "GRbeta expression in nasal polyp inflammatory cells and its relationship to the anti-inflammatory effects of intranasal fluticasone." J Allergy Clin Immunol **108**(1): 59-68.

Hammond, G. L. (1990). "Molecular properties of corticosteroid binding globulin and the sex-steroid binding proteins." Endocr Rev **11**(1): 65-79.

Hardy, R., Rabbitt, E. H., Filer, A., et al. (2008). "Local and systemic glucocorticoid metabolism in inflammatory arthritis." Ann Rheum Dis **67**(9): 1204-10.

Hardy, R. S., Filer, A., Cooper, M. S., et al. (2006). "Differential expression, function and response to inflammatory stimuli of 11beta-hydroxysteroid dehydrogenase type 1 in human fibroblasts: a mechanism for tissue-specific regulation of inflammation." Arthritis Res Ther **8**(4): R108.

Harris, H. J., Kotelevtsev, Y., Mullins, J. J., et al. (2001). "Intracellular regeneration of glucocorticoids by 11beta-hydroxysteroid dehydrogenase (11beta-HSD)-1 plays a key role in regulation of the hypothalamic-pituitary-adrenal axis: analysis of 11beta-HSD-1-deficient mice." Endocrinology **142**(1): 114-20.

Haselbach, M., Wegener, J., Decker, S., et al. (2001). "Porcine Choroid plexus epithelial cells in culture: regulation of barrier properties and transport processes." Microsc Res Tech **52**(1): 137-52.

Heijl, A., Lindgren, G. and Olsson, J. (1987). "A package for statistical analysis of computerized fields." Doc Ophthalmol **49**: 153-168

Hermanowski-Vosatka, A., Balkovec, J. M., Cheng, K., et al. (2005). "11beta-HSD1 inhibition ameliorates metabolic syndrome and prevents progression of atherosclerosis in mice." J Exp Med **202**(4): 517-27.

Higgins, J. N., Cousins, C., Owler, B. K., et al. (2003). "Idiopathic intracranial hypertension: 12 cases treated by venous sinus stenting." J Neurol Neurosurg Psychiatry **74**(12): 1662-6.

Higgins, J. N., Gillard, J. H., Owler, B. K., et al. (2004). "MR venography in idiopathic intracranial hypertension: unappreciated and misunderstood." J Neurol Neurosurg Psychiatry **75**(4): 621-5.

Hiraoka, A., Miura, I., Hattori, M., et al. (1994). "Proton magnetic resonance spectroscopy of cerebrospinal fluid as an aid in neurological diagnosis." Biol Pharm Bull **17**(1): 1-4.

Ho, C. K., Tetsuka, M. and Hillier, S. G. (1999). "Regulation of 11beta-hydroxysteroid dehydrogenase isoforms and glucocorticoid receptor gene expression in the rat uterus." J Endocrinol **163**(3): 425-31.

Hollenberg, S. M., Weinberger, C., Ong, E. S., et al. (1985). "Primary structure and expression of a human glucocorticoid receptor cDNA." Nature **318**(19): 635-641.

Holman, D. W., Grzybowski, D. M., Mehta, B. C., et al. (2005). "Characterization of cytoskeletal and junctional proteins expressed by cells cultured from human arachnoid granulation tissue." Cerebrospinal Fluid Res **2**: 9.

Holmes, E., Loo, R. L., Stamler, J., et al. (2008). "Human metabolic phenotype diversity and its association with diet and blood pressure." Nature **453**(7193): 396-400.

Holmes, E., Tsang, T. M., Huang, J. T., et al. (2006a). "Metabolic profiling of CSF: evidence that early intervention may impact on disease progression and outcome in schizophrenia." PLoS Med **3**(8): e327.

Holmes, E., Tsang, T. M. and Tabrizi, S. J. (2006b). "The application of NMR-based metabonomics in neurological disorders." NeuroRx **3**(3): 358-72.

Holmes, M. C., Sangra, M., French, K. L., et al. (2006c). "11beta-Hydroxysteroid dehydrogenase type 2 protects the neonatal cerebellum from deleterious effects of glucocorticoids." Neuroscience **137**(3): 865-73.

Holmes, M. C. and Seckl, J. R. (2006). "The role of 11beta-hydroxysteroid dehydrogenases in the brain." Mol Cell Endocrinol **248**(1-2): 9-14.

Honda, M., Orii, F., Ayabe, T., et al. (2000). "Expression of glucocorticoid receptor beta in lymphocytes of patients with glucocorticoid-resistant ulcerative colitis." Gastroenterology **118**(5): 859-66.

Hoogendijk, W. J., Meynen, G., Endert, E., et al. (2005). "Increased cerebrospinal fluid cortisol level in Alzheimer's disease is not related to depression." Neurobiol Aging **27**(5): 780.

Horton, R., Pasupuletti, V. and Antonipillai, I. (1993). "Androgen induction of steroid 5 alpha-reductase may be mediated via insulin-like growth factor-I." Endocrinology **133**(2): 447-451.

Hosking, G. P. and Elliston, H. (1978). "Benign intracranial hypertension in a child with eczema treated with topical steroids." Br Med J **1**(6112): 550-1.

Ireland, B., Corbett, J. J. and Wallace, R. B. (1990). "The search for causes of idiopathic intracranial hypertension. A preliminary case-control study." Arch Neurol **47**(3): 315-20.

Ishibashi, T., Takagi, Y., Mori, K., et al. (2002). "cDNA microarray analysis of gene expression changes induced by dexamethasone in cultured human trabecular meshwork cells." Invest Ophthalmol Vis Sci **43**(12): 3691-7.

Issa, A. M., Rowe, W., Gauthier, S., et al. (1990). "Hypothalamic-pituitary-adrenal activity in aged, cognitively impaired and cognitively unimpaired rats." J Neurosci **10**(10): 3247-54.

Ivancic, R. and Pfadenhauer, K. (2004). "Pseudotumor cerebri after hormonal emergency contraception." Eur Neurol **52**(2): 120.

Ivey, K. J. and Denssesten, L. (1969). "Pseudotumor cerebri associated with corticosteroid therapy in an adult." JAMA **208**(9): 1698-700.

Jacobson, N., Andrews, M., Shepard, A. R., et al. (2001). "Non-secretion of mutant proteins of the glaucoma gene myocilin in cultured trabecular meshwork cells and in aqueous humor." Hum Mol Genet **10**(2): 117-25.

Jakimiuk, A. J., Weitsman, S. R. and Magoffin, D. A. (1999). "5alpha-reductase activity in women with polycystic ovary syndrome." J Clin Endocrinol Metab **84**(7): 2414-8.

Jamieson, A., Wallace, A. M., Andrew, R., et al. (1999). "Apparent cortisone reductase deficiency: a functional defect in 11beta-hydroxysteroid dehydrogenase type 1." J Clin Endocrinol Metab **84**(10): 3570-4.

Jang, C., Obeyesekere, V. R., Alford, F. P., et al. (2009). "Skeletal muscle 11beta hydroxysteroid dehydrogenase type 1 activity is upregulated following elective abdominal surgery." Eur J Endocrinol **160**(2): 249-55.

Janny, P., Chazal, J., Colnet, G., et al. (1981). "Benign intracranial hypertension and disorders of CSF absorption." Surg Neurol **15**(3): 168-74.

Janzik, H. H. (1973). "[Benign increase in intracranial pressure during oral contraception (author's transl)]." Dtsch Med Wochenschr **98**(43): 2028-9.

Jellinck, P. H., Pavlides, C., Sakai, R. R., et al. (1999). "11beta-hydroxysteroid dehydrogenase functions reversibly as an oxidoreductase in the rat hippocampus in vivo." J Steroid Biochem Mol Biol **71**(3-4): 139-44.

Jenkins, E. P., Hsieh, C. L., Milatovich, A., et al. (1991). "Characterization and chromosomal mapping of a human steroid 5 alpha-reductase gene and pseudogene and mapping of the mouse homologue." Genomics **11**(4): 1102-12.

Jennum, P. and Borgesen, S. E. (1989). "Intracranial pressure and obstructive sleep apnea." Chest **95**(2): 279-83.

Jewell, D. P. (1972). "Benign intracranial hypertension and ulcerative colitis." Am J Dig Dis **17**(1): 89-91.

Jiang, S., Chappa, A. K. and Proksch, J. W. (2009). "A rapid and sensitive LC/MS/MS assay for the quantitation of brimonidine in ocular fluids and tissues." J Chromatogr B Analyt Technol Biomed Life Sci **877**(3): 107-14.

Johansen, K. M., W. Beal, F. Aasly, JO. Bogdanov, M. (2007). "Metabolomic analysis in LRRK2 Parkinson's disese." Movement Disorders **22**(S16): S184 E-abstract 603.

Johnson, L. N., Krohel, G. B., Madsen, R. W., et al. (1998). "The role of weight loss and acetazolamide in the treatment of idiopathic intracranial hypertension (pseudotumor cerebri)." Ophthalmology **105**(12): 2313-7.

Johnston, I., Besser, M. and Morgan, M. K. (1988). "Cerebrospinal fluid diversion in the treatment of benign intracranial hypertension." J Neurosurg **69**(2): 195-202.

Johnston, I., Kollar, C., Dunkley, S., et al. (2002). "Cranial venous outflow obstruction in the pseudotumour syndrome: incidence, nature and relevance." J Clin Neurosci **9**(3): 273-8.

Johnston, I. and Paterson, A. (1974). "Benign intracranial hypertension. II. CSF pressure and circulation." Brain **97**(2): 301-12.

Johnston, M., Zakharov, A., Papaiconomou, C., et al. (2004). "Evidence of connections between cerebrospinal fluid and nasal lymphatic vessels in humans, non-human primates and other mammalian species." Cerebrospinal Fluid Res **1**(1): 2.

Johnston, P. K., Corbett, J. J. and Maxner, C. E. (1991). "Cerebrospinal fluid protein and opening pressure in idiopathic intracranial hypertension (pseudotumor cerebri)." Neurology **41**(7): 1040-2.

Karahalios, D. G., Rekate, H. L., Khayata, M. H., et al. (1996). "Elevated intracranial venous pressure as a universal mechanism in pseudotumor cerebri of varying etiologies." Neurology **46**(1): 198-202.

Karssen, A. M., Meijer, O. C., van der Sandt, I. C., et al. (2001). "Multidrug resistance P-glycoprotein hampers the access of cortisol but not of corticosterone to mouse and human brain." Endocrinology **142**(6): 2686-94.

Keltner, J. L., Albert, D. M., Lubow, M., et al. (1977). "Optic nerve decompression. A clinical pathologic study." Arch Ophthalmol **95**(1): 97-104.

Kesler, A. and Gadoth, N. (2001). "Epidemiology of idiopathic intracranial hypertension in Israel." J Neuroophthalmol **21**(1): 12-4.

Kesler, A., Kliper, E., Shenkerman, G., et al. (2009). "Idiopathic Intracranial Hypertension Is Associated with Lower Body Adiposity." Ophthalmology **117**(1): 169-74.

Khonsari, R. H., Wegener, M., Leruez, S., et al. (2009). "[Optic disc drusen or true papilledema?]." Rev Neurol (Paris) **166**(1): 32-8.

Kida, S., Yamashima, T., Kubota, T., et al. (1988). "A light and electron microscopic and immunohistochemical study of human arachnoid villi." J Neurosurg **69**(3): 429-35.

Kiehna, E. N., Keil, M., Lodish, M., et al. (2010). "Pseudotumor Cerebri after Surgical Remission of Cushing's Disease." J Clin Endocrinol Metab **95**(4): 1528-32.

Kind, T., Tolstikov, V., Fiehn, O., et al. (2007). "A comprehensive urinary metabolomic approach for identifying kidney cancerr." Anal Biochem **363**(2): 185-95.

King, J. O., Mitchell, P. J., Thomson, K. R., et al. (1995). "Cerebral venography and manometry in idiopathic intracranial hypertension." Neurology **45**(12): 2224-8.

King, J. O., Mitchell, P. J., Thomson, K. R., et al. (2002). "Manometry combined with cervical puncture in idiopathic intracranial hypertension." Neurology **58**(1): 26-30.

Kinnear, P. R. and Sahraie, A. (2002). "New Farnsworth-Munsell 100 hue test norms of normal observers for each year of age 5-22 and for age decades 30-70." Br J Ophthalmol **86**(12): 1408-11.

Kling, M. A., DeBellis, M. D., O'Rourke, D. K., et al. (1994). "Diurnal variation of cerebrospinal fluid immunoreactive corticotropin-releasing hormone levels in healthy volunteers." J Clin Endocrinol Metab **79**(1): 233-9.

Klok, M. D., Jakobsdottir, S. and Drent, M. L. (2007). "The role of leptin and ghrelin in the regulation of food intake and body weight in humans: a review." Obes Rev **8**(1): 21-34.

Kollar, C., Parker, G. and Johnston, I. (2001). "Endovascular treatment of cranial venous sinus obstruction resulting in pseudotumor syndrome. Report of three cases." J Neurosurg **94**(4): 646-51.

Koschorek, F., Offermann, W., Stelten, J., et al. (1993). "High-resolution 1H NMR spectroscopy of cerebrospinal fluid in spinal diseases." Neurosurg Rev **16**(4): 307-15.

Kosinski, M., Bayliss, M. S., Bjorner, J. B., et al. (2003). "A six-item short-form survey for measuring headache impact: the HIT-6." Qual Life Res **12**(8): 963-74.

Kostopoulos, V., Douzinas, E. E., Kypriades, E. M., et al. (2006). "A new method for the early diagnosis of brain edema/brain swelling. An experimental study in rabbits." J Biomech **39**(16): 2958-65.

Kotelevtsev, Y., Holmes, M. C., Burchell, A., et al. (1997). "11β-hydroxysteroid dehydrogenase type 1 knockout mice show attenuated glucocorticoid-inducible responses and resist hyperglycaemia on obesity and stress." Proceedings of the National Academy of Sciences of the United States of America **94**: 1492-14929.

Ku, Y. H., Koo, B. K., Kwak, S. H., et al. (2009). "Regulatory effect of common promoter polymorphisms on the expression of the 11beta-hydroxysteroid dehydrogenase type 1 gene." Horm Res **72**(1): 25-32.

Kupersmith, M. J., Gamell, L., Turbin, R., et al. (1998). "Effects of weight loss on the course of idiopathic intracranial hypertension in women." Neurology **50**(4): 1094-8.

Kushnir, M. M., Neilson, R., Roberts, W. L., et al. (2004). "Cortisol and cortisone analysis in serum and plasma by atmospheric pressure photoionization tandem mass spectrometry." Clin Biochem **37**(5): 357-62.

Kushnir, M. M., Rockwood, A. L. and Bergquist, J. (2009). "Liquid chromatography-tandem mass spectrometry applications in endocrinology." Mass Spectrom Rev **29**(3): 480-502.

Lakshmi, V. and Monder, C. (1988). "Purification and characterization of the corticosteroid 11 beta-dehydrogenase component of the rat liver 11 beta-hydroxysteroid dehydrogenase complex." Endocrinology **123**(5): 2390-8.

Lakshmi, V., Sakai, R. R., McEwen, B. S., et al. (1991). "Regional distribution of 11 beta-hydroxysteroid dehydrogenase in rat brain." Endocrinology **128**(4): 1741-8.

Lampl, Y., Eshel, Y., Kessler, A., et al. (2002). "Serum leptin level in women with idiopathic intracranial hypertension." J Neurol Neurosurg Psychiatry **72**(5): 642-3.

Landfield, P. W., Waymire, J. C. and Lynch, G. (1978). "Hippocampal aging and adrenocorticoids: quantitative correlations." Science **202**(4372): 1098-102.

Laughlin, G. A. and Barrett-Connor, E. (2000). "Sexual dimorphism in the influence of advanced aging on adrenal hormone levels: the Rancho Bernardo Study." J Clin Endocrinol Metab **85**(10): 3561-8.

Lavery, G. G., Walker, E. A., Tiganescu, A., et al. (2008). "Steroid biomarkers and genetic studies reveal inactivating mutations in hexose-6-phosphate dehydrogenase in patients with cortisone reductase deficiency." J Clin Endocrinol Metab **93**(10): 3827-32.

Lee, G. C. a. W., D.L. (2004). "Beam search for peak alignment of NMR signals." Analytica Chimica Acta **513**: 413-416.

Lennon, V. A., Kryzer, T. J., Pittock, S. J., et al. (2005). "IgG marker of optic-spinal multiple sclerosis binds to the aquaporin-4 water channel." J Exp Med **202**(4): 473-7.

Lennon, V. A., Wingerchuk, D. M., Kryzer, T. J., et al. (2004). "A serum autoantibody marker of neuromyelitis optica: distinction from multiple sclerosis." Lancet **364**(9451): 2106-12.

Levy, J. C., Matthews, D. R. and Hermans, M. P. (1998). "Correct homeostasis model assessment (HOMA) evaluation uses the computer program." Diabetes Care **21**(12): 2191-2.

Li, X., Lindquist, S., Chen, R., et al. (2007). "Depot-specific messenger RNA expression of 11 beta-hydroxysteroid dehydrogenase type 1 and leptin in adipose tissue of children and adults." Int J Obes (Lond) **31**(5): 820-8.

Li, Z., Maglione, M., Tu, W., et al. (2005). "Meta-analysis: pharmacologic treatment of obesity." Ann Intern Med **142**(7): 532-46.

Lindon, J. C., Nicholson, J. K., Holmes, E., et al. (2003). "Contemporary issues in toxicology the role of metabonomics in toxicology and its evaluation by the COMET project." Toxicol Appl Pharmacol **187**(3): 137-46.

Lipton, H. L. and Michelson, P. E. (1972). "Pseudotumor cerebri syndrome without papilledema." JAMA **220**(12): 1591-2.

Liu, G. T., Glaser, J. S. and Schatz, N. J. (1994). "High-dose methylprednisolone and acetazolamide for visual loss in pseudotumor cerebri." Am J Ophthalmol **118**(1): 88-96.

Liu, W., Wang, J., Sauter, N. K., et al. (1995). "Steroid receptor heterodimerization demonstrated *in-vitro* and *in-vivo*." Proceedings of the National Academy of Sciences of the United States of America **92**: 12480-12484.

Llobet, A., Gasull, X. and Gual, A. (2003). "Understanding trabecular meshwork physiology: a key to the control of intraocular pressure?" News Physiol Sci **18**: 205-9.

Lloyd, D. J., Helmering, J., Cordover, D., et al. (2009). "Antidiabetic effects of 11beta-HSD1 inhibition in a mouse model of combined diabetes, dyslipidaemia and atherosclerosis." Diabetes Obes Metab **11**(7): 688-99.

Lolli, F., Rovero, P., Chelli, M., et al. (2006). "Toward biomarkers in multiple sclerosis: new advances." Expert Rev Neurother **6**(5): 781-94.

Loong, T.-W. (2003). "Understanding sensitivity and specificity with the right side of the brain." BMJ **327**(7417): 716-719.

Lorenzo, Y. D. I. J. and Avellanal, C. (1961). "[Benign endocranial hypertension ("cerebral pseudotumor") during corticosteroid therapy.]." Arch Pediatr Urug **32**: 347-52.

Lorrot, M., Bader-Meunier, B., Sebire, G., et al. (1999). "[Benign intracranial hypertension: an unrecognized complication of corticosteroid therapy]." Arch Pediatr **6**(1): 40-2.

Losel, R. M., Falkenstein, E., Feuring, M., et al. (2003). "Nongenomic steroid action: controversies, questions, and answers." Physiol Rev **83**(3): 965-1016.

Lovie-Kitchin, J. E. and Brown, B. (2000). "Repeatability and intercorrelations of standard vision tests as a function of age." Optom Vis Sci **77**(8): 412-20.

Low, S. C., Assaad, S. N., Rajan, V., et al. (1993). "Regulation of 11 beta-hydroxysteroid dehydrogenase by sex steroids in vivo: further evidence for the existence of a second dehydrogenase in rat kidney." J Endocrinol **139**(1): 27-35.

Low, S. C., Chapman, K. E., Edwards, C. R., et al. (1994). "Sexual dimorphism of hepatic 11 beta-hydroxysteroid dehydrogenase in the rat: the role of growth hormone patterns." J Endocrinol **143**(3): 541-8.

Lucas, A., Coll, J., Salinas, I., et al. (1991). "[Benign intracranial hypertension following the suspension of corticotherapy in a female patient previously operated on for Cushing's disease]." Med Clin (Barc) **97**(12): 473.

Lueck, C. and McIlwaine, G. (2002). "Interventions for idiopathic intracranial hypertension." Cochrane Database Syst Rev(3): CD003434.

Lueck, C. and McIlwaine, G. (2005). "Interventions for idiopathic intracranial hypertension." Cochrane Database Syst Rev(3): CD003434.

Lupien, S. J., de Leon, M., de Santi, S., et al. (1998). "Cortisol levels during human aging predict hippocampal atrophy and memory deficits." Nat Neurosci **1**(1): 69-73.

Lupien, S. J., Nair, N. P., Briere, S., et al. (1999). "Increased cortisol levels and impaired cognition in human aging: implication for depression and dementia in later life." Rev Neurosci **10**(2): 117-39.

Lutz, N. W., Maillet, S., Nicoli, F., et al. (1998). "Further assignment of resonances in 1H NMR spectra of cerebrospinal fluid (CSF)." FEBS Lett **425**(2): 345-51.

Lutz, N. W., Viola, A., Malikova, I., et al. (2007). "Inflammatory multiple-sclerosis plaques generate characteristic metabolic profiles in cerebrospinal fluid." PLoS ONE **2**: e595.

Lutz, N. W., Yahi, N., Fantini, J., et al. (1996). "Analysis of individual purine and pyrimidine nucleoside di- and triphosphates and other cellular metabolites in PCA extracts by using multinuclear high resolution NMR spectroscopy." Magn Reson Med **36**(5): 788-95.

Lynch, J., Peeling, J., Auty, A., et al. (1993). "Nuclear magnetic resonance study of cerebrospinal fluid from patients with multiple sclerosis." Can J Neurol Sci **20**(3): 194-8.

Madan Mohan, P., Noushad, T. P., Sarita, P., et al. (1993). "Hypoparathyroidism with benign intracranial hypertension." J Assoc Physicians India **41**(11): 752-3.

Maher, A. D., Zirah, S. F., Holmes, E., et al. (2007). "Experimental and analytical variation in human urine in 1H NMR spectroscopy-based metabolic phenotyping studies." Anal Chem **79**(14): 5204-11.

Malavasi, E. L., Kelly, V., Nath, N., et al. (2009). "Functional Effects of Polymorphisms in the Human Gene Encoding 11{beta}-Hydroxysteroid Dehydrogenase Type 1 (11{beta}-HSD1): A Sequence Variant at the Translation Start of 11{beta}-HSD1 Alters Enzyme Levels." Endocrinology **151**(1): 195-202.

Malm, J., Kristensen, B., Markgren, P., et al. (1992). "CSF hydrodynamics in idiopathic intracranial hypertension: a long-term study." Neurology **42**(4): 851-8.

Marcelis, J. and Silberstein, S. D. (1991). "Idiopathic intracranial hypertension without papilledema." Arch Neurol **48**(4): 392-9.

Marin, P., Darin, N., Amemiya, T., et al. (1992). "Cortisol secretion in relation to body fat distribution in obese premenopausal women." Metabolism **41**(8): 882-6.

Martens, H. and Naes, T. (1989). "Multivariate Calibration." John Wiley & Sons, New York.

Marynick, S. P., Havens, W. W., 2nd, Ebert, M. H., et al. (1976). "Studies on the transfer of steroid hormones across the blood-cerebrospinal fluid barrier in the Rhesus Monkey." Endocrinology **99**(2): 400-5.

Marynick, S. P., Smith, G. B., Ebert, M. H., et al. (1977). "Studies on the transfer of steroid hormones across the blood-cerebrospinal fluid barrier in the rhesus monkey. II." Endocrinology **101**(2): 562-7.

Masuzaki, H., Paterson, J., Shinyama, H., et al. (2001). "A transgenic model of visceral obsity and the metabolic syndrome." Science **294**: 2166-2170.

Masuzaki, H., Yamamoto, H., Kenyon, C. J., et al. (2003). "Transgenic amplification of glucocorticoid action in adipose tissue causes high blood pressure in mice." J Clin Invest **112**(1): 83-90.

Masuzawa, T., Hasegawa, T., Nakahara, N., et al. (1984). "Localization of carbonic anhydrase in the rat choroid plexus epithelial cell." Ann N Y Acad Sci **429**: 405-7.

Masuzawa, T. and Sato, F. (1983). "The enzyme histochemistry of the choroid plexus." Brain **106 (Pt 1)**: 55-99.

McComb, J. G. (1983). "Recent research into the nature of cerebrospinal fluid formation and absorption." J Neurosurg **59**(3): 369-83.

McDonald, W. I., Compston, A., Edan, G., et al. (2001). "Recommended diagnostic criteria for multiple sclerosis: guidelines from the International Panel on the diagnosis of multiple sclerosis." Ann Neurol **50**(1): 121-7.

McGonigal, A., Bone, I. and Teasdale, E. (2004). "Resolution of transverse sinus stenosis in idiopathic intracranial hypertension after L-P shunt." Neurology **62**(3): 514-5.

McGraw, P., Winn, B. and Whitaker, D. (1995). "Reliability of the Snellen chart." BMJ **310**(6993): 1481-2.

Meaney, M. J., O'Donnell, D., Rowe, W., et al. (1995). "Individual differences in hypothalamic-pituitary-adrenal activity in later life and hippocampal aging." Exp Gerontol **30**(3-4): 229-51.

Medeiros, F. A., Moura, F. C., Vessani, R. M., et al. (2003). "Axonal loss after traumatic optic neuropathy documented by optical coherence tomography." Am J Ophthalmol **135**(3): 406-8.

Medeiros, F. A., Zangwill, L. M., Bowd, C., et al. (2004). "Comparison of the GDx VCC scanning laser polarimeter, HRT II confocal scanning laser ophthalmoscope, and

stratus OCT optical coherence tomograph for the detection of glaucoma." <u>Arch Ophthalmol</u> **122**(6): 827-37.

Mercer, J. G., Hoggard, N., Williams, L. M., et al. (1996). "Localization of leptin receptor mRNA and the long form splice variant (Ob-Rb) in mouse hypothalamus and adjacent brain regions by in situ hybridization." <u>FEBS Lett</u> **387**(2-3): 113-6.

Meyer, J. S., Sawada, T., Kitamura, A., et al. (1968). "Cerebral Oxygen, Glucose, Lactate, and Pyruvate Metabolism in Stroke: Therapeutic Considerations." <u>Circulation</u> **37**(6): 1036-1048.

Michailidou, Z., Jensen, M. D., Dumesic, D. A., et al. (2007). "Omental 11beta-hydroxysteroid dehydrogenase 1 correlates with fat cell size independently of obesity." <u>Obesity (Silver Spring)</u> **15**(5): 1155-63.

Miller, D. B. and O'Callaghan, J. P. (2005). "Aging, stress and the hippocampus." <u>Ageing Res Rev</u> **4**(2): 123-40.

Miller, J. D., Stanek, A. and Langfitt, T. W. (1972). "Concepts of cerebral perfusion pressure and vascular compression during intracranial hypertension." <u>Prog Brain Res</u> **35**: 411-32.

Miller, N., Newman, N. J., Biousse, V., et al. (1999). "Clinical Neuro-Ophthalmology: The Essentials." (Second Edition): 57-58.

Miyamoto, Y., Morisaki, H., Yamanaka, I., et al. (2009). "Association study of 11beta-hydroxysteroid dehydrogenase type 1 gene polymorphisms and metabolic syndrome in urban Japanese cohort." <u>Diabetes Res Clin Pract</u> **85**(2): 132-8.

Mode, A. and Norstedt, G. (1982). "Effects of gonadal steroid hormones on the hypothalamo-pituitary-liver axis in the control of sex differences in hepatic steroid metabolism in the rat." <u>J Endocrinol</u> **95**(2): 181-7.

Moisan, M. P., Seckl, J. R. and Edwards, C. R. (1990). "11 beta-hydroxysteroid dehydrogenase bioactivity and messenger RNA expression in rat forebrain: localization in hypothalamus, hippocampus, and cortex." <u>Endocrinology</u> **127**(3): 1450-5.

Moore, R. Y. and Silver, R. (1998). "Suprachiasmatic nucleus organization." <u>Chronobiol Int</u> **15**(5): 475-87.

Morton, N. M., Holmes, M. C., Fievet, C., et al. (2001). "Improved lipid and lipoprotein profile, hepatic insulin sensitivity, and glucose tolerance in 11beta-hydroxysteroid dehydrogenase type 1 null mice." <u>J Biol Chem</u> **276**(44): 41293-300.

Mowry, E. M., Loguidice, M. J., Daniels, A. B., et al. (2009). "Vision related quality of life in multiple sclerosis: correlation with new measures of low and high contrast letter acuity." <u>J Neurol Neurosurg Psychiatry</u> **80**(7): 767-72.

Murphy, V. A. and Johanson, C. E. (1989). "Alteration of sodium transport by the choroid plexus with amiloride." <u>Biochim Biophys Acta</u> **979**(2): 187-92.

Nappi, G., Jensen, R., Nappi, R. E., et al. (2006). "Diaries and calendars for migraine. A review." <u>Cephalalgia</u> **26**(8): 905-16.

Nawashiro, H., Huang, S., Brenner, M., et al. (2002). "ICP monitoring following bilateral carotid occlusion in GFAP-null mice." <u>Acta Neurochir Suppl</u> **81**: 269-70.

Neville, L. and Egan, R. A. (2005). "Frequency and amplitude of elevation of cerebrospinal fluid resting pressure by the Valsalva maneuver." <u>Can J Ophthalmol</u> **40**(6): 775-7.

Newborg, B. (1974). "Pseudotumor cerebri treated by rice reduction diet." <u>Arch Intern Med</u> **133**(5): 802-7.

Newman, P. K., Snow, M. and Hudgson, P. (1980). "Benign intracranial hypertension and Cushing's disease." <u>Br Med J</u> **281**(6233): 113.

Newton, M. and Cooper, B. T. (1994). "Benign intracranial hypertension during prednisolone treatment for inflammatory bowel disease." Gut **35**(3): 423-5.

Newton, R. and Holden, N. S. (2007). "Separating transrepression and transactivation: a distressing divorce for the glucocorticoid receptor?" Mol Pharmacol **72**(4): 799-809.

Ngumah, Q. C., Buchthal, S. D. and Dacheux, R. F. (2006). "Longitudinal non-invasive proton NMR spectroscopy measurement of vitreous lactate in a rabbit model of ocular hypertension." Exp Eye Res **83**(2): 390-400.

Nichols, B. E., Thompson, H. S. and Stone, E. M. (1997). "Evaluation of a significantly shorter version of the Farnsworth-Munsell 100-hue test in patients with three different optic neuropathies." J Neuroophthalmol **17**(1): 1-6.

Nicoli, F., Vion-Dury, J., Confort-Gouny, S., et al. (1996). "Cerebrospinal fluid metabolic profiles in multiple sclerosis and degenerative dementias obtained by high resolution proton magnetic resonance spectroscopy." C R Acad Sci III **319**(7): 623-31.

Nielsen, S., Smith, B. L., Christensen, E. I., et al. (1993). "Distribution of the aquaporin CHIP in secretory and resorptive epithelia and capillary endothelia." Proc Natl Acad Sci U S A **90**(15): 7275-9.

Nishi, M. and Kawata, M. (2006). "Brain corticosteroid receptor dynamics and trafficking: implications from live cell imaging." Neuroscientist **12**(2): 119-33.

Noggle, J. D. and Rodning, C. B. (1986). "Rapidly advancing pseudotumor cerebri associated with morbid obesity: an indication for gastric exclusion." South Med J **79**(6): 761-3.

Nogradi, A., Kelly, C. and Carter, N. D. (1993). "Localization of acetazolamide-resistant carbonic anhydrase III in human and rat choroid plexus by immunocytochemistry and in situ hybridisation." Neurosci Lett **151**(2): 162-5.

Nwe, K. H., Hamid, A., Morat, P. B., et al. (2000). "Differential regulation of the oxidative 11beta-hydroxysteroid dehydrogenase activity in testis and liver." Steroids **65**(1): 40-5.

Oakley, R. H., Sar, M. and Cidlowski, J. A. (1996). "The human glucocorticoid receptor beta isoform. Expression, biochemical properties, and putative function." J Biol Chem **271**(16): 9550-9.

Odermatt, A. and Atanasov, A. G. (2009). "Mineralocorticoid receptors: emerging complexity and functional diversity." Steroids **74**(2): 163-71.

Onyimba, C. U., Vijapurapu, N., Curnow, S. J., et al. (2006). "Characterisation of the prereceptor regulation of glucocorticoids in the anterior segment of the rabbit eye." J Endocrinol **190**(2): 483-93.

Orcutt, J. C., Page, N. G. and Sanders, M. D. (1984). "Factors affecting visual loss in benign intracranial hypertension." Ophthalmology **91**(11): 1303-12.

Orefice, G., Celentano, L., Scaglione, M., et al. (1992). "Radioisotopic cisternography in benign intracranial hypertension of young obese women. A seven-case study and pathogenetic suggestions." Acta Neurol (Napoli) **14**(1): 39-50.

Palermo, M., Gomez-Sanchez, C., Roitmann, E., et al. (1996). "Quantification of cortisol and related 3-oxo-4-ene steroids in urine using gas chromatography/mass spectrometry with stable isotope labeled internal standards." Steroids **61**: 583-589.

Pampapathi, M. R. and Kabuubi, J. B. (1987). "Benign intracranial hypertension: a clinical lesson." J R Army Med Corps **133**(2): 82-4.

Pandit, J. C. (1994). "Testing acuity of vision in general practice: reaching recommended standard." BMJ **309**(6966): 1408.

Papadimitriou, A. and Priftis, K. N. (2009). "Regulation of the hypothalamic-pituitary-adrenal axis." Neuroimmunomodulation **16**(5): 265-71.

Parry, B. L., Javeed, S., Laughlin, G. A., et al. (2000). "Cortisol circadian rhythms during the menstrual cycle and with sleep deprivation in premenstrual dysphoric disorder and normal control subjects." Biol Psychiatry **48**(9): 920-31.

Pasquali, R., Cantobelli, S., Casimirri, F., et al. (1993). "The hypothalamic-pituitary-adrenal axis in obese women with different patterns of body fat distribution." J Clin Endocrinol Metab **77**(2): 341-346.

Paterson, J. M., Morton, N. M., Fievet, C., et al. (2004). "Metabolic syndrome without obesity: Hepatic overexpression of 11beta-hydroxysteroid dehydrogenase type 1 in transgenic mice." Proc Natl Acad Sci U S A **101**(18): 7088-93.

Paterson, R., Depasquale, N. and Mann, S. (1961). "Pseudotumor cerebri." Medicine (Baltimore) **40**: 85-99.

Paulmyer-Lacroix, O., Boullu, S., Oliver, C., et al. (2002). "Expression of the mRNA coding for 11beta-hydroxysteroid dehydrogenase type 1 in adipose tissue from obese patients: an in situ hybridization study." J Clin Endocrinol Metab **87**(6): 2701-5.

Paulsen, S. K., Pedersen, S. B., Fisker, S., et al. (2007). "11Beta-HSD type 1 expression in human adipose tissue: impact of gender, obesity, and fat localization." Obesity (Silver Spring) **15**(8): 1954-60.

Petroff, O. A., Yu, R. K. and Ogino, T. (1986). "High-resolution proton magnetic resonance analysis of human cerebrospinal fluid." J Neurochem **47**(4): 1270-6.

Petrone, A., Civitillo, R. M., Galante, L., et al. (1999). "Usefulness of a 12-month treatment with finasteride in idiophathic and polycystic ovary syndrome-associated hirsutism." Clin Exp Obstet Gynecol **26**(3-4): 213-6.

Phillipov, G., Palermo, M. and Shackleton, C. H. (1996). "Apparent cortisone reductase deficiency: a unique form of hypercortisolism." J Clin Endocrinol Metab **81**(11): 3855-60.

Pickard, J. D., Czosnyka, Z., Czosnyka, M., et al. (2008). "Coupling of sagittal sinus pressure and cerebrospinal fluid pressure in idiopathic intracranial hypertension--a preliminary report." Acta Neurochir Suppl **102**: 283-5.

Poisson, M., Pertuiset, B. F., Moguilewsky, M., et al. (1984). "[Steroid receptors in the central nervous system. Implications in neurology]." Rev Neurol (Paris) **140**(4): 233-48.

Polansky, J. R., Fauss, D. J., Chen, P., et al. (1997). "Cellular pharmacology and molecular biology of the trabecular meshwork inducible glucocorticoid response gene product." Ophthalmologica **211**: 126-139.

Polman, C. H., Reingold, S. C., Edan, G., et al. (2005). "Diagnostic criteria for multiple sclerosis: 2005 revisions to the "McDonald Criteria"." Ann Neurol **58**(6): 840-6.

Popp, J., Schaper, K., Kolsch, H., et al. (2009). "CSF cortisol in Alzheimer's disease and mild cognitive impairment." Neurobiol Aging **30**(3): 498-500.

Praetorius, J. (2007). "Water and solute secretion by the choroid plexus." Pflugers Arch **454**(1): 1-18.

Prakash, A. and Matta, B. F. (2008). "Hyperglycaemia and neurological injury." Curr Opin Anaesthesiol **21**(5): 565-9.

Pratt, W. B. and Toft, D. O. (1997). "Steroid receptor interactions with heat shock protein and immunophilin chaperones." Endocrine Reviews **18**(3): 306-369.

Pryse-Phillips, W. (2002). "Evaluating migraine disability: the headache impact test instrument in context." Can J Neurol Sci **29 Suppl 2**: S11-5.

Purcell, E. M., Torrey, H.C. and Pound, R.V. (1946). "Resonance Absorption by Nuclear Magnetic Moments in a Solid." Phys Rev **69**: 37-38.

Quincke, H., Deuttsche, Z. and Nervenheilk (1897). "Uber meningitis serosa und verwandete zustande " Deutsche Zeitschrift fur Nervenheilkunde **6**: 140-168.

Radhakrishnan, K., Thacker, A. K., Bohlaga, N. H., et al. (1993). "Epidemiology of idiopathic intracranial hypertension: a prospective and case-control study." J Neurol Sci **116**(1): 18-28.

Rajan, V., Edwards, C. R. W. and Seckl, J. R. (1996). "11β-hydroxysteroid dehydrogenase in cultured hippocampal cells reactivates inert 11-dehydrocorticosterone, potentiating neurotoxicity." Journal of Neuroscience **16**: 65-70.

Rajpal, S., Niemann, D. B. and Turk, A. S. (2005). "Transverse venous sinus stent placement as treatment for benign intracranial hypertension in a young male: case report and review of the literature." J Neurosurg **102**(3 Suppl): 342-6.

Ramadan, Z., Jacobs, D., Grigorov, M., et al. (2006). "Metabolic profiling using principal component analysis, discriminant partial least squares, and genetic algorithms." Talanta **68**(5): 1683-1691.

Rask, E., Olsson, T., Soderberg, S., et al. (2001). "Tissue-specific dysregulation of cortisol metabolism in human obesity." J Clin Endocrinol Metab **86**(3): 1418-21.

Rauz, S., Cheung, C. M., Wood, P. J., et al. (2003a). "Inhibition of 11beta-hydroxysteroid dehydrogenase type 1 lowers intraocular pressure in patients with ocular hypertension." Qjm **96**(7): 481-90.

Rauz, S., Walker, E. A., Hughes, S. V., et al. (2003b). "Serum- and glucocorticoid-regulated kinase isoform-1 and epithelial sodium channel subunits in human ocular ciliary epithelium." Invest Ophthalmol Vis Sci **44**(4): 1643-51.

Rauz, S., Walker, E. A., Murray, P. I., et al. (2003c). "Expression and distribution of the serum and glucocorticoid regulated kinase and the epithelial sodium channel subunits in the human cornea." Exp Eye Res **77**(1): 101-8.

Rauz, S., Walker, E. A., Shackleton, C. H., et al. (2001). "Expression and putative role of 11 beta-hydroxysteroid dehydrogenase isozymes within the human eye." Invest Ophthalmol Vis Sci **42**(9): 2037-42.

REA-SPCW, G. (2004). "Revised 2003 consensus on diagnostic criteria and long-term health risks related to polycystic ovary syndrome." Fertility and Sterility **81**(1): 19-25.

Rebolleda, G. and Munoz-Negrete, F. J. (2009). "Follow-up of Mild Papilledema in Idiopathic Intracranial Hypertension with Optical Coherence Tomography." Invest Ophthalmol Vis Sci **50**(11): 5197-200.

Reeves, G. D. and Doyle, D. A. (2002). "Growth hormone treatment and pseudotumor cerebri: coincidence or close relationship?" J Pediatr Endocrinol Metab **15 Suppl 2**: 723-30.

Reichardt, H. M. and Schutz, G. (1998). "Glucocorticoid signalling--multiple variations of a common theme." Mol Cell Endocrinol **146**(1-2): 1-6.

Reul, J. M. and de Kloet, E. R. (1985). "Two receptor systems for corticosterone in rat brain: microdistribution and differential occupation." Endocrinology **117**(6): 2505-11.

Reynolds, R. M., Walker, B. R., Syddall, H. E., et al. (2001). "Altered control of cortisol secretion in adult men with low birth weight and cardiovascular risk factors." J Clin Endocrinol Metab **86**(1): 245-50.

Ricketts, M. L., Verhaeg, J. M., Bujalska, I., et al. (1998). "Immunohistochemical localization of type 1 11beta-hydroxysteroid dehydrogenase in human tissues." J Clin Endocrinol Metab **83**(4): 1325-35.

Ridsdale, L. and Moseley, I. (1978). "Thoracolumbar intraspinal tumours presenting features of raised intracranial pressure." J Neurol Neurosurg Psychiatry **41**(8): 737-45.

Robitaille, J., Brouillette, C., Houde, A., et al. (2004). "Molecular screening of the 11beta-HSD1 gene in men characterized by the metabolic syndrome." Obes Res **12**(10): 1570-5.

Robson, A. C., Leckie, C. M., Seckl, J. R., et al. (1998). "11 Beta-hydroxysteroid dehydrogenase type 2 in the postnatal and adult rat brain." Brain Res Mol Brain Res **61**(1-2): 1-10.

Rodahl, K. and Moore, T. (1943). "The vitamin A content and toxicity of bear and seal liver." Biochem J **37**(2): 166-8.

Roland, B. L., Li, K. X. and Funder, J. W. (1995). "Hybridization histochemical localization of 11 beta-hydroxysteroid dehydrogenase type 2 in rat brain." Endocrinology **136**(10): 4697-700.

Ropper, A. H. and Marmarou, A. (1984). "Mechanism of pseudotumor in Guillain-Barre syndrome." Arch Neurol **41**(3): 259-61.

Rosenberg, M. L., Corbett, J. J., Smith, C., et al. (1993). "Cerebrospinal fluid diversion procedures in pseudotumor cerebri." Neurology **43**(6): 1071-2.

Rosenfeld, W. E. (1997). "Topiramate: a review of preclinical, pharmacokinetic, and clinical data." Clin Ther **19**(6): 1294-308.

Rosenstock, J., Banarer, S., Fonseca, V., et al. (2009). "Efficacy and Safety of the 11-beta-HSD1 Inhibitor, INCB13739, Added to Metformin Therapy in Patients with Type 2 Diabetes." Proc 69th Scientific Sessions Meeting of the American Diabetes Association, New Orleans **Abstract 7-LB**.

Rowe, F. J. and Sarkies, N. J. (1998). "Assessment of visual function in idiopathic intracranial hypertension: a prospective study." Eye **12 (Pt 1)**: 111-8.

Rozsa, F. W., Reed, D. M., Scott, K. M., et al. (2006). "Gene expression profile of human trabecular meshwork cells in response to long-term dexamethasone exposure." Mol Vis **12**: 125-41.

Russell, D. W. and Wilson, J. D. (1994). "Steroid 5 alpha-reductase: two genes/two enzymes." Annu Rev Biochem **63**: 25-61.

Rusvai, E. and Naray-Fejes-Toth, A. (1993). "A new isoform of 11 beta-hydroxysteroid dehydrogenase in aldosterone target cells." J Biol Chem **268**(15): 10717-20.

Sacks, F. M., Bray, G. A., Carey, V. J., et al. (2009). "Comparison of weight-loss diets with different compositions of fat, protein, and carbohydrates." N Engl J Med **360**(9): 859-73.

Saigusa, K., Takei, H., Shishido, T., et al. (2002). "[Benign intracranial hypertension resulting from corticosteroid withdrawal: case report]." No Shinkei Geka **30**(1): 57-62.

Sanchez-Tocino, H., Bringas, R., Iglesias, D., et al. (2006). "[Utility of optic coherence tomography (OCT) in the follow-up of idiopathic intracranial hypertension in childhood.]." Arch Soc Esp Oftalmol **81**(7): 383-9.

Sandeep, T. C., Andrew, R., Homer, N. Z., et al. (2005). "Increased in vivo regeneration of cortisol in adipose tissue in human obesity and effects of the 11beta-hydroxysteroid dehydrogenase type 1 inhibitor carbenoxolone." Diabetes **54**(3): 872-9.

Sandeep, T. C., Yau, J. L., MacLullich, A. M., et al. (2004). "11Beta-hydroxysteroid dehydrogenase inhibition improves cognitive function in healthy elderly men and type 2 diabetics." Proc Natl Acad Sci U S A **101**(17): 6734-9.

Sandrini, G., Farkkila, M., Burgess, G., et al. (2002). "Eletriptan vs sumatriptan: a double-blind, placebo-controlled, multiple migraine attack study." Neurology **59**(8): 1210-7.

Sapolsky, R. M., Uno, H., Rebert, C. S., et al. (1990). "Hippocampal damage associated with prolonged glucocorticoid exposure in primates." J Neurosci **10**(9): 2897-902.

Sarnat, H. B. (1998). "Histochemistry and immunocytochemistry of the developing ependyma and choroid plexus." Microsc Res Tech **41**(1): 14-28.

Savini, G., Bellusci, C., Carbonelli, M., et al. (2006). "Detection and Quantification of Retinal Nerve Fiber Layer Thickness in Optic Disc Edema Using Stratus OCT." Arch Ophthalmol **124**(8): 1111-1117.

Schwalbe, G. (1869). "Der Arachnoidalraum ein Lymphraum und sein Zusammenhang mit den Perichoriodalraum." Zentralbl Med Wiss **7**: 465-467.

Sellebjerg, F., Christiansen, M., Jensen, J., et al. (2000). "Immunological effects of oral high-dose methylprednisolone in acute optic neuritis and multiple sclerosis." Eur J Neurol **7**(3): 281-9.

Senay, L. C., Jr. and Tolbert, D. L. (1984). "Effect of arginine vasopressin, acetazolamide, and angiotensin II on CSF pressure at simulated altitude." Aviat Space Environ Med **55**(5): 370-6.

Serafini, P. and Lobo, R. A. (1985). "Increased 5 alpha-reductase activity in idiopathic hirsutism." Fertil Steril **43**(1): 74-8.

Sergott, R. C., Savino, P. J. and Bosley, T. M. (1990). "Optic nerve sheath decompression: a clinical review and proposed pathophysiologic mechanism." Aust N Z J Ophthalmol **18**(4): 365-73.

Serratrice, J., Granel, B., Conrath, J., et al. (2002). "Benign intracranial hypertension and thyreostimulin suppression hormonotherapy." Am J Ophthalmol **134**(6): 910-1.

Shackleton, C. H., Neres, M. S., Hughes, B. A., et al. (2008). "17-Hydroxylase/C17,20-lyase (CYP17) is not the enzyme responsible for side-chain cleavage of cortisol and its metabolites." Steroids **73**(6): 652-6.

Shackleton, C. H. and Whitney, J. O. (1980). "Use of Sep-pak cartridges for urinary steroid extraction: evaluation of the method for use prior to gas chromatographic analysis." Clin Chim Acta **107**(3): 231-43.

Sheedy, J. (1993.). "Standards for visual acuity measurement. In: Eye care technology forum proceedings." Bethesda, Maryland: National Institutes of Health,.

Shimojo, M., Ricketts, M. L., Perelli, M. D., et al. (1997). "Immunodetection of 11β-hydroxysteroid dehydrogenase type 2 in human mineralocorticoid target tissues: evidence of nuclear localizaton." Endocrinology **138**(3): 1305-1311.

Shin, H. E., Park, J. W., Kim, Y. I., et al. (2008). "Headache Impact Test-6 (HIT-6) Scores for Migraine Patients: Their Relation to Disability as Measured from a Headache Diary." J Clin Neurol **4**(4): 158-63.

Shinar, H. and Navon, G. (1986). "Sodium-23 NMR relaxation times in body fluids." Magn Reson Med **3**(6): 927-34.

Siger, M., Dziegielewski, K., Jasek, L., et al. (2008). "Optical coherence tomography in multiple sclerosis: thickness of the retinal nerve fiber layer as a potential measure of axonal loss and brain atrophy." J Neurol **255**(10): 1555-60.

Silva, P., Stoff, J., Field, M., et al. (1977). "Mechanism of active chloride secretion by shark rectal gland: role of Na-K-ATPase in chloride transport." Am J Physiol **233**(4): F298-306.

Simone, I. L., Federico, F., Trojano, M., et al. (1996). "High resolution proton MR spectroscopy of cerebrospinal fluid in MS patients. Comparison with biochemical changes in demyelinating plaques." J Neurol Sci **144**(1-2): 182-90.

Sinclair, A. J., Ball, A. K., Burdon, M. A., et al. (2008). "Exploring the pathogenesis of IIH: An inflammatory perspective." J Neuroimmunol **201-202C**: 212-220.

Sinclair, A. J., Viant, M. R., Ball, A. K., et al. (2009). "NMR-based metabolomic analysis of cerebrospinal fluid and serum in neurological diseases - a diagnostic tool?" NMR Biomed **23**(2): 123-32.

Siva, A., Altintas, A. and Saip, S. (2004). "Behcet's syndrome and the nervous system." Curr Opin Neurol **17**(3): 347-57.

Small, G. R., Hadoke, P. W., Sharif, I., et al. (2005). "Preventing local regeneration of glucocorticoids by 11beta-hydroxysteroid dehydrogenase type 1 enhances angiogenesis." Proc Natl Acad Sci U S A **102**(34): 12165-70.

Smit, P., Dekker, M. J., de Jong, F. J., et al. (2007). "Lack of Association of the 11beta-hydroxysteroid dehydrogenase type 1 gene 83,557insA and hexose-6-phosphate dehydrogenase gene R453Q polymorphisms with body composition, adrenal androgen production, blood pressure, glucose metabolism, and dementia." J Clin Endocrinol Metab **92**(1): 359-62.

Smith, J. L. (1985). "Whence pseudotumor cerebri?" J Clin Neuroophthalmol **5**(1): 55-6.

Snellen, H. (1862). "Probebuchstaben zur Bestimmung der Sehschdrfe." Utrecht: P.W. van de Weijer.

Soler, D., Cox, T., Bullock, P., et al. (1998). "Diagnosis and management of benign intracranial hypertension." Arch Dis Child **78**(1): 89-94.

Sorensen, P. S., Krogsaa, B. and Gjerris, F. (1988). "Clinical course and prognosis of pseudotumor cerebri. A prospective study of 24 patients." Acta Neurol Scand **77**(2): 164-72.

Sowers, M. F., Zheng, H., McConnell, D., et al. (2009). "Testosterone, sex hormone-binding globulin and free androgen index among adult women: chronological and ovarian aging." Hum Reprod **24**(9): 2276-85.

Speake, T., Whitwell, C., Kajita, H., et al. (2001). "Mechanisms of CSF secretion by the choroid plexus." Microsc Res Tech **52**(1): 49-59.

Spence, J. D. (2006). "Homocysteine and stroke prevention: have the trials settled the issue?" Int J Stroke **1**(4): 242-4.

Stacy, M. and Jankovic, J. (1992). "Differential diagnosis of Parkinson's disease and the parkinsonism plus syndromes." Neurol Clin **10**(2): 341-59.

Staner, L. (2006). "Surrogate outcomes in neurology, psychiatry, and psychopharmacology." Dialogues Clin Neurosci **8**(3): 345-52.

Starkman, M. N., Gebarski, S. S., Berent, S., et al. (1992). "Hippocampal formation volume, memory dysfunction, and cortisol levels in patients with Cushing's syndrome." Biol Psychiatry **32**(9): 756-65.

Stewart, P. M., Boulton, A., Kumar, S., et al. (1999). "Cortisol metabolism in human obesity: impaired cortisone-->cortisol conversion in subjects with central adiposity." J Clin Endocrinol Metab **84**(3): 1022-7.

Stewart, P. M., Corrie, J. E., Shackleton, C. H., et al. (1988). "Syndrome of apparent mineralocorticoid excess. A defect in the cortisol-cortisone shuttle." J Clin Invest **82**(1): 340-9.

Stewart, P. M. and Krozowski, Z. S. (1999). "11 beta-Hydroxysteroid dehydrogenase." Vitam Horm **57**: 249-324.

Stewart, P. M., Shackleton, C. H., Beastall, G. H., et al. (1990). "5 alpha-reductase activity in polycystic ovary syndrome." Lancet **335**(8687): 431-3.

Stone, M. B. (2009). "Ultrasound diagnosis of papilledema and increased intracranial pressure in pseudotumor cerebri." Am J Emerg Med **27**(3): 376 e1-376 e2.

Subramaniam, R. M., Tress, B. M., King, J. O., et al. (2004). "Transverse sinus septum: a new aetiology of idiopathic intracranial hypertension?" Australas Radiol **48**(2): 114-6.

Subramanian, A., Gupta, A., Saxena, S., et al. (2005). "Proton MR CSF analysis and a new software as predictors for the differentiation of meningitis in children." NMR Biomed **18**(4): 213-25.

Sugerman, H., Windsor, A., Bessos, M., et al. (1997). "Intra-abdominal pressure, sagittal abdominal diameter and obesity comorbidity." J Intern Med **241**(1): 71-9.

Sugerman, H. J., Felton, W. L., 3rd, Salvant, J. B., Jr., et al. (1995). "Effects of surgically induced weight loss on idiopathic intracranial hypertension in morbid obesity." Neurology **45**(9): 1655-9.

Sussman, J., Leach, M., Greaves, M., et al. (1997). "Potentially prothrombotic abnormalities of coagulation in benign intracranial hypertension." J Neurol Neurosurg Psychiatry **62**(3): 229-33.

Svendsen, P. F., Madsbad, S., Nilas, L., et al. (2009). "Expression of 11[beta]-hydroxysteroid dehydrogenase 1 and 2 in subcutaneous adipose tissue of lean and obese women with and without polycystic ovary syndrome." Int J Obes **33**(11): 1249-56.

Swan, E. E., Peppi, M., Chen, Z., et al. (2009). "Proteomics analysis of perilymph and cerebrospinal fluid in mouse." Laryngoscope **119**(5): 953-8.

Swanton, J. K., Rovira, A., Tintore, M., et al. (2007). "MRI criteria for multiple sclerosis in patients presenting with clinically isolated syndromes: a multicentre retrospective study." Lancet Neurol **6**(8): 677-86.

t Hart, B. A., Vogels, J. T., Spijksma, G., et al. (2003). "1H-NMR spectroscopy combined with pattern recognition analysis reveals characteristic chemical patterns in urines of MS patients and non-human primates with MS-like disease." J Neurol Sci **212**(1-2): 21-30.

Tamburrelli, C., Salgarello, T., Caputo, C. G., et al. (2000). "Ultrasonographic evaluation of optic disc swelling: comparison with CSLO in idiopathic intracranial hypertension." Invest Ophthalmol Vis Sci **41**(10): 2960-6.

Tan, J. C., Peters, D. M. and Kaufman, P. L. (2006). "Recent developments in understanding the pathophysiology of elevated intraocular pressure." Curr Opin Ophthalmol **17**(2): 168-74.

Tanaka, K., Budd, M. A., Efron, M. L., et al. (1966). "Isovaleric acidemia: a new genetic defect of leucine metabolism." Proc Natl Acad Sci U S A **56**(1): 236-42.

Tannin, G. M., Agarwal, A. K., Monder, C., et al. (1991). "The human gene for 11 beta-hydroxysteroid dehydrogenase. Structure, tissue distribution, and chromosomal localization." J Biol Chem **266**(25): 16653-8.

Taplu, A., Gokmen, N., Erbayraktar, S., et al. (2003). "Effects of pressure- and volume-controlled inverse ratio ventilation on haemodynamic variables, intracranial pressure and cerebral perfusion pressure in rabbits: a model of subarachnoid haemorrhage under isoflurane anaesthesia." Eur J Anaesthesiol **20**(9): 690-6.

Thieringer, R., Grande, C. B. L., Carbin, L., et al. (2001). "11β-hydroxysteroid dehydrogenase type 1 is induced in human monocytes upon differentiation to macrophages." Journal of Immunology **167**: 30-35.

Thigpen, A. E., Silver, R. I., Guileyardo, J. M., et al. (1993). "Tissue distribution and ontogeny of steroid 5 alpha-reductase isozyme expression." J Clin Invest **92**(2): 903-10.

Tian, S., Poukka, H., Palvimo, J. J., et al. (2002). "Small ubiquitin-related modifier-1 (SUMO-1) modification of the glucocorticoid receptor." <u>Biochem J</u> **367**(Pt 3): 907-11.

Tiziani, S., Emwas, A. H., Lodi, A., et al. (2008). "Optimized metabolite extraction from blood serum for 1H nuclear magnetic resonance spectroscopy." <u>Anal Biochem</u> **377**(1): 16-23.

Tomlinson, J. W., Finney, J., Hughes, B. A., et al. (2008). "Reduced glucocorticoid production rate, decreased 5{alpha}-reductase activity and adipose tissue insulin sensitization following weight loss." <u>Diabetes</u> **57**(6): 1536-43.

Tomlinson, J. W., Moore, J. S., Clark, P. M., et al. (2004a). "Weight loss increases 11beta-hydroxysteroid dehydrogenase type 1 expression in human adipose tissue." <u>J Clin Endocrinol Metab</u> **89**(6): 2711-6.

Tomlinson, J. W., Sinha, B., Bujalska, I., et al. (2002). "Expression of 11beta-hydroxysteroid dehydrogenase type 1 in adipose tissue is not increased in human obesity." <u>J Clin Endocrinol Metab</u> **87**(12): 5630-5.

Tomlinson, J. W., Walker, E. A., Bujalska, I. J., et al. (2004b). "11β-Hydroxysteroid Dehydrogenase Type 1: A Tissue-Specific Regulator of Glucocorticoid Response." <u>Endocrine Reviews</u> **25**(5): 831-866.

Towers, R., Naftali, T., Gabay, G., et al. (2005). "High levels of glucocorticoid receptors in patients with active Crohn's disease may predict steroid resistance." <u>Clin Exp Immunol</u> **141**(2): 357-62.

Tripathi, B. J. and Tripathi, R. C. (1974). "Vacuolar transcellular channels as a drainage pathway for cerebrospinal fluid." <u>J Physiol</u> **239**(1): 195-206.

Tsilchorozidou, T., Honour, J. W. and Conway, G. S. (2003). "Altered cortisol metabolism in polycystic ovary syndrome: insulin enhances 5alpha-reduction but not the elevated adrenal steroid production rates." <u>J Clin Endocrinol Metab</u> **88**(12): 5907-13.

Tsilchorozidou, T., Overton, C. and Conway, G. S. (2004). "The pathophysiology of polycystic ovary syndrome." <u>Clin Endocrinol (Oxf)</u> **60**(1): 1-17.

Turner, L. (1961). "The structure of arachnoid granulations with observations on their physiological and pathological significance." <u>Ann R Coll Surg Engl</u> **29**: 237-64.

Turner, R. C., Holman, R. R., Matthews, D., et al. (1979). "Insulin deficiency and insulin resistance interaction in diabetes: estimation of their relative contribution by feedback analysis from basal plasma insulin and glucose concentrations." <u>Metabolism</u> **28**(11): 1086-96.

Ueda, J., Wentz-Hunter, K. and Yue, B. Y. (2002). "Distribution of myocilin and extracellular matrix components in the juxtacanalicular tissue of human eyes." <u>Invest Ophthalmol Vis Sci</u> **43**(4): 1068-76.

Ueda, K., Okamura, N., Hirai, M., et al. (1992). "Human P-glycoprotein transports cortisol, aldosterone, and dexamethasone, but not progesterone." <u>J Biol Chem</u> **267**(34): 24248-52.

Uhl, E., Wrba, E., Nehring, V., et al. (1999). "Technical note: a new model for quantitative analysis of brain oedema resolution into the ventricles and the subarachnoid space." <u>Acta Neurochir (Wien)</u> **141**(1): 89-92.

Upton, M. L. and Weller, R. O. (1985). "The morphology of cerebrospinal fluid drainage pathways in human arachnoid granulations." <u>J Neurosurg</u> **63**(6): 867-75.

Uutela, P., Reinila, R., Harju, K., et al. (2009). "Analysis of intact glucuronides and sulfates of serotonin, dopamine, and their phase I metabolites in rat brain microdialysates by liquid chromatography-tandem mass spectrometry." <u>Anal Chem</u> **81**(20): 8417-25.

Valentine, G. H. (1959). "Triamcinolone and intracranial hypertension: a side-effect." Lancet **1**(7078): 892.

Van Cauter, E., Leproult, R. and Kupfer, D. J. (1996). "Effects of gender and age on the levels and circadian rhythmicity of plasma cortisol." J Clin Endocrinol Metab **81**(7): 2468-73.

van der Vaart, M. and Schaaf, M. J. (2009). "Naturally occurring C-terminal splice variants of nuclear receptors." Nucl Recept Signal **7**: e007.

van Steensel, B., van Binnendijk, E. P., Hornsby, C. D., et al. (1996). "Partial colocalization of glucocorticoid and mineralocorticoid receptors in discrete compartments in nuclei of rat hippocampus neurons." J Cell Sci **109 (Pt 4)**: 787-92.

Vassiliadi, D. A., Barber, T. M., Hughes, B. A., et al. (2009). "Increased 5 alpha-reductase activity and adrenocortical drive in women with polycystic ovary syndrome." J Clin Endocrinol Metab **94**(9): 3558-66.

Veilleux, A., Rheaume, C., Daris, M., et al. (2009). "Omental adipose tissue type 1 11 beta-hydroxysteroid dehydrogenase oxoreductase activity, body fat distribution, and metabolic alterations in women." J Clin Endocrinol Metab **94**(9): 3550-7.

Venero, J. L., Vizuete, M. L., Ilundain, A. A., et al. (1999). "Detailed localization of aquaporin-4 messenger RNA in the CNS: preferential expression in periventricular organs." Neuroscience **94**(1): 239-50.

Verkman, A. S. (2009). "Aquaporins: translating bench research to human disease." J Exp Biol **212**(11): 1707-1715.

Viant, M. R. (2003). "Improved methods for the acquisition and interpretation of NMR metabolomic data." Biochem Biophys Res Commun **310**(3): 943-8.

Vogeser, M. (2003). "Liquid chromatography-tandem mass spectrometry--application in the clinical laboratory." Clin Chem Lab Med **41**(2): 117-26.

Vogh, B. P., Godman, D. R. and Maren, T. H. (1987). "Effect of AlCl3 and other acids on cerebrospinal fluid production: a correction." J Pharmacol Exp Ther **243**(1): 35-9.

Vyas, C. K., Talwar, K. K., Bhatnagar, V., et al. (1981). "Steroid-induced benign intracranial hypertension." Postgrad Med J **57**(665): 181-2.

Walker, A. E. and Adamkiewicz, J. J. (1964). "Pseudotumor Cerebri Associated with Prolonged Corticosteroid Therapy. Reports of Four Cases." JAMA **188**: 779-84.

Wall, M., Dollar, J. D., Sadun, A. A., et al. (1995). "Idiopathic intracranial hypertension. Lack of histologic evidence for cerebral edema." Arch Neurol **52**(2): 141-5.

Wall, M. and George, D. (1991). "Idiopathic intracranial hypertension. A prospective study of 50 patients." Brain **114 (Pt 1A)**: 155-80.

Wallace, T. M., Levy, J. C. and Matthews, D. R. (2004). "Use and Abuse of HOMA Modeling." Diabetes Care **27**(6): 1487-1495.

Wang, S. J., Silberstein, S. D., Patterson, S., et al. (1998). "Idiopathic intracranial hypertension without papilledema: a case-control study in a headache center." Neurology **51**(1): 245-9.

Warner, J. E., Larson, A. J., Bhosale, P., et al. (2007). "Retinol-binding protein and retinol analysis in cerebrospinal fluid and serum of patients with and without idiopathic intracranial hypertension." J Neuroophthalmol **27**(4): 258-62.

Watanabe, A., Kinouchi, H., Horikoshi, T., et al. (2008). "Effect of intracranial pressure on the diameter of the optic nerve sheath." J Neurosurg **109**(2): 255-8.

Weber, K. T., Singh, K. D. and Hey, J. C. (2002). "Idiopathic intracranial hypertension with primary aldosteronism: report of 2 cases." Am J Med Sci **324**(1): 45-50.

Webster, S. P., Ward, P., Binnie, M., et al. (2007). "Discovery and biological evaluation of adamantyl amide 11beta-HSD1 inhibitors." Bioorg Med Chem Lett **17**(10): 2838-43.

Welch, K. (1963). "Secretion of Cerebrospinal Fluid by Choroid Plexus of the Rabbit." Am J Physiol **205**: 617-24.

Weller, R. O. (1974). "Mechanisms of cerebrospinal fluid absorption." Dev Med Child Neurol **16**(1): 85-7.

Westheimer, G. (2001). "Updating the classical approach to visual acuity." Clin Exp Optom **84**(5): 258-263.

Wevers, R. A., Engelke, U., Wendel, U., et al. (1995). "Standardized method for high-resolution 1H-NMR of cerebrospinal fluid." Clin Chem **41**(5): 744-51.

Whiteley, W., Al-Shahi, R., Warlow, C. P., et al. (2006). "CSF opening pressure: reference interval and the effect of body mass index." Neurology **67**(9): 1690-1.

Whorwood, C. B., Franklyn, J. A., Sheppard, M. C., et al. (1992). "Tissue localization of 11 beta-hydroxysteroid dehydrogenase and its relationship to the glucocorticoid receptor." J Steroid Biochem Mol Biol **41**(1): 21-8.

Whorwood, C. B., Mason, J. I., Ricketts, M. L., et al. (1995). "Detection of human 11β-hydroxysteroid dehydrogenase isoforms using reverse-transcriptase-polymerase chain reaction and localisation of type 2 isoform to renal collecting ducts." Molecular and Cellular Endocrinology **110**(3): R7-R12.

Wiggs, J. L., Allingham, R. R., Vollrath, D., et al. (1998). "Prevalence of mutations in TIGR/Myocilin in patients with adult and juvenile primary open-angle glaucoma." Am J Hum Genet **63**(5): 1549-52.

Williams, G. (2010). "Withdrawal of sibutramine in Europe." BMJ **340**: c824.

Williams, M. A., Moutray, T. N. and Jackson, A. J. (2008). "Uniformity of visual acuity measures in published studies." Invest Ophthalmol Vis Sci **49**(10): 4321-7.

Wishart, D. S., Tzur, D., Knox, C., et al. (2007). "HMDB: the Human Metabolome Database." Nucleic Acids Res **35**(Database issue): D521-6.

Wolf, O. T. (2003). "HPA axis and memory." Best Pract Res Clin Endocrinol Metab **17**(2): 287-99.

Wong, R., Madill, S. A., Pandey, P., et al. (2007). "Idiopathic intracranial hypertension: the association between weight loss and the requirement for systemic treatment." BMC Ophthalmol **7**: 15.

Woodruff, E. (1947). "Visual Acuity and the Selection of Test Letters." Hatton Press London.

Wright, E. M. (1978). "Transport processes in the formation of the cerebrospinal fluid." Rev Physiol Biochem Pharmacol **83**: 3-34.

Wu, Q., Delpire, E., Hebert, S. C., et al. (1998). "Functional demonstration of Na+-K+-2Cl- cotransporter activity in isolated, polarized choroid plexus cells." Am J Physiol **275**(6 Pt 1): C1565-72.

Yang, Y., Li, C., Nie, X., et al. (2007). "Metabonomic Studies of Human Hepatocellular Carcinoma Using High-Resolution Magic-Angle Spinning (1)H NMR Spectroscopy in Conjunction with Multivariate Data Analysis." J Proteome Res **6**(7): 2605-2614.

Younger, D. S. (2004). "Vasculitis of the nervous system." Curr Opin Neurol **17**(3): 317-36.

Zeuthen, T. and Wright, E. M. (1978). "An electrogenic NA+/K+ pump in the choroid plexus." Biochim Biophys Acta **511**(3): 517-22.

Zeuthen, T. and Wright, E. M. (1981). "Epithelial potassium transport: tracer and electrophysiological studies in choroid plexus." J Membr Biol **60**(2): 105-28.

Zhang, T. Y., Ding, X. and Daynes, R. A. (2005). "The Expression of 11β-Hydroxysteroid Dehydrogenase Type I by Lymphocytes Provides a Novel Means for Intracrine Regulation of Glucocorticoid Activities." Journal of Immunology **174**: 879-889.

Zhang, X., Zhou, Z., Yang, H., et al. (2009a). "4-(Phenylsulfonamidomethyl)benzamides as potent and selective inhibitors of the 11beta-hydroxysteroid dehydrogenase type 1 with efficacy in diabetic ob/ob mice." Bioorg Med Chem Lett **19**(15): 4455-8.

Zhang, Y. L., Zhong, X., Gjoka, Z., et al. (2009b). "H6PDH interacts directly with 11beta-HSD1: implications for determining the directionality of glucocorticoid catalysis." Arch Biochem Biophys **483**(1): 45-54.

Zillig, M., Wurm, A., Grehn, F. J., et al. (2005). "Overexpression and properties of wild-type and Tyr437His mutated myocilin in the eyes of transgenic mice." Invest Ophthalmol Vis Sci **46**(1): 223-34.

Zupping, R., Kaasik, A. E. and Raudam, E. (1971). "Cerebrospinal fluid metabolic acidosis and brain oxygen supply. Studies in patients with brain infarction." Arch Neurol **25**(1): 33-8.

Publications arising from this thesis

Sinclair AJ, Burdon MA, Ball AK, Nightingale NG, Good P, Matthews TD, Jacks A, Lawden M, Clarke CE, Walker EA, Tomlinson J, Stewart PM, and Rauz S. Low calorie diet and intracranial pressure in idiopathic intracranial hypertension: a prospective cohort study. BMJ in press (accepted 13/04/2010).

Sinclair AJ, Viant MR, Ball AK, Burdon MA, Walker EA. Stewart PM, Rauz S, Young S. Diagnostic Metabolomic Biomarkers in Neurology NMR Biomed. 2009 Aug 18. [Epub ahead of print]).

Ball A[*], **Sinclair AJ**[*], Curnow SJ, Tomlinson JW, Burdon MA, Walker EA, Stewart PM, Nightingale PG, Clarke CE, Rauz S. Elevated CSF leptin in idiopathic intracranial hypertension: Evidence for hypothalamic leptin resistance? (Clin Endocrinol (Oxf). 2009 Jun;70(6):863-9. Epub 2008 Sep 2). *** Joint first author.**

Sinclair AJ, Ball AK, Burdon MA, Clarke CE, Stewart PM, Curnow SJ and Rauz S. Exploring the Pathogenesis of Idiopathic Intracranial Hypertension: An inflammatory perspective. J Neuroimmunology 2008 Sep 15;201-202:212-20. Epub 2008 Aug 3.

Sinclair AJ, Onyimba C, Khosla P, Hughes S, Tomlinson J, Stewart P, Burdon M, Murray P, Walker E and Rauz S. Corticosteroids, 11β-Hydroxysteroid Dehydrogenase Isozymes and the Rabbit Choroid Plexus. J Neuroendocrinol. 2007 Aug;19(8):614-620.

Submitted

Sinclair AJ, Tomlinson J, Hughes BA, van Beek AP, Kema IP, Burdon MA, Nightingale MA, Walker EA, Stewart PM, Rauz S. Cerebrospinal fluid corticosteroid levels and cortisol metabolism in patients with Idiopathic Intracranial Hypertension: a link between 11β-HSD1 and intracranial pressure regulation? Submitted to The Journal of Clinical Endocrinology & Metabolism.